Asymmetric Ligands Derived from Carbohydrates

THE UNIVERSITY OF
WAIKATO
Te Whare Wānanga o Waikato

A thesis submitted in fulfilment of

the requirements for the degree of

Doctor of Philosophy of Chemistry

at

The University of Waikato

by

Bevan Peter Jarman

The University of Waikato

2011

Abstract

This thesis describes the incorporation of carbohydrate groups in thiourea, **1**, or iminophosphorane, **2**, ligands.

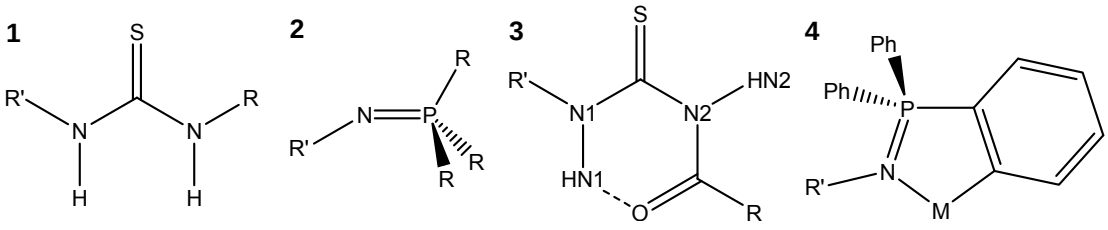

R´ is a sugar derived moiety

Several carbohydrate acyl thioureas, **3**, were synthesised from the reaction of protected and unprotected D-glucosamine with acyl isothiocyanates, RCONCS. Internal hydrogen-bonding forms a planar six-membered ring, which locks the thiourea into an Z,E,Z-anti conformation as shown by ^{1}H NMR spectroscopy and confirmed by X-ray structure determination of two examples. As neutral ligands to Rh(III), Rh(I), Ru(II), Pd(II), Pt(II) and Au(I) they bond through the sulfur atom with retention of the six-membered ring and the Z,E,Z-anti conformation. This was confirmed by two X-ray structure determinations on Rh(III) and Pd(II) examples which also showed the new hydrogen-bond formed by HN2 to a halide on the metal.

Deprotonation of the ligands **3** with NaOAc gave anionic species which formed bidentate chelating complexes with metals. When attached to Rh(III), Ru(II) or with two thiourea bonding to Pd(II) it forms a four-membered ring through the S and N2 atoms which retains the hydrogen-bond. If Rh(I) or (C,N-dimethylbenzylamine-Pd) is used a six-membered ring is formed through the S and O atoms which disrupts the hydrogen-bond. This disruption of the hydrogen-bond is apparent from the chemical shift of HN1. For examples where

coordination led to a chiral metal complex (e.g. for Cp*RhCl(*N*,*S*-thiourea)) NMR measurements showed that the natural chirality of the ligand did not provide any selectivity with equal proportions of the two diastereoisomers formed.

Iminophosphoranes were produced by the reaction of protected sugar azides with phosphines via the Staudinger reaction. Cyclometalated complexes, **4**, could not be formed directly which an X-ray structure determination suggested was because of steric crowding of the nitrogen. An indirect transmetalation route was developed where the sugar azides were reacted with the mercurated diphosphine, $Hg(2\text{-}C_6H_4PPh_2)_2$, and the resulting iminophosphoranes transmetalated with $[NMe_4][AuCl_4]$ to produce cyclometalated Au(III) dichloride complexes. Two X-ray structure determinations showed that the five-membered metalocyclic ring was in an envelope conformation. The chlorides were labile and able to be displaced by PPh_3 and thiosalicylic acid.

A series of *N*-sugar and *N*-phenyl iminophosphorane Au(III) complexes were shown to catalyse the addition of 2-methyl furan to methyl vinyl ketone.

Acknowledgments

Having finished this thesis there are many people who helped me get to this point and need to be thanked. Firstly to the University of Waikato for providing funding for my research. Next is the academic staff in the chemistry department, who were all willing to help. Special mention must go to Professor Alastair Wilkins who always helped with running the NMR and detailed explanations, and to Dr Graham Saunders who was ready to offer advice and answer questions. And more importantly he was always generous in “lending” me his expensive rhodium materials. My secondary supervisors Associate Professor Merilyn Manley-Harris and Professor Bill Henderson were also very helpful, always willing to stop what they were doing to help me out. The technicians Pat Gread and Wendy Jackson were very helpful with the instruments and were happy to stop what they were doing and let me into C.3.08 to get chemicals.

Of the students I must acknowledge, first must be Dr Kelly Kilpin who was helpful, friendly and always had a Simpsons quote ready. Secondly Jonathan Puddick who could be counted on for a cup of tea and our Wednesday coffees. And to the rest of the students past and present who made the department a great place to work in.

My family has provided me with an amazing amount of support. They have looked after me, shared times of celebrations, and gave me the encouragement to carry on.

And finally I wish to thank my supervisor Professor Brian Nicholson without whom I could not have done this. He has shown unfailing patience while I completed my thesis. He could calmly look at a difficult problem and solve it for me.

Table of Contents

Appendices

List of Figures

Chapter One: Introduction

Chapter Two: Sugar thioureas as neutral ligands

Chapter Three: Sugar thioureas as anionic ligands

Chapter Four: Sugar gold(III) iminophosphoranes

List of Schemes

List of Tables

Chapter Two: Sugar thioureas as neutral ligands

List of Abbreviations

General Abbreviations

COD 1,5-Cyclooctadiene

Cp* ..... η^5-C_5Me_5 (penta methyl cyclopentadienyl)

DMAB ..... Dimethylbenzylamine

DMSO ..... Dimethyl sulfoxide

ESI-MS ..... Electrospray Ionisation-Mass Spectrometry

THT ..... Tetrahydrothiophene

NMR Abbreviations

b..... Broad signal

d..... Doublet

dd..... Doublet of doublets

ddd ..... Doublet of doublet of doublets

dt ..... Doublet of triplets

COSY ..... **CO**rrelation **S**pectroscop**Y**

HSQC..... **H**eteronuclear **S**ingle **Q**uantum **C**oherence

HMBC ..... **H**eteronuclear **M**ultiple **B**ond **C**oherrence

Hz..... Hertz

m..... Multiplet

NMR..... Nuclear magnetic resonance

ppm ..... Parts per million

SELTOCSY..... **SEL**ected 1D **TO**tal **C**orrelation **S**pectroscop**Y**

t ..... Triplet

Chapter One
Introduction

Carbohydrates are an extremely important class of biomolecules and are the most abundant class of molecules in the biosphere comprising two thirds of all carbon in the biosphere [1]. Cellulose is the most abundant carbohydrate being half of all organic carbon [2]; 10^{15} kilograms of cellulose are synthesized and decomposed each year [2]. The simplest sugars, monosaccharides, have the general formula $C_nH_{2n}O_n$, or $C_n(H_2O)_n$, which is the origin of their name as they were thought to be hydrated carbon [3]. Carbohydrates have a large number of different biological roles including structural, cellulose in plants and chitin in arthropods; energy storage, glycogen in animals and starch in plants; as well as in processes such as cell recognition [4]. There are a large number of simple carbohydrates and many ways that they can be joined, meaning that there is a huge variety of carbohydrates that are available for use synthetically as well as in biological systems. Carbohydrates are an excellent way to introduce a number of interesting properties into compounds, such as chirality, water solubility and bioactivity.

1.1 Use of carbohydrates with metals

1.1.1 Using metals for synthesis of carbohydrates

There is a large background of material for the use of metals in synthetic carbohydrate chemistry [5]. The Koenigs-Knorr reaction is a classic example of this, a glycosidation reaction between an acylated α-glycosyl halide and an alcohol with an insoluble silver salt, either silver oxide or silver carbonate [6, 7], Scheme 1.1. Many other metal salts have been used for this reaction such as mercury oxide and mercury bromide [8], cadmium carbonate [9] and silver triflate [10] to name a few. Organometallic reagents also find other uses in

synthetic carbohydrate chemistry; alkyl stannylenes have been used to activate specific sugar hydroxyl groups [11]; carbohydrate complexes with titanium have been used to promote diastereoselective reactions [12].

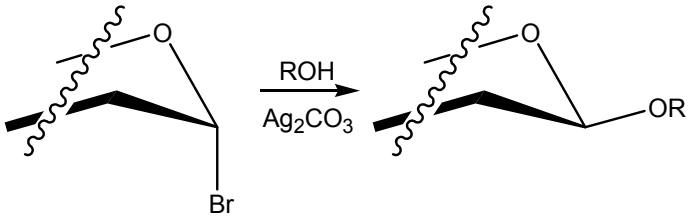

Scheme 1.1 *General scheme of the original Koenigs-Knorr reaction between glycosyl bromide and an alcohol in the presence of silver carbonate.*

1.1.2 Carbohydrates as ligands

Carbohydrates have been widely studied as ligands. This review will be selective and only touch on the basics of such a wide topic. For more comprehensive details a number of reviews have been published. Reviews have been written on carbohydrates as coordination ligands [13, 14], their biological applications [15, 16], and the use of carbohydrates as asymmetric catalysts [17-19].

1.1.2.1 Carbohydrates as coordination ligands

With their large number of pendant hydroxyl groups, natural abundance and large variability it is little wonder that carbohydrates have been extremely widely studied as coordination ligands.

1.1.2.2 Non-modified carbohydrates as coordination ligands

There are significant difficulties involved in the study of the coordination of non-modified carbohydrates to metals. Because of the large number of hydroxyl

groups available for coordination and the different configurational isomers that are possible, complex equilibria are often established and this complicates isolation and characterization [20]. As a general rule trivalent ions form stronger complexes than the mono and divalent ions.

1.1.2.3 Modified carbohydrates as coordination ligands

Because of the issues involved in non-modified sugar-metal complexes carbohydrates are often modified before complexing. These additional groups can enhance the binding affinities to metals, as well as making the complexes more crystalline. For example the condensation of 4,6-*O*-ethylidene-β-D-glucopyranosylamine with salicylaldehyde produces a ligand with a pendant group that can act as a chelating group [21]. The vanadium complex is shown in Figure 1.1; molybdenum, uranium [21] and copper analogues are known [22].

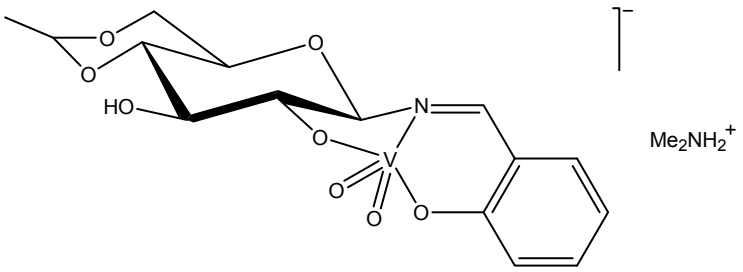

Figure 1.1 *A di-oxo vanadium complex with a carbohydrate featuring a pendant chelating group [21].*

Carbohydrates can be modified by derivatising the hydroxyl groups for example a 2,3-bis-*O*-(diarylphosphinite) [23], or by replacing the hydroxyl groups with other functionalities such as thioethers [24], Figure 1.2. Many other examples are known, that also show interesting properties, such as the *N,N* palladium chelate shown in Figure 1.3, which can be used for the hydrogenation of olefins [25].

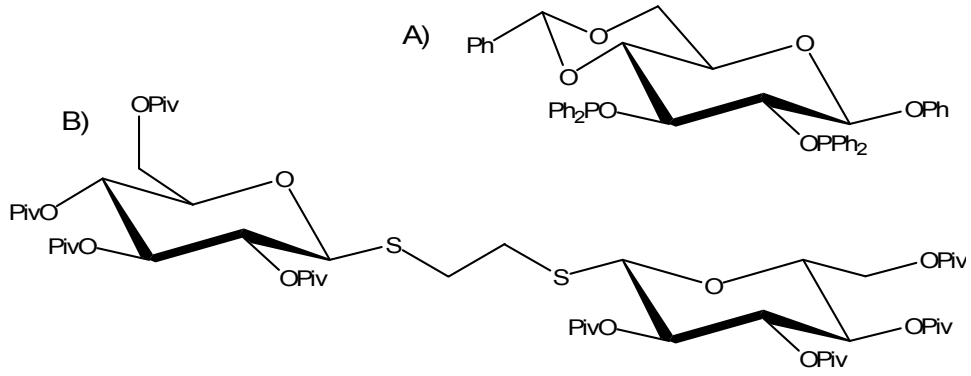

Figure 1.2 *A) A 2,3-bis-O-(diarylphosphinite) [23]; B) A Dithioether [24].*

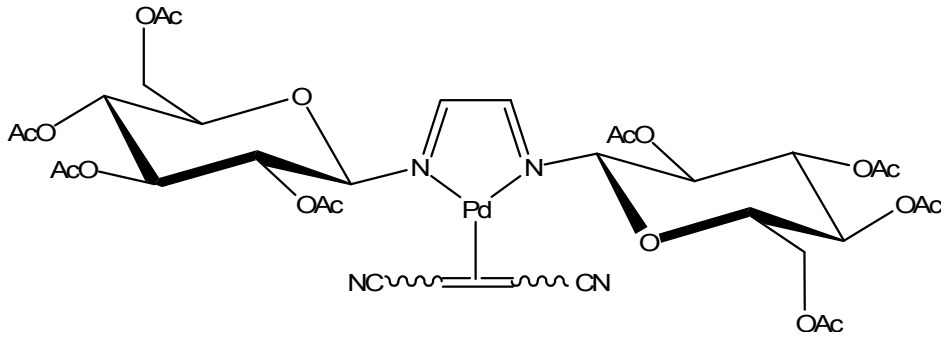

Figure 1.3 *An N,N palladium chelate based on glucose used for hydrogenation of olefins [25].*

1.1.2.4 Carbohydrates as organometallic ligands

A large number of organometallic ligands are based on carbohydrates. While the carbohydrate is generally modified with a pendant group that binds to the metal, there are examples where the metal is directly bonded to one of the carbohydrate carbons. Figure 1.4 shows compounds where the metal is directly bonded to the anomeric carbon, with iridium [26], manganese pentacarbonyl [27] and tributyl tin [28] examples. A common feature of these compounds and most of the ones for this work is that there are no free hydroxyl groups, they have all been protected. While the hydroxyl groups may impart water solubility as a desirable trait, often this gives major difficulties. The hydroxyl groups may preclude the use of common organic solvents and the presence of free hydroxyl groups can interfere with reactions. For these reasons the hydroxyl groups are

often protected. There are many options for the protecting groups including *inter alia* acetate, benzoyl, benzyl, trityl, acetal and silyl ethers.

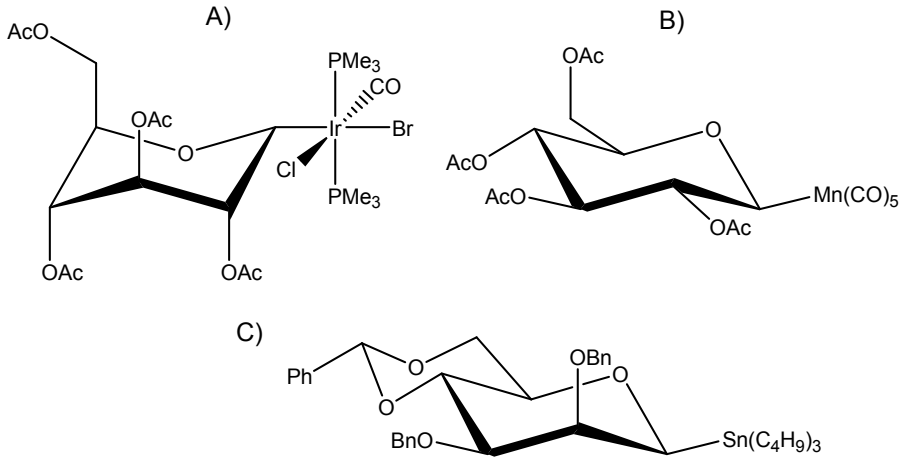

Figure 1.4 *Examples of organometallic complexes with the metal bonded to the anomeric carbon. A) An iridium example [26]; B) A manganese pentacarbonyl example [27]; C) A tributyl tin example [28].*

Figure 1.5 shows examples where a pendant group is bonding to the metal. Such compounds have shown a very wide range of properties including; antitumor [29], antimalarial [30], radioactive imaging [31], as well as catalysts for epoxidation [32] and hydrogenation [25] of olefins.

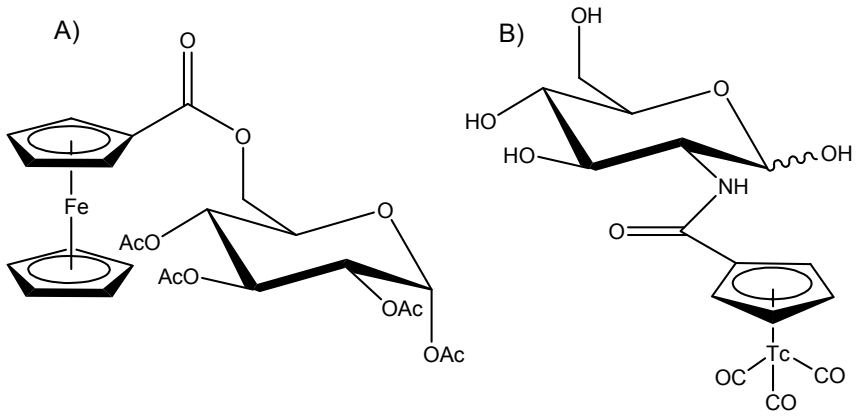

Figure 1.5 *A) [6-O-(1,2,3,4-Tetra-O-acetyl-β-D-glucopyranose)]-1-ferrocene carboxylate [30]; B) A tricarbonylcyclopentadienyl technetium(I) core with 2-amino-2-deoxy-D-glucose attached [31].*

1.2 Properties of carbohydrates to be exploited

There are three main properties of carbohydrates that have potential use in organometallic chemistry: water solubility, chirality and biofunctionality. There are many examples in the literature where water solubility is an important feature supplied by carbohydrates such as in water-soluble catalysts [25] and radioactive tracers for medical use [31]. Of more local relevance, other workers at the University of Waikato have produced organometallic compounds which show some activity as anti-cancer agents such as phosphine gold(I) thiourea complexes [33] and gold(III) iminophosphoranes [34], however these are made from water-insoluble ligands which limits their use as drugs. If they could be modified to include an unprotected carbohydrate moiety this would boost their water-solubility.

Secondly carbohydrates are a useful source of chirality; glucopyranose has five chiral centres. In a reaction that generates a chiral centre in the absence of any asymmetric influence, a racemic mixture will be produced; while if there is some asymmetric influence differing proportions of enantiomers can be formed [4]. It is possible to use carbohydrates to induce an asymmetric influence on a reaction which is very important in today's chemistry. Many of today's drugs are enantiopure compounds and this class is becoming more important. Of the drugs submitted to the FDA over 1992 to 2003, the number that are achiral or a racemic mixture were declining while the number of enantiopure drugs was increasing [35]. In a racemic mixture the "inactive" enantiomer may contribute to adverse side effects [36]. Carbohydrates can be bound to a reactant giving a local chiral influence with the carbohydrate being removed after the reaction has occurred or a reagent can be made with a carbohydrate attached [4]. For example an asymmetric borohydride with a glucofuranose derivative attached can reduce aryl ketones with high selectivity [37], Figure 1.6. Carbohydrates can also be used as chiral catalysts. Chiral catalysts have been made with iridium complexes of derivatised xylose based ligands [38]. Carbohydrate ligands have

also been included in catalysts that have been used for asymmetric hydrogenations [23, 39], asymmetric hydroformylation [40], hydrocyanation [41], epoxidation of olefins [42, 43] and allylic alkylation [44].

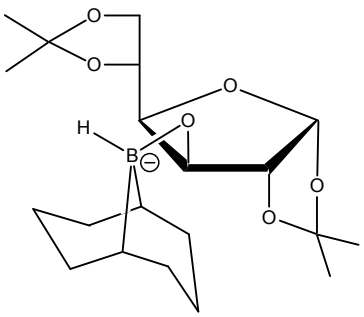

Figure 1.6 *A carbohydrate bound reagent, the borohydride can selectively reduce aryl ketones [4].*

Thirdly carbohydrates are important for providing biofunctionality. They are widely used in nature as mono-, oligo- and polysaccharides, as well as being attached to other biomolecules to form glycolipids and glycoproteins. Carbohydrates are also involved in cell-cell interactions with for example the adhesion of neurons in the development of the nervous system being mediated by carbohydrates [2]. Different pendant oligosaccharides on red blood cells produce the different blood groups [3]. Lectins are a class of proteins that bind carbohydrates, and have important roles such as mediating immune responses and infectious cycles. β-Galactosyl glycoconjugates are specifically up taken by lectins in the liver [2, 45]. Using a carbohydrate based ligand can potentially reduce toxicity and improve molecular targeting [45]. For example MRI agents have been developed that use the biofunctionality of carbohydrates in their action; one example uses a β-galactopyranose blocking group to prevent water molecules interacting with the gadolinium, Figure 1.7. In the body it is exposed to the β-galactosidase enzyme which cleaves the blocking group allowing access to water molecules altering the gadolinium's properties [46]. Another example has similar properties with a β-glucuronic acid portion that can be hydrolysed by a β-

glucuronidase enzyme [47], Figure 1.7. Both examples use the biofunctional properties of carbohydrates to elicit a change in the behaviour of the drug.

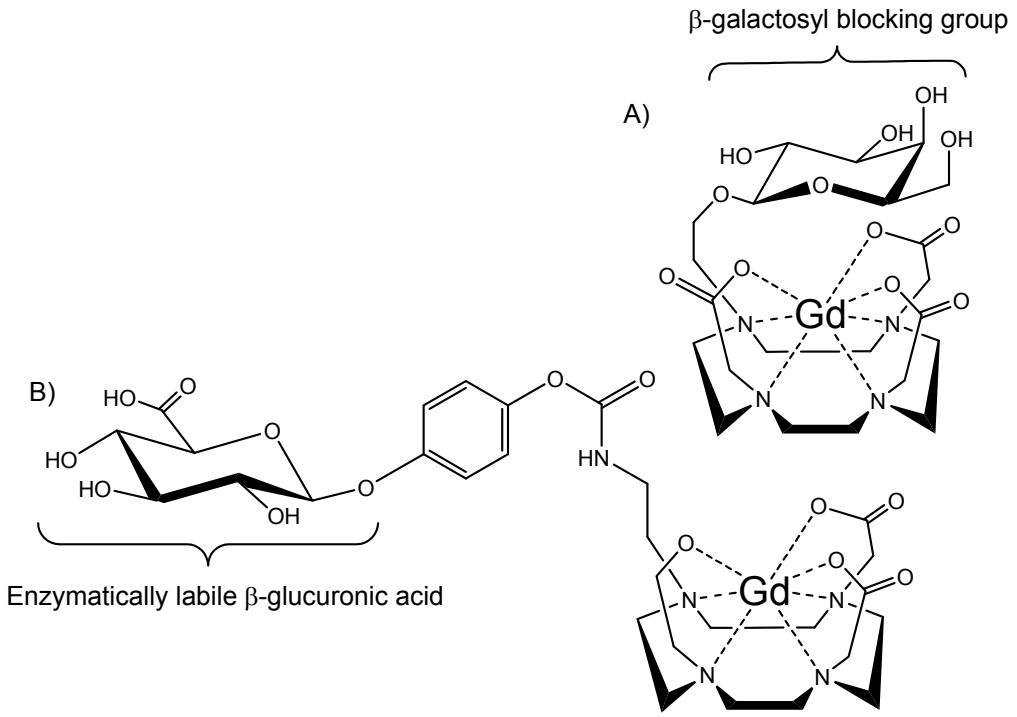

Figure 1.7 *Examples of medical imaging agents sensitive to the enzymes; A) β-galactosidase [45] ; B) β-glucuronidase [45].*

1.3 Research goals for the project

There were four main goals for this project. The first was to see if it was possible to produce thiourea and iminophosphorane complexes that contained protected carbohydrate functionality and to characterise the new compounds. The second goal was to investigate if it was possible to produce and characterise complexes with unprotected carbohydrate groups. Thirdly the biological activity of some of the compounds was to be investigated to see if there was any improvement over non-carbohydrate based analogues. It was hoped that this would tie into the previous goal, since complexes with unprotected sugars would be expected to be more water soluble which had the potential to boost the biological activity of the complexes compared to the protected analogues. Finally the carbohydrate

complexes were to be investigated to see if they could act as catalysts. This was important as if they were catalysts, there was the potential for them to act as chiral catalysts.

1.4 Overview of work covered

This was only a brief review of a very large area and more specific details and literature references will be referred to in each individual chapter. Chapter Two will discuss the use of sugar-derivatised thioureas as neutral ligands with various metals, while Chapter Three will look at their uses as anionic ligands. Chapter Four will detail the use of carbohydrate iminophosphoranes in cyclometalation reactions to gold(III). Chapter Five will describe some catalytic properties of the new complexes.

1.5 References

1. Sinnott, M.L., *Catalytic mechanisms of enzymic glycosyl transfer.* Chem. Rev., 1990. **90**, 1171-1202.
2. Stryer, L., *Biochemistry*. 3rd ed. 1988, New York: W.H. Freeman and Company.
3. Rao, V.S.R., Qasba, P.K., Balaji, P.V., and Chandrasekaran, R., *Conformation of carbohydrates*. 1998, Amsterdam: Harwood academic publishers.
4. Collins, P. and Ferrier, R., *Monosaccharides: Their chemistry and their roles in natural products*. 1995, Chichester: John Wiley & Sons, Ltd.
5. Whitfield, D.M., Stojkovski, S., and Sarkar, B., *Metal coordination to carbohydrates. Structures and function.* Coord. Chem. Rev., 1993. **122**, 171-225.
6. Koenigs, W. and Knorr, E., *Derivatives of grape sugar and galactose.* Ber., 1901. **34**, 957-981.
7. Igarashi, K., *The Koenigs-Knorr reaction.* Adv. Carbohydr. Chem. Biochem., 1977. **34**, 243-283.
8. Chen, Y., Heeg, M.J., Braunschweiger, P.G., Xie, W., and Wang, P.G., *A carbohydrate-linked cisplatin analogue having antitumor activity.* Angew. Chem. Int. Ed., 1999. **38**, 1768-1769.

9. Conrow, R.B. and Bernstein, S., *Steroid conjugates. VI. An improved Koenigs-Knorr synthesis of aryl glucuronides using cadmium carbonate, a new and effective catalyst.* J. Org. Chem., 1971. **36**, 863-870.

10. Lemieux, R.U., Takeda, T., and Chung, B.Y., *Synthesis of 2-amino-2-deoxy-β-D-glucopyranosides. Properties and use of 2-deoxy-2-phthalimidoglycosyl halides.* ACS. Symp. Ser., 1976. **39**, 90-115.

11. David, S. and Hanessian, S., *Regioselective manipulation of hydroxyl groups via organotin derivatives.* Tetrahedron, 1985. **41**, 643-663.

12. Duthaler, R.O., Herold, P., Wyler-Helfer, S., and Riediker, M., *Enantio- and diastereoselective aldol-reaction of 2,6-dimethylphenyl propionate using titanium-carbohydrate complexes.* Helv. Chim. Acta, 1990. **73**, 659-673.

13. Steinborn, D. and Junicke, H., *Carbohydrate complexes of platinum-group metals.* Chem. Rev., 2000. **100**, 4283-4317.

14. Alexeev, Y.E., Vasilchenko, I.S., Kharisov, B.I., Blanco, L.M., Garnovskii, A.D., and Zhdanov, Y.A., *Review: Synthetically modified carbohydrates as ligands.* J. Coord. Chem., 2004. **57**, 1447-1517.

15. Gottschaldt, M. and Schubert, U.S., *Prospects of metal complexes peripherally substituted with sugars in biomedicinal applications.* Chem. Eur. J., 2009. **15**, 1548-1557.

16. Hartinger, C.G., Nazarov, A.A., Ashraf, S.M., Dyson, P.J., and Keppler, B.K., *Carbohydrate-metal complexes and their potential as anticancer agents.* Curr. Med. Chem., 2008. **15**, 2574-2591.

17. Diéguez, M., Pàmies, O., Ruiz, A., Díaz, Y., Castillón, S., and Claver, C., *Carbohydrate derivative ligands in asymmetric catalysis.* Coord. Chem. Rev., 2004. **248**, 2165-2192.

18. Woodward, S., Diéguez, M., and Pàmies, O., *Use of sugar-based ligands in selective catalysis: Recent developments.* Coord. Chem. Rev., 2010. **254**, 2007-2030.

19. Diéguez, M., Claver, C., and Pàmies, O., *Recent progress in asymmetric catalysis using chiral carbohydrate-based ligands.* Eur. J. Org. Chem., 2007. **2007**, 4621-4634.

20. Piarulli, U. and Floriani, C., *Assembling sugars and metals: Novel architectures and reactivities in transition metal chemistry.* Prog. Inorg. Chem., 1997. **45**, 393-429.

21. Sah, A.K., Rao, C.P., Saarenketo, P.K., Wegelius, E.K., Kolehmainen, E., and Rissanen, K., *First crystallographic investigation of complexes of cis-VO_2^+, cis-MoO_2^+, and trans-UO_2^+ species with Schiff-base molecules derived from 4,6-O-ethylidene-β-D-glucopyranosylamine.* Eur. J. Inorg. Chem., 2001. **11**, 2773-2781.

22. Sah, A.K., Kato, M., and Tanase, T., *Trinuclear coordinatively labile Cu(II) complex of 4,6-O-ethylidene-β-D-glucopyranosylamine derived Schiff base ligand and its reactivity towards primary alcohols and amines.* Chem. Commun., 2005. **5**, 675-677.

23. RajanBabu, T.V., Ayers, T., Halliday, G.A., You, K.K., Calabrese, J.C., and Casalnuovo, A.L., *Carbohydrate phosphinites as practical ligands in asymmetric catalysis: Electronic effects and dependence of backbone chirality in Rh-catalyzed asymmetric hydrogenations. Synthesis of R- or S-amino acids using natural sugars as ligand precursors.* J. Org. Chem., 1997. **62**, 6012-6028.

24. Khiar, N., Araújo, C.S., Alvarez, E., and Fernández, I., *C_2-Symmetric bis-thioglycosides as new ligands for palladium-catalyzed allylic substitutions.* Tetrahedron Lett., 2003. **44**, 3401-3404.

25. Borriello, C., Ferrara, M.L., Orabona, I., Panunzi, A., and Ruffo, F., *[Pd^0(N,N-chelate)(olefin)] complexes containing nitrogen chelates derived from carbohydrates and their use in mild hydrogenation of olefins in water.* J. Chem. Soc., Dalton Trans., 2000. **15**, 2545-2550.

26. Pelczar, E.M., Munro-Leighton, C., and Gagné, M.R., *Oxidative addition of glycosylbromides to trans-$Ir(PMe_3)_2(CO)Cl$.* Organometallics, 2009. **28**, 663-665.

27. DeShong, P., Soli, E.D., Slough, G.A., Sidler, D.R., Elango, V., Rybczynski, P.J., Vosejpka, L.J.S., Lessen, T.A., Le, T.X., Anderson, G.B., von Philipsborn, W., Vöhler, M., Rentsch, D., and Zerbe, O., *Glycosylmanganese pentacarbonyl complexes: an organomanganese-based approach to the synthesis of C-glycosyl derivatives.* J. Organomet. Chem., 2000. **593-594**, 49-62.

28. Uhlmann, P., Nanz, D., Bozo, E., and Vasella, A., *Glycosylidene carbenes. Part 18. Insertion of glycosylidene carbenes into the Sn-H bond of tributyl- and triphenylstannane: a synthesis of stannoglycosides.* Helv. Chim. Acta, 1994. **77**, 1430-1440.

29. Tsubomura, T., Ogawa, M., Yano, S., Kobayashi, K., Sakurai, T., and Yoshikawa, S., *Highly active antitumor platinum(II) complexes of amino sugars.* Inorg. Chem., 1990. **29**, 2622-2626.

30. Ferreira, C.L., Ewart, C.B., Barta, C.A., Little, S., Yardley, V., Martins, C., Polishchuk, E., Smith, P.J., Moss, J.R., Merkel, M., Adam, M.J., and Orvig, C., *Synthesis, structure, and biological activity of ferrocenyl carbohydrate conjugates.* Inorg. Chem., 2006. **45**, 8414-8422.

31. Ferreira, C.L., Ewart, C.B., Bayly, S.R., Patrick, B.O., Steele, J., Adam, M.J., and Orvig, C., *Glucosamine conjugates of tricarbonylcyclopentadienyl rhenium(I) and technetium(I) cores.* Inorg. Chem., 2006. **45**, 6979-6987.

32. Tanase, T., Mano, K., and Yamamoto, Y., *Synthesis and characterization of copper(II) complexes containing N-glycoside ligands and their use in catalytic epoxidation of olefins.* Inorg. Chem., 1993. **32**, 3995-4003.

33. Henderson, W., Nicholson, B.K., and Tiekink, E.R.T., *Synthesis, characterisation, supramolecular aggregation and biological activity of phosphine gold(I) complexes with monoanionic thiourea ligands.* Inorg. Chim. Acta, 2006. **359**, 204-214.

34. Kilpin, K.J., Linklater, R.A., Henderson, W., and Nicholson, B.K., *Synthesis and characterisation of isomeric cycloaurated complexes derived from the iminophosphorane $Ph_3PNC(O)Ph$.* Inorg. Chim. Acta, 2010. **363**, 1021-1030.

35. Farina, V., Reeves, J.T., Senanayake, C.H., and Song, J.J., *Asymmetric synthesis of active pharmaceutical ingredients.* Chem. Rev., 2006. **106**, 2734-2793.

36. Ariëns, E.J., *Stereochemistry, a basis for sophisticated nonsense in pharmacokinetics and clinical pharmacology.* Eur. J. Clin. Pharmacol., 1984. **26**, 663-668.

37. Brown, H.C., Park, W.S., and Cho, B.T., *Potassium 9-O-(1,2:5,6-Di-O-isopropylidene-α-D-glucofuranosyl)-9-boratabicyclo[3.3.1]nonane. A new, effective chiral borohydride reagent.* J. Org. Chem., 1986. **51**, 1934-1936.

38. Pàmies, O., Diéguez, M., Net, G., Ruiz, A., and Claver, C., *Iridium complexes containing the first sugar dithioether ligands. Application as catalyst precursors in asymmetric hydrogenation.* J. Chem. Soc., Dalton Trans., 1999. **19**, 3439-3444.

39. Borriello, C., Cucciolito, M.E., Panunzi, A., Ruffo, F., and Saporito, A., *A hydrophillic chiral diamine from D-glucose in the Rh(I) catalysed asymmetric hydrogenation of acetophenone.* Inorg. Chem. Commun., 2003. **6**, 1081-1085.

40. Buisman, G.J.H., Martin, M.E., Voss, E.J., Klootwijk, A., Kamer, P.C.J., and van Leeuwen, P.W.N.M., *Rhodium catalysed asymmetric hydroformylation with diphosphite ligands based on sugar backbones.* Tetrahedron: Asymm., 1995. **6**, 719-738.

41. RajanBabu, T.V. and Casalnuovo, A.L., *Electronic effects in asymmetric catalysis: enantioselective carbon-carbon bond forming processes.* Pure Appl. Chem., 1994. **66**, 1535-1542.

42. Borriello, C., Litto, R.D., Panunzi, A., and Ruffo, F., *A supported Mn(III) catalyst based on D-glucose in the asymmetric epoxidation of styrenes.* Inorg. Chem. Commun., 2005. **8**, 717-721.

43. Borriello, C., Litto, R.D., Panunzi, A., and Ruffo, F., *Mn(III) complexes of chiral 'salen' type ligands derived from carbohydrates in the asymmetric epoxidation of styrenes.* Tetrahedron: Asymm., 2004. **15**, 681-686.

44. Khiar, N., Suárez, B., and Fernández, I., *Mixed S/N and S/P/N ligands from carbohydrates: Synthesis and application in palladium-catalyzed allylic alkylation.* Inorg. Chim. Acta, 2006. **359**, 3048-3053.

45. Storr, T., Thompson, K.H., and Orvig, C., *Design of targeting ligands in medicinal inorganic chemistry.* Chem. Soc. Rev., 2006. **35**, 534-544.

46. Moats, R.A., Fraser, S.E., and Meade, T.J., *A "smart" magnetic resonance imaging agent that reports on specific enzymatic activity.* Angew. Chem. Int. Ed., 1997. **36**, 726-728.

47. Duimstra, J.A., Femia, F.J., and Meade, T.J., *A gadolinium chelate for detection of β-glucuronidase: A self-immolative approach.* J. Am. Chem. Soc., 2005. **127**, 12847-12855.

Chapter Two

Sugar thioureas as neutral ligands

2.1 Thioureas as ligands

Thioureas are compounds with the general formula $R_1R_2N(C=S)NR_3R_4$, and are analogous to ureas with the oxygen replaced with sulfur. Thioureas are very versatile ligands capable of acting as neutral [1], monoanionic [2] or dianionic ligands [3], Figure 2.1. They have been widely studied for many applications including liquid-liquid extraction, and pre-concentration and separation of platinum group metals (PGMs) and as sequestering agents for copper sulfides and mercury. Several drugs have the thiourea functional group such as sulfathiourea which is an antibacterial agent. The sulfur atom is very soft and readily forms complexes with soft metals such as Au [4] and Hg [5], although it can also bond to harder metals such as Fe [6] and Zn [7].

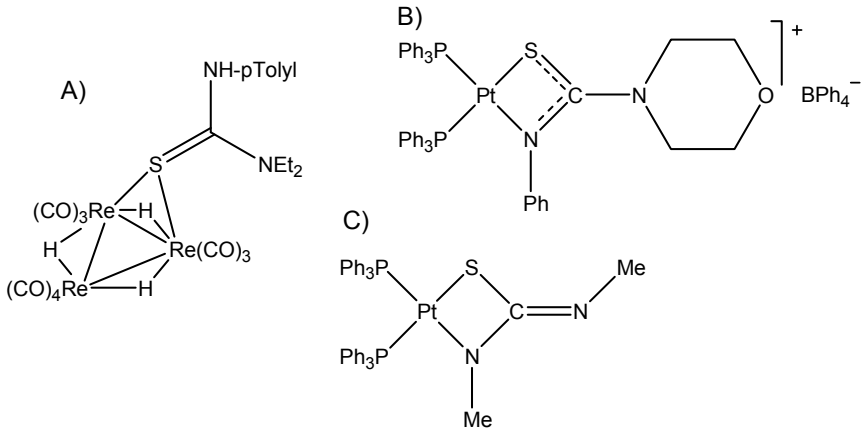

Figure 2.1 *Binding modes of thioureas; A) Neutral [1]; B) Monoanionic [2]; C) Dianionic [3].*

2.1.1 Benzoyl thioureas as ligands

Benzoyl based thioureas have been extensively studied as neutral ligands to a wide array of metals, including Pt, Pd, Hg, Cu, Ni, Co. The most important factor in their coordination is the potential to form an intra-molecular hydrogen-bond. In *N*-alkyl-*N*´-benzoyl thioureas a hydrogen-bond is formed between the thioamide proton (HN1) and the carbonyl, which forms a flat six-membered ring, Figure 2.2. For *N*,*N*-di-alkyl-*N*´-benzoyl thioureas this hydrogen-bond cannot occur, Figure 2.2. This can be clearly seen in a comparison of the crystal structures of *N*-propyl-*N*´-benzoyl thiourea [8], **1**, and *N*,*N*-di-*n*-propyl-*N*´-(2-chlorobenzoyl)-thiourea [9], Figure 2.3, where for the latter compound the six-membered ring has been twisted, bringing the C=S group towards the carbonyl.

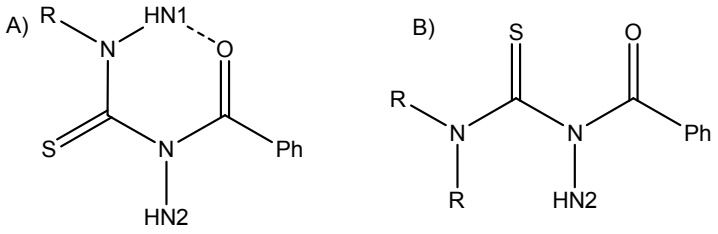

Figure 2.2 *A) An N-alkyl-N´-benzoyl thiourea showing the intra-molecular hydrogen-bond between the carbonyl and HN1; B) An N,N-di-alkyl-N´-benzoyl thiourea with no intra-molecular hydrogen-bond.*

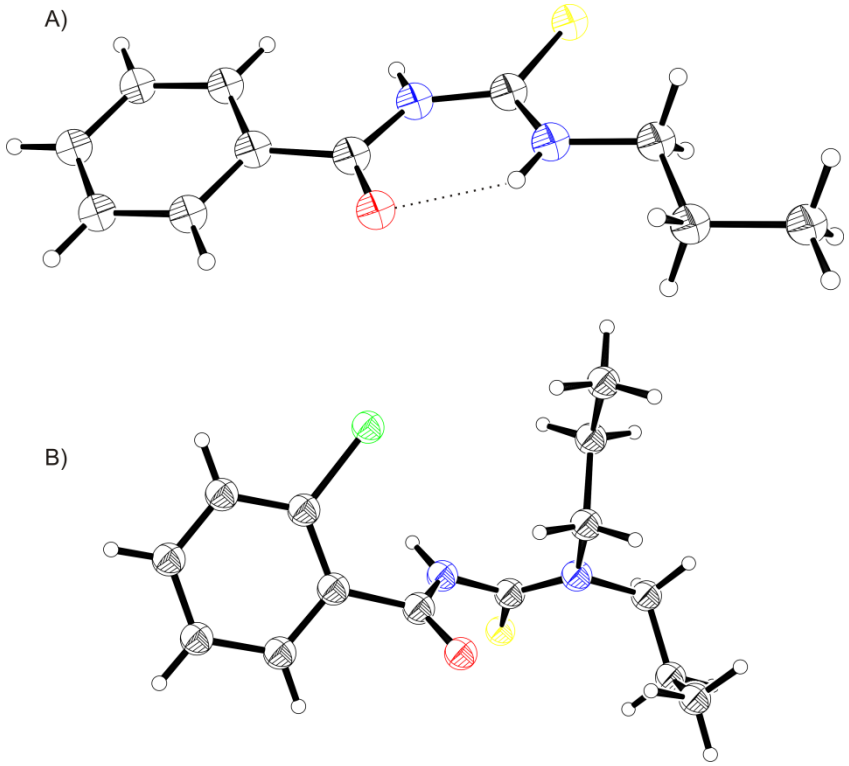

Figure 2.3 *Comparison of the geometry of N-alkyl- and N,N-di-alkyl-N´-benzoyl thioureas. A) **1** [8]; B) N,N-di-n-propyl-N´-(2-chlorobenzoyl)-thiourea; only one of the two independent structures from the unit cell is shown [9].*

Because the *N*-alkyl thioureas are locked into an internal six membered ring, they strongly favour being monodentate ligands through the sulfur atom, while the *N*,*N*-di-alkyl thioureas prefer to act as bidentate ligands coordinating through the sulfur and carboxyl oxygen with concomitant loss of the HN2 proton to form an anionic ligand. A comparison of the two different bonding modes is shown in Figure 2.4.

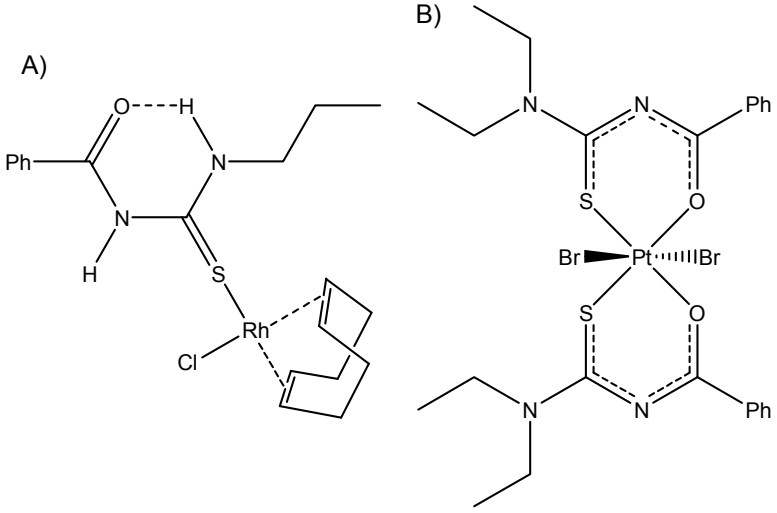

Figure 2.4 *Comparison of the different bonding modes for N-alkyl- and N,N-di-alkyl-N´-benzoyl thioureas; A) Neutral thiourea coordinating though the sulfur atom [10]; B) Monoanionic thiourea coordinating through the sulfur and oxygen atoms [11].*

1 has been widely studied as a neutral ligand. Figure 2.5 shows **1** and examples of complexes it forms. Neutral complexes with the thiourea coordinated through the sulfur atom have been reported with palladium [12], copper [12], rhodium [10] and platinum [13]. It shows the features that are expected when an *N*-alkyl-*N´*-benzoyl thiourea is coordinated to a metal. The thiourea acts as a monodentate ligand, and coordinates to the metals through the sulfur atom. Crystal structures of different complexes show that the intra-molecular hydrogen-bond is still present in the complexes, and that the HN2 proton forms a hydrogen-bond to the halide on the metal [10, 12-14].

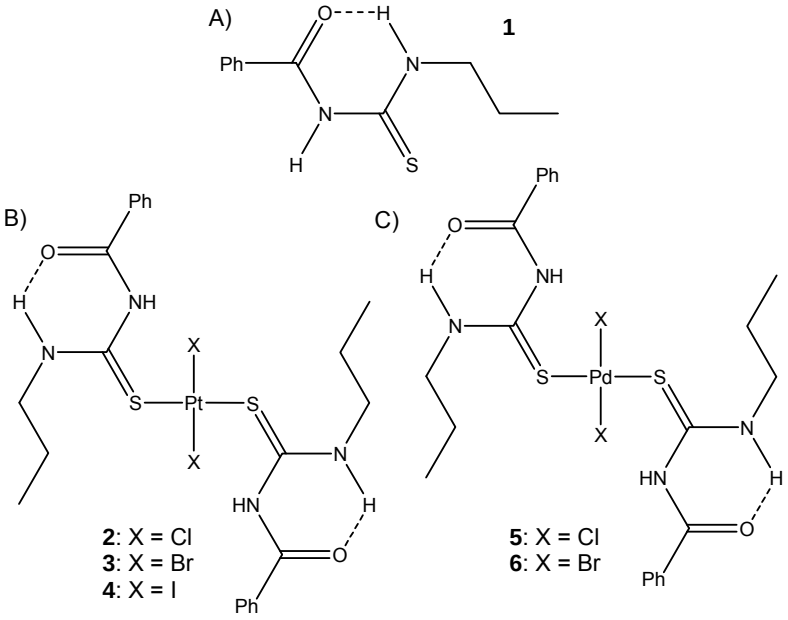

Figure 2.5 *1 and complexes it forms; A) **1**; B) **2-3**, Platinum complexes [14]; C) **5-6**, Palladium complexes [14].*

Acyl thioureas act in a similar fashion to benzoyl thioureas, with the carbonyl acting as the donor for the hydrogen-bond, Figure 2.6. *N*-(4-methylphenyl)-*N*'-ethoxycarbonyl-thiourea forms complexes with copper [15]. Related examples are *N*-phosphorylated thioureas, with the P=O group producing the same six-membered ring as the benzoyl thioureas [16].

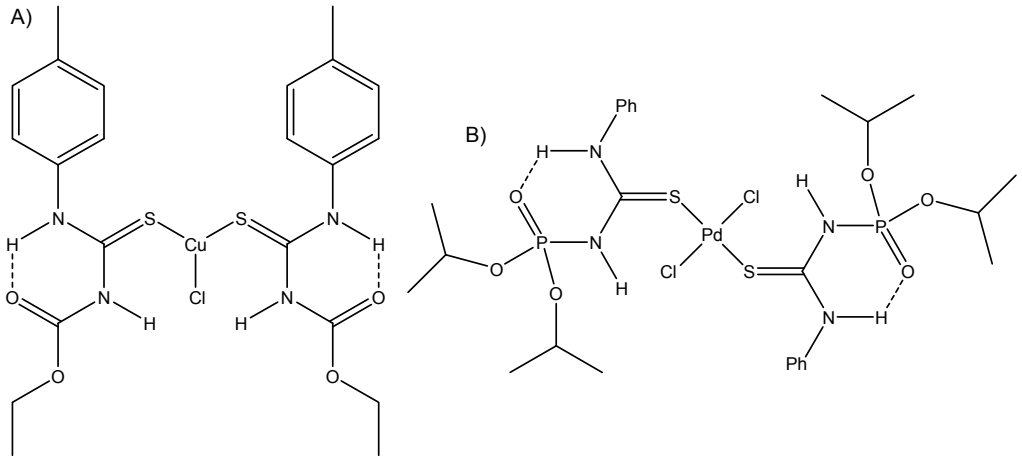

Figure 2.6 *Examples of acyl and related thioureas with similar features as benzoyl thioureas; A) Ethoxycarbonyl thiourea copper(I) complex [15]; B) N-phosphorylated thiourea palladium complex [16].*

2.2 Sugar thioureas

Sugars with a thiourea group are well established with many examples in the literature. The thiourea group has been used to link a series of disaccharides into a cyclic structure [17], Figure 2.7. Closely related thiosemicarbazones have been made [18], Figure 2.7. Sugar thioureas have been studied for a variety of reasons such as biological activity, for example they can act as *N*-acetyl-β-D-hexosaminidase inhibitors [19]. They are also used as precursors to ureas by desulfurization of the thiourea with HgO [20, 21], which avoids the use of phosgene.

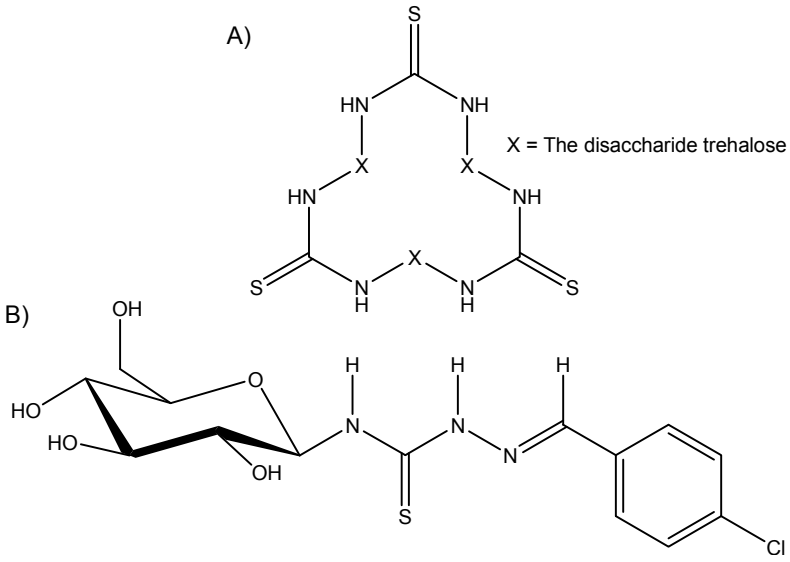

Figure 2.7 *A) Cyclic sugar with thiourea linkers [17]; B) Example of a sugar thiosemicarbazone [18].*

While there are a large number of sugar derived thioureas, much less is known about their chemistry as coordination ligands. The thiourea group is often used merely as a way of linking the sugar to another functional group which coordinates to the metal. For example sugars have been linked via a thiourea to a chelating group that was used to bind europium [22], as well as a cyclam which bound Cu^{2+}, Co^{2+}, Ni^{2+} and Zn^{2+} [23], Figure 2.8. Ferrocene has been linked to sugars via a thiosemicarbazone [24].

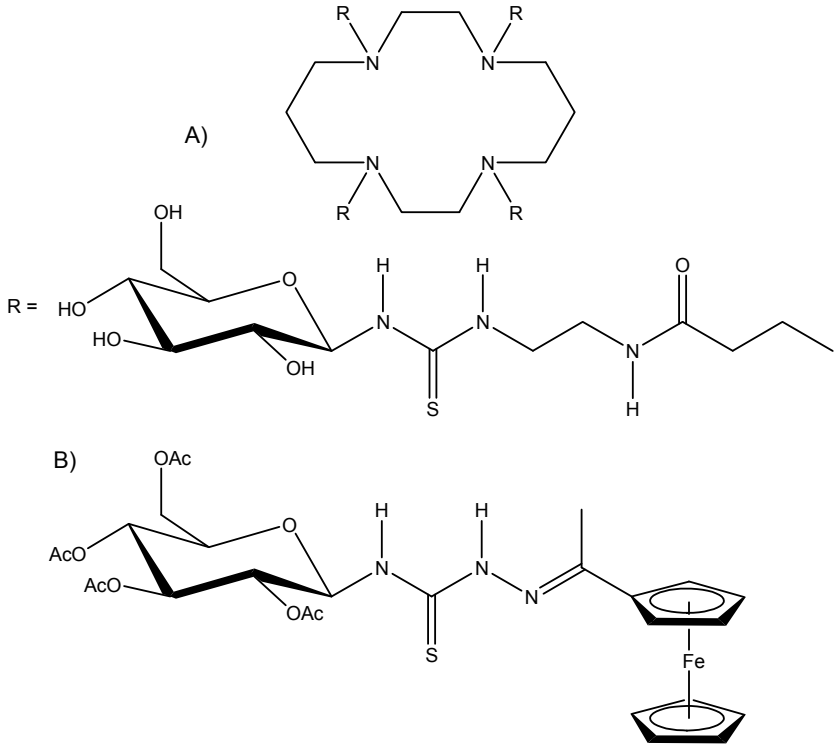

Figure 2.8 *A) Cyclam used to bind Cu^{2+}, Co^{2+}, Ni^{2+} and Zn^{2+} [23]; B) A sugar linked to ferrocene via a thiosemicarbazone [24].*

There are very few compounds where the thiourea is a neutral ligand bonding directly to the metal through the sulfur atom, and to our knowledge a German group has published the only paper on this [25]. They took the thiourea shown in Figure 2.9 and used it as a neutral ligand to form complexes with $[Cp^*MCl_2]_2$ (M = Rh or Ir), $PdCl_2$, $PtCl_2$, $(Me_2S)AuCl$ and $[Pd(C,N\text{-DMAB})Cl]_2$ [25]. As discussed in more detail in Chapter Three there is little more known about sugar thioureas as anionic ligands, with only two previous papers.

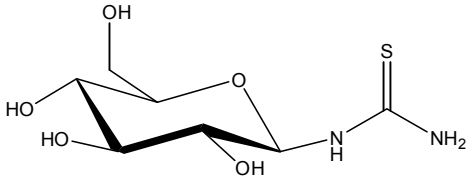

Figure 2.9 *Sugar thiourea used as a neutral ligand to form metal complexes [25].*

In light of the lack of knowledge of the properties of coordination to metals via the sulfur atom of sugar thioureas, a number of acyl sugar thioureas were synthesised. Once in hand their coordination to metals as neutral ligands was investigated. A non-acyl sugar thiourea was synthesised to see if it was similar to the acyl sugar thiourea in its coordination behaviour.

2.2.1 Synthesis of sugar thioureas

To investigate their properties as ligands, carbohydrates with thiourea functionality were required. Thioureas can be synthesised by a number of different routes. One common method is the reaction of an amine with an isothiocyanate with the addition reaction giving the desired thiourea. This pathway requires an amino sugar (a sugar with a hydroxyl group replaced with an amine). While amines can be introduced synthetically into a sugar, glucosamine is a ready source of a natural amino sugar. It is found in chitin which is the basis for the exoskeletons of crustaceans and insects and is the precursor to all amino sugars in nature [26]. To use glucosamine in reactions it is preferred that the hydroxyl groups are acetylated while the amine is still free. 1,3,4,6-tetra-*O*-acetyl-β-D-glucosamine, **7**, is conveniently prepared by protection of the amino group by conversion to a benzylidene with 4-methoxybenzaldehyde; acetylation followed by deprotection with hydrochloric acid gives **7**·HCl [27]. This is readily converted to the free amine **7**, Scheme 2.1.

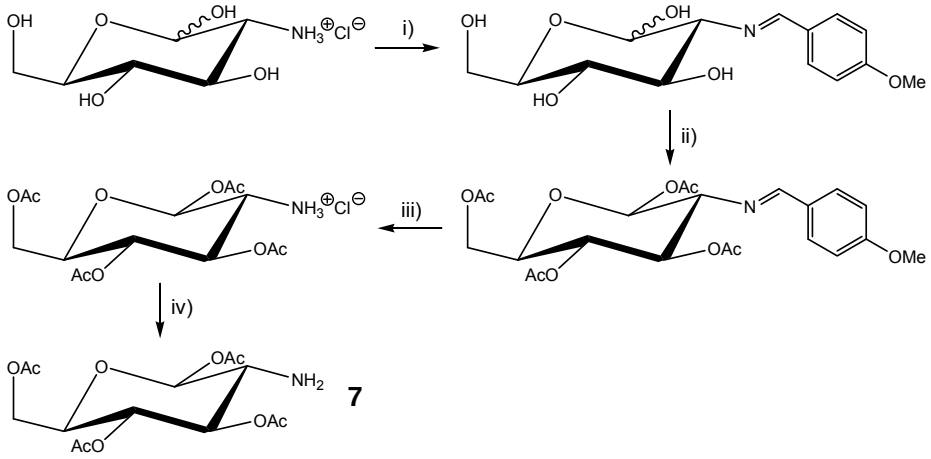

Scheme 2.1 *Protection of glucosamine with acetate groups. Reagents and conditions: i) NaOH, 4-methoxybenzaldehyde, H_2O; ii) Pyridine, acetic anhydride; iii) Acetone, HCl; iv) $NaHCO_3$, H_2O [27].*

2.2.2 Sugar acyl thioureas

Benzoyl chloride reacts with potassium thiocyanate in refluxing acetone to form benzoyl isothiocyanate, which can be reacted with **7** to form the sugar thiourea, **8a** [28, 29], Figure 2.10. The overall general reaction is shown in Scheme 2.2.

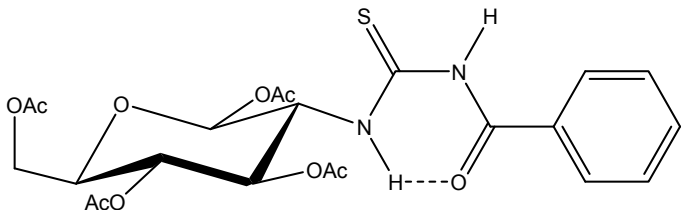

Figure 2.10 *Sugar benzoyl thiourea **8a**.*

To investigate different acyl thioureas other aromatic acyl isothiocyanates were used. The three that were chosen were *p*-nitrobenzoyl, 2-furoyl and 2-thiophene carbonyl isothiocyanate. These were of particular interest as they have additional functionality. All were accessible from the reaction of the appropriate acid chloride with a thiocyanate salt; *p*-nitrobenzoyl chloride was refluxed in

acetonitrile with potassium thiocyanate [30], while 2-furoyl chloride and 2-thiophene carbonyl chloride were refluxed in acetone with ammonium thiocyanate [30, 31]. These isothiocyanates reacted readily as above to form the novel thioureas **8b**, **8c** and **8d**.

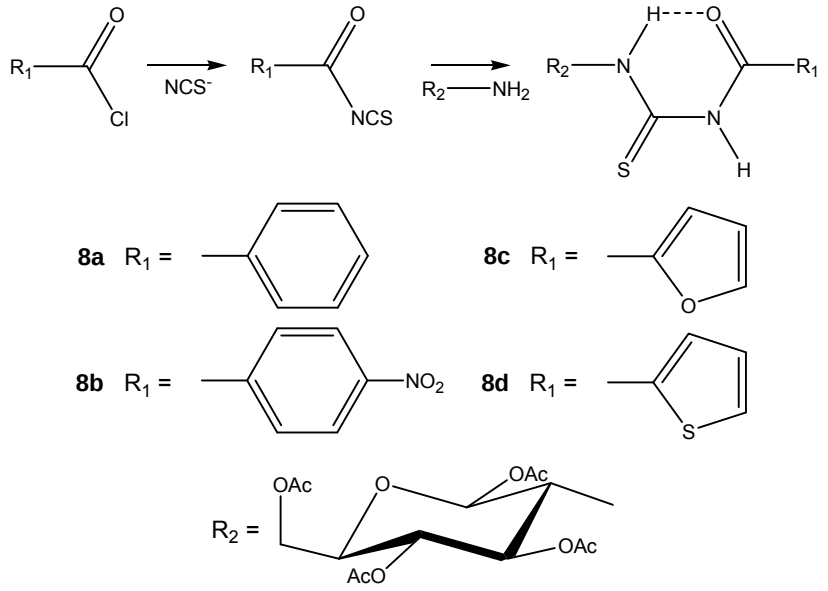

Scheme 2.2 *General reaction scheme for synthesising protected acyl thioureas.*

The benzoyl thiourea, **8a**, used for this work has been made previously, as well its analogue where the thiourea is attached to the C1 carbon of the sugar [32, 33]. All of the thioureas in this work are on C2. In 1966 2-Furoyl and 2-thiophene carbonyl isothiocyanate were reacted with unprotected glucosamine [31]. While the 2-furoyl thiourea was formed, 2-thiophene carbonyl isothiocyanate reacted to give the amide substitution product rather than the desired thiourea addition product [31], Scheme 2.3. These are the only examples of the use of these two isothiocyanates with sugars in the literature. No reaction of *p*-nitrobenzoyl isothiocyanate with a sugar has been reported.

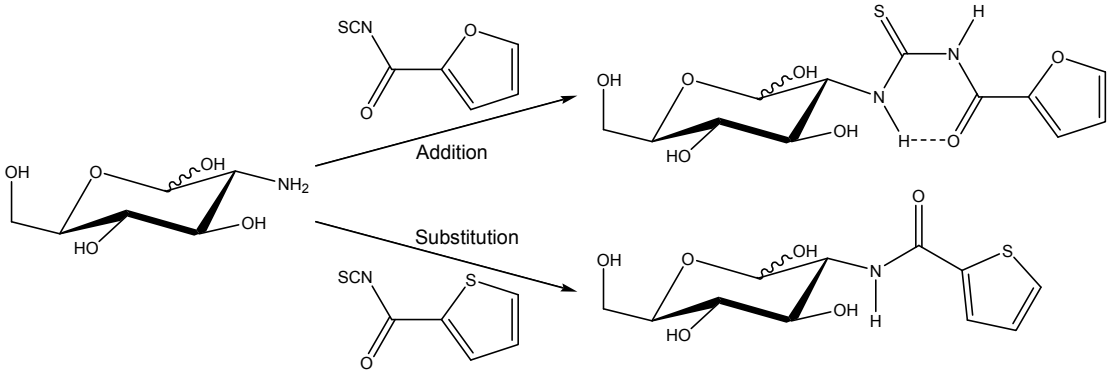

Scheme 2.3 *Previous reaction of 2-furoyl and 2-thiophene carbonyl isothiocyanate with unprotected glucosamine and the difference in the products [31].*

As mentioned above benzoyl thioureas have been widely studied as ligands. Much less is known for thioureas derived from the other three acyl groups studied in this work. While non-sugar thioureas have been made with the *p*-nitro benzoyl and 2-thiophene carbonyl groups there are no metal complexes reported using them as neutral monodentate ligands. For 2-furoyl thioureas as neutral ligands the only examples are complexes with cadmium and mercury halides such as the CdL_4Cl_2 example shown in Figure 2.11 [34].

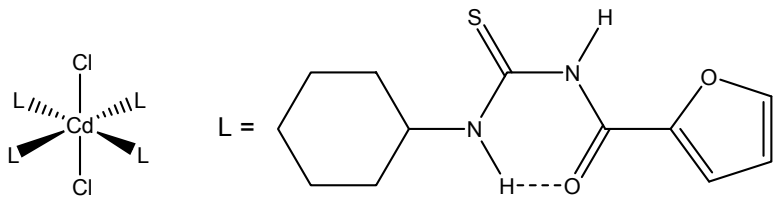

Figure 2.11 *Example of a 2-furoyl thiourea cadmium complex with S-bonded thioureas [34].*

2.2.2.1 ESI-MS of the acyl thioureas

High resolution electrospray ionisation mass spectrometry (ESI-MS) was carried out on all the compounds in this work. The spectra of the thioureas showed

similar ions, with $[M+Na]^+$, $[M+K]^+$ and $[2M+Na]^+$ ions being observed (where M = each thiourea). These ions are expected as there is generally plenty of background Na^+ and K^+ in the system to form these adducts. See Appendix One for ESI-MS experimental details.

2.2.2.2 ^{1}H and ^{13}C NMR assignment of the acyl thioureas

Different NMR experiments were used to characterise the compounds in this work. Appendix Two describes in detail the assignment of one compound to illustrate the NMR procedures and how compounds were characterised. The ^{1}H NMR spectrum of **8a** was as previously reported [29] except that the aromatic signals were now able to be assigned. Figure 2.12 shows the labelling scheme while Figure 2.13 shows a portion of the ^{1}H NMR spectrum of **8a**.

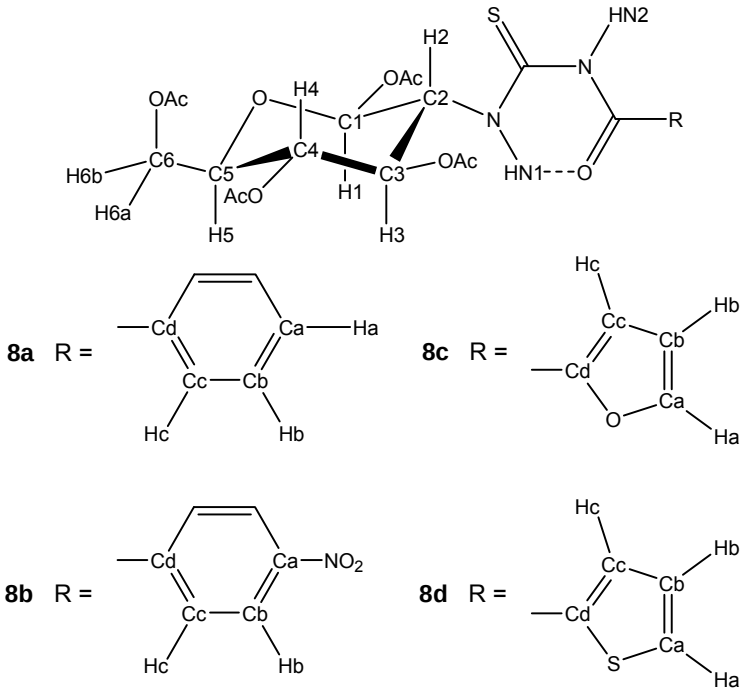

Figure 2.12 *^{1}H and ^{13}C NMR labelling scheme for the acyl thioureas **8a-d**.*

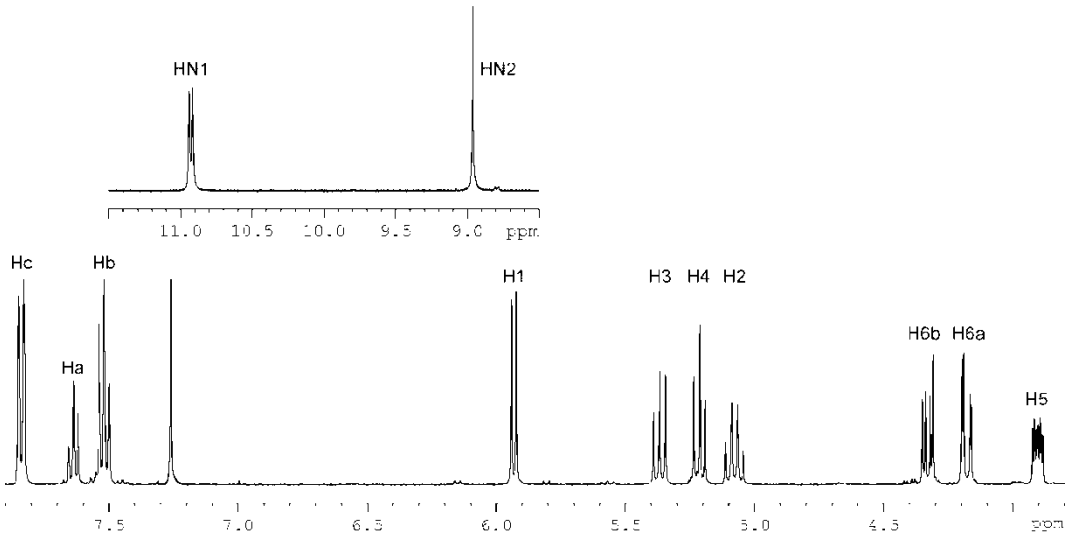

Figure 2.13 *Portion of the ^{1}H NMR spectrum of **8a**; inset shows the N–H signals.*

There are several signals that convey the most information. The first are the N–H protons, HN1 and HN2. HN1 is a doublet that is far downfield (10.92 ppm). Since it is involved in an intramolecular hydrogen-bond the carbonyl oxygen withdraws a lot of electron density causing the proton to be highly deshielded and shifted far downfield. This deshielding effect from a hydrogen-bond is seen in related molecules such as the enol form of acetylacetone, where the proton that is involved in an intramolecular hydrogen-bond with the carbonyl comes at ~15.4 ppm [35]. Anything that affects the hydrogen-bond will have a large effect on the chemical shift.

HN1 is a doublet, split by H2 with a coupling constant of 9.2 Hz. Based on this coupling constant H2 and HN1 are likely to have the anti conformation. The six-membered ring prevents rotation around the N1–C15 bond, so only rotation around the C2–N1 bond can occur. A previous determination of **8a** proposed that because of this data the thiourea has the Z,E,Z-anti conformation [28], Figure 2.14. As shown below by a X-ray structure determination (Section 2.2.4) of **8a** this proposal was correct.

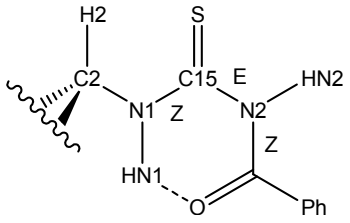

Figure 2.14 *Diagram showing the six-membered ring the thiourea **8a** forms and the anti conformation H2 and HN1 have giving the Z,E,Z-anti-conformation.*

The other proton, HN2, is a singlet and while it is not as far downfield as HN1 it still has a large chemical shift (8.97 ppm). These signals are a clear sign of how the thiourea is bonding; if both are present in the complex it is a neutral ligand, while if one is missing it must be monoanionic.

The other important signals are ones on the sugar portion of the molecule. The two that are most important are H1 and H2. Since H2 is now adjacent to a thiourea rather than an amine there is a large downfield shift of approximately 2 ppm compared to glucosamine. Since H2 is the closest to the thiourea it changes the most of the sugar signals if something happens on the thiourea. The other important sugar signal is H1; generally it has the highest chemical shift of the sugar signals so is easily identified. It also gives information about which anomer the D-glucose residue has formed, a coupling constant of ~3 Hz is α while ~8 Hz is β for D-glucose, Figure 2.15. All of the acetylated sugar thioureas were the β anomers. This was expected since the protection of the amine group of glucosamine (Section 2.2.1) only produces the β anomer upon acetylation and this configuration remains through all the reactions. If the unprotected version of **8a** is acetylated a mixture of anomers is formed [29].

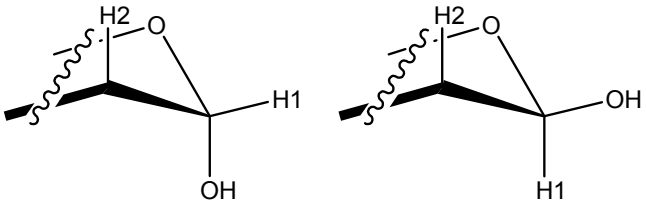

α: J_3 H1-H2 ~3 Hz β: J_3 H1-H2 ~8 Hz

Figure 2.15 *Comparison of α and β anomers of D-glucose and the approximate J_3 coupling constants of H1 to H2.*

As would be expected for parts of the sugar more removed from the thiourea functional group there is little change in H6a, H6b, H5, H4 and H3 as compared to glucosamine and little change is seen for them no matter what happens on the thiourea. Resolution enhancement (see Appendix Two) helps to determine the multiplicity of the carbohydrate and aromatic signals and what is seen for **8a** is typical for the rest of the thioureas and any complexes that form. Generally for the aromatic signals, only Hc undergoes shifts if a complex has formed as would be expected since it is the closest to the thiourea. After resolution enhancement Ha is seen as a triplet of triplets and Hb and Hc are multiplets.

The ^{13}C NMR spectrum of **8a** matched the literature values [29], shown in Figure 2.16. The ^{13}C NMR signals were much less diagnostic than the ^{1}H NMR signals and showed fewer and smaller shifts upon the formation of a complex. The carbons that changed the most were C2, C=S and the C=O of the amide as would be expected since they are the closest to the coordinating sulfur.

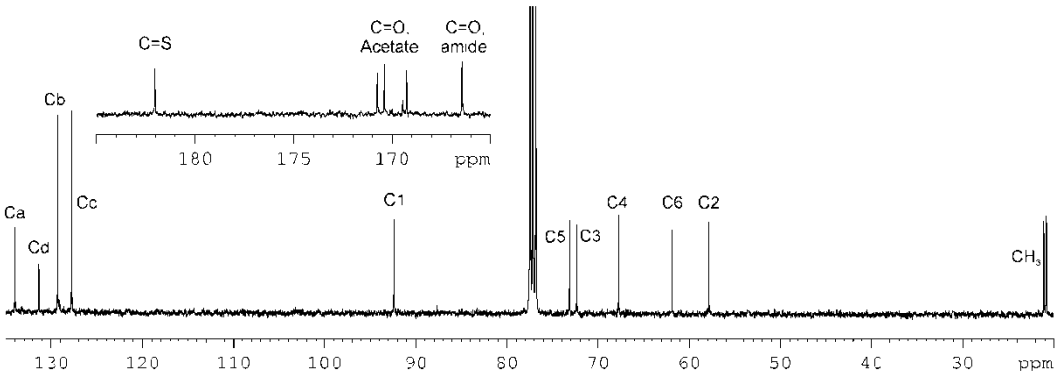

Figure 2.16 *^{13}C NMR spectrum of **8a**; inset shows the carbonyl and C=S carbons.*

The ^{1}H NMR spectra of **8b-d**, showed many of the same features as **8a**. Figure 2.17 is a comparison of the ^{1}H NMR spectra of **8a-d**, and Table 2.1 summarises selected chemical shifts and coupling constants for **8a-d**. The N–H and carbohydrate signals were in similar positions to **8a**, with a slightly more upfield position for HN1 compared with **8a**. The coupling constants for HN1 of **8b-d** are slightly larger than for **8a**. The coupling constants suggest the thioureas have the Z,E,Z-anti conformation of **8a**.

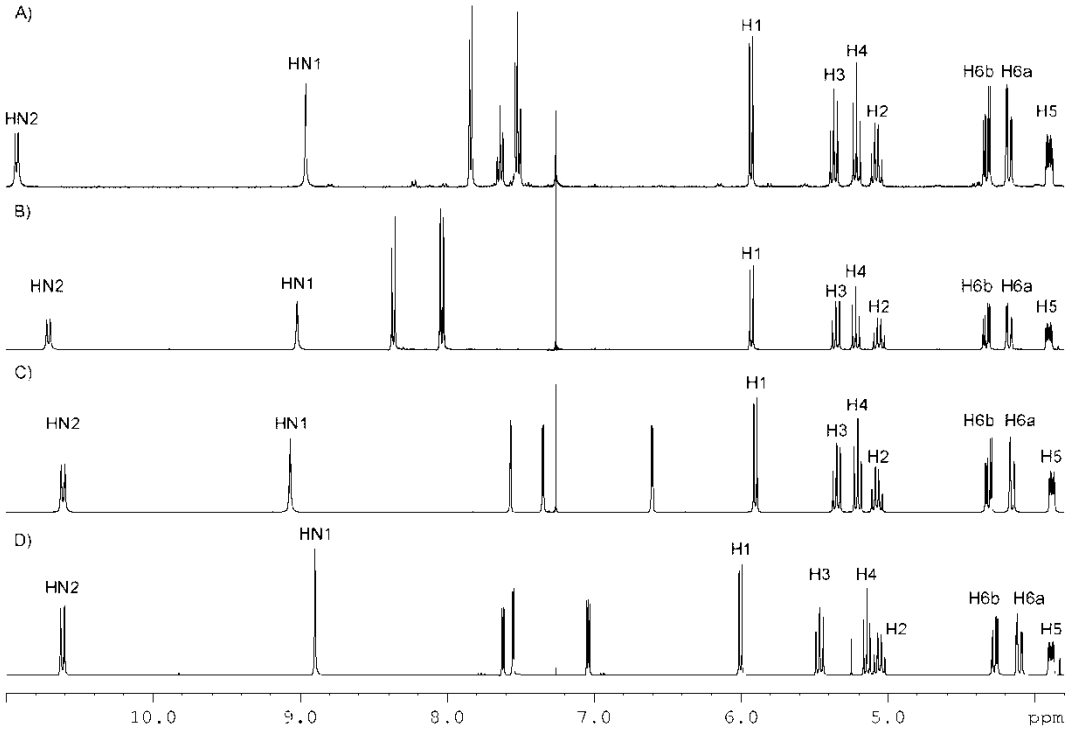

Figure 2.17 *Portion of the ^{1}H NMR spectrum comparing the acyl thioureas; A) **8a**; B) **8b**; C) **8c**; D) **8d**.*

	HN1	HN2	Hc	H2	C=S	C=O, amide	C2
8a	10.92, 9.2 Hz	8.97	7.82	5.08	182.0	166.5	57.9
8b	10.71, 9.4 Hz	9.02	8.04	5.06	181.3	164.5	58.0
8c	10.61, 9.5 Hz	9.07	7.35	5.07	181.6	156.4	57.9
8d	10.62, 9.5 Hz	8.90	7.55	5.06	181.5	160.5	57.8

Table 2.1 *Selected chemical shifts and coupling constants from the NMR spectra of the acyl thioureas **8a-d**.*

The major differences in the ^{1}H NMR spectra were in the aromatic region. In the aromatic region of **8b** there are now only two signals because of the replacement of the *para* proton with the nitro group which has also shifted the other two aromatic signals downfield, which appear as two doublets of triplets. They show virtual coupling which is why they produce a doublet of triplets rather than a doublet. **8c** and **8d** have similar patterns in the aromatic region, with doublets of

doublets for the three protons on the aromatic ring. The coupling constants for **8c** range from 0.8-3.6 Hz while for **8d** the range is 1.2-5.0 Hz. With the exception of the aromatic portion the ^{13}C NMR spectra of **8b-d** are similar to **8a**.

2.2.3 Unprotected sugar acyl thioureas

The reaction with benzoyl isothiocyanate can also be carried out using unprotected glucosamine. Since the amine is much more nucleophilic than the hydroxyl groups and water, the reaction can be carried out in a mixture of acetone and water. This produces the thiourea **8e** [28]. While this reaction is successful with benzoyl isothiocyanate, phenyl isothiocyanate cannot be used with unprotected sugars, since when the thiourea is formed it undergoes an intramolecular cyclisation that sees the anomeric hydroxyl group attack N2 forming a number of products, one of which is shown in Figure 2.18 [28].

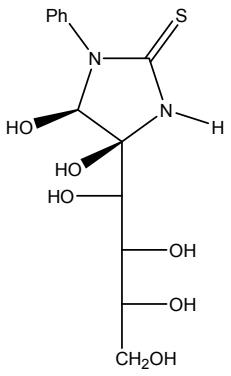

Figure 2.18 *One of the products formed when glucosamine is reacted with phenyl isothiocyanate [28].*

2.2.4 Crystal structures of 8a and 8e

Crystals of **8a** and **8e** suitable for single crystal X-ray diffraction were grown. **8a** was recrystallised by the slow evaporation of an ethanol solution, while **8e** was

recrystallised by the slow cooling of a hot solution of **8e** in a mixture of ethanol and water. General details of the structure solution and refinement are discussed in Appendix Three. Both form orthorhombic crystals, space group $P2_12_12_1$. For **8a** the asymmetric unit contains two independent molecules and Figure 2.19 shows the geometry of one of them. The two structures are very similar differing mainly in the orientation of the phenyl ring. Figure 2.20 shows the geometry of **8e**. Protons bound to carbon were placed using a riding model. The position of protons bound to nitrogen or oxygen atoms were found in a difference map. Their positions were allowed to refine and isotropic *U* values were constrained to 1.2 times the U_{eq} value of the atom they were bound to.

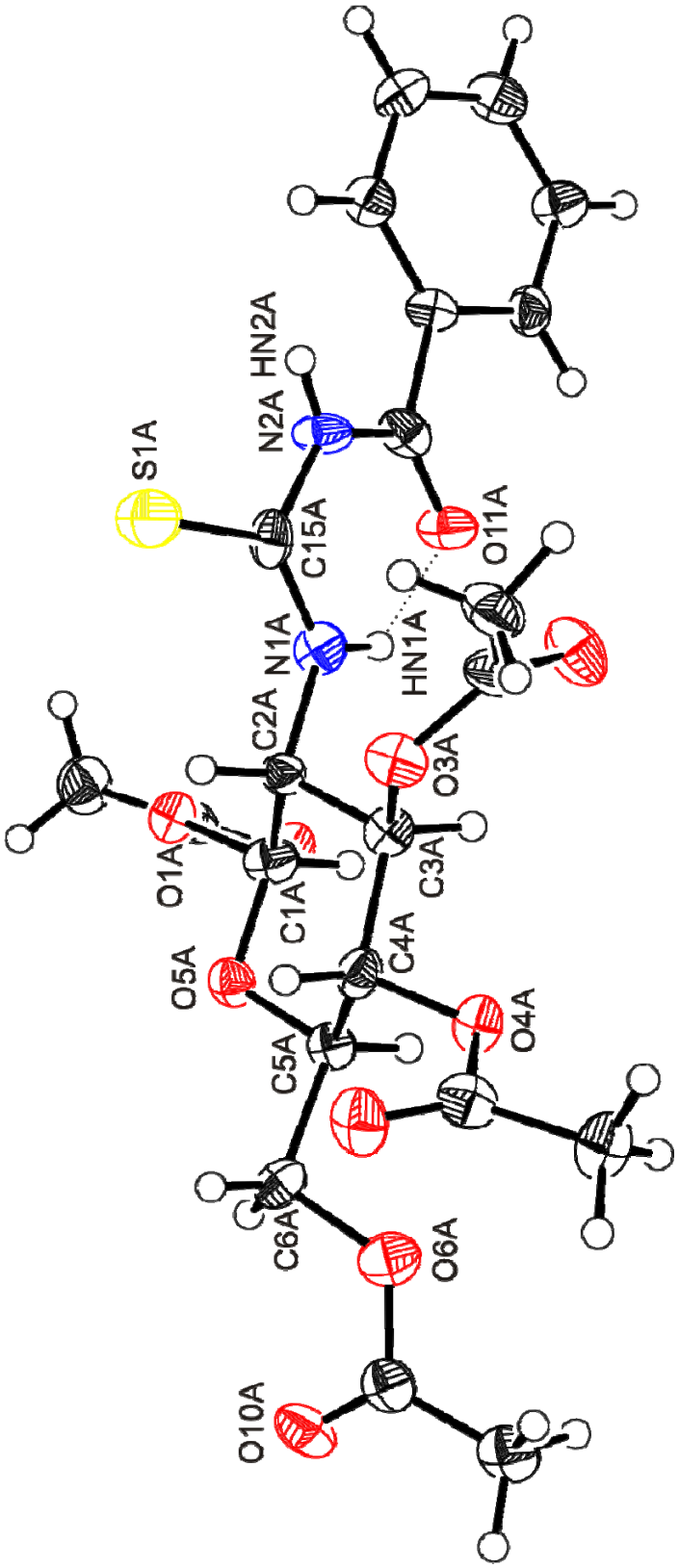

Figure 2.19 *The geometry of **8a** showing the atom labelling scheme and thermal ellipsoids at the 50% probability level. Only molecule A from the unit cell is shown.*

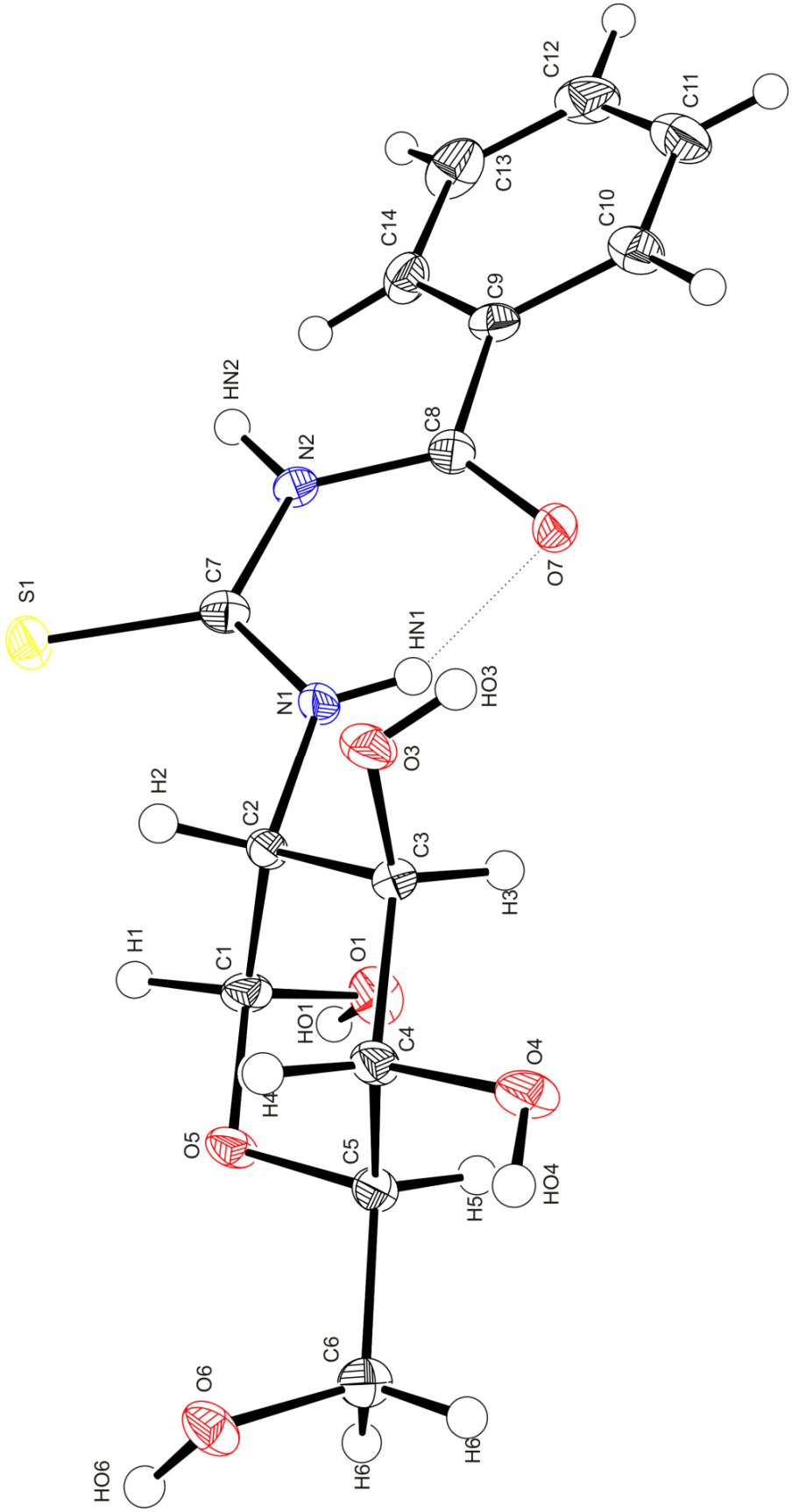

Figure 2.20 *The geometry of* ***8e*** *showing the atom labelling scheme and thermal ellipsoids at the 50% probability level.*

While crystal structures of sugars with thioureas on C1 are known, these structures are the first with the thiourea moiety on C2. Despite the differences between **8a** and **8e** there are common features between the two. Table 2.2 has selected bond lengths and angles for **8a** and **8e**, and are compared to the structure of **1** [8]. The three structures all show very similar bond lengths and angles.

	8a		**8e**	**1**
	Molecule A	**Molecule B**		
C=S	1.670(6)	1.669(6)	1.680(2)	1.678(4)
N1–C=S	1.316(8)	1.324(7)	1.319(3)	1.332(7)
N2–C=S	1.387(8)	1.402(8)	1.402(3)	1.392(5)
C=O, amide	1.216(7)	1.231(7)	1.234(3)	1.226(5)
C2–N1	1.453(8)	1.443(7)	1.458(3)	NA
S=C–N1	125.2(5)	126.7(6)	123.16(19)	124.1(3)
S=C–N2	118.9(5)	117.4(5)	119.78(18)	118.5(3)

Table 2.2 *Selected bond lengths (Å) and angles (°) of **8a**, **8e** and **1** [8].*

As discussed above published NMR evidence suggested that **8a** had an internal hydrogen-bond and a Z,E,Z-anti conformation [28]. The structure determination shows that both of these proposals were correct. There is an internal hydrogen-bond between HN1•••O11 of 2.08(6) Å and 1.92(6) Å for the A and B molecules respectively. The Z,E,Z-anti conformation can also be seen, the torsion angle for C2–N1–C15–S1 is 2.5(10)° and 1.7(9)° for the A and B molecules respectively. These features are also seen for **8e**, with an HN1•••O7 distance of 1.92(3) Å, similar to both bonds in **8a**. This compares with 1.80(6) Å for **1** [8]. The Z,E,Z-anti conformation is seen again with the C2–N1–C7–S1 torsion angle measuring 0.3(3)°. This conformation is also seen in the structure of a urea derivative of glucosamine in which the corresponding torsion angle is 1.2(9)° despite lacking the internal hydrogen-bond [36]. The internal hydrogen-bond locks the ring into

a rigid plane; a plane defined by N1, C15, S1, C16 and O11 for **8a** has a largest deviation of 0.077(4) Å for O11A and 0.018(5) Å for C15B for molecule A and B respectively, with a RMS deviation of 0.06 and 0.01 respectively. For **8e** the plane defined by N1, C7, S1, C8 and O7 has a largest deviation of 0.040(1) Å for O7, with a RMS deviation of 0.029. The phenyl ring is twisted out of plane with respect to the six-membered ring. The angle of the twist is 7.9(3)° and 33.1(2)° for molecule A and B respectively in **8a**, while in **8e** it is 21.9(1)°.

The definition of a hydrogen-bond is deceptively simple, being defined as the interaction between a proton donor group, A–H (where the proton is covalently bonded to A), and a proton acceptor group B [37]. However in practice deciding what counts as an interaction is more difficult. A previously well-accepted rule of thumb was that the A•••B distance was less than the sum of the van der Waals radii for A and B, but this was shown to be flawed with the hydrogen-bond continuing to be important past this threshold [38]. The minimum criteria for assigning a hydrogen-bond is that there is evidence of bond formation and that this new bond linking A–H and B specifically involves the hydrogen already bonded to A [38, 39]. On this basis for **8a** a further weak hydrogen-bond is seen between HN2 and the carbonyl oxygen from the acetate on O6 of the adjacent molecule. All the hydrogen-bonds for **8a** are summarised in Table 2.3, and Figure 2.21 shows the hydrogen-bonding network for molecule A.

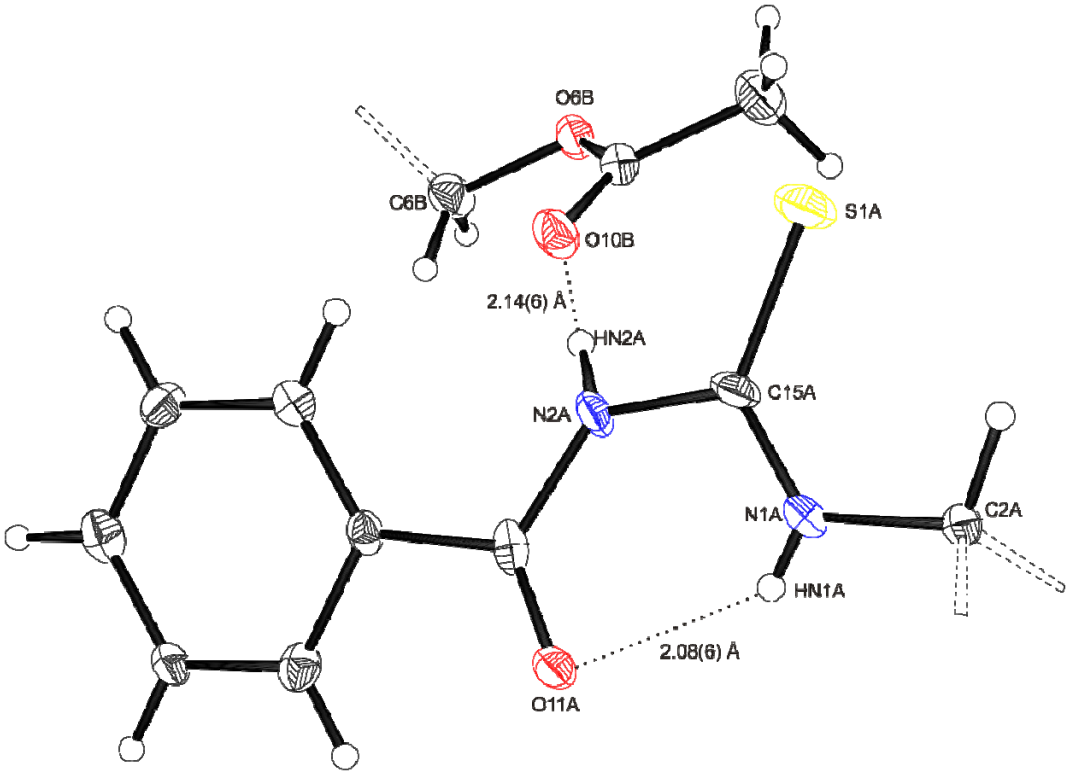

Figure 2.21 *Hydrogen-bonding network for molecule A of **8a** with e.s.d. values in parentheses.*

D–H•••A	d(D–H) (Å)	d(H•••A) (Å)	d(D•••A) (Å)	<(DHA) (°)
N1A–HN1A•••O11A	0.69(6)	2.08(6)	2.619(6)	136(8)
N1B–HN1B•••O11B	0.88(5)	2.14(6)	2.995(7)	165(5)
N2A–HN2A•••O10B^{i}	0.91(5)	1.92(6)	2.667(7)	138(5)
N2B–HN2B•••O10A^{ii}	0.90(5)	2.61(6)	3.277(7)	132(5)

Table 2.3 *Table of hydrogen-bond geometry data for **8a**.*

For **8e**, as well as the intramolecular hydrogen-bond between HN1 and the carbonyl oxygen, there is a large network of intermolecular hydrogen-bonding in the crystal as compared to **8a**, as would be expected for an unprotected sugar. Figure 2.22 shows the network of hydrogen-bonding, while Table 2.4 summarises the data. If a hydroxyl group is acting as an acceptor for a hydrogen bond as well as a donor, it is termed cooperative and forms a stronger hydrogen-bond than a hydroxyl group that only acts as an acceptor [40]. All hydroxyl groups in **8e**

except OH3 are cooperative. The H•••O distances in **8e** are slightly longer than the average distance of 1.805 Å found in a survey of neutron diffraction of carbohydrates [41]. There is a similarity in the hydrogen-bond that HN2 forms in the structures of **8a** and **8e**, with **8e** forming a hydrogen-bond to the O6 hydroxyl compared to the O6 acetate for **8a**. In the solid state **1** forms a dimer with a hydrogen-bond between HN2 and the sulfur atom of an adjacent molecule [8]. For **8e** the sulfur atom forms a hydrogen-bond to HO4 on an adjacent molecule, while the sulfur atoms in **8a** show no sign of hydrogen-bonds. This form of dimer is not seen for either **8a** or **8e** with other functional groups present acting as the acceptor for HN2.

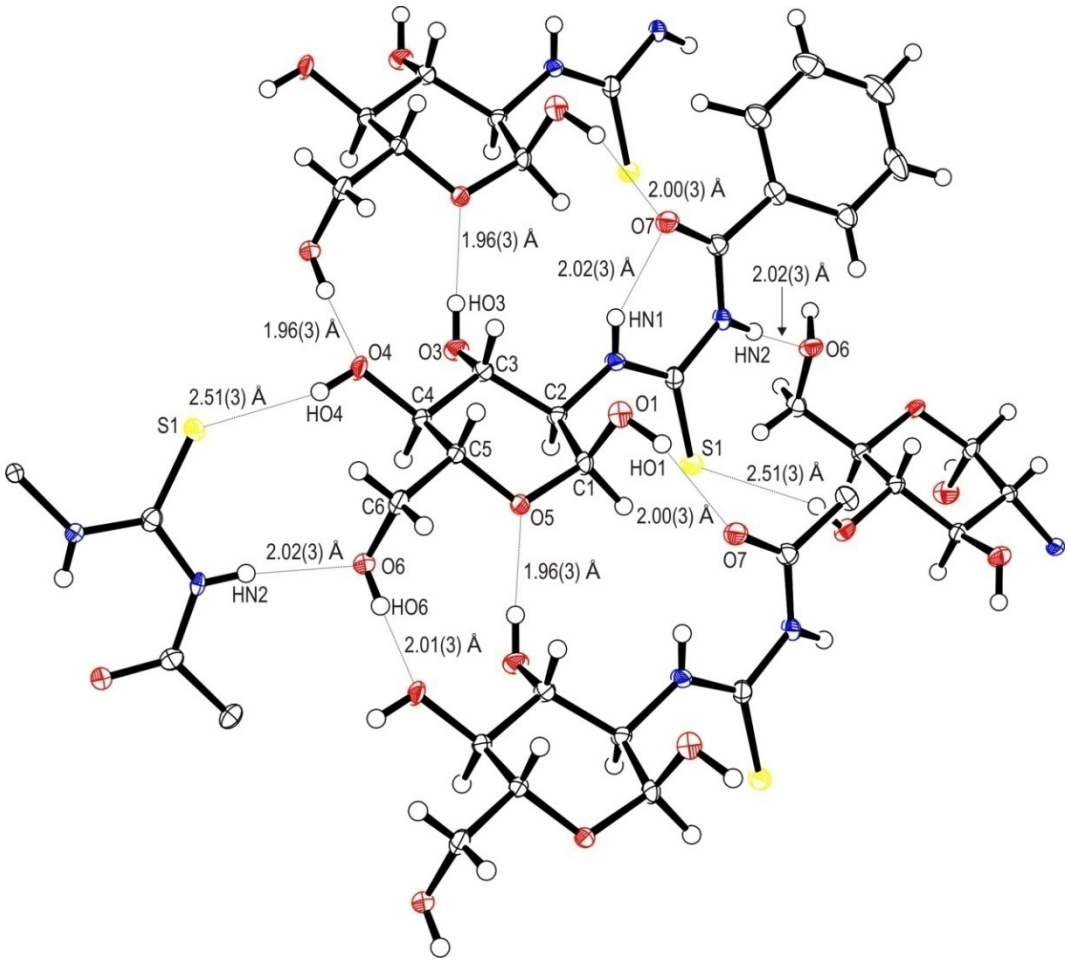

Figure 2.22 *Hydrogen-bond network in **8e** with e.s.d. values in parentheses.*

D–H•••A	d(D–H) (Å)	d(H•••A) (Å)	d(D•••A) (Å)	<(DHA) (°)
N1–HNA•••O7	0.81(3)	1.92(3)	2.623(3)	145(3)
N2–HNB•••O6^{i}	0.84(2)	2.02(3)	2.848(3)	168(3)
O1–HO1•••O7^{ii}	0.92(3)	2.00(3)	2.827(3)	149(2)
O3–HO3•••O5^{iii}	0.78(3)	1.96(3)	2.733(2)	172(3)
O4–HO4•••S1^{iv}	0.79(3)	2.51(3)	3.2571(2)	160(3)
O6–HO6•••O4^{ii}	0.82(3)	2.01(3)	2.791(2)	159(2)

Table 2.4 *Table of hydrogen-bond geometry data for **8e**.*

In both structures the glucopyranose ring is in the expected $^{4}C_{1}$ conformation. This is the most stable conformation as it places the groups on the sugar, particularly the acetylated hydroxymethyl, into equatorial positions which are more stable than axial positions [42]. A hydroxymethyl group can have one of three different conformations as shown in Figure 2.23 [42]. An equilibrium of the three conformations exists in solution, while in the solid state only one conformation is expected. Looking at **8a** the two independent molecules have different conformations for their acetylated hydroxymethyl groups; molecule A has the *tg* conformation while molecule B has the *gg* conformation, Figure 2.20 shows the A molecule. In **8e** the hydroxymethyl group has adopted the *gg* conformation.

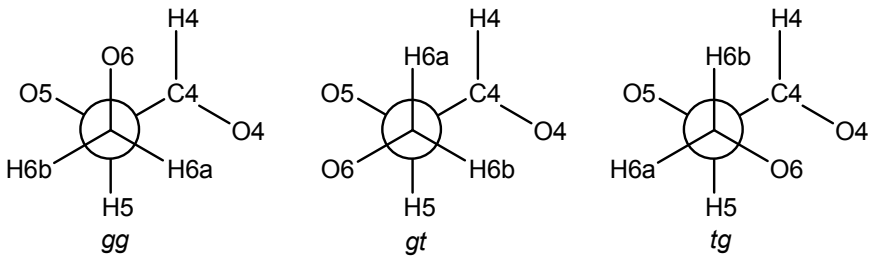

Figure 2.23 *The three conformations that a hydroxymethyl group can adopt.*

One difference between the structures is in the anomer they form. **8a** forms the β anomer, while **8e** has formed the α anomer. The β anomer is seen for **8a** since **7** has the β anomer and this is retained upon formation of the thiourea. **8e** was poorly soluble in water; a sample was left to stand in D_2O, and after 48 hours the supernatant was removed and analyzed by ^{1}H NMR spectroscopy. The signals were very weak but with a large number of scans the anomeric protons could be seen. A mixture of the two anomers was observed in the ratio 69:31 (α:β). In this and subsequent spectra the two anomers could be identified by their coupling constants (~3.6 Hz for α, ~8.4 Hz for β). To see if only the α anomer had crystallised out, the ^{1}H NMR spectrum of recrystallised **8e** was recorded in DMSO since mutarotation between the anomers will not occur in this solvent [43]; only the α anomer was seen. If **8e** was dissolved in a 1:1 mixture of D_2O and DMSO the β anomer appeared; after standing for 24 hours the ratio was 83:17 (α: β). Leaving it for a further 48 hours did not change the ratio. The anomeric effect is the preference for a group on the anomeric carbon to go into the sterically unfavoured axial position; the stronger the effect the higher the proportion of the axial position [43]. Since the anomeric effect is stronger in non-polar solvents it is not surprising that the proportion of the α anomer is higher in the D_2O and DMSO mixture than D_2O only. This is a high proportion of the α anomer as compared with glucosamine in D_2O (36:64, α:β) [44]. It was found that protonation or acetylation on the amine caused the proportion of the α anomer to increase to 63% and 68% respectively [45], showing that there is an increase of the anomeric effect. These are similar values to **8e**. Horton *et al* suggested that this increase was because of hydrogen-bonding between the hydroxyl group on C1 and the group on C2 [45]. In the analysis of hydrogen-bonding for **8e** above, the closest possible group on the thiourea for hydrogen-bonding to the anomeric hydroxyl was HN1 which was 2.90 Å away, Figure 2.24. This is becoming too distant to be a credible bond; if this is a bond it is only a very weak interaction. Of course the structure determination was carried out on the solid, and this means that the conformation in solution may be different. Also the structure only shows one conformation and in solution a mixture of

conformations would be expected. As seen in Figure 2.24 the thiourea has twisted so HN1 is pointed away from the hydroxyl group. While the gross features of the structure are not likely to alter in solution (i.e. the thiourea's six-membered ring or the $^4C_1$ chair conformation are retained in solution) the thiourea could rotate around the C–N bond to bring HN1 closer to the hydroxyl group. Theoretical studies are needed to confirm it is hydrogen-bonding that increases the anomeric effect, or if it is an electronic effect or a combination of the two.

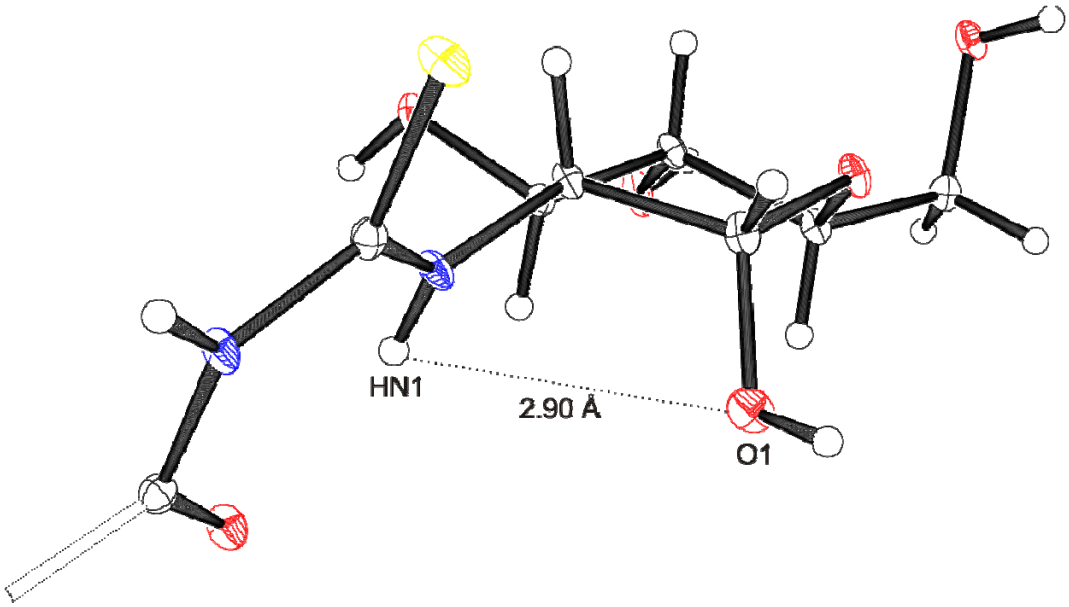

Figure 2.24 *The position of the anomeric hydroxyl and thiourea in **8e**.*

Regardless of what causes the effect, when **8e** is dissolved in ethanol and water for recrystallisation a mixture of the two anomers would form with the α anomer predominating. From this mixture the α anomer crystallises out either because that form is favoured in the crystal packing or the fact that it is present in a higher concentration and once it starts crystallising this drives the equilibrium of anomers towards the α anomer.

2.2.5 Non-acyl thioureas

To compare thioureas without the internal hydrogen-bond a non-acyl thiourea was needed. Acetylated glucosamine reacts with phenyl isothiocyanate to produce **8f** [28], Figure 2.25. The ^{1}H NMR spectrum of **8f** has all the same signals that **8a** has but they occur in very different positions, Figure 2.26 shows the comparison of ^{1}H NMR spectrum of **8a** and **8f**. The major difference is in the N–H protons. Lacking the ability to form the internal hydrogen-bond, HN1 is much further upfield at 5.96 ppm compared with 10.92 ppm for **8a**. HN2 has also shifted upfield but to a lesser extent. The aromatic and carbohydrate signals are also further downfield. The coupling constant for HN1 of 9.2 Hz suggests that the thiourea also has the Z,E,Z-anti conformation. The ESI-MS of **8f** showed similar ionisation modes with $[M+Na]^{+}$ and $[M+K]^{+}$.

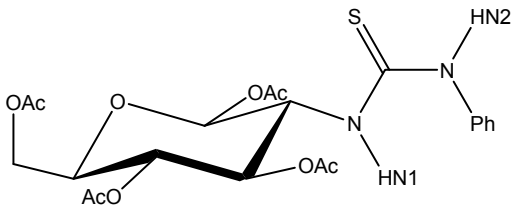

Figure 2.25 *The non-acyl thiourea **8f**.*

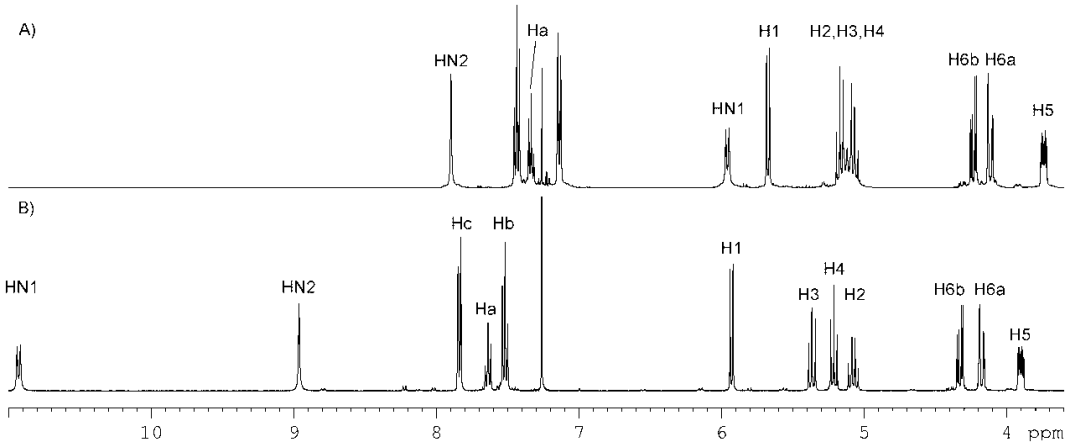

Figure 2.26 *Portion of the ^{1}H NMR spectrum comparing; A) **8f**; B) **8a**.*

2.3 Complexes with sugar thioureas

Two main synthetic routes were used to prepare complexes, Scheme 2.4. The first used a thiourea to displace a bridging ligand in a dimer; the second was reacting the thiourea with an M(II) halide. Each lead to a four-coordinate neutral molecule. Some work was also done using gold(I).

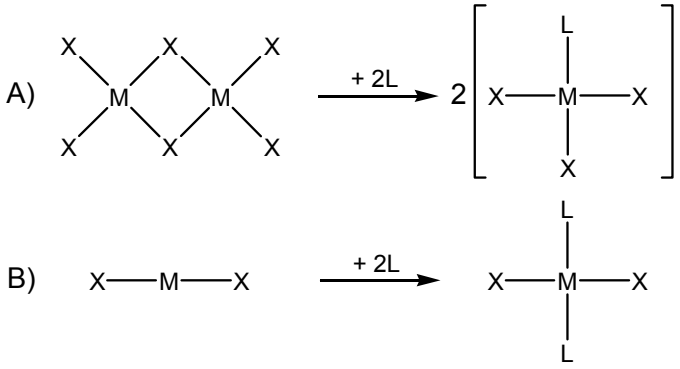

Scheme 2.4 *Synthesis of thiourea complexes; A) Thiourea displacing a bridging ligand in a dimer; B) Two thioureas complexing to a M(II) halide to form a four coordinate complex.*

2.4 Reaction of thioureas with $[Cp^*RhCl_2]_2$

If **8a** is reacted with $[Cp^*RhCl_2]_2$ in CH_2Cl_2 in a 2:1 ratio the thiourea displaces the bridging chloride bond and acts as a monodentate neutral ligand forming the complex **9a**, Figure 2.27. ESI-MS shows different ions arising from the loss of at least one chloride and proton from the complex. The most intense peak comes from the ion $[M–HCl–Cl]^+$. The rest of the ions are very weak, see Table 2.5 for details. No molecular ion was observed for **9a**. While the loss of a chloride is a common route of ionisation for transition metal complexes [46], no ions were seen from this mode of ionisation. The driving force behind the ionisation seen was from the loss of HCl. The loss of one HCl gives rise to a complex where the thiourea is anionic and acting as a bidentate ligand. These complexes are discussed in greater detail in Chapter Three. The complex can lose another HCl so

that the thiourea is dianionic thiourea, in Chapter Three complexes where the thiourea is dianionic could not be made so the structure of this fragment ion cannot be verified.

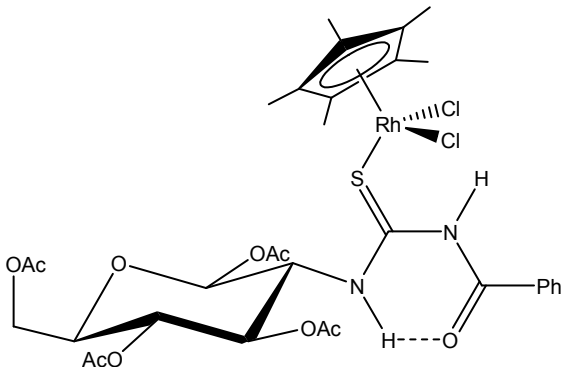

Figure 2.27 ***9a*** *with* ***8a*** *acting as a monodentate ligand to* Cp^*RhCl_2.

Ion	Observed m/z	Calculated m/z	Intensity
$[(M–Cl–HCl]^+$	747.149	747.145	strong
$[(M–2HCl)+Na]^+$	769.131	769.127	weak
$[(M–HCl)+Na]^+$	805.108	805.104	weak
$[(M–2HCl)(M-HCl)+H]^+$	1529.260	1529.260	weak
$[(M–2HCl)(M-HCl)+Na]^+$	1551.243	1551.242	weak
$[2(M–HCl)+Na]^+$	1587.225	1587.219	weak

Table 2.5 *Ions observed in the ESI-MS spectrum of* ***9a****.*

^{1}H NMR confirmed the neutral monodentate binding mode, with both N–H protons still present and shifted downfield; Figure 2.28 shows the ^{1}H NMR spectrum with a comparison to **8a**. While there is little change in the carbohydrate chemical shifts, the N–H and aromatic signals show more change. HN1 and HN2 are both shifted slightly upfield. Hc shifts the most of the aromatic signals, moving 0.44 ppm downfield while Ha and Hb only move downfield slightly (0.10 ppm and 0.07 ppm respectively). The coupling constant for HN1 of

8.5 Hz suggests that the thiourea still has the Z,E,Z-anti conformation. This conformation is seen for other thioureas acting as neutral ligands such as acyl thioureas with a cyclohexane attached to N1 [34] and cyclic thioureas with an isopropyl group attached to N1 [47, 48]. The conformation was confirmed by an X-ray structure determination discussed below.

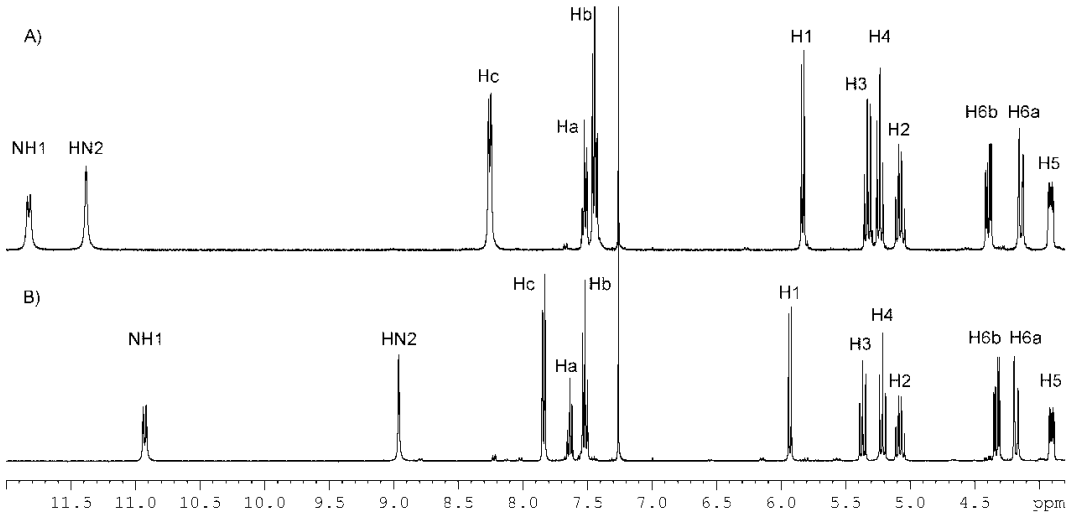

Figure 2.28 *Portion of the ^{1}H NMR spectrum comparing; A) **9a**; B) **8a**.*

The ^{13}C NMR spectrum of **9a** shows little change compared to **8a** as shown in Figure 2.29. If the ^{13}C NMR spectrum was processed with no line broadening the amide carbonyl was observed as a broad singlet as a shoulder on one of the acetyl signals, the broadening would be because of the nitrogen next to it, Figure 2.30. It has been shifted downfield relative to the parent thiourea. While this is the biggest shift in the spectrum the signal has only moved a small amount shifting 3.2 ppm. In comparison the C=S carbon only moved 0.3 ppm downfield even though it is directly attached to the bonding sulfur.

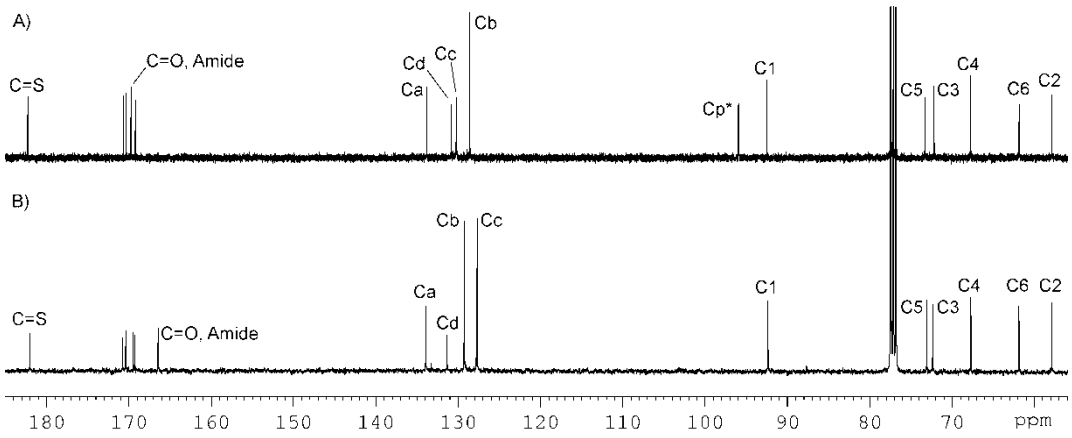

Figure 2.29 *Portion of the ^{13}C NMR spectrum comparing; A) **9a**; B) **8a**.*

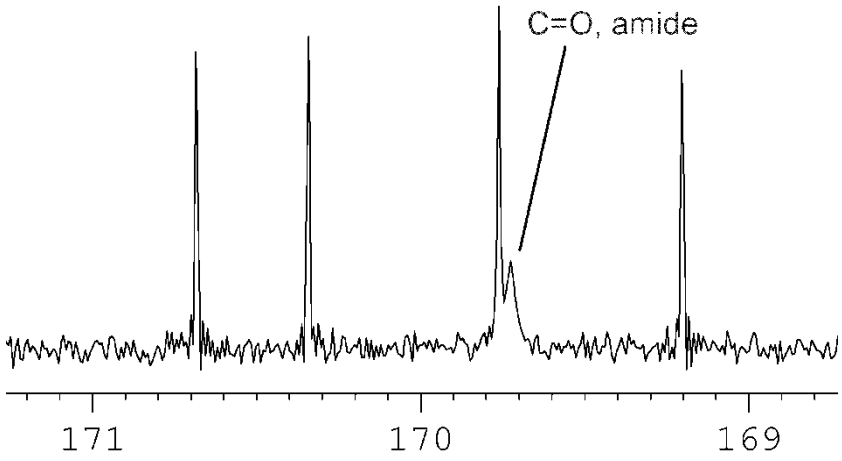

Figure 2.30 *^{13}C NMR spectrum of the carbonyl region of **9a**, processed with no line broadening. The acetate carbonyls can be seen as sharp signals, while the amide carbonyl is a broad signal at 169.7 ppm.*

There are a few similar compounds reported where a thiourea is a neutral ligand to Cp*Rh(III). One is shown in Figure 2.31. **10** is a DNA intercalating agent that is cytotoxic [49].

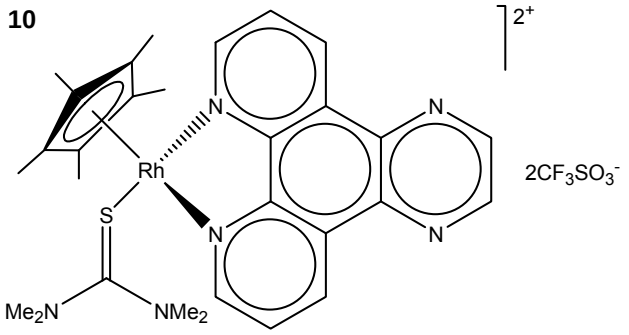

Figure 2.31 *Reported thiourea complex of Cp*Rh(III), **10**, which is a cytotoxic DNA intercalating agent [49].*

2.4.1 Crystal structure of 9a

Crystals of **9a** suitable for X-ray diffraction were grown by vapour diffusion of hexane into an ethanol solution of **9a**. **9a** forms orthorhombic crystals, space group $P2_12_12_1$. The asymmetric unit contains two independent molecules called A and B; molecule B had a disordered Cp^*RhCl_2. One of the disordered portions was called portion C. The crystal was of poor quality (R factor ~0.12) leading to oblate displacement ellipsoids. Figure 2.32 shows the geometry of **9a**. A number of the acetate groups showed very large displacement ellipsoids from unresolvable disorder, and for C13A its position was not allowed to refine and was fixed. Only the overall features merit discussion. This is the first structure of a neutral thiourea acting as a monodentate ligand for the type of complex Cp^*RhCl_2L.

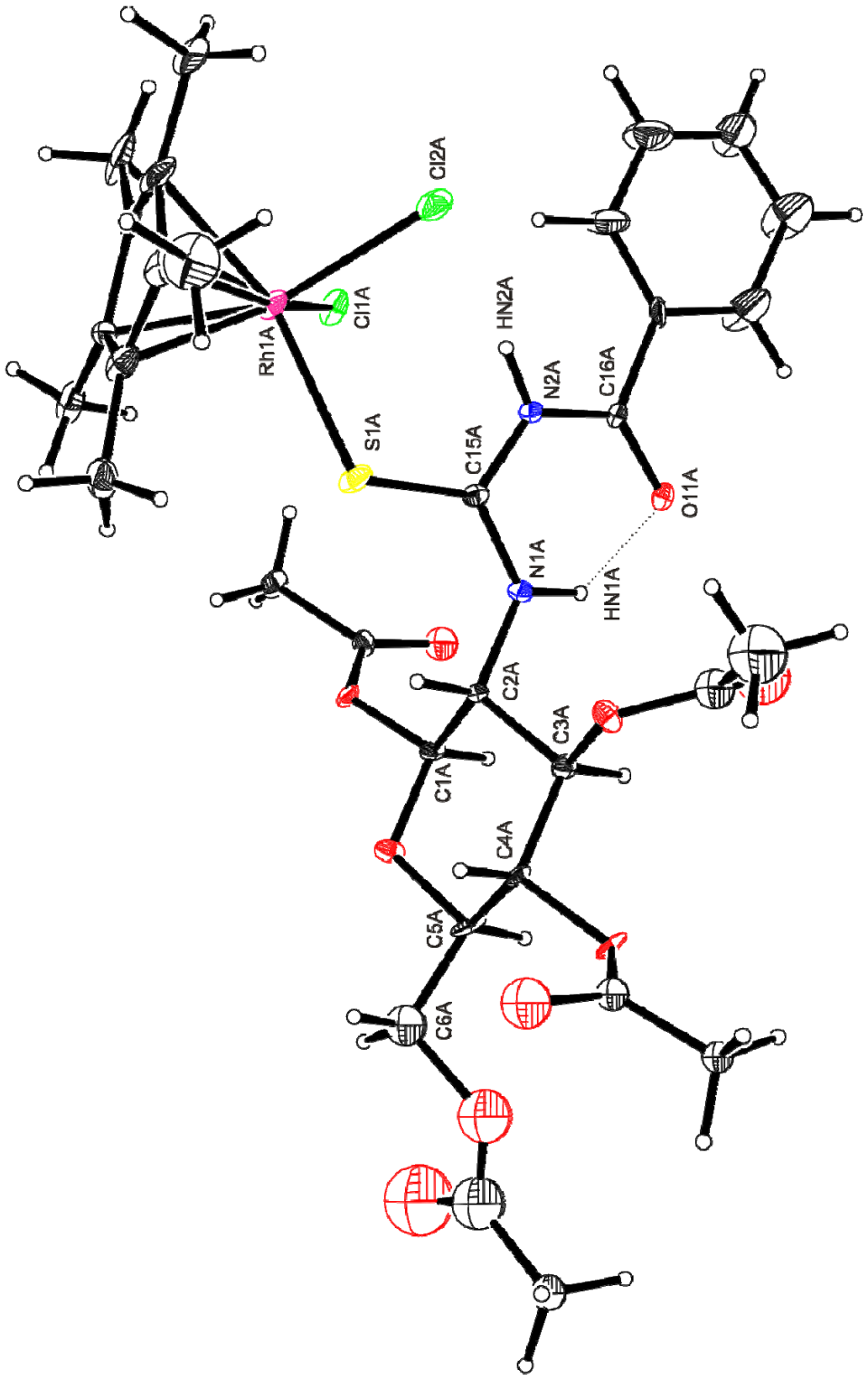

Figure 2.32 *The geometry of **9a** showing the atom labelling scheme and thermal ellipsoids at the 15% probability level. Only one molecule from the independent unit has been shown.*

Selected bond lengths and angles for **9a** and **10** are summarised in Table 2.6. The comparison of molecule A of **9a** (which lacks the disorder) with **10** shows that both the Rh–S bond and the Rh–S=C angle are smaller. The polypyridyl ligand of **10** is much bulkier than the two chlorides, and so distorts the environment around the rhodium, which increases the bond length and angle. Both independent molecules show similar features, the only difference being the conformation of the acetylated hydroxymethyl group. Molecules A and B have the *tg* and *gt* conformations respectively. The internal hydrogen-bond is still present holding the thiourea into the six-membered ring. Both molecules also have the Z,E,Z-anti conformation suggested by NMR data.

	Molecule A	**Molecule B Portion B**	**Molecule B Portion C**	**10**
Rh–S	2.386(3)	2.295(4)	2.605(5)	2.416
Rh-Cp*[1]	1.782(6)	1.80(1)	1.80(1)	1.814
Rh–Cl1	2.403(4)	2.396(8)	2.403(8)	NA
Rh–Cl2	2.422(3)	2.448(7)	2.435(8)	NA
Rh–S–C15	114.7(4)	118.2(5)	114.2(6)	133.8

1: Measured as the distance between the rhodium and the plane defined by the quaternary carbons of the Cp* ring.

Table 2.6 *Table of selected bond lengths (Å) and angles (°) for **9a** and **10** [49].*

As shown in Figure 2.33, one of the molecules has disorder on the Cp*$RhCl_2$ portion of the structure. There appears to be no disorder on the sulfur atom. The disorder refines to approximately 50% occupancy for both portions of the disorder. The disordered portion shows the same bond lengths and angles for the two parts with the exception of the Rh–S distance, with 2.396(8) Å and 2.605(5) Å for portion B and C respectively which is likely an artefact of the disorder.

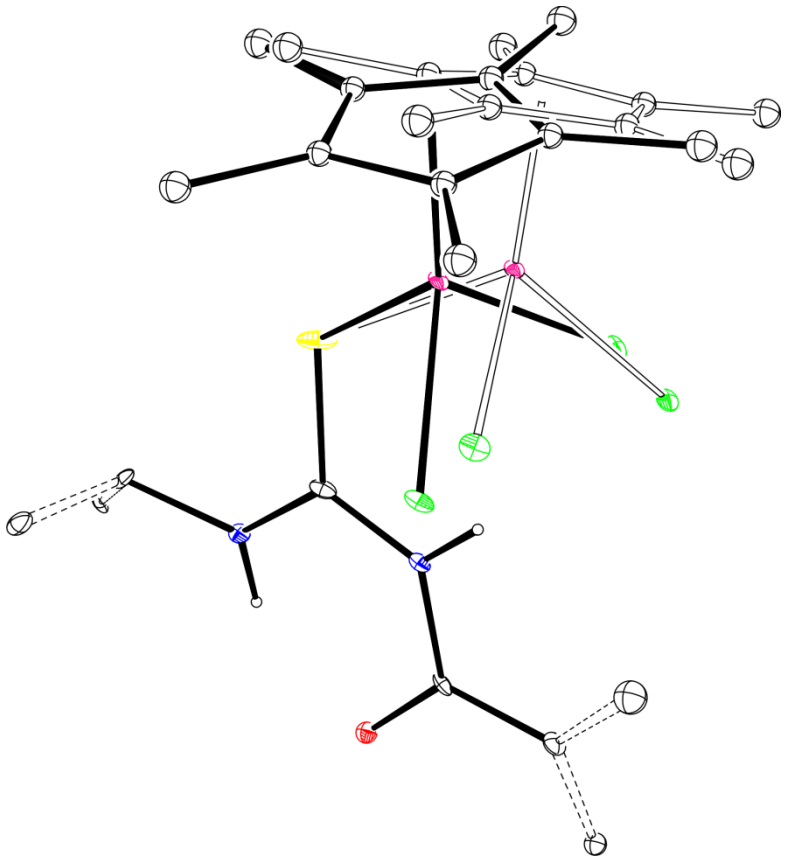

Figure 2.33 *The disorder of the Cp*RhCl$_2$ on molecule B of **9a**. Methyl protons have been omitted for clarity.*

2.5 Reaction of thioureas with [Rh(COD)Cl]$_2$

Since the thiourea readily displaced the bridging chloride in [Cp*RhCl$_2$]$_2$ to form a neutral compound, reactions with other dimers with bridging chlorides were examined. The benzoyl thiourea **8a** was reacted with [Rh(COD)Cl]$_2$ in CH_2Cl_2 as above for **9a**. The thiourea again formed a neutral complex, **11a**, acting as a monodentate ligand through the sulfur, Figure 2.34.

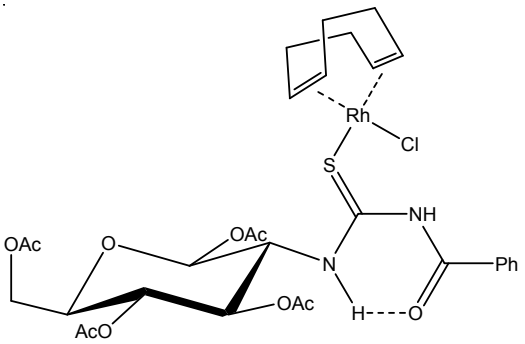

Figure 2.34 ***11a*** *with* ***8a*** *acting as a monodentate ligand to (COD)RhCl.*

ESI-MS showed a similar loss of HCl to **9a**, however the spectrum has many fewer ions since there is only one chloride on the metal to lose. There are only two ions observed, they are assigned as $[(M–HCl)+Na]^+$ and $[2(M–HCl)+Na]^+$. These ions form from the loss of an N–H proton from the thiourea and a chloride from the Rh(I) so the thiourea acts a bidentate anionic ligand as discussed further in Chapter Three.

The ^{1}H NMR spectrum of **11a** showed similar changes from the ligand as for **9a** with the N–H signals shifted downfield, with HN2 again coming further downfield than HN1. The sugar signals and aromatic signals have shifted the same as for **9a**. The coupling constant for HN1 of 9.7 Hz suggests that the thiourea still has the Z,E,Z-anti conformation. The signals in the ^{13}C NMR spectrum of **11a** have also shifted in the same manner as **9a**.

2.6 Reaction of thioureas with $[(p\text{-cymene})RuCl_2]_2$

8a was reacted with $[(p\text{-cymene})RuCl_2]_2$ in CH_2Cl_2 in a 2:1 ratio as above to form **12a**, Figure 2.35. ESI-MS of the reaction mixture showed only one peak which was identified as $[(M–HCl–Cl]^+$. If sodium formate was added as a calibrant, two additional peaks were observed which corresponded to $[(M–HCl)+Na]^+$ and [(M–

2HCl)+Na]$^+$. The mixture was filtered through Celite and precipitated with petroleum spirits to give an orange powder.

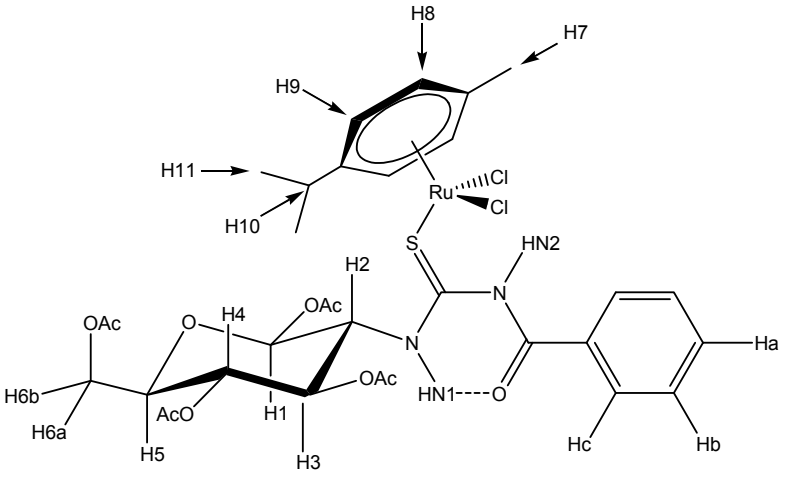

Figure 2.35 ***12a*** *with* ***8a*** *acting as a monodentate ligand, with the* ^{1}*H NMR labelling scheme.*

^{1}H NMR of **12a** confirmed the thiourea was a monodentate ligand by the presence of the two N–H protons, shifted downfield, Figure 2.36. The aromatic signals H8 overlapped with H3, but the 2D experiments and a SELTOCSY spectrum allowed them to be distinguished, see Appendix Two for more detail. The coupling constant for HN1 of 9.6 Hz suggests that the thiourea still has the Z,E,Z-anti conformation. The aromatic signals are upfield, at 5.45 and 5.30 ppm, compared to where aromatic signals would be expected because of the metal pulling electron density off the aromatic ring. The signals in the ^{13}C NMR spectrum of **12a** have also shifted in the same manner as **9a**.

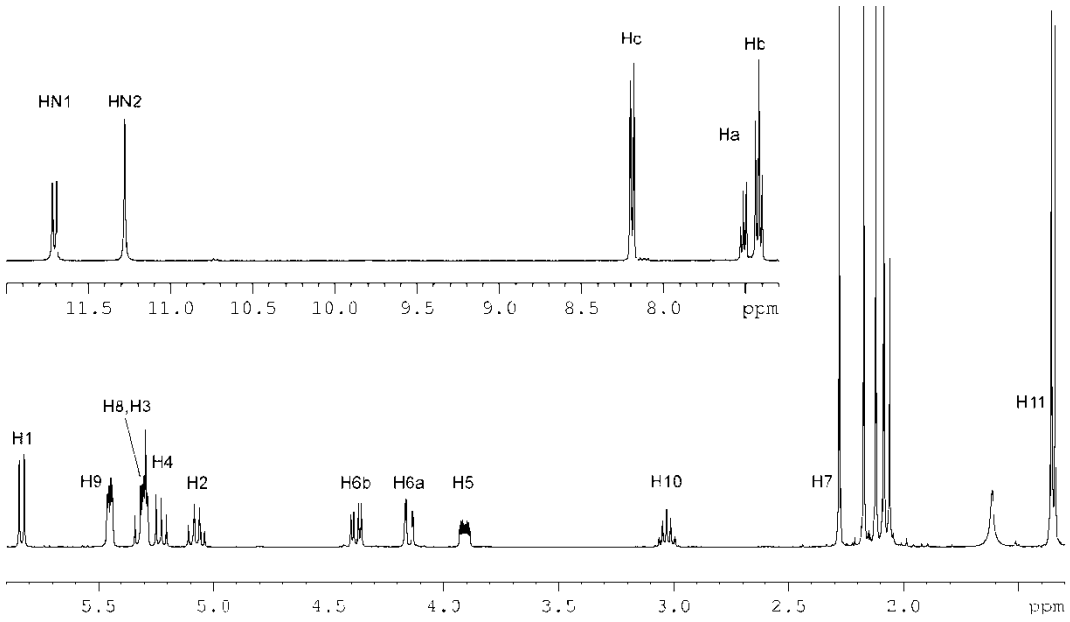

Figure 2.36 *^{1}H NMR spectrum of **12a**; inset shows N–H and aromatic region.*

The only other similar compound is where a thiosemicarbazone derivative of vitamin K_3 was used as a non-acyl monodentate ligand [50], Figure 2.37.

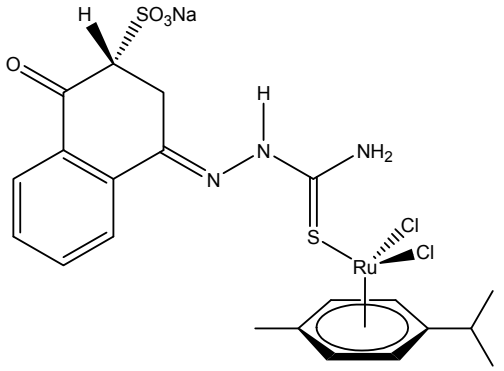

Figure 2.37 *Example of a thiourea as a neutral monodentate ligand to $RuCl_2$(p-cymene) [50].*

2.7 Reaction of thioureas with [Pd(*C,N*-DMBA)Cl]$_2$

8a was reacted with [Pd(*C,N*-DMBA)Cl]$_2$ in CH_2Cl_2 as above. ESI-MS of **13a** showed a number of ions. Assuming that the thiourea was binding as a neutral

monodentate ligand as previously seen, Figure 2.38, the most intense ion was assigned as $[M–Cl]^+$; two other smaller peaks were $[(M–HCl)+Na]^+$ and $[(M–HCl)+K]^+$ corresponding to the thiourea losing one proton with a concomitant loss of the chloride to form a bidentate ligand, see Chapter Three for more details.

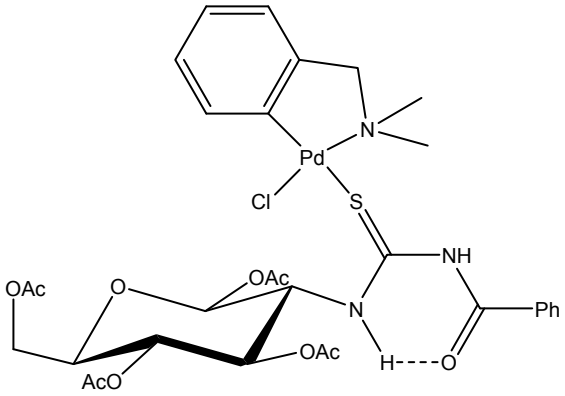

Figure 2.38 ***13a*** *with* ***8a*** *acting as a neutral monodentate ligand.*

^{1}H NMR of **13a** clearly showed the thiourea was acting as a monodentate ligand. ESI-MS cannot distinguish between the mono and bidentate forms of the complexes since there is no way to know if the loss of HCl from the complex was happening in the instrument or before it was analysed. The ^{1}H NMR indicated that the rearrangement to form the bidentate complex was happening in the instrument as the two N–H proton signals were present and shifted downfield. The bidentate complex is discussed further in the next Chapter. The coupling constant for HN1 of 9.2 Hz suggests that the thiourea still has the Z,E,Z-anti conformation. Unfortunately **13a** was unstable in solution and after several hours in $CDCl_3$ started decomposing precluding full characterisation.

Thiourea complexes with Pd(*C,N*-DMBA)X have shown anti-tumour and anti-mycobacterial properties [51], Figure 2.39. Since **13a** was so unstable in solution, this precluded further testing. While the structure of the complex could not be confirmed, it was assumed that the sulfur was *trans* to the metalated carbon as

seen in other structures. A sugar thiourea has been reported bonding as a neutral ligand to Pd(*C*,*N*-DMBA)Cl [25], see Section 2.2 (Pages 22-23).

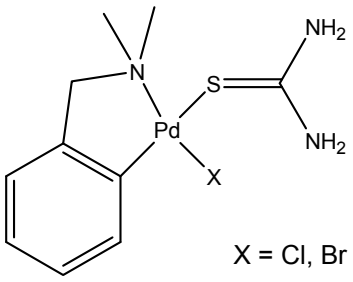

Figure 2.39 *Thiourea complexes with Pd(C,N-DMBA)X (X = Cl, Br) which shows anti-tumour and anti-mycobacterial properties [51].*

2.8 Reaction of thioureas with PdX_2 (X = Cl, Br or I)

There are a large number of examples in the literature of palladium halide complexes with benzoyl thioureas. Previous methods of making the complexes include reacting $Pd(PhCN)_2Cl_2$ and the thiourea in CH_2Cl_2 [12], or stirring $K_2[PdCl_4]$ and the thiourea in a 1:1 water:acetonitrile mixture [52]. A complicated method required adding dropwise a solution of $PdCl_2$ or $PdBr_2$ in 2:1 acetonitrile:1M acid (HCl and HBr respectively) to a solution of the ligand in the same solvent [14]. A simpler route to these complexes was developed for this work. The ligand and PdX_2 (X = Cl, Br or I) were stirred together in acetonitrile to give a clear solution, the solvent was evaporated, and the residue dissolved in CH_2Cl_2 and filtered through Celite. Precipitation with petroleum spirits gave high yields and required no further purification of the complexes, Figure 2.40. That the PdL_2I_2 complex can be made by this method is particularly interesting as the acetonitrile:acid method was unsuccessful [14].

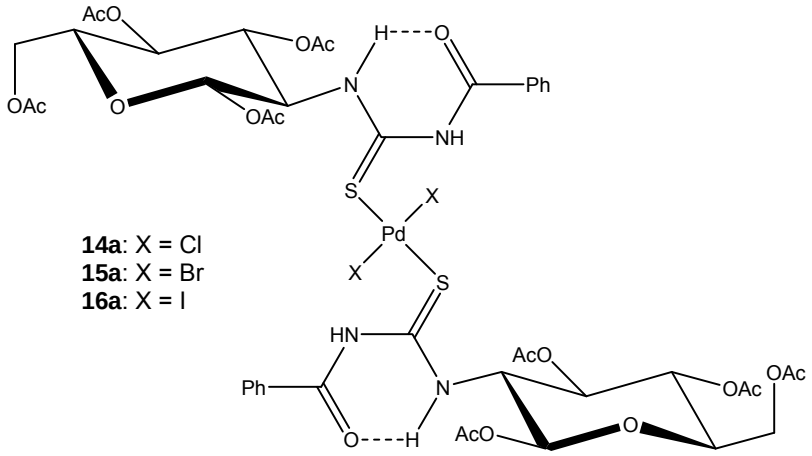

Figure 2.40 *Palladium(II) halide complexes with **8a** acting as a neutral monodentate ligand. Shown are the trans isomers.*

ESI-MS of **14a** showed a peak corresponding to $[M–2HCl+H]^+$. Immediately after the use of sodium formate, this peak disappeared and was replaced with $[M–2HCl+Na]^+$. All the palladium complexes of the form PdL_2X_2 in this report showed analogous signals, involving the loss of HX ($X = Cl^-$, Br^- or I^-).

The ^1H NMR spectra of **14a** clearly showed the thiourea was bonding to the palladium as a neutral ligand with both N–H protons still present and with downfield shifts in their positions. The coupling constant for HN1 of 9.8 Hz suggests that the thiourea still has the Z,E,Z-anti conformation. The HN1 proton is only shifted a relatively short distance. This is caused by the metal centre pulling electron density from the ligand. On the basis of previous crystal structures [12, 14] and the crystal structure of **14b** reported below it is known that the HN2 proton forms a hydrogen-bond to the chloride. This shifts HN2 much further downfield in comparison to HN1 since the chloride is pulling electron density off the proton, combining with the electron withdrawing effect of the metal. Figure 2.41 shows the aromatic and sugar portion of the ^1H NMR spectra comparing **14a** with **8a**. The H2 signal has been moved upfield, while for the aromatic region Hc has moved downfield.

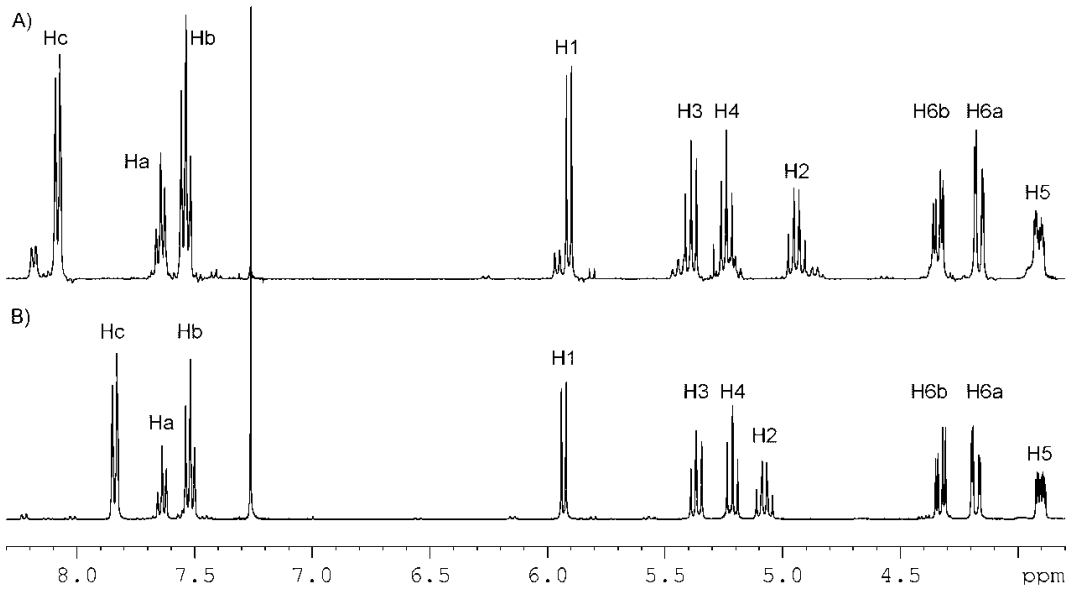

Figure 2.41 *Portion of the ^{1}H NMR spectrum comparing; A) **14a**; B) **8a**.*

Since palladium(II) forms square planar complexes an equilibrium of *cis* and *trans* isomers is possible, Figure 2.42. As seen in Figure 2.41 there are several small signals next to the main peaks which can be assigned as the other isomer. Figure 2.43 shows the N–H portion of the ^{1}H NMR spectra again showing that two isomers have formed. Based on X-ray crystal structure information detailed below (Section 2.8.2, Page 64), the main isomer was assigned as the *trans* isomer. This assignment was also suggested by **5** for which it was shown that the *trans* isomer predominates in $CDCl_3$ with an equilibrium constant K value of 2.33 at 25°C [14].

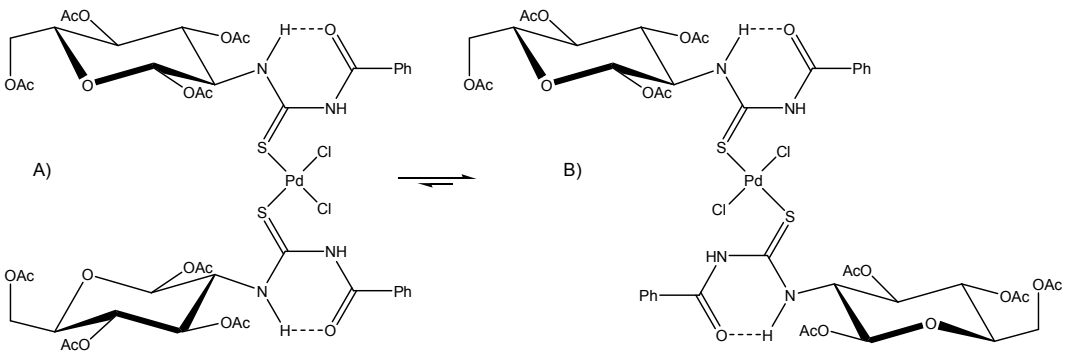

Figure 2.42 *Diagram showing the equilibrium between the cis (A) and trans (B) form of **14a**.*

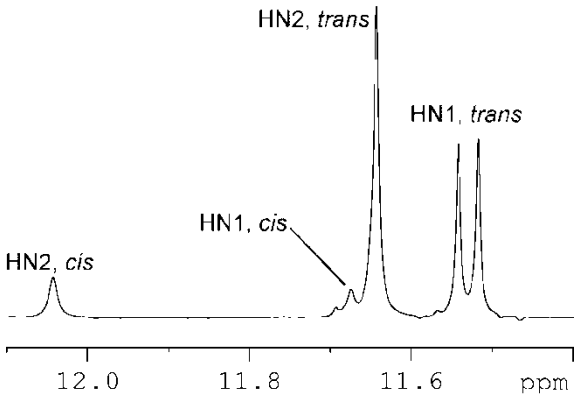

Figure 2.43 *^{1}H NMR spectrum of the N–H region of **14a** showing the two sets of signals coming from the cis and trans isomers. The doublet of HN1, cis is overlapping with HN2, trans.*

Comparing ^{1}H NMR spectra as the halide on the metal is changed, a clear trend can be seen for the N–H signals, with the more electronegative the halide the more upfield the signal, Figure 2.44. For the bromide and iodide complexes HN2 is more upfield than HN1 as the hydrogen bond HN2 forms is weaker. The other signals in the spectra show smaller shifts from the parent thiourea going from Cl^- > Br^- > I^-. Neither the bromide or iodide versions of the complex showed signs of equilibrium between the two isomers. It was assumed that it was the *trans* isomer that was observed. This was based on the *trans* effect, which increases from Cl^- to I^- [53], and so the *cis* isomer would be expected to disappear.

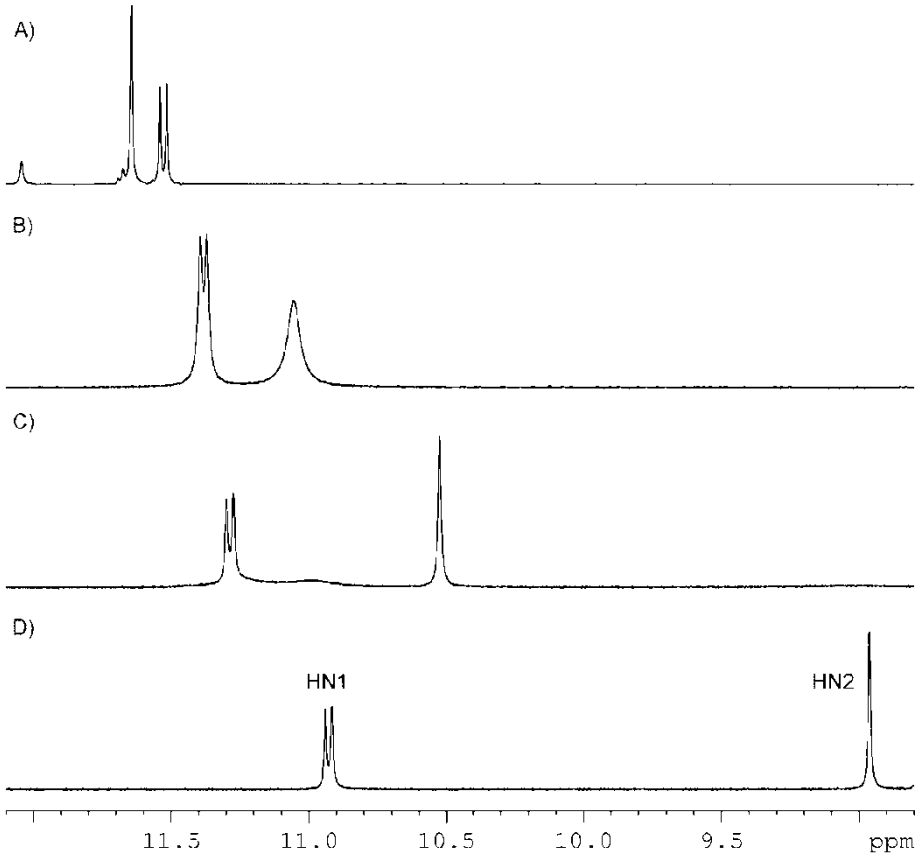

Figure 2.44 *^{1}H NMR spectrum of the N–H region comparing; A) **14a**; B) **15a**; C) **16a**; D) **8a**.*

The reaction was also carried out using the other acyl thioureas **8b-d**. While **8b** reacted in the same fashion, the acetonitrile mixtures of $PdCl_2$ and **8c** or **8d** did not produce clear solutions, but gave orange precipitates. This indicates that these complexes are much more insoluble than the other two. While products from **8b** and **8c** could be isolated, **8d** showed the presence of the product in ESI-MS but attempts to isolate a product gave complex mixtures. Both ESI-MS and NMR of **14b** and **14c** showed similar features to **14a**, Table 2.7 summarises selected chemical shifts and coupling constants from the NMR spectra of the palladium thiourea complexes.

	HN1	HN2	Hc	H2	C=S	C=O, amide	C2
8a	10.92, 9.2 Hz	8.97	7.82	5.08	182.0?	166.5	57.9
***trans*-14a**	11.53, 9.8 Hz	10.64	8.16	4.92	181.2	169.6	59.6
***cis*-14a**	11.55, NA	12.04	8.13	4.90	181.1	169.5	59.6
***trans*-15a**	11.38, 9.7 Hz	11.05	8.10	4.93	181.6	167.9	59.1
***trans*-16a**	11.29, 10.0 Hz	10.49	8.01	4.91	181.4	167.1	59.0
8b	10.71, 9.4 Hz	9.02	8.04	5.06	181.3	164.5	58.0
***trans*-14b**	11.23, 9.5 Hz	11.07	8.27	4.95	180.4	167.7	58.9
8c	10.61, 9.5 Hz	9.07	7.35	5.07	181.6	156.4	57.9
***trans*-14c**	11.17, 9.7 Hz	11.63	7.58	4.93	181.1	158.2	58.4
***cis*-14c**	11.20, NA	11.92	7.57	4.91	181.0	158.3	58.5

NA : Not determined

Table 2.7 *Selected chemical shifts and coupling constants from the NMR spectra of the acyl thioureas and their complexes with palladium(II) halides.*

While complex **14c** showed equilibrium between the *cis* and *trans* isomers, **14b** did not. When its ^{1}H NMR spectrum was recorded only one set of signals was seen, which was assumed to be the *trans* isomer, Figure 2.45. The nitro group is affecting the equilibrium in some fashion. To calculate equilibrium constants for the complexes accurate integration of the ^{1}H NMR signals was required. To ensure there was no saturation of the signals so quantitative integration could be carried out, D1 was increased in a series of experiments and the integrations compared to ensure there was no variation. Two signals that were well separated were chosen and integrated. The Table 2.8 summarises the equilibrium constants. The equilibrium for **14a** and **14c** both lie towards the *trans* isomer more than for **5**. This preference for the *trans* isomer is likely to be because of bulkiness of the sugar group compared to propyl.

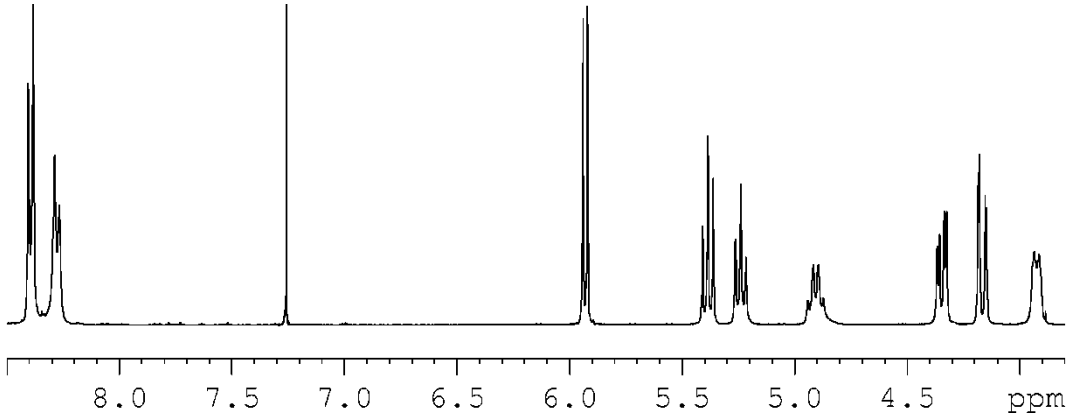

Figure 2.45 *Aromatic and sugar portion of the ^{1}H NMR spectrum of **14b** showing only one isomer.*

	Equilibrium constant for *cis* ↔ *trans*
5[1] [14]	2.33
14a	4.2
14c	4.3

Table 2.8 *Equilibrium constants for the equilibrium cis ↔ trans for a series of PdL_2Cl_2 compounds at 27°C.*

2.8.1 PdL_2Cl_2 type complexes with unprotected thioureas

Using **8e** under the same conditions as above gave an orange powder that was difficult to analyse. ESI-MS of the compound showed ions consistent with the complex forming with the same ions as for **14a**. ^{1}H NMR was difficult due to its solubility; running **14e** in DMSO gave a spectrum corresponding to **8e**, meaning that if a complex had formed the DMSO was breaking it apart. Using a mixture of acetone and $CDCl_3$ (90:10) gave slightly better results. Although the signals were broad which made identification of individual signals difficult, in the N–H region changes were seen that suggested that the complex had formed. Figure 2.46 shows that it appears that the N–H signals have moved downfield, and that there are several signals from the different isomers. This however is not definitive. IR spectra of **8e** and **14e** were run and showed a shift in $\nu_{C=S}$ indicative of

coordination to a metal. Repeated attempts at elemental analysis gave inconsistent results. While there is some indication that a complex has formed it cannot be confirmed with certainty.

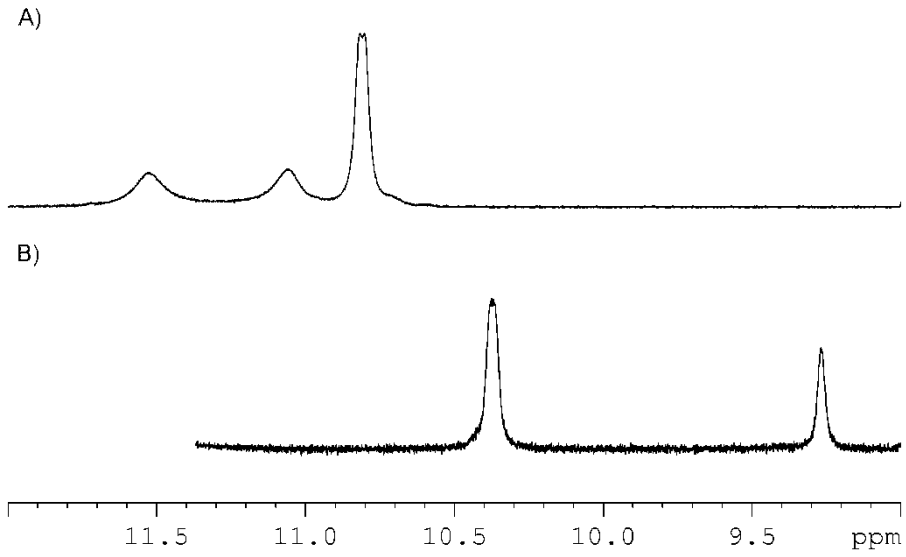

Figure 2.46 *N–H portion of the ^{1}H NMR spectrum comparing; A) **14e**; B) **8e**.*

2.8.2 Crystal structure of 14b

14b was recrystallised by the vapour diffusion of hexane into a mixture of THF and hexane at 4°C to produce crystals suitable for single crystal X-ray diffraction. **14b** forms orthorhombic crystals, space group $P2_12_12_1$. General details of the structure solution are discussed in Appendix Three. There were three THF molecules as solvent of crystallisation. One molecule of THF was well defined and its oxygen atom could be assigned and formed a hydrogen-bond. The other two were more highly disordered and were not near any groups that might form a bond. They were first refined as carbon atoms, and the atom with the lowest temperature factor was arbitrarily assigned as the oxygen atom. The structure was poor with voids in the structure that may have highly disordered solvent. Because of the quality of the data, the N–H protons were placed using a riding model. Figure 2.47 shows the geometry of **14b**.

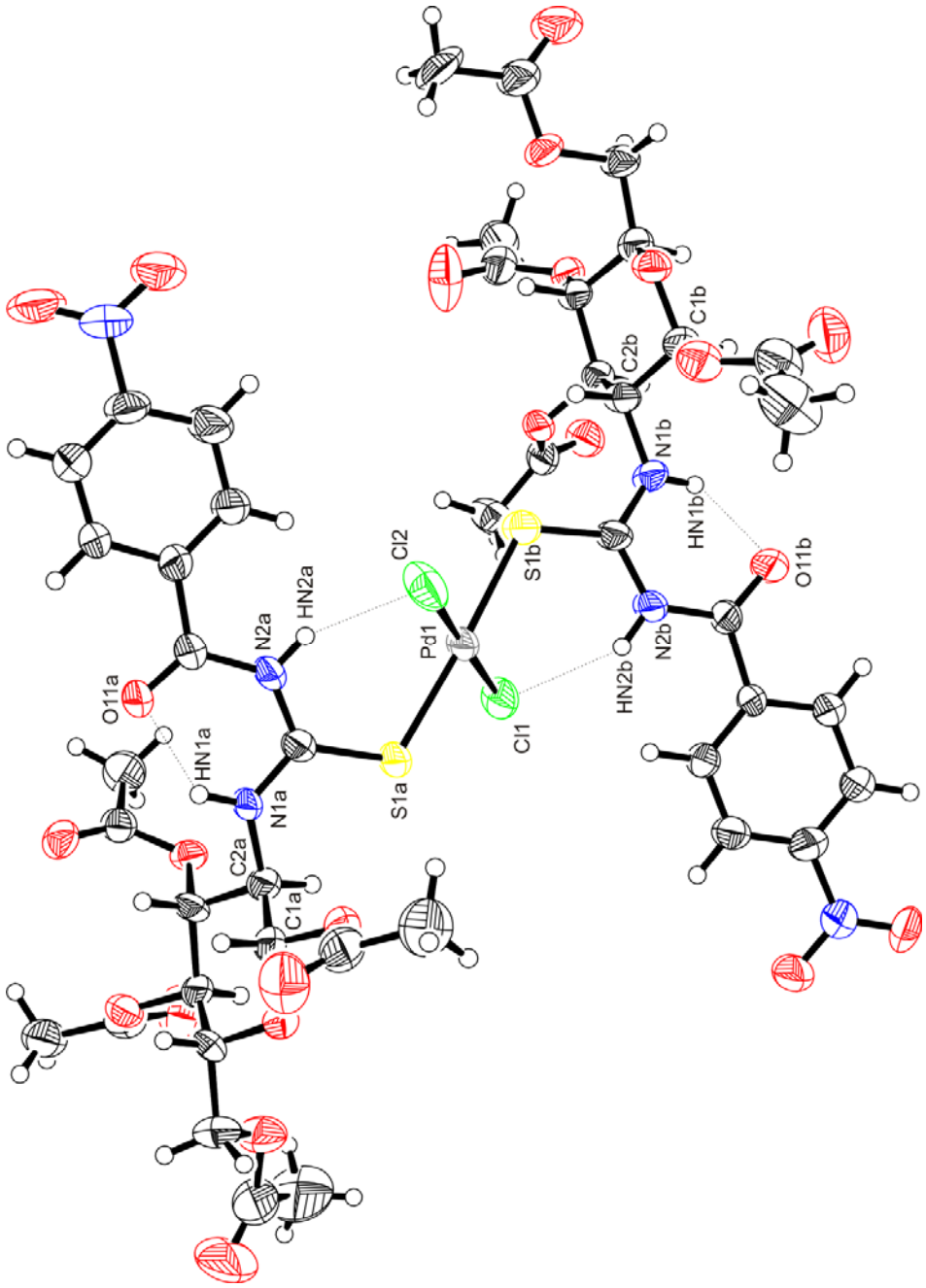

Figure 2.47 *The geometry of **14b**, showing the atom labelling scheme and thermal ellipsoids at the 50% probability level. Solvent molecules are excluded for clarity.*

While the two sugar thioureas are very similar for **14b** they were crystallographically unique, and are referred to as sugar A and B. Table 2.9 has selected bond lengths and angles for **14b**, **5** [12] and **6**, [14]. The bond lengths and angles are similar for the three structures. Both the *N*-propyl-*N´*-benzoyl-thiourea structures are triclinic with the $P\bar{1}$ space group and the palladium on the inversion centre so only half the structures are crystallographically unique.

The palladium has a square planar geometry; the plane defined by Pd1, S1A, S1B, Cl1 and Cl2 has the largest deviation for S1B of 0.0545(17) Å with a RMS deviation of 0.0452. The thioureas have bonded as the *trans* isomer as seen for **5** and **6**. The Z,E,Z-anti conformation is seen for both thioureas, with torsion angles for C2–N1–C15–S1 of 2.5(10)° and 1.7(9)° for the A and B respectively.

	14b **Sugar A**	**Sugar B**	**5**	**6**
Pd–S1	2.334(2)	2.314(3)	2.322(3)	2.3164(10)
Pd–Cl1	2.294(3)	NA	2.311(2)	NA
Pd–Cl2	2.312(3)	NA	NA	NA
Pd–Br	NA	NA	NA	2.4415(5)
C15A=S1A	1.704(10)	1.705(10)	1.690(1)	1.689(4)
C15A–N1A	1.330(12)	1.320(12)	1.327(11)	1.315(5)
C15A–N2A	1.339(12)	1.399(12)	1.376(7)	1.379(5)
C2A–N1A	1.473(11)	1.466(12)	1.456(8)	1.315
S1A–Pd1–Cl2	93.97(10)	NA	94.3(1)	85.46(3)
S1B–Pd1–Cl1	NA	93.69(11)	NA	NA

Table 2.9 *Table of selected bond lengths (Å) and angles (°) for **14b, 5** [12] and **6** [14].*

Figure 2.48 shows the hydrogen-bond network in **14b** while Table 2.10 summarises the hydrogen-bond geometry data. Since the N–H hydrogen atoms

were placed using a riding model, there are only e.s.d. values for the D•••A distances. The internal hydrogen-bond is still present holding the thiourea into the six-membered ring. However both NH1 protons are bifurcated, with an additional hydrogen-bond to the carbonyl O8 on the adjacent molecule (i.e. HN1A•••O8B and HN1B•••O8A). The plane defined by N1, C15, S1, C16 and O11 has a largest deviation of 0.1189(45) Å for S1A and 0.1267(70) Å for N2B for molecule A and B respectively, with a RMS of 0.0901 and 0.099 respectively. Also there is a weak hydrogen-bond seen between the HN2 protons and the chlorides on the palladium, with a distance of 2.32 Å for HN2A•••Cl2 and 2.52 Å for HN2B•••Cl1. This was expected and confirms that the reason for the large downfield shift in the position of the HN2 signal in the ^{1}H NMR spectrum is the formation of a new hydrogen-bond. **5** has a N•••Cl distance of 3.158(7) Å [12], which compares with 3.128(9) and 3.218(9) Å for **14b**. HN2B is also bifurcated with a bond to the oxygen on one of the THF molecules, this hydrogen-bond is likely to be holding the THF in a more well defined position explaining why it has smaller temperature factors than the other two THF molecules.

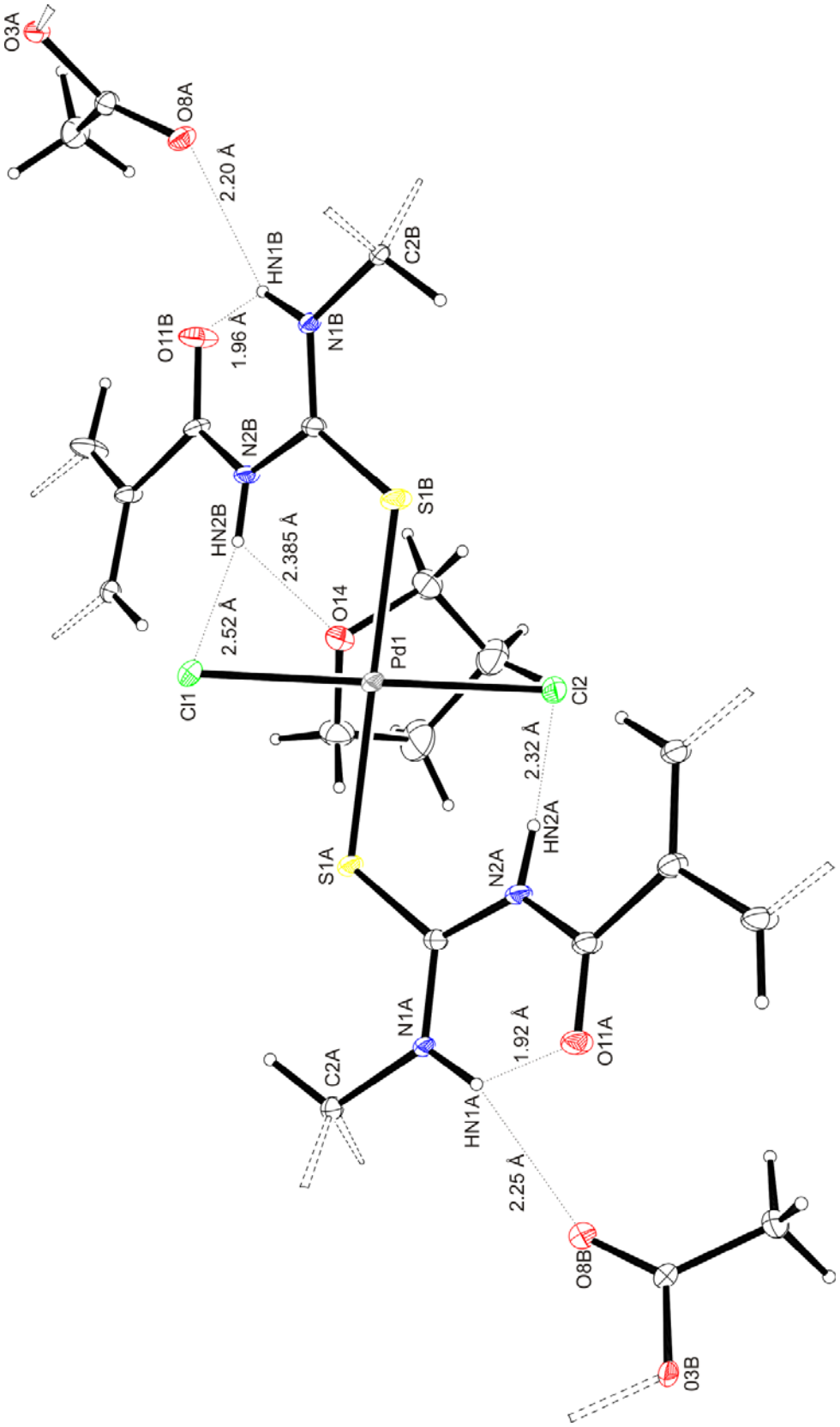

Figure 2.48 *Diagram of the hydrogen-bond network in **14b**.*

D-H•••A	d(D-H) (Å)	d(H•••A) (Å)	d(D•••A) (Å)	<(DHA) (°)
N1A-HN1A•••O11A	0.880	1.92	2.578(10)	130.5
N1A-HN1A•••O8B[i]	0.880	2.25	2.988(10)	140.7
N2A-HN2A•••Cl2	0.880	2.32	3.128(9)	152.9
N1B-HN1B•••O11B	0.880	1.96	2.620(11)	130.4
N2B-HN2B•••O8A[ii]	0.880	2.20	2.915(10)	137.6
N2B-HN2B•••Cl1	0.880	2.52	3.218(9)	136.8
N2B-HN2B•••O14	0.880	2.385	2.868(12)	114.9

Table 2.10 *Table of hydrogen-bond geometry data for **14b**.*

Both aromatic rings have twisted slightly with respect to the thiourea ring, with angles of 4.4(5)° and 17.1 (5)° for molecules A and B respectively. This difference in the twist is the main difference between the two sugar thioureas in the complex. The glycopyranose rings have the expected $^4C_1$ conformation and the acetylated hydroxymethyl groups on both sugars have the *gg* conformation.

2.8.3 8a with the PdL_4 motif

When $PdCl_2(MeCN)_2$ was reacted with a four molar equivalent of the cyclic thiourea shown in Figure 2.49, a $[PdL_4]Cl_2$ complex was formed [54]. If a four molar equivalent of **8a** was reacted with $PdCl_2$ in acetonitrile, the analogous compound was formed. ESI-MS of **17a** showed a complex mixture of ions, which are listed in Table 2.11. The main peaks are from the thiourea **8a**, with a number of other ions with increasing numbers of thioureas bonding to the palladium.

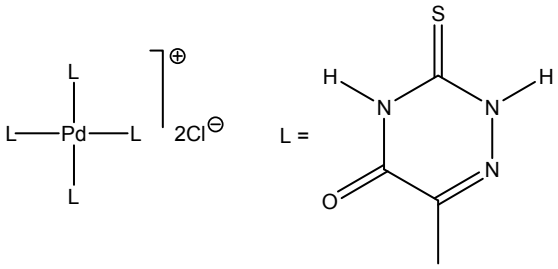

Figure 2.49 *Example of a $[PdL_4]^{2+}$ type complex where the thiourea bonds through the sulfur atom [54].*

	Observed m/z	Calculated m/z	Intensity
[8a+Na]$^+$	533.114	533.120	strong
[8a+K]$^+$	549.099	549.093	strong
[(8a–H)$_2$Pd+H]$^+$	1125.151	1125.158	weak
[(8a–H)$_2$Pd+Na]$^+$	1147.143	1147.140	weak
[(8a–H)$_2$Pd+K]$^+$	1163.110	1163.114	weak
[(8a–H)$_2$(8a)Pd+H]$^+$	1635.296	1635.290	medium
[(8a–H)$_2$(8a)Pd+Na]$^+$	1657.276	1657.272	medium
[(8a–H)$_2$(8a)Pd+K]$^+$	1673.251	1673.245	medium
[(8a–H)$_2$(8a)$_2$Pd+K]$^+$	2185.3	2185.4[1]	very weak
[(8a–H)$_4$Pd$_2$+H]$^+$	2251.2	2251.3[1]	very weak
[(8a–H)$_4$Pd$_2$+Na]$^+$	2273.2	2273.3[1]	very weak
[(8a–H)$_4$Pd$_2$+K]$^+$	2289.2	2289.3[1]	very weak

1: These peaks were beyond the effective calibration range of the instrument and so are only reported to one decimal place.

Table 2.11 *Ions seen in ESI-MS of **17a**.*

The ^{1}H NMR spectrum was similar to the PdL_2Cl_2 complex, as shown in Figure 2.50. The broadening of the N–H signals means that the coupling constant of HN1 cannot be determined, and so while it is likely that the thiourea still has the Z,E,Z-anti conformation it cannot be confirmed. The ^{13}C NMR spectrum was almost identical to **14a**.

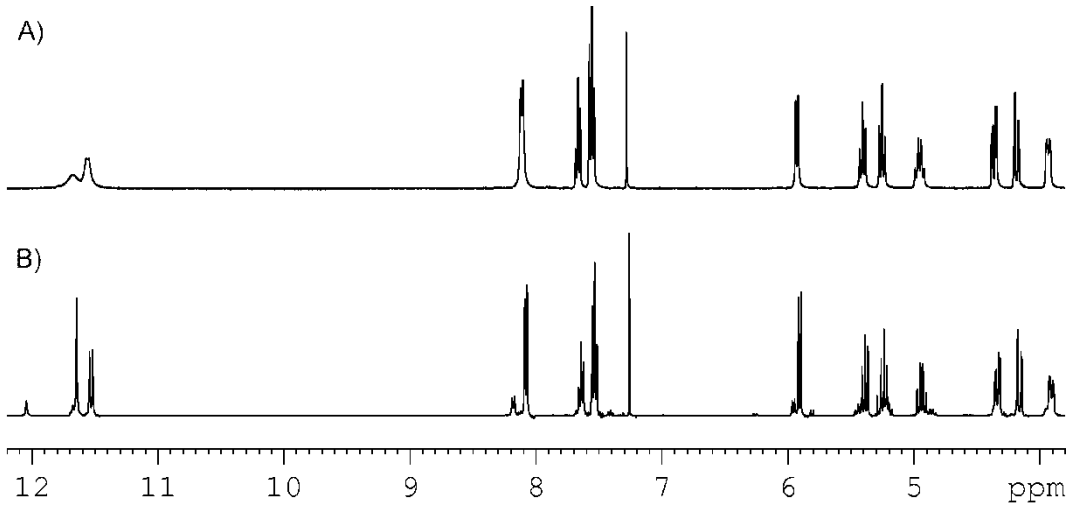

Figure 2.50 *Portion of the ^{1}H NMR spectrum comparing; A) **17a**; B) **14a**.*

In one of a number of attempts to produce single crystals, a recrystallisation of **17a** was carried out by vapour diffusion of hexane into THF. Analysis of the resulting crystals showed **14a** had crystallized out, indicating an equilibrium was involved and that THF favoured the displacement of two of the thiourea ligands for the chloride counter ions in solution, Scheme 2.5.

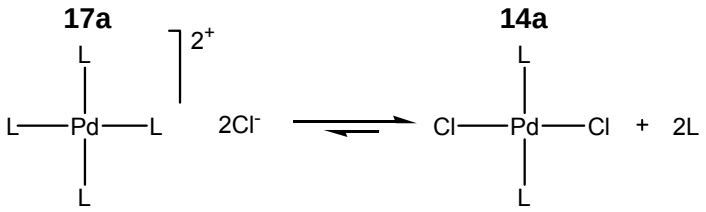

Scheme 2.5 *Equilibrium of **17a** and **14a** in THF which favours the chloride ions coordinated to the palladium.*

2.9 Reaction of thioureas with PtX_2 (X = Cl, Br or I)

Since the benzoyl thioureas formed complexes with palladium halides so readily other d^8 square planar metals were investigated. Isoelectronic platinum(II) was chosen. $K_2[PtCl_4]$ and **8a** were suspended in acetonitrile and left to stir as for the palladium complexes. After approximately three days all solids had dissolved to

give a yellow solution. ESI-MS of the reaction mixture showed several peaks; if it was assumed the analogous complex had formed, Figure 2.51, the ions could be assigned as $[M–HCl–Cl]^+$ and $[M–2HCl+Na]^+$.

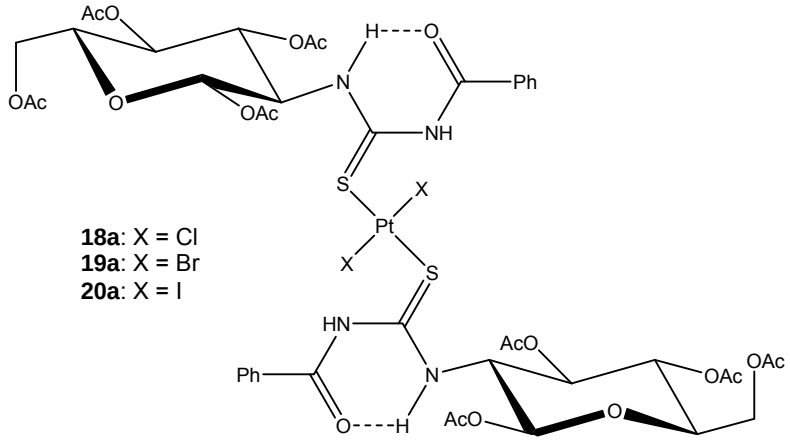

Figure 2.51 *Platinum(II) halide complexes with **8a** acting as a neutral monodentate ligand. Shown are the trans isomers.*

Since the very long reaction time was likely to be a solubility issue the reaction was repeated using a 10:1 mixture of acetonitrile and water. After 2 hours all solids had dissolved and given a yellow solution. The solvent was removed and the residue suspended in CH_2Cl_2, filtered though Celite and precipitated with petroleum spirits to give a yellow powder. Other methods that have been used involved a similar method to one mentioned above for the palladium complexes; adding dropwise a solution of $[PtCl_4]^{-2}$ in 2:1 acetonitrile:1M HCl to a solution of the ligand in the same solvent. By adding a 25 molar excess of NaBr or NaI to the $K_2[PtCl_4]$ solution and stirring for an hour before the thiourea was added, the bromide and iodide versions of the complex could be made.

When the ^{1}H NMR spectrum of the precipitated **18a** was examined it was clear that **8a** was acting as a neutral monodentate ligand. All the features were the same as the palladium analogues with the shifts. The coupling constant for HN1

of 10.0 and 9.9 Hz suggests that the thiourea still has the Z,E,Z-anti conformation. That a mixture of *cis* and *trans* isomers had formed was apparent with two sets of signals seen. Unlike the palladium complex the two isomers were present in similar proportions. The ^{1}H NMR spectrum shows that the two isomers have different chemical shifts for most of the signals, Figure 2.52, and are more separated than for the palladium isomers. The signals that are the most distant from the thiourea, H5, H6a and H6b, show little difference in chemical shift.

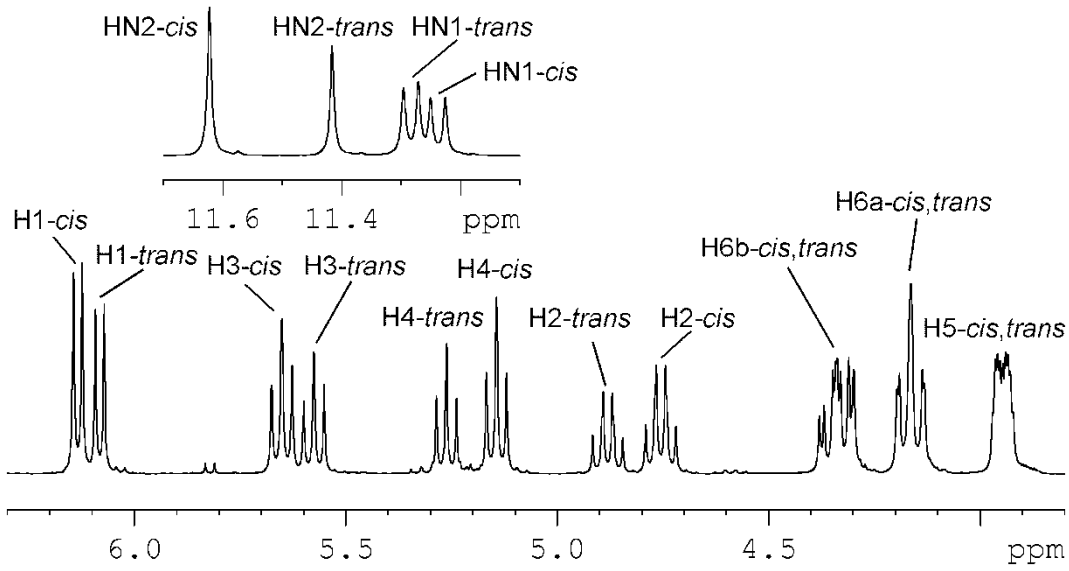

Figure 2.52 *Sugar region of the ^{1}H NMR spectrum of **18a** showing the two sets of signals observed from the cis and trans isomers; inset shows the N–H region.*

A ^{1}H-^{1}H COSY spectrum can be used to trace which sugar signals and which HN1 protons belong to which isomer. However as seen in Figure 2.52 the H5, H6a and H6b signals overlap. Using a SELTOCSY spectrum with a long mixing time separated the signals, Figure 2.53. Unlike the palladium series there is less of a trend in the N–H protons. Figure 2.54 shows an overlay of the N–H portion of the ^{1}H NMR spectra of the series of platinum complexes and **8a**. When the ^{1}H NMR spectrum of the bromide and iodide complexes, **19a** and **20a**, was recorded, isomerisation was also seen.

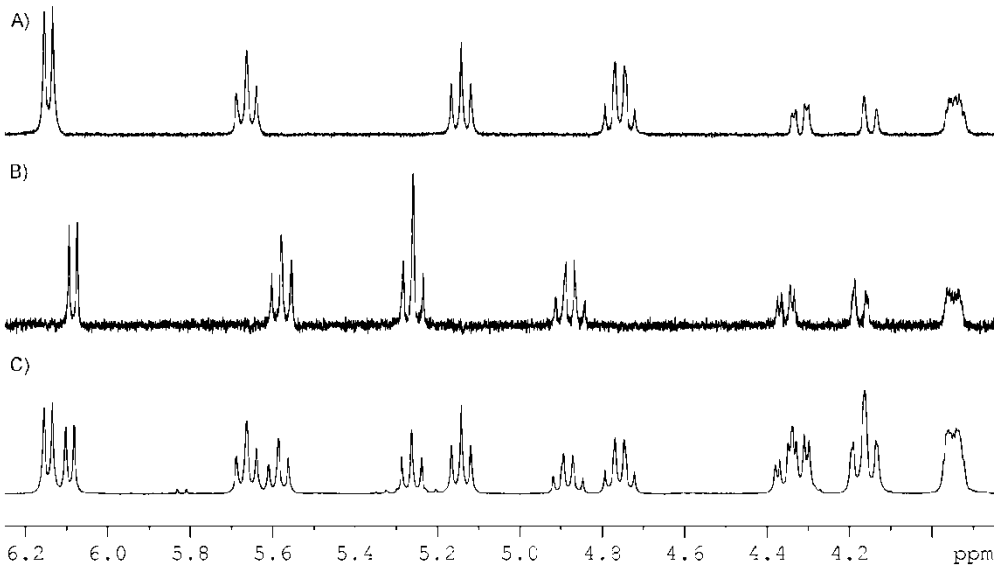

Figure 2.53 *Sugar portion of the ^{1}H NMR spectrum of **18a** comparing A) SELTOCSY spectrum irradiating first H1; B) SELTOCSY spectrum irradiating second H1; C) Standard ^{1}H NMR.*

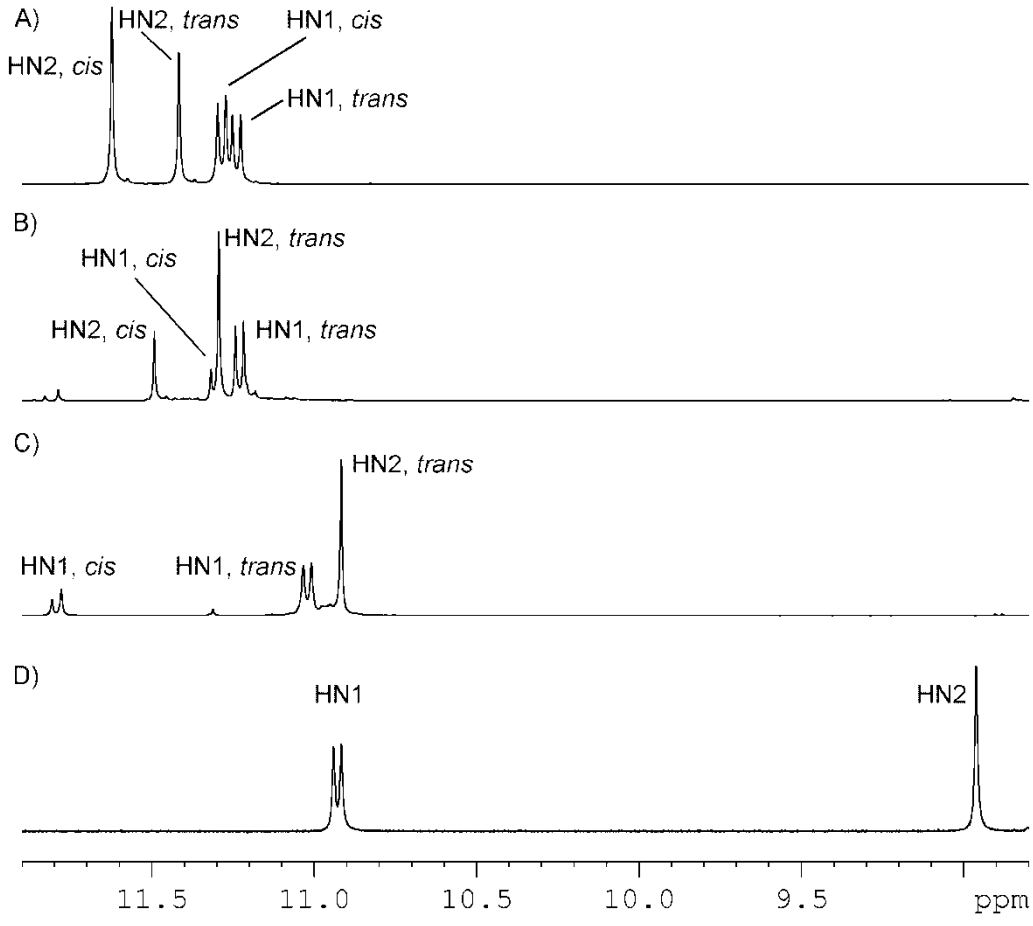

Figure 2.54 *^{1}H NMR spectrum of the N–H region of Pt**8a**$_2$X$_2$ complexes and the ligand showing the changes in chemical shift; A) **18a**; B) **19a**; C) **20a**; D) **8a**.*

As with the palladium chloride analogues the other acyl thiourea **8b**, **8c** and **8d** were used. Table 2.12 summarises selected NMR signals for the complexes. However the **8d** complex was difficult to analyse by NMR. When dissolved in $CDCl_3$ it formed a gel leading to large line broadening of the signals. Only very dilute solutions of the complex could be analysed, so ^{13}C NMR was not run. The coupling constants for HN1 of the complexes were all within the range that suggests the Z,E,Z-anti conformation.

	HN1	**HN2**	**Hc**	**H2**	**C=S**	**C=O, amide**	**C2**
8a	10.92, 9.2 Hz	8.97	7.82	5.08	182.0	166.5	57.9
***trans*-18a**	11.26, 9.9 Hz	11.43	8.01	4.88	178.9	167.3	59.1
***cis*-18a**	11.30, 10.0 Hz	11.64	8.09	4.76	178.0	167.4	59.3
***trans*-19a**	11.22, 10.2 Hz	11.29	8.10	4.81	178.2	167.1	59.3
***cis*-19a**	11.30, NA	11.48	8.21	4.67	177.5	167.3	59.4
***trans*-20a**	11.02, 10.0 Hz	10.92	8.03	4.83	176.4	166.3	59.6
***cis*-20a**	11.79, 11.4 Hz	NA	8.27	4.64	175.5	166.0	59.7
8b	10.71, 9.4 Hz	9.02	8.04	5.06	181.3	164.5	58.0
***trans*-18b**	11.13, 9.9 Hz	11.67	8.41	4.84	178.8	165.9	59.2
***cis*-18b**	11.23, 10.0 Hz	12.01	8.41	4.70	178.3	166.1	59.2
8c	10.61, 9.5 Hz	9.07	7.35	5.07	181.6	156.4	57.9
***trans*-18c**	10.99, 9.9 Hz	11.52	7.75	4.81	178.9	157.3	59.0
***cis*-18c**	10.95, 10.0 Hz	11.58	7.81	4.68	177.9	157.3	59.2
8d	10.62, 9.5 Hz	8.90	7.55	5.06	181.5	160.5	57.8
***trans*-18d**	11.15, NA	11.48	8.18	4.83	NA	NA	NA
***cis*-18d**	11.15, 9.4 Hz	11.69	8.07	4.73	NA	NA	NA

NA: Not determined.

Table 2.12 *Table of selected changes in chemical shifts in the NMR spectra of the acyl thioureas and their complexes with platinum(II) halides.*

If the precipitated mixture of *cis* and *trans* isomers of **18a** was recrystallised from $CHCl_3$ and hexane only one isomer crystallised out; this was apparent since when they were first dissolved in $CDCl_3$ only one set of signals were seen. X-ray diffraction of the crystals was attempted but the crystals were twinned and no structure could be determined. This made it difficult to assign which isomer was from each signal. In a study of the analoguous complexes that **5** makes with platinum(II) it was found that the *cis* isomer had HN2 further downfield than the *trans* isomer [14]. On this basis it could be assumed that the same would be seen for these complexes. Looking at the bromide analogue supports this assumption since the HN1 signal that has gotten smaller, and so is the *cis* isomer, is further downfield, see spectra A) and B) from Figure 2.54. This is also seen for the palladium complexes with the HN2 proton of the *cis* isomer coming further downfield, Figure 2.43. That the isomers may in fact be switched cannot be ruled out however. For this work it was assumed that the *cis* isomer does have its HN2 proton further downfield.

Within several minutes of the recrystallised **18a** being dissolved in $CDCl_3$, the second isomer started to appear. Over a period of 2 hours the compound underwent isomerisation back to the mixture of isomers. Figure 2.55 shows a series of ^1H NMR spectra showing the change, while Figure 2.56 is a graph showing the change in concentration over time.

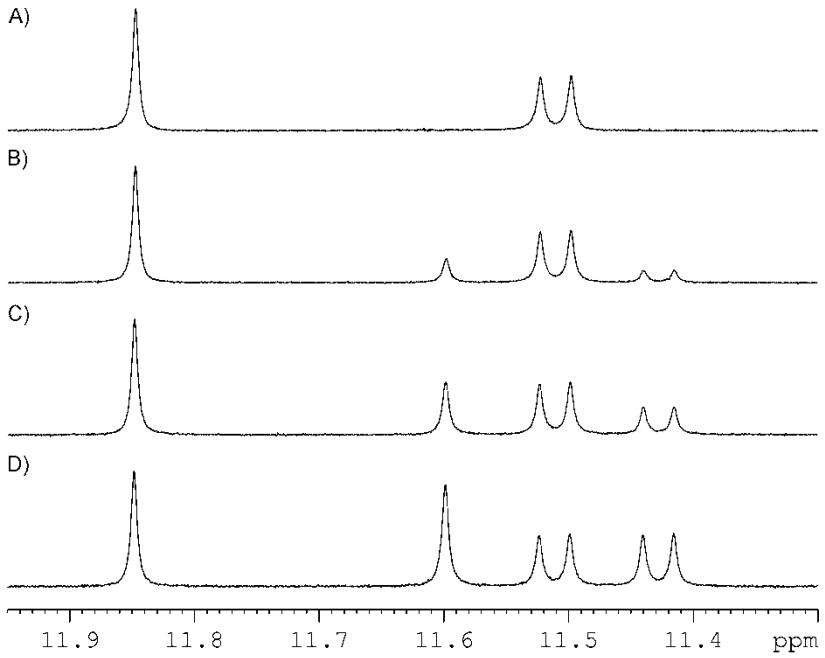

Figure 2.55 *Series of ^{1}H NMR spectra showing the isomerisation of **18a** over time in $CDCl_3$; A) 1 minute after dissolving; B) 30 minutes; C) 1 hour; D) 2 hours.*

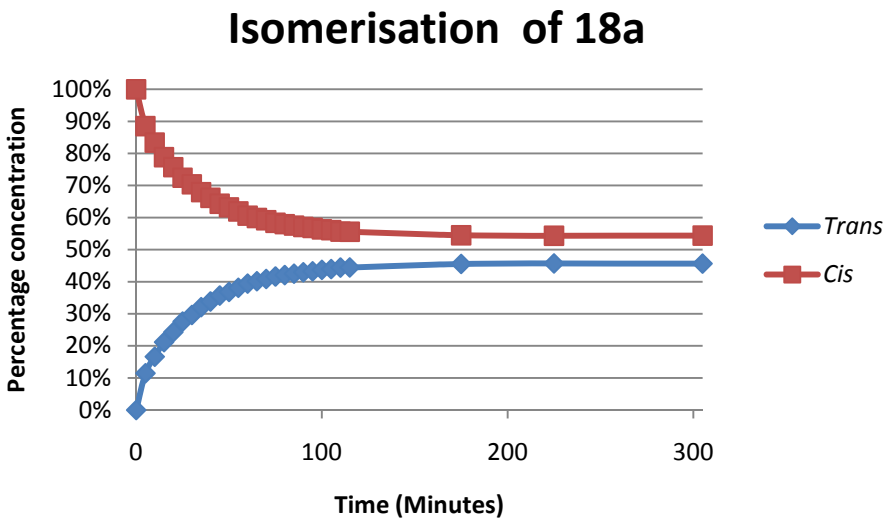

Figure 2.56 *Graph showing the isomerisation of **18a** over time in $CDCl_3$.*

To find the equilibrium constants, the complexes were dissolved in $CDCl_3$ at 27°C and left for 24 hours in the NMR tube. If no change was observed in the peak integration, the integrals were used to get equilibrium constants. Table 2.13

summarises the equilibrium constants. It can be seen as the complexes go from Cl^- > I^- the equilibrium constants shift to favour the *trans* isomer. From the trend in the *trans* effect, it is expected that the *trans* isomer forms the major compound in the bromide and iodide complexes. For **18a**, **18c** and **18d** the *cis* isomers are favoured, while for **18b** the *trans* isomer is slightly favoured. This is a weaker effect than was seen for the palladium complexes where **14b** only formed the *cis* isomer. The other values are different to the palladium analogues where the *trans* isomers are favoured. Except for **18d** all of the complexes favoured the *trans* isomer more than **2**, which again suggests that the bulky thioureas prefer the *trans* isomer more than **1**.

	Equilibrium constant for *cis* ↔ *trans*
2 [14]	0.47
3 [14]	1.41
4 [14]	15.4
18a	0.8
19a	1.9
20a	3.3
18b	1.1
18c	0.6
18d	0.2

Table 2.13 *Equilibrium constants for the equilibrium cis ↔ trans for a series of PtL_2X_2 compounds at 27 °C. It is assumed for the chloride complexes that the cis HN2 signal is further downfield than trans HN2.*

2.10 Reaction of thioureas with HgX_2 (X = Cl, Br or I)

Mercury(II) is a particularly soft cation and so has a preference for sulfur [55]. A number of cyclic thiourea complexes are known [56, 57]. The first benzoyl

thiourea mercury complex was bis(*o*-chlorophenylbenzoylthiourea-κS)-diiodomercury(II) [58], Figure 2.57. There are a number of other structures reported for mercury(II) and thiourea complexes, with different coordination. For example a μ-chloride bridged mercury dimer has been reported [59], Figure 2.57.

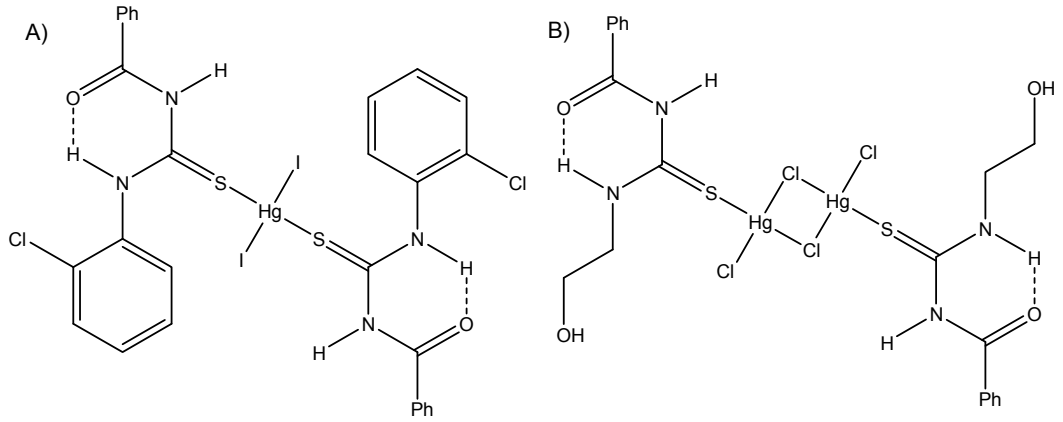

Figure 2.57 *Mercury(II) thiourea complexes with benzoyl thioureas; A) First benzoyl thiourea mercury complex [58]; B) μ-Chloride bridged mercury dimer [59].*

2.10.1 Reaction with 8a

Complexes with mercury could be made by dissolving a two molar equivalent of the thiourea and a mercury(II) halide in a 1:1 mixture of ethanol and acetone stirring for 3 hours, removing the solvent, dissolving the residue in CH_2Cl_2 and filtering through Celite and precipitating with petroleum spirits. Yields were generally high (greater than 95%) and the products needed no further purification and formed the neutral monodentate complex showed in Figure 2.58.

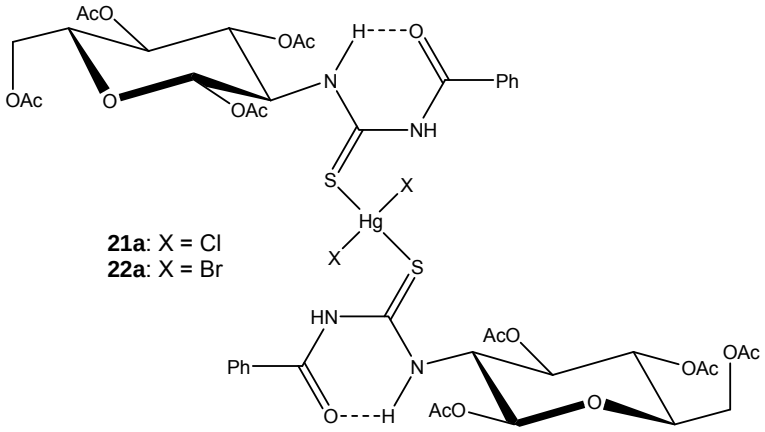

Figure 2.58 *Mercury(II) halide complexes with **8a** acting as a neutral monodentate ligand.*

ESI-MS of complex **21a** only showed very weak ions corresponding to the complexes. The largest peak came from the sodium adduct of the uncoordinated thiourea. Medium intensity ions from the complex were assigned as $[M–2HCl+H]^+$ and $[M–2HCl+Na]^+$. For **22a** the uncoordinated thiourea was the largest peak again and there was only one peak corresponding to the complex. It was of medium intensity and was assigned as $[M–Br]^+$.

The chloride and bromide complexes were soluble in chloroform; however the iodide was much more intractable. Upon dissolution in chloroform HgI_2 quickly precipitated out leaving the uncomplexed thiourea in solution. This could be clearly seen by the ^1H NMR spectra, with chemical shifts matching **8a**, and an orange solid forming in the NMR tube after starting with a white solid. This could be because of an equilibrium between the mercury iodide complexed and uncomplexed with the thiourea and mercury iodide precipitating out of the $CDCl_3$ driving the reaction towards precipitating mercury iodide.

To try and increase the solubility of the mercury iodide so it wouldn't precipitate the complex was analysed in DMSO. It however proved to be unsuitable as a solvent for the iodide complex, as it displaced the thiourea from the complex, again as shown by the ^1H NMR which again showed the chemical shifts at the

position **8a**. This was also seen for the chloride and bromide complexes. To investigate this, a 20 mg sample of **21a** was dissolved in $CDCl_3$ and increasing amounts of DMSO were added, Figure 2.59 shows the series of spectra with increasing amounts of DMSO added. As more DMSO is added the chemical shifts of the N–H proton slowly shift, this is presumably an average signal from a mixed complex that forms in solution. As the concentration increases the protons shift further and further towards the position of the starting thiourea. There are reported structures of mercury(II) halides with DMSO bonding through its oxygen atom [60-63]. The sulfur–mercury bond in these complexes is apparently weak enough to allow the excess of DMSO to displace it.

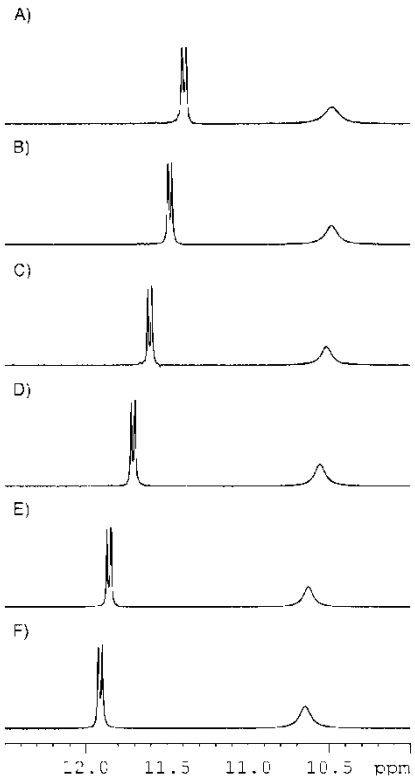

Figure 2.59 *Portion of the ^1H NMR spectrum of **21a** in $CDCl_3$ showing the N–H protons with increasing amounts of DMSO. A) 30 M of DMSO; B) 20 M of DMSO; C) 10 M of DMSO; D). 5 M of DMSO; E) 1 M of DMSO; F) No DMSO added.*

Table 2.14 shows selected chemical shifts and coupling constants. Figure 2.60 shows a portion of the ^{1}H NMR spectra comparing **21a**, **22a** and **8a**. Since mercury(II) forms tetrahedral complexes no isomers were expected, unlike the square planar palladium(II) and platinum(II).

	HN1	HN2	Hc	H2	C=S	C=O, amide	C2
8a	10.92, 9.2 Hz	8.97	7.82	5.08	182.0	166.5	57.9
21a	12.00, 9.6 Hz	10.65	8.12	4.98	181.2	169.6	59.0
22a	11.43, 9.5 Hz	9.58	7.98	4.98	181.6	167.9	58.4

Table 2.14 *Selected chemical shifts and coupling constants from the NMR spectra of **8a** and its complexes with mercury(II) halides.*

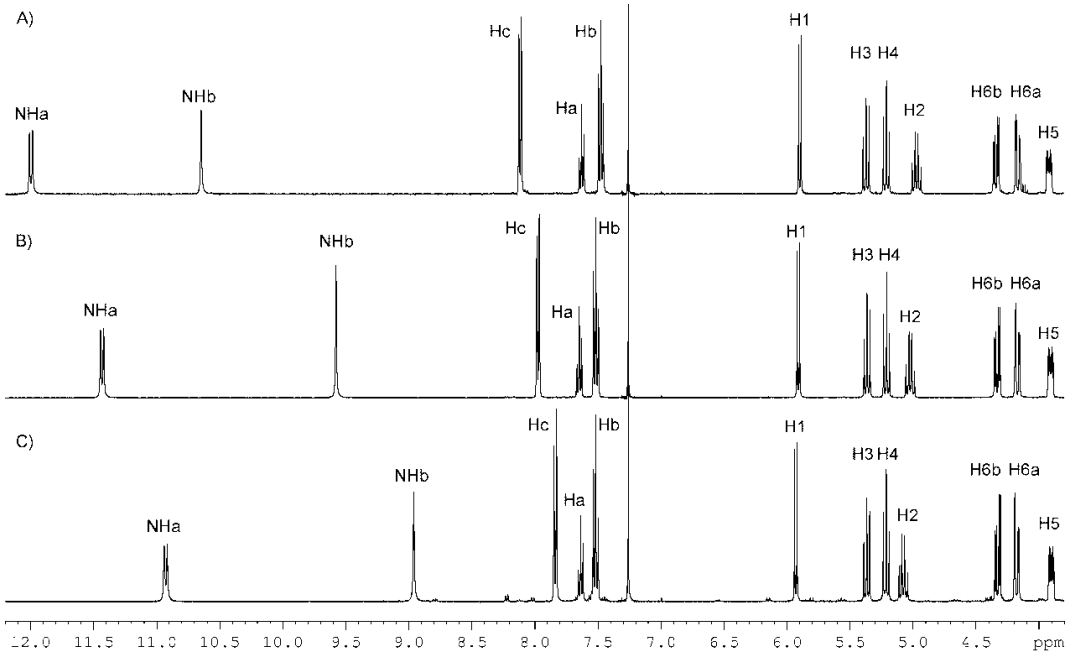

Figure 2.60 *Portion of the ^{1}H NMR spectrum comparing; A) **21a**; B) **22a**; C) **8a**.*

The ^{1}H NMR spectrum shows the thiourea acting as a neutral ligand with both N–H protons present and shifted downfield. This is the same as the previous complexes with the metal pulling electron density off the thiourea and the halide

forming a new hydrogen-bond to HN2. The more electronegative chloride forms a stronger hydrogen-bond and shifts the proton signal further downfield compared to bromide. This effect is also seen for the other signals, with the largest changes in chemical shift from **8a** for the chloride analogue. The coupling constant for HN1 suggests that the thiourea still has the Z,E,Z-anti conformation for both complexes. Unlike the palladium or platinum complexes there is only a small shift for the H2 signal and there is no change for the other carbohydrate signals. Of the aromatic signals only Hc has shifted. There is little change in the chemical shift of the C=S carbon despite being complexed to a metal. The slightly smaller shifts for the sugar signals may be caused by the differences in electronegativity since mercury(II) has a lower electronegativity than palladium(II), platinum(II) and rhodium(III) [64].

2.10.2 Reaction with 8f

The above reaction was repeated with **8f** to investigate the differences a non-acyl thiourea had. Reaction of **8f** with HgX_2 proceeded the same as above. They did not ionise as well as the acyl analogues and no ions were observed by ESI-MS. The ^{1}H NMR spectra of the complexes **21f** and **22f** were not as well defined as **21a** and **22a** with the N–H protons seen as broad signals suggesting they were not as tightly bound as for **21a** and **22a**, and exchanging more rapidly as shown in Figure 2.61 which compares **22f** with **8f**. The broadening is worse for **21f** with HN2 almost completely disappeared. Since H2 couples to the broadened HN1 proton, it is also broad.

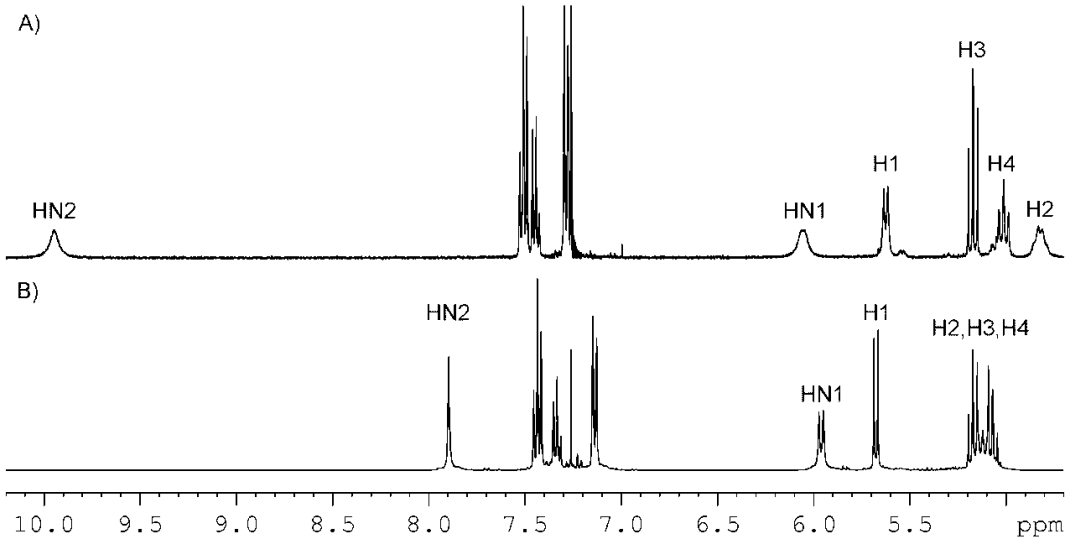

Figure 2.61 *Portion of the ^{1}H NMR spectrum comparing; A) **22f**; B) **8f**.*

Apart from the N–H signals the changes are what would be expected. While HN1 has not moved far, HN2 has shifted downfield as it forms a hydrogen-bond to the halide, and the chloride has shifted HN2 more than the bromide. The sugar signals have moved upfield. Since there is no internal hydrogen-bond for the non-acyl thiourea little can be said about the conformation the thiourea takes. To make things more difficult, without the coupling constant of HN1 nothing is known about the orientation of H2 with respect to HN1. Table 2.15 has selected chemical shifts from the NMR spectrum of **21f**, **22f** and **8f**.

	HN1	HN2	Hc	H2	C=S	C2
8f	5.96	7.90	7.14	5.13	182.0	58.2
21f	12.00	10.65	7.26	4.79	176.8	58.9
22f	11.43	9.58	7.29	4.82	177.5	58.8

Table 2.15 *Selected chemical shifts from the NMR spectra of **8f** and its complexes with mercury(II) halides.*

2.11 Thiourea complexes with Au(I)

2.11.1 LAuCl compounds (L = thiourea)

The neutral ligand, tetrahydrothiophene (THT), in (THT)AuX (where X is an anion) is only weakly bound to the gold(I) atom and is very easily displaced. The sulfur atom on a thiourea is very soft and therefore has a strong affinity for gold making it ideal to displace the ligand. Many sulfur compounds have been used in this reaction including thiourea examples. Other methods have been used such as using a reducing agent to produce gold(I) *in situ*. For example gold(III) halides were reduced with SO_2 before addition of the thiourea [65]. The thiourea itself can act as a reducing agent so when an excess of tetramethyl thiourea reacted with Au_2O_3 and HBr a mixture of products was formed, one of which was LAuBr [66]. The displacement of THT has been used with a DNA intercalating molecule with a thiourea side chain that was reacted with a range of (THT)AuX (Cl, Br or NCS^-) compounds to produce complexes that showed potent activity against *Mycobacterium tuberculosis* [67]. Gold(I) compounds are of interest as there is a very long history of known gold compounds with biological activity such as Robert Koch's discovery in 1890 that $K[Au(CN)_2]$ had anti-bacterial properties [68]. Auranofin is used in the treatment of rheumatoid arthritis [69] and Sanocrysin has long been studied for its activity against *Mycobacterium tuberculosis* [70], Figure 2.62. The sugar thiourea in Figure 2.9 was reacted with $(Me_2S)AuCl$ to produce a RAuCl complex [25].

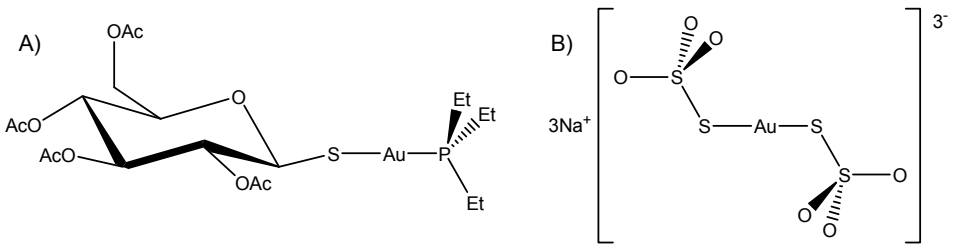

Figure 2.62 *Gold complexes with biological activity; A) Auranofin used in the treatment of arthritis [69]; B) Sanocrysin potent against Mycobacterium tuberculosis [70].*

If **8a** is stirred with a molar equivalent of (THT)AuCl in dichloromethane overnight, a white solid can be isolated. Figure 2.63 shows **23a**. The ^{1}H NMR spectrum shows that the thiourea is still a neutral ligand with the two N–H protons still seen. Figure 2.64 has the ^{1}H NMR spectrum of **23a**.

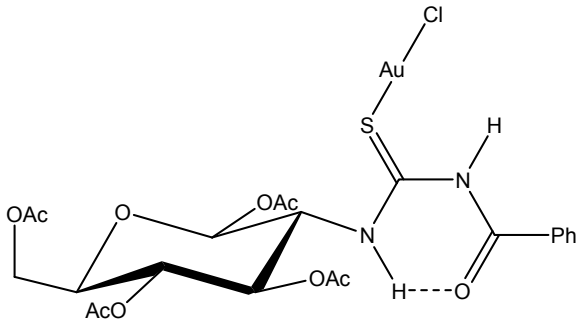

Figure 2.63 **23a** *with* ***8a*** *acting as a neutral monodenatate ligand.*

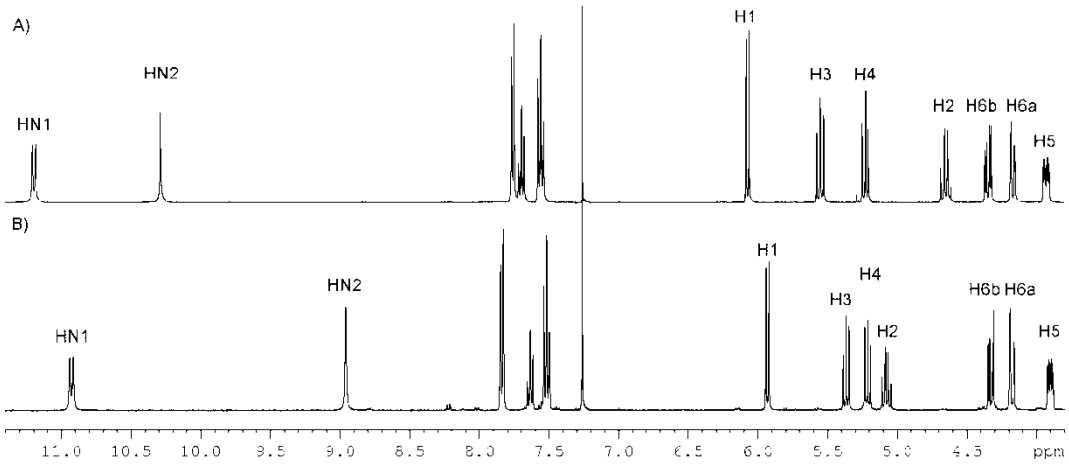

Figure 2.64 *Portion of the ^{1}H NMR spectra comparing; A)* ***23a****; B)* ***8a****.*

Both N–H signals have been shifted upfield, with HN2 shifting more because of the removal of electron density by the metal centre affecting it much more since the HN1 proton has already lost a lot of electron density because of the hydrogen-bond. Unlike with the other examples of metal halide complexes mentioned already (i.e. L_2PdCl_2 or $LRhCp^*Cl_2$ etc) the HN2 proton is not likely to be forming a hydrogen-bond to the chloride because of the linear bonding of

gold(I). As shown with two examples in Figure 2.65, the hydrogen–chloride distance is further than would be credible. The coupling constant for HN1 suggests that the thiourea still has the Z,E,Z-anti conformation. The carbohydrate region also sees shifts from the metal pulling electron density off the thiourea. There are small shifts for H1 and H3, while H4, H5, H6a and H6b show negligible shifts as would be expected since they are further from any change. The biggest shift is for H2 which has moved 0.43 ppm upfield to 4.65 ppm. In the ^{13}C NMR spectrum there is very little change. The C=S carbon has shifted upfield to 179.6 from 182.0 ppm. The amide C=O carbon has a negligible shift (166.4 from 166.5 ppm). For the carbohydrate region the only change comes from C2 which shifts downfield to 59.4 from 57.9 ppm.

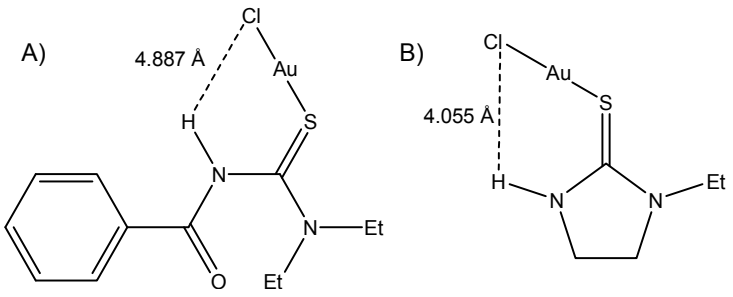

Figure 2.65 *Diagram showing distance between the proton and chloride in two thiourea–AuCl crystal structures; A) [71]; B) [72].*

The other acyl thioureas also react with (THT)AuCl to form neutral complexes. They all formed white solids except for the *p*-nitro analogue which was yellow. Their NMR spectra were similar to **23a** and selected chemical shifts and coupling constants are given in Table 2.16. The stability of the complexes was tested by dissolving **23a** in deuterated DMSO and recording the ^{1}H NMR spectrum. This showed the ^{1}H NMR shifts coming at the same positions as the parent thiourea, evidence that the gold has been displaced. The thiourea sulfur–gold (I) bond is apparently weak enough for the DMSO to displace.

	HN1	HN2	Hc	H2	C=S	C=O, amide	C2
8a	10.92, 9.2 Hz	8.97	7.82	5.08	182.0	166.5	57.9
23a	11.20, 10.0 Hz	10.29	7.76	4.65	179.6	166.2	60.5
24a	11.12, 9.7 Hz	9.76	7.82	4.83	180.7	166.4	59.4
8b	10.71, 9.4 Hz	9.02	8.04	5.06	181.3	164.5	58.0
23b	11.08, 9.6 Hz	10.55	8.30	4.81	180.2	165.4	59.5
8c	10.61, 9.5 Hz	9.07	7.35	5.07	181.6	156.4	57.9
24c	10.75, 9.8 Hz	9.82	7.43	4.78	180.1	156.0	59.7
8d	10.62, 9.5 Hz	8.90	7.55	5.06	181.5	160.5	57.8
23d	10.78, 10.1 Hz	10.05	7.30	4.64	178.8	160.2	60.8

Table 2.16 *Selected chemical shifts and coupling constants from the NMR spectra of acyl thioureas and their complexes with gold(I).*

The complexes were unstable if exposed to light and at room temperature. They decomposed to elemental gold, with samples turning purple overnight. This was also seen for the analogous complex made with the sugar thiourea in Figure 2.9 (Page 22) [25]. Accurate elemental analysis could not be determined for these complexes.

2.11.2 $[L_2Au]Cl$ compounds (L = thiourea)

If two molar equivalents of the thiourea are reacted with (THT)AuCl in dichloromethane both the THT and the chloride are displaced giving the cationic species $[L_2Au]Cl$. Such compounds have been made before, for example a four molar excess of thiourea ($H_2N(C=S)NH_2$) was reacted with $HAuCl_4$ to produce $[L_2Au]Cl$ [73]. A cyclic thiourea has been used recently to form a complex of the form $[L_2Au]Cl$ and was shown to be cytotoxic to cancer cells as well as an inhibitor of thioredoxin reductase [74].

The ^{1}H NMR spectrum is very similar to LAuCl. The major difference is that HN2 has been shifted downfield less than with LAuCl. The coupling constant for HN1 of 9.7 Hz suggests that the thiourea still has the Z,E,Z-anti conformation. The carbohydrate portion also shows smaller shifts, for example H2 has only shifted to 4.83 ppm, compared with 4.65 ppm for LAuCl. Evidently the RAuR moiety removes less electron density than RAuCl, which makes sense since the electronegative chloride is no longer directly attached to the molecule. There is little change in the aromatic signals. Figure 2.66 shows the comparison of ^{1}H NMR of **24a**, **23a** and **8a**. The ^{13}C NMR spectrum is also very similar with the main changes coming from C=S and C2. Table 2.16 has selected chemical shifts and coupling constants for **24a**.

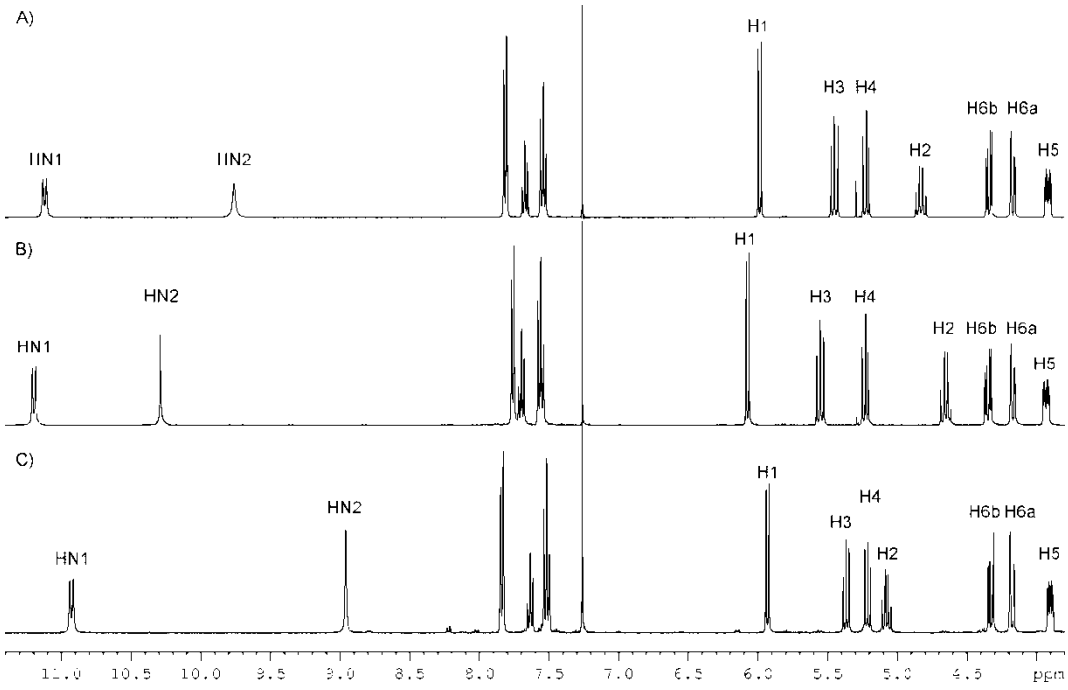

Figure 2.66 *Portion of the ^{1}H NMR spectrum comparing; A) **24a** B) **23a**; C) **8a**.*

2.11.3 [LAuPPh$_3$]Cl compounds (L = thiourea)

Previously thioureas have been reacted with R_3PAuCl in methanol to give complexes of the form $[R_3PAuL]Cl$, where the thiourea has bonded as a neutral ligand to the gold(I) forming a cationic species [75]. When the reaction was

carried out with Ph_3PAuCl and **8a**, ESI-MS showed the presence of an ion corresponding to [**8a**$AuPPh_3$]$^+$ but when the reaction was worked up unreacted Ph_3PAuCl was obtained. A different synthesis to get a similar product was to react Ph_3PAuCl with $AgNO_3$ and filter off the AgCl before adding the thiourea [67]. This was attempted with **8a**, but gave no product that could be isolated.

2.12 Conclusions

The acyl thioureas make excellent neutral ligands. They are able to form monodenatate ligands to a wide variety of metals. The internal hydrogen-bond the acyl thioureas have is a vital part of their bonding, and remains when they form complexes. The hydrogen-bond helps to drive the Z,E,Z-anti conformation seen for the acyl thiourea, and could be inferred from the value of the coupling constant of HN1. For all the complexes formed where coupling constant for HN1 could be determined showed values of 8.8-10.0 Hz. This is consistent with retention of the Z,E,Z-anti conformation, and remains despite large changes such as; the oxidation number of the metal (I, II or III); the type of anions on the metal (Cp*, *p*-cymene, COD or a halide); and the coordination number (2 or 4).

^{1}H NMR was an excellent technique for characterization of the complexes showing clear changes upon coordination. When a complex had formed the ^{1}H NMR signals for the N–H protons are shifted downfield by the metal centre withdrawing electron density from the thiourea portion of the molecule and if possible the formation of hydrogen-bond to a halide on the metal.

The importance of the hydrogen-bond could be seen with the non-acyl thiourea, **8f**, complexes with mercury(II) halides. The ^{1}H NMR showed very broad N–H signals unlike any of the acyl thioureas. Despite this they still formed complexes readily.

The functionality on the aromatic group was also important, with it imparting different properties on the complexes. For example the presence of the thiophene moiety caused the PtL_2Cl_2 complex to form a gel. Another example was the *p*-nitro moiety causing the PdL_2Cl_2 complex to only form the *trans* isomer.

2.13 Experimental

The general experimental procedures are in Appendix One with the synthesis of **7**·HCl and **7**. NMR information is in Appendix Two and X-ray diffraction details are in Appendix Three. D-Glucosamine hydrochloride, 4-methoxybenzaldehyde and phenyl isothiocyanate were purchased from Aldrich and used without further purification. **8e** [28], **8f** [28], $[Cp^*RhCl_2]_2$ [76] and (THT)AuCl [77] were made according to literature procedures.

Table 2.17 *Summary of the crystallographic data for the structures in Chapter Two.*

	8a	**8e**	**9a**	**14b**
Molecular formula	$2\cdot(C_{22}H_{26}N_2O_{10}S)$	$C_{14}H_{18}N_2O_6S$	$2\cdot(C_{32}H_{41}N_2O_{10}SCl_2Rh)$	$C_{44}H_{50}N_6O_{24}S_2Cl_2Pd\cdot3(C_4H_8O)$
Lattice	Orthorhombic	Orthorhombic	Orthorhombic	Orthorhombic
Space group	$P2_12_12_1$	$P2_12_12_1$	$P2_12_12_1$	$P2_12_12_1$
Z	8	4	8	4
a (Å)	8.8623(11)	6.1311(2)	16.4914(4)	15.9834(7)
b (Å)	21.342(4)	12.9802(4)	47.0882(13)	21.7896(12)
c (Å)	26.328(4)	19.2667(6)	9.3446(2)	22.5637(11)
α (°)	90	90	90	90
β (°)	90	90	90	90
γ (°)	90	90	90	90
Unit cell volume ($Å^3$)	4979.7(13)	1533.30(8)	7256.6(3)	7858.3(7)
Calculated density (g cm^{-3})	1.362	1.483	1.500	1.272
θ range (°)	2.49 to 26.49	1.89 to 27.94	1.31 to 26.47	1.30 to 27.93
Reflections collected, unique	41827 / 10158	11727, 3665	152951, 14947	61506, 18398
R(int)	0.2232	0.0571	0.0849	0.0987
Data, restraints, parameters	10158 / 0 / 651	3665, 0, 263	14947, 673, 715	18398 / 704 / 805
Goodness-of-fit on F^2	0.918	1.010	1.028	0.943
Final R indices [I>2σ(I)]; R1, wR2	0.0630, 0.1060	0.0442, 0.0821	0.1226, 0.2974	0.0932, 0.2469
R indices (all data); R1, wR2	0.2209, 0.1512	0.0622, 0.0895	0.1368, 0.3089	0.2003, 0.3118
Largest diff. peak and hole (e $Å^{-3}$)	0.298 and -0.361	0.340 and -0.270	1.463 and -1.513	1.631 and -0.700
Flack parameter	0.18(13)	0.04(9)	0.12(7)	-0.05(5)

8a

Benzoyl chloride (0.19 mL, 0.295 g, 2.10 mmol) and KSCN (0.204 g, 2.10 mmol) were refluxed in dry acetone (15 mL) for 10 minutes. **7** (0.730 g, 2.10 mmol) was dissolved in dry CH_2Cl_2 (10 mL) and added to the acetone suspension and stirred overnight at room temperature. Water (30 mL) was added and the organic phase collected, the aqueous layer was washed with dichloromethane (2 × 20 mL). The organic phases were combined, dried ($MgSO_4$), filtered and evaporated under reduced pressure. The residue was recrystallised from hot ethanol to give white crystals of **8a** (0.808 g, 75.4%).

^{1}H NMR: δ 10.92 (d, 1H, $J_{NH,H2}$, 9.2 Hz, HN1), 8.97 (s, 1H, HN2), 7.82 (m, 2H, Hc), 7.62 (m, 1H, Ha), 7.51 (m, 2H, Hb), 5.94 (d, 1H, $J_{H1,H2}$, 8.1 Hz, H1), 5.38 (dd, 1H, $J_{H3,H4}$ 8.8 Hz, $J_{H2,H3}$ 9.8 Hz, H3), 5.21 (m, 1H, H4), 5.08 (m, 1H, H2), 4.32 (dd, 1H, $J_{H5,H6b}$ 4.8 Hz, $J_{H6a,H6b}$ 12.4 Hz, H6b), 4.17 (dd, 1H, $J_{H5,H6a}$ 2.7 Hz, $J_{H6a,H6b}$ 12.4 Hz, H6a), 3.91 (ddd, 1H, $J_{H5,H6a}$ 2.7 Hz, $J_{H5,H6b}$ 4.8 Hz, $J_{H4,H5}$ 9.4 Hz, H5), 2.12, 2.10, 2.06, 2.05 (4s, 12H, 4 × OAc) ppm. ^{13}C NMR: δ 182.0 (C=S), 170.8, 170.4, 169.5, 169.2 (4 × C=O, acetyl), 166.5 (C=O, amide), 134.0 (Ca), 131.4 (Cd), 129.3 (Cb), 127.7 (Cc), 92.4 (C1), 73.1 (C5), 72.4 (C3), 67.7 (C4), 61.9 (C6), 57.9 (C2), 21.1, 20.9, 20.8, 20.7 (4 × CH_3) ppm. MS: *m/z*: 533.119 (strong, $[M + Na]^+$, calc. 533.120), 549.091 (medium, $[M + K]^+$, calc. 549.094), 1043.251 (strong, $[2M + Na]^+$, calc. 1043.251), 1059.222 (weak, $[2M + K]^+$, calc. 1059.225).

8b

p-Nitrobenzoyl chloride (0.750 g, 4.04 mmol) was dissolved in dry acetonitrile (10 mL) under N_2 and cooled to 0 °C. KNCS (0.392 g, 4.04 mmol) was added and stirred for 1 hour at 0 °C. The mixture was allowed to warm to room temperature and **7** (1.404 g, 4.04 mmol) in dry CH_2Cl_2 (10 mL) was added and stirred for 16 hours. The mixture was poured into water (100 mL) and the organic layer separated, the aqueous phase was washed with CH_2Cl_2 (2 × 15 mL), the organic phases were combined, dried ($MgSO_4$), filtered and evaporated under reduced

pressure to give a pale yellow foam. The crude product was recrystallised from hot ethanol to give **8b** as a pale yellow solid (2.036 g, 90.7%).

^{1}H NMR: δ 10.71 (d, 1H, $J_{H2,HN1}$ 9.4 Hz, HN1), 9.02 (s, 1H, HN2), 8.36 (dt, 2H, Hb), 8.04 (dt, 2H, Hc), 5.93 (d, 1H, $J_{H1,H2}$ 8.1 Hz, H1), 5.35 (dd, 1H, $J_{H3,H4}$ 8.7 Hz, $J_{H2,H3}$ 9.8 Hz, H3), 5.21 (t, 1H, H4), 5.06 (dt, 1H, H2), 4.33 (dd, 1H, $J_{H5,H6b}$ 4.8 Hz, $J_{H6a,H6b}$ 12.4 Hz, H6b), 4.18 (dd, 1H, $J_{H5,H6a}$ 2.7 Hz, $J_{H6a,H6b}$ 12.4 Hz, H6a), 3.91 (ddd, 1H, $J_{H5,H6a}$ 2.7 Hz, $J_{H5,H6b}$ 4.8 Hz, $J_{H4,H5}$ 9.4 Hz, H5), 2.13, 2.11, 2.07, 2.05 (4s, 12H, 4 × OAc) ppm. ^{13}C NMR: δ 181.3 (C=S), 170.8, 170.5, 169.4, 169.2 (4 × C=O, acetyl), 164.5 (C=O, amide), 151.0 (Ca), 136.8 (Cd), 129.1 (Cb), 124.4 (Cc), 92.3 (C1), 73.1 (C5), 72.3 (C3), 67.6 (C4), 61.8 (C6), 58.0 (C2), 21.2, 20.9, 20.8, 20.7 (4 × CH_3) ppm. *Anal.* Calcd for $C_{22}H_{25}N_3O_{12}S$ (555.512): C, 47.57; H, 4.54; N, 7.56. Found: C, 47.46; H, 4.70; N, 7.29. MS: *m/z*: 578.110 (strong, $[M + Na]^+$, calc. 578.105), 594.078 (weak, $[M + K]^+$, calc. 594.079), 1133.219 (weak, $[2M + Na]^+$, calc. 1133.221).

8c

2-Furoyl chloride (0.5 mL, 0.622 g, 5.07 mmol) was dissolved in dry acetone (10 mL) under nitrogen, NH_4NCS (0.386 g, 5.07 mmol) was added and refluxed for 10 minutes. **7** (1.762 g, 5.07 mmol) in dry CH_2Cl_2 (10 mL) was added and stirred for 16 hours. The mixture was poured into water (100 mL) and the organic layer separated, the aqueous phase was washed with CH_2Cl_2 (3 × 15 mL), the organic phases were combined, dried ($MgSO_4$), filtered and evaporated under reduced pressure to give a pale yellow foam. The crude product was recrystallised from hot ethanol to give white crystals of **8c** (2.119 g, 83.5%).

^{1}H NMR: δ 10.61 (d, 1H, $J_{H2,HN1}$ 9.5 Hz, HN1), 9.07 (s, 1H, HN2), 7.57 (dd, 1H, $J_{Ha,Hc}$ 0.8 Hz, $J_{Ha,Hb}$ 1.8 Hz, Ha), 7.35 (dd, 1H, $J_{Ha,Hc}$ 0.8 Hz , $J_{Hb,Hc}$ 3.6 Hz, Hc), 6.61 (dd, 1H, $J_{Ha,Hb}$ 1.8 Hz , $J_{Hb,Hc}$ 3.6 Hz, Hb), 5.90 (d, 1H, $J_{H1,H2}$ 8.3 Hz, H1), 5.33 (dd, 1H, $J_{H3,H4}$ 8.9 Hz, $J_{H2,H3}$ 9.9 Hz, H3), 5.20 (t, 1H, H4), 5.07 (dt, 1H, H2), 4.32 (dd, 1H, $J_{H5,H6b}$ 4.7 Hz, $J_{H6a,H6b}$ 12.4 Hz, H6b), 4.16 (dd, 1H, $J_{H5,H6a}$ 2.5 Hz, $_{H6a,H6b}$

12.4 Hz, H6a), 3.88 (ddd, 1H, $J_{H5,H6a}$ 2.5 Hz, $J_{H5,H6b}$ 4.7 Hz, $J_{H4,H5}$ 9.5 Hz, H5), 2.12, 2.10, 2.05, 2.04 (4s, 12H, 4 × OAc) ppm. ^{13}C NMR: δ 181.6 (C=S), 170.8, 170.4, 169.5, 169.3 (4 × C=O, acetyl), 156.4 (C=O, amide), 146.5 (Ca), 144.9 (Cd), 119.4 (Cc), 113.6 (Cb), 92.4 (C1), 73.1 (C5), 72.4 (C3), 67.7 (C4), 61.8 (C6), 57.9 (C2), 21.1, 20.9, 20.8, 20.7 (4 × CH_3) ppm. *Anal.* Calcd for $C_{20}H_{24}N_2O_{11}S$ (500.476): C, 48.00; H, 4.83; N, 5.60. Found: C, 48.48; H, 4.86; N, 5.61. MS: *m/z*: 523.099 (strong, $[M + Na]^+$, calc. 523.099), 539.078 (weak, $[M + K]^+$, calc. 539.073), 1023.211 (medium, $[2M+Na]^+$, calc 1023.209).

8d

8d was made using the same method as **8c**, 2-Thiophene carbonyl chloride (0.5 mL, 0.686 g, 4.68 mmol), NH_4NCS (0.356 g, 4.68 mmol) and **7** (1.624 g, 4.68 mmol). Worked up to give white crystals of **8d** (2.118 g, 87.7%).

^{1}H NMR: δ 10.62 (d, 1H, $J_{H2,HN1}$ 9.5 Hz, HN1), 8.90 (s, 1H, HN2), 7.62 (dd, 1H, $J_{Ha,Hc}$ 1.2 Hz, $J_{Ha,Hb}$ 5.0 Hz, Ha), 7.55 (dd, 1H, $J_{Ha,Hc}$ 1.2 Hz, $J_{Hb,Hc}$ 3.9 Hz, Hc), 7.04 (dd, 1H, $J_{Hb,Hc}$ 3.9 Hz, $J_{Ha,Hb}$ 5.0 Hz, Hb), 6.01 (d, 1H, $J_{H1,H2}$ 8.3 Hz, H1), 5.47 (dd, 1H, $J_{H3,H4}$ 8.9 Hz, $J_{H2,H3}$ 10.0 Hz, H3), 5.14 (t, 1H, H4), 5.06 (dt, 1H, H2), 4.27 (dd, 1H, $J_{H5,H6b}$ 4.7 Hz , $J_{H6a,H6b}$ 12.4 Hz, H6b), 4.11 (dd, 1H, $J_{H5,H6a}$ 2.6 Hz, $J_{H6a,H6b}$ 12.4 Hz, H6a), 3.89 (ddd, 1H, $J_{H5,H6a}$ 2.6 Hz, $J_{H5,H6b}$ 4.7 Hz, $J_{H4,H5}$ 9.6 Hz, H5), 2.06, 2.03, 1.99, 1.98 (4s, 12H, 4 × OAc) ppm. ^{13}C NMR: δ 181.5 (C=S), 170.6, 170.4, 169.4 × 2 (4 × C=O, acetyl), 160.5 (C=O, amide), 135.8 (Cd), 134.4 (Ca), 130.8 (Cc), 128.4 (Cb), 92.1 (C1), 72.7 (C5), 72.3 (C3), 67.8 (C4), 61.8 (C6), 57.8 (C2), 21.0, 20.7 × 2, 20.6 (4 × CH_3) ppm. *Anal.* Calcd for $C_{20}H_{24}N_2O_{10}S_2$ (516.542): C, 46.50; H, 4.68; N, 5.42. Found: C, 46.66; H, 4.70; N, 5.41. MS: *m/z*: 539.078 (strong, $[M + Na]^+$, calc. 539.077), 555.051 (weak, $[M + K]^+$, calc. 555.050), 1055.164 (medium, $[2M + Na]^+$, calc. 1055.164).

9a

8a (27.3 mg, 0.0535 mmol) and $[Cp^*RhCl_2]_2$ (16.5 mg, 0.0267 mmol) were dissolved in CH_2Cl_2 (10 mL) and stirred for 2 hours. The solution was filtered through Celite and the solvent removed under reduced pressure. The residue was recrystallised from CH_2Cl_2 and petroleum spirits to give **9a** (23.4 mg, 53.4%).

^{1}H NMR: δ 11.83 (d, 1H, $J_{HN1,H2}$ 8.5 Hz, HN1), 11.38 (s, 1H, HN2), 8.26 (m, 2H, Hc), 7.52 (m, 1H, Ha), 7.44 (m, 2H, Hb), 5.83 (d, 1H, $J_{H1,H2}$ 8.3 Hz, H1), 5.33 (dd, 1H, $J_{H3,H4}$ 9.0 Hz, $J_{H2,H3}$ 9.9 Hz, H3), 5.23 (t, 1H, H4), 5.08 (dt, 1H, H2), 4.39 (dd, 1H, $J_{H5,H6b}$ 5.0 Hz, $J_{H6a,H6b}$ 12.5 Hz, H6b), 4.14 (dd, 1H, $J_{H5,H6a}$ 2.4 Hz, $J_{H6a,H6b}$ 12.5 Hz, H6a), 3.91 (ddd, 1H, $J_{5,6a}$ 2.5 Hz, $J_{5,6b}$ 5.0 Hz, $J_{4,5}$ 9.6 Hz, H5), 2.21, 2.06 (2s, 6H, 2 × OAc), 2.12 (1s, 6H, 2 × OAc) ppm. ^{13}C NMR: δ 182.3 (C=S), 170.9, 170.3, 169.8, 169.2 (4 × C=O, acetyl), 169.7 (bs, C=O, amide), 133.8 (Ca), 130.8 (Cd), 130.2 (Cc), 128.6 (Cb), 92.5 (C1), 73.3 (C5), 72.2 (C3), 67.8 (C4), 61.9 (C6), 57.9 (C2), 21.3, 21.0, 20.8, 20.8 (4 × CH_3) ppm. *Anal.* Calcd for $C_{32}H_{41}N_2O_{10}SCl_2Rh$ (819.552): C, 46.90; H, 5.04; N, 3.42. Found: C, 47.16; H, 4.84; N, 3.72. MS: *m/z*: 747.149 (strong, $[M–H–2Cl]^+$, calc. 747.145), 769.131 (weak, $[M–2HCl+Na]^+$, calc. 769.127), 805.108 (weak, $[M–HCl+Na]^+$, calc. 805.104), 1529.260 (weak, $[2(M–H–2Cl)+Cl]^+$, calc. 1529.260), 1551.243 (weak, $[2(M–2HCl)+NaCl+H]^+$, calc. 1551.242), 1587.225 (weak, $[2(M–HCl)+Na]^+$, calc. 1587.219).

11a

8a (104 mg, 0.203 mmol) and $[Rh(COD)Cl]_2$ (50.0 mg, 0.101 mmol) were dissolved in CH_2Cl_2 (15 mL) and stirred for 1 hour. The solution was filtered through Celite and the solvent removed under reduced pressure. The residue was recrystallised with CH_2Cl_2 and petroleum spirits to give **11a** (128 mg, 83.3%).

^{1}H NMR: δ 12.34 (s, 1H, HN2), 11.53 (d, 1H, $J_{HN1,H2}$ 9.7 Hz, HN1), 8.12 (m, 2H, Hc), 7.58 (m, 1H, Ha), 7.47 (m, 2H, Hb), 5.85 (d, 1H, $J_{H1,H2}$ 8.3 Hz, H1), 5.33 (dd, 1H, $J_{H3,H4}$ 9.0 Hz, $J_{H2,H3}$ 9.8 Hz, H3), 5.17 (t, 1H, H4), 4.93 (dt, 1H, H2) 4.33 (dd,

1H, $J_{H5,H6b}$ 4.7 Hz, $J_{H6a,H6b}$ 12.4 Hz, H6b), 4.31 (b, 4H, CH), 4.13 (dd, 1H, $J_{H5,H6a}$ 2.4 Hz, $J_{H6a,H6b}$ 12.4 Hz, H6a), 3.89 (ddd, 1H, $J_{5,6a}$ 2.4 Hz, $J_{5,6b}$ 4.6 Hz, $J_{4,5}$ 9.5 Hz, H5), 2.46 (m, 4H, CH_2), 2.16, 2.09, 2.08, 2.04 (4s, 12H, 4 × OAc), 1.88 (m, 4H, CH_2) ppm. ^{13}C NMR: δ 182.6 (C=S), 170.7, 170.2, 169.5, 169.1 (4 × C=O, acetyl), 169.5 (C=O, amide), 134.1 (Ca), 131.0 (Cd), 129.4 (Cc), 128.8 (Cb), 92.2 (C1), 73.1 (C5), 72.3 (C3), 67.6 (C4), 61.7 (C6), 57.6 (C2), 31.1 (4 × CH_2), 21.2, 20.8 × 2, 20.7 (4 × CH_3) ppm. *Anal.* Calcd for $C_{30}H_{38}N_2O_{10}SClRh$ (757.054): C, 47.60; H, 5.06; N, 3.70. Found: C, 47.16; H, 4.84; N, 3.72. MS: *m/z*: 743.117 (strong, $[M–HCl+Na]^+$, calc. 743.112).

12a

8a (83.4 mg, 0.163 mmol) and [(*p*-cymene)$RuCl_2$]$_2$ (50.0 mg, 0.0816 mmol) were dissolved in CH_2Cl_2 (10 mL) and stirred for 1 hour. The solution was filtered through Celite and the solvent removed under reduced pressure. The residue was recrystallised with CH_2Cl_2 and petroleum spirits to give **12a** (0.102 mg, 76.4%).

^{1}H NMR: δ 11.71 (d, 1H, $J_{H2,NH}$ 9.6 Hz, HN1), 11.28 (s, 1H, HN2), 8.19 (m, 2H, Hc), 7.51 (m, 1H, Ha), 7.42 (m, 1H, Hb), 5.83 (d, 1H, $J_{H1,H2}$ 8.4 Hz, H1), 5.45 (m, 2H, H9), 5.30 (m, 2H, H8), 5.32 (dd, 1H, $J_{H3,H4}$ 9.0 Hz, $J_{H2,H3}$ 10.0 Hz, H3), 5.23 (t, 1H, H4), 5.07 (dt, 1H, $J_{1,2}$ 8.4 Hz, $J_{H2,HN1}$; $J_{H2,H3}$ 10.0 Hz, H2), 4.38 (dd, 1H, $J_{H5,H6b}$ 4.9 Hz , $J_{H6a,H6b}$ 12.5, H6b), 4.15 (dd, 1H, $J_{H5,H6a}$ 2.4 Hz, $J_{H6a,H6b}$ 12.5 Hz, H6a), 3.91 (ddd, 1H, $J_{H5,6a}$ 2.4 Hz, $J_{H5,H6b}$ 4.9 Hz, $J_{H4,H5}$ 9.6 Hz, H5), 3.03 (qn, 1H, H10), 2.28 (s, 3H, H7), 2.18, 2.12, 2.09, 2.06 (4s, 12H, 4 × OAc), 1.35 (d, 6H, H11) ppm. ^{13}C NMR: δ 183.5 (C=S), 170.7, 170.3, 169.7, 169.1 (4 × C=O, acetyl), 169.4 (C=O, amide), 133.8 (Ca), 130.8 (Cd), 130.1 (Cc), 128.6 (Cb), 103.5 (C11), 100.0 (C8), 92.3 (C1), 84.2, 84.0 (C10), 83.1, 83.0 (C9), 73.3 (C5), 72.2 (C3), 67.7 (C4), 61.8 (C6), 58.0 (C2), 30.6 (C12), 22.3 (C13), 21.2, 20.9, 20.9, 20.7 (4 × CH_3) 18.5 (C7) ppm. *Anal.* Calcd for $C_{32}H_{40}N_2O_{10}SCl_2Ru$ (816.708): C, 47.06; H, 4.94; N, 3.43. Found: C, 47.48; H, 4.82; N, 3.49. MS: *m/z:* 745.137 (strong, $[(M–2HCl)+H]^+$, calc 745.137).

13a

8a (100 mg, 0.196 mmol) and [Pd(*C*,*N*-DMAB)Cl]$_2$ (54.1 mg, 0.0979 mmol) were dissolved in CH_2Cl_2 (15 mL) under N_2 and stirred for 1 hour. The solution was filtered through Celite and the addition of petroleum spirits gave **13a** (103.2 mg, 67%)

^{1}H NMR: δ 12.38 (s, 1H, HN2), 11.57 (d, 1H, $J_{H2,NH}$ 9.8 Hz, HN1), 8.19 (m, 2H, Hc), 7.62 (m, 1H, Ha), 7. 14 (m, 2H, Hb), 7.56 (m, 1H, Arom.), 7.41 (m, 2H, Arom.), 6.94 (m, 1H, Arom.), 5.94 (d, 1H, $J_{1,2}$ 8.0 Hz, H1), 5.41 (t, 1H, H3), 5.22 (t, 1H, H4), 5.07 (m, 1H, H2), 4.39 (dd, 1H, $J_{5,6b}$ 5.0 Hz , $J_{6a,6b}$ 12.7 Hz, H6b), 4.20 (b, 1H, CH_2), 4.19 (m, 1H, H6a), 4.94 (b, 1H, CH_2), 3.94 (m, 1H, H5), 2.94 (s, 3H, Me), 2.78 (s, 3H, Me), 2.17, 2.16, 2.09, 2.08 (4s, 12H, 4 × OAc) ppm. *Anal.* Calcd for $C_{31}H_{38}N_3O_{10}SClPd$ (786.59): C, 47.34; H, 4.87; N, 5.34. Found: C, 47.06; H, 4.78; N, 5.11. MS: *m/z*: 750.134 (strong, $[M–Cl]^+$, calc. 750.131), 772.116 (medium, $[M–HCl+K]^+$, calc. 772.114), 788.092 (weak, $[M–HCl+K]^+$, calc. 788.088).

14a

8a (100 mg, 0.196 mmol) and $PdCl_2$ (17.4 mg, 0.0980 mmol) were dissolved in acetonitrile (7 mL) and stirred for 4 hours. The solvent was removed under reduced pressure and the residue dissolved in CH_2Cl_2 and filtered through Celite. Solvent was reduced and petroleum spirits added to give an orange powder of **14a** (103 mg, 87%).

trans isomer: ^{1}H NMR: δ 11.64 (s, 1H, HN2), 11.53 (d, 1H, $J_{H2,NH}$ 9.8 Hz, HN1), 8.08 (m, 2H, Hc), 7.64 (m, 1H, Ha), 7.54 (m, 2H, Hb), 5.91 (d, 1H, $J_{1,2}$ 8.3 Hz, H1), 5.39 (dd, 1H, $J_{H3,H4}$ 9.1 Hz, $J_{H2,H3}$ 10.0 Hz, H3), 5.24 (t, 1H, H4), 4.94 (dt, 1H, $J_{1,2}$ 8.3 Hz, $J_{H2,HN1}$; $J_{H2,H3}$ 9.9 Hz, H2), 4.34 (dd, 1H, $J_{5,6b}$ 4.4 Hz , $J_{6a,6b}$ 12.5 Hz, H6b), 4.17 (dd, 1H, $J_{5,6a}$ 2.3 Hz, $J_{6a,6b}$ 12.5, H6a), 3.91 (ddd, 1H, $J_{5,6a}$ 2.4 Hz, $J_{5,6b}$ 4.3 Hz, $J_{4,5}$ 9.7 Hz, H5), 2.19, 2.13, 2.10, 2.06 (4s, 12H, 4 × OAc) ppm. ^{13}C NMR: δ 180.3 (C=S), 170.8, 170.7, 169.4, 169.4 (4 × C=O, acetyl), 168.7 (C=O, amide), 134.7

(Ca), 130.3 (Cd), 129.3 (Cb), 129.0 (Cc), 92.2 (C1), 73.2 (C5), 72.4 (C3), 67.5 (C4), 61.6 (C6), 58.5 (C2), 21.2, 20.9, 20.9, 20.7 (4 × CH_3) ppm. *cis* isomer: ^{1}H NMR: δ 12.04 (s, 1H, HN2), 11.67 (d, 1H, HN1), 8.18 (m, 2H, Hc), 7.64 (m, 1H, Ha), 7.54 (m, 2H, Hb), 5.96 (d, 1H, $J_{1,2}$ 8.2 Hz, H1), 5.45 (dd, 1H, $J_{H3,H4}$ 9.2 Hz, $J_{H2,H3}$ 9.8 Hz, H3), 5.20 (t, 1H, H4), 4.87 (dt, 1H, H2), 4.34 (m, 1H, H6b), 4.17 (m, 1H , H6a), 3.91 (m, 1H, H5), 2.19, 2.13, 2.10, 2.06 (4s, 12H, 4 × OAc) ppm. *Anal.* Calcd for $C_{44}H_{52}N_4O_{20}S_2Cl_2Pd$ (1198.35): C, 44.10; H, 4.37; N, 4.68. Found: C, 44.32; H, 4.49; N, 4.75. MS: *m/z*: 1147.140 (strong, $[M–2H–2Cl+Na]^+$, calc 1147.140), 1125.157 (weak, $[M–H–2Cl]^+$ calc 1125.158).

14b

14b was produced using the same method as for **14a**. **8b** (100 mg, 0.180 mmol) and $PdCl_2$ (15.6 mg, 0.090 mmol), worked up to give an orange powder of **14b** (103 mg, 89%).

^{1}H NMR: δ 11.90 (s, 1H, HN2), 11.28 (d, 1H, $J_{H2,HN1}$ 9.6 Hz, HN1), 8.39 (m, 2H, Hc), 8.28 (m, 1H, Hb), 5.93 (d, 1H, $J_{H1,H2}$ 8.3 Hz, H1), 5.39 (dd, 1H, $J_{H3,H4}$ 9.1 Hz, $J_{H2,H3}$ 9.7 Hz, H3), 5.24 (t, 1H, H4), 4.91 (dt, 1H, H2), 4.35 (dd, 1H, $J_{H5,H6b}$ 4.5 Hz, $J_{H6a,H6b}$ 12.6 Hz, H6b), 4.17 (dd, 1H, $J_{H5,H6a}$ 2.4 Hz, $J_{H6a,H6b}$ 12.6 Hz, H6a), 3.92 (ddd, 1H, $J_{H5,H6a}$ 2.4 Hz, $J_{H5,H6b}$ 4.5Hz, $J_{H4,H5}$ 9.6 Hz, H5), 2.21, 2.12, 2.10, 2.07 (4s, 12H, 4 × OAc) ppm. ^{13}C NMR: δ 180.0 (C=S), 170.7, 169.3 (4 × C=O, acetyl), 166.8 (C=O, amide), 151.2 (Ca), 135.6 (Cd), 130.3 (Cb), 124.3 (Cc), 92.0 (C1), 73.2 (C5), 72.2 (C3), 67.3 (C4), 61.5 (C6), 58.8 (C2), 21.2, 20.9, 20.8, 20.7 (4 × CH_3) ppm. *Anal.* Calcd for $C_{44}H_{50}N_6O_{24}S_2Cl_2Pd$ (1288.350): C, 41.02; H, 3.91; N, 6.52. Found: C, 41.19; H, 4.14; N, 6.35. MS: *m/z*: 1215.122 (weak, $[M–2HCl+H]^+$, calc 1215.128), 1237.108 [strong, $[M–2HCl+Na]^+$, calc 1237.110), 1253.081 [weak, $[M–2HCl+K]^+$, calc 1253.084), 1297.065 (weak, $[M–2HCl+NaCl+Na]^+$ calc 1297.068) , 1313.042 (weak, $[M–2HCl+NaCl+K]^+$ calc 1313.042).

14c

14c was produced using the same method as for **14a**. **8c** (100 mg, 0.200 mmol) and $PdCl_2$ (17.7 mg, 0.100 mmol), worked up to give an orange powder of **14c** (94.5 mg, 80%).

trans isomer: ^{1}H NMR: δ 11.63 (s, 1H, HN2), 11.17 (d, 1H, $J_{H2,HN1}$ 9.8 Hz, HN1), 7.73 (dd, 1H, $J_{Ha,Hc}$ 0.6 Hz, $J_{Ha,Hb}$ 1.7 Hz, Ha), 7.56 (m, 1H, $J_{Ha,Hc}$ 0.6 Hz, $J_{Hb,Hc}$ 3.6 Hz, Hc), 6.61 (m, 1H, $J_{Ha,Hb}$ 1.7 Hz, $J_{Hb,Hc}$ 3.6 Hz, Hb), 5.91 (d, 1H, $J_{H1,H2}$ 8.1 Hz, H1), 5.38 (dd, 1H, $J_{H3,H4}$ 9.1 Hz, $J_{H2,H3}$ 10.0, H3), 5.22 (t, 1H, H4), 4.91 (dt, 1H, H2), 4.33 (dd, 1H, $J_{H5,H6b}$ 4.2 Hz, $J_{H6a,H6b}$ 12.5 Hz, H6b), 4.15 (dd, 1H, $J_{H5,H6a}$ 2.4 Hz, $J_{H6a,H6b}$ 12.5 Hz, H6a), 3.90 (ddd, 1H, $J_{H5,H6a}$ 2.4 Hz, $J_{H5,H6b}$ 4.2 Hz, $J_{H4,H5}$ 9.7 Hz, H5), 2.18, 2.12, 2.10, 2.05 (4s, 12H, 4 × OAc) ppm. ^{13}C NMR: δ 180.0 (C=S), 170.8, 170.8, 169.5, 169.4 (4 × C=O, acetyl), 158.1 (C=O, amide), 148.6 (Ca), 144.1 (Cd), 121.0 (Cc), 113.5 (Cb), 92.1 (C1), 73.2 (C5), 72.4 (C3), 67.5 (C4), 61.5 (C6), 58.6 (C2), 21.2, 20.9, 20.9, 20.7 (4 × CH_3) ppm. *cis* isomer: ^{1}H NMR: δ 11.92 (s, 1H, HN2), 11.21 (d, 1H, $J_{H2,HN1}$ 10.1 Hz, HN1), 7.77 (m, 1H, Ha), 7.56 (m, 1H, Hc), 6.61 (m, 1H, Hb), 6.00 (d, 1H, $J_{H1,H2}$ 8.2 Hz, H1), 5.49 (t, 1H, H3), 5.18 (t, 1H, H4), 4.82 (dt, 1H, H2), 4.34 (m, 1H, H6b), 4.16 (m, 1H, H6a), 3.94 (m, 1H, H5), 2.23, 2.13, 2.09, 2.08 (4s, 12H, 4 × OAc) ppm. *Anal.* Calcd for $C_{40}H_{48}N_4O_{22}S_2Cl_2Pd$ (1178.279): C, 40.77; H, 4.11; N, 4.75. Found: C, 40.25; H, 3.96; N, 4.79. MS: *m/z*: 1127.096 [strong, $[M–2HCl+Na]^+$, calc 1127.099), 1143.075 [weak, $[M–2HCl+K]^+$, calc 1143.073).

15a

$PdCl_2$ (17.4 mg, 0.098 mmol) and NaBr (252.0 mg, 2.45 mmol, 25 M excess) was dissolved in acetonitrile and water (1:1, 7 mL) and stirred for ½ an hour. The solvent was removed under reduced pressure. **8a** (100 mg, 0.196 mmol) was added and acetonitrile (7 mL) added and stirred for 16 hours. The solvent was removed under reduced pressure and the residue dissolved in CH_2Cl_2 and filtered

through Celite. Solvent was reduced and petroleum spirits added to give an orange powder of **15a** (97.5 mg, 77%).

^{1}H NMR: δ 11.38 (d, 1H, $J_{H2,NH}$ 9.7 Hz, HN1), 11.05 (s, 1H, HN2), 8.10 (m, 2H, Hc) 7.66 (m, 1H, Ha), 7.55 (m, 2H, Hb), 5.95 (d, 1H, $J_{1,2}$ 8.4 Hz, H1), 5.43 (dd, 1H, $J_{H3,H4}$ 9.1 Hz, $J_{H2,H3}$ 10.0 Hz, H3), 5.24 (t, 1H, H4), 4.93 (dt, 1H, H2), 4.35 (dd, 1H, $J_{5,6b}$ 4.5 Hz , $J_{6a,6b}$ 12.5 Hz, H6b), 4.17 (dd, 1H, $J_{5,6a}$ 2.3 Hz, $J_{6a,6b}$ 12.5, H6a), 3.92 (ddd, 1H, $J_{5,6a}$ 2.4 Hz, $J_{5,6b}$ 4.4 Hz, $J_{4,5}$ 9.8 Hz, H5), 2.21, 2.13, 2.11, 2.07 (4s, 12H, 4 × OAc) ppm. ^{13}C NMR: δ 179.1 (C=S), 170.8, 170.7, 169.5, 169.4 (4 × C=O, acetyl), 167.9 (C=O, amide), 134.7 (Ca), 130.0 (Cd), 129.4 (Cb), 128.9 (Cc), 92.2 (C1), 73.2 (C5), 72.4 (C3), 67.6 (C4), 61.6 (C6), 59.1 (C2), 21.3, 21.0, 20.9, 20.7 (4 × CH_3) ppm. *Anal.* Calcd for $C_{44}H_{52}N_4O_{20}S_2Br_2Pd$ (1287.26): C, 41.05; H, 4.07; N, 4.35. Found: C, 41.16; H, 3.97; N, 4.23. MS: *m/z*: 1147.140 (strong, $[M–2HBr+Na]^+$, calc 1147.140)

16a

16a was produced using the same method as **15a**. $PdCl_2$ (17.4 mg, 0.098 mmol), NaI (367.2 mg, 2.45 mmol, 25 M excess) and **8a** (100 mg, 0.196 mmol), worked up to give **16a** (113 mg, 84.3%).

^{1}H NMR: δ 11.29 (d, 1H, $J_{H2,HN1}$ 10.0 Hz, HN1), 10.53 (s, 1H, HN2), 8.14 (m, 2H, Hc), 7.68 (m, 1H, Ha), 7.56 (m, 2H, Hb), 5.87 (d, 1H, $J_{H1,H2}$ 8.3 Hz, H1), 5.36 (dd, 1H, $J_{H3,H4}$ 9.1 Hz, $J_{H2,H3}$ 10.1 Hz, H3), 5.26 (t, 1H, H4), 4.91 (dt, 1H, H2), 4.36 (dd, 1H, $J_{H5,H6b}$ 4.2 Hz, $J_{H6a,H6b}$ 12.5 Hz, H6b), 4.17 (dd, 1H, $J_{H5,H6a}$ 2.2 Hz, $J_{H6a,H6b}$ 12.5 Hz, H6a), 3.90 (ddd, 1H, $J_{H5,H6a}$ 2.2 Hz, $J_{H5,H6b}$ 4.2 Hz, $J_{H4,H5}$ 9.8 Hz, H5), 2.23, 2.15, 2.13, 2.07 (4s, 12H, 4 × OAc) ppm. ^{13}C NMR: δ 181.4 (C=S), 170.8, 170.7, 169.4, 169.4 (4 × C=O, acetyl), 167.1 (C=O, amide), 134.7 (Ca), 130.3 (Cd), 129.3 (Cb), 129.0 (Cc), 92.2 (C1), 73.2 (C5), 72.3 (C3), 67.5 (C4), 61.5 (C6), 58.8 (C2), 21.2, 20.9, 20.9, 20.7 (4 × CH_3) ppm. *Anal.* Calcd for $C_{44}H_{52}N_4O_{20}S_2I_2Pd$ (1381.26): C, 38.26; H, 3.79; N, 4.06. Found: C, 37.91; H, 3.92; N, 4.27. MS: *m/z*: 1147.145 (100%, $[M–2HI+Na]^+$, calc 1147.140).

17a

17a was produced using the same method as **14a** except a four molar excess of **8a** was used. $PdCl_2$ (8.7 mg, 0.049 mmol) and **8a** (100 mg, 0.196 mmol), worked up to give an orange powder of **17a** (51.2 mg, 76%).

^{1}H NMR: δ 11.67 (b, 1H, HN2), 11.56 (b, 1H, HN1), 8.12 (m, 2H, Hc), 7.67 (m, 1H, Ha), 7.56 (m, 2H, Hb), 5.93 (d, 1H, $J_{H1,H2}$ 8.4 Hz, H1), 5.41 (t, 1H, H3), 5.26 (t, 1H, H4), 4.95 (m, 1H, H2), 4.37 (dd, 1H, $J_{H5,H6b}$ 4.6 Hz, $J_{H6a,H6b}$ 12.6 Hz, H6b), 4.19 (dd, 1H, $J_{H5,H6a}$ 2.2 Hz, $J_{H6a,H6b}$ 12.6 Hz, H6a), 3.94 (ddd, 1H, $J_{H5,H6a}$ 2.2 Hz, $J_{H5,H6b}$ 4.6 Hz, $J_{H4,H5}$ 9.6 Hz, H5), 2.21, 2.15, 2.13, 2.09 (4s, 12H, 4 × OAc) ppm. ^{13}C NMR: δ 180.3 (C=S), 170.7, 170.6, 169.4, 169.3 (4 × C=O, acetyl), 168.7 (C=O, amide), 134.7 (Ca), 130.3 (Cd), 129.3 (Cb), 129.0 (Cc), 92.2 (C1), 73.2 (C5), 72.4 (C3), 67.5 (C4), 61.6 (C6), 58.5 (C2), 21.2, 20.9, 20.9, 20.7 (4 × CH_3) ppm. *Anal.* Calcd for $C_{44}H_{52}N_4O_{20}S_2I_2Pd$ (1381.26): C, 38.26; H, 3.79; N, 4.06. Found: C, 38.57; H, 3.82; N, 4.26.

18a

8a (100 mg, 0.196 mmol) and $K_2[PtCl_4]$ (40.7 mg, 0.098 mmol) were dissolved in acetonitrile:water (10:1, 11 mL) and stirred for 4 hours. The solvent was removed under vacuum and the residue dissolved in CH_2Cl_2 and filtered through Celite. The solvent was removed under vacuum and recrystallised from CH_2Cl_2 and petroleum spirits to give a yellow powder of **18a** (115 mg, 91%).

trans isomer: ^{1}H NMR: δ 11.43 (s, 1H, HN2), 11.26 (d, 1H, $J_{H2,HN1}$ 9.9 Hz, HN1), 8.02 (m, 2H, Hc), 7.60 (m, 1H, Ha), 7.53 (m, 2H, Hb), 6.05 (d, 1H, $J_{1,2}$ 8.3 Hz, H1), 5.55 (dd, 1H, $J_{H3,H4}$ 9.1 Hz, $J_{H2,H3}$ 10.1 Hz, H3), 5.26 (t, 1H, H4), 4.87 (dt, 1H, $J_{1,2}$ 8.4 Hz, $J_{H2,HN1}$; $J_{H2,H3}$ 10.0 Hz, H2), 4.35 (dd, 1H, $J_{5,6b}$ 4.5 Hz , $J_{6a,6b}$ 12.6 Hz, H6b), 4.18 (dd, 1H, $J_{5,6a}$ 2.3 Hz, $J_{6a,6b}$ 12.6 Hz, H6a), 3.94 (m, 1H, H5) 2.26, 2.18, 2.07, 2.06 (4s, 12H, 4 × OAc) ppm. ^{13}C NMR: δ 178.9 (C=S), 171.0, 170.7, 169.8, 169.4 (4 × C=O, acetyl), 167.3 (C=O, amide), 134.6 (Ca), 129.9 (Cd), 129.4 (Cb), 128.5

(Cc), 92.0 (C1), 73.1 (C5), 72.3 (C3), 67.8 (C4), 61.6 (C6), 59.1 (C2), 21.2, 21.0, 20.8, 20.7 (4 × CH_3) ppm. *cis* isomer: ^{1}H NMR: δ 11.64 (s, 1H, HN2), 11.30 (d, 1H, $J_{H2,HN1}$ 10.0 Hz, HN1), 8.10 (m, 2H, Hc), 7.60 (m, 1H, Ha), 7.53 (m, 2H, Hb), 6.10 (d, 1H, $J_{1,2}$ 8.4 Hz, H1), 5.62 (dd, 1H, $J_{H3,H4}$ 9.2 Hz, $J_{H2,H3}$ 10.2 Hz, H3), 5.14 (t, 1H, H4), 4.75 (dt, 1H, $J_{1,2}$ 8.4 Hz, $J_{H2,HN1}$; $J_{H2,H3}$ 10.0 Hz, H2), 4.32 (dd, 1H, $J_{5,6b}$ 4.7 Hz, $J_{6a,6b}$ 12.4 Hz, H6b), 4.15 (dd, 1H, $J_{5,6a}$ 2.1 Hz, $J_{6a,6b}$ 12.4 Hz, H6a), 3.94 (m, 1H, H5), 2.21, 2.13, 2.11, 2.06 (4s, 12H, 4 × OAc) ppm. ^{13}C NMR: δ 177.9 (C=S), 170.8, 171.6, 169.7, 169.3 (4 × C=O, acetyl), 167.4 (C=O, amide), 134.8 (Ca), 129.7 (Cd), 129.5 (Cb), 128.7 (Cc), 91.9 (C1), 73.1 (C5), 72.2 (C3), 67.9 (C4), 61.7 (C6), 59.3 (C2), 21.2, 20.9, 20.8, 20.6 (4 × CH_3) ppm. *Anal.* Calcd for $C_{44}H_{52}N_4O_{20}S_2Cl_2Pt$ (1287.012): C, 41.06; H, 4.07; N, 4.35. Found: C, 40.61; H, 4.38; N, 4.26. MS: *m/z*: 1215.216 (weak, $[M–2HCl+H]^+$ calc 1215.219), 1237.204 (strong, $[M–2HCl+Na]^+$, calc 1237.201), 1253.177 (weak, $[M–2HCl+K]^+$ calc 1253.175).

18b

18b was produced using the same method as for **18a**. **8b** (50 mg, 0.090 mmol) and $K_2[PtCl_4]$ (18.7 mg, 0.045 mmol) with acetonitrile:water (10:1, 11 mL). Gave a yellow powder of **18b** (53.4 mg, 89%).

cis isomer: ^{1}H NMR: δ 12.01 (s, 1H, HN2), 11.23 (d, 1H, $J_{H2,HN1}$ 9.7 Hz, HN1), 8.41 (m, 2H, Hc), 8.29 (m, 1H, Hb), 5.94 (d, 1H, $J_{H1,H2}$ 8.2 Hz, H1), 5.44 (dd, 1H, $J_{H3,H4}$ 9.0 Hz, $J_{H2,H3}$ 10.0 Hz, H3), 5.27 (t, 1H, H4), 4.85 (dt, 1H, H2), 4.36 (dd, 1H, $J_{H5,H6b}$ 3.9 Hz, $J_{H6a,H6b}$ 12.5 Hz, H6b), 4.19 (dd, 1H, $J_{H5,H6a}$ 2.3 Hz, $J_{H6a,H6b}$ 12.5 Hz, H6a), 3.94 (m, 1H, H5), 2.23, 2.15, 2.09, 2.08 (4s, 12H, 4 × OAc) ppm. ^{13}C NMR: δ 178.3 (C=S), 170.6, 170.6, 169.4, 169.1 (4 × C=O, acetyl), 166.1 (C=O, amide), 151.4 (Ca), 135.1 (Cd), 130.4 (Cb), 129.6 (Cc), 92.0 (C1), 73.4 (C5), 72.2 (C3), 67.5 (C4), 61.7 (C6), 59.3 (C2), 21.2, 20.9, 20.8, 20.7 (4 × CH_3) ppm. *trans* isomer: ^{1}H NMR: δ 11.67 (s, 1H, HN2), 11.13 (d, 1H, $J_{H2,HN1}$ 9.7 Hz, HN1), 8.41 (m, 2H, Hc), 8.29 (m, 1H, Hb), 5.98 (d, 1H, $J_{H1,H2}$ 8.1 Hz, H1), 5.41 (dd, 1H, $J_{H3,H4}$ 9.0 Hz, $J_{H2,H3}$ 9.6 Hz, H3), 5.18 (t, 1H, H4), 4.70 (dt, 1H, H2), 4.34 (dd, 1H, $J_{H5,H6b}$ 4.6 Hz, $J_{H6a,H6b}$ 12.9 Hz, H6b), 4.16 (dd, 1H, $J_{H5,H6a}$ 2.3 Hz, $J_{H6a,H6b}$ 12.9 Hz, H6a), 3.94 (m,

1H, H5), 2.21, 2.14, 2.12, 2.09 (4s, 12H, 4 × OAc) ppm. ^{13}C NMR: δ 178.9 (C=S), 170.9, 170.7, 169.5, 169.3 (4 × C=O, acetyl), 165.9 (C=O, amide), 151.3 (Ca), 135.4 (Cd), 130.0 (Cb), 124.5 (Cc), 92.1 (C1), 73.3 (C5), 72.3 (C3), 67.4 (C4), 61.5 (C6), 59.2 (C2), 21.2, 20.9, 20.9, 20.7 (4 × CH_3) ppm. *Anal.* Calcd for $C_{44}H_{50}N_6O_{24}S_2Cl_2Pt$ (1326.949): C, 38.38; H, 3.66; N, 6.10. Found: C, 38.53; H, 3.64; N, 6.14. MS: *m/z*: 1327.167 (100%, $[M–2HCl+Na]^+$, calc 1327.171), 1343.143 (38.7%, $[M–2HCl+K]^+$, calc 1343.145), 1385.128 (6.4%, $[M-2HCl+NaCl+Na]^+$ calc 1385.129), 1401.103 (6.4%, $[M-2HCl+NaCl+K]^+$ calc 1401.103).

18c

18c was produced using the same method as for **18a**. **8c** (50 mg, 0.100 mmol) and $K_2[PtCl_4]$ (20.8 mg, 0.050 mmol) with acetonitrile:water (10:1, 11 mL). Gave yellow powder of **18c** (52.9 mg, 84%).

trans isomer ^{1}H NMR: δ 11.52 (s, 1H, HN2), 10.99 (d, 1H, $J_{H2,HN1}$ 10.0 Hz, HN1), 7.75 (dd, 1H, $J_{Ha,Hc}$ 0.7 Hz, $J_{Ha,Hb}$ 1.7 Hz, Ha), 7.50 (dd, 1H, $J_{Ha,Hc}$ 0.7 Hz, $J_{Hb,Hc}$ 3.7 Hz, Hc), 6.60 (dd, 1H, $J_{Ha,Hb}$ 1.7 Hz, $J_{Hb,Hc}$ 3.7 Hz, Hb), 5.95 (d, 1H, $J_{H1,H2}$ 8.4 Hz, H1), 5.43 (dd, 1H, $J_{H3,H4}$ 9.1 Hz, $J_{H2,H3}$ 10.0 Hz, H3), 5.24 (t, 1H, H4), 4.81 (dt, 1H, H2), 4.34 (dd, 1H, $J_{H5,H6b}$ 4.4 Hz, $J_{H6a,H6b}$ 12.5 Hz, H6b), 4.15 (m, 1H, H6a), 3.91 (m, 1H, H5), 2.20, 2.13, 2.12, 2.06 (4s, 12H, 4 × OAc) ppm. ^{13}C NMR: δ 178.9 (C=S), 170.9, 170.7, 169.7, 169.4 (4 × C=O, acetyl), 157.3 (C=O, amide), 148.5 (Ca), 148.5 (Cd), 120.8 (Cc), 113.6 (Cb), 91.9 (C1), 73.1 (C5), 72.2 (C3), 67.8 (C4), 61.6 (C6), 59.1 (C2), 21.2, 21.0, 20.9, 20.7 (4 × CH_3) ppm. *cis* isomer ^{1}H NMR: δ 11.58 (s, 1H, HN2), 10.95 (d, 1H, $J_{H2,HN1}$ 10.0 Hz, HN1), 7.81 (dd, 1H, $J_{Ha,Hc}$ 0.7 Hz, $J_{Ha,Hb}$ 1.7 Hz, Ha), 7.64 (dd, 1H, $J_{Ha,Hc}$ 0.7 Hz, $J_{Hb,Hc}$ 3.7 Hz, Hc), 6.59 (dd, 1H, $J_{Ha,Hb}$ 1.7 Hz, $J_{Hb,Hc}$ 3.6 Hz, Hb), 6.05 (d, 1H, $J_{H1,H2}$ 8.5 Hz, H1), 5.55 (dd, 1H, $J_{H3,H4}$ 9.2 Hz, $J_{H2,H3}$ 10.3 Hz, H3), 5.14 (t, 1H, H4), 4.69 (dt, 1H, H2), 4.31 (dd, 1H, $J_{H5,H6b}$ 4.5 Hz, $J_{H6a,H6b}$ 12.4 Hz, H6b), 4.15 (m, 1H, H6a), 3.91 (m, 1H, H5), 2.26, 2.15, 2.08, 2.06 (4s, 12H, 4 × OAc) ppm. ^{13}C NMR: δ 177.9 (C=S), 171.0, 170.6, 169.7, 169.4 (4 × C=O, acetyl), 157.3 (C=O, amide), 149.7 (Ca), 149.2 (Cd), 121.3 (Cc), 113.6 (Cb), 92.1 (C1), 73.2 (C5), 72.4 (C3), 67.5 (C4), 61.7 (C6), 59.2 (C2), 21.3, 20.9, 20.9, 20.7 (4 × CH_3) ppm.

Anal. Calcd for $C_{40}H_{48}N_4O_{22}S_2Cl_2Pt$ (1266.937): C, 37.92; H, 3.82; N, 4.42. Found: C, 37.81; H, 3.88; N, 4.54. MS: *m/z*: 1243.179 (weak, $[M–2HCl+H]^+$, calc 1243.178), 1265.162 (strong, $[M–2HCl+Na]^+$, calc 1265.160).

18d

18d was produced using the same method as for **18a**. **8d** (50 mg, 0.097 mmol) and $K_2[PtCl_4]$ (19.9 mg, 0.048 mmol) with acetonitrile:water (10:1, 11 mL). Gave yellow powder of **18d** (58.4 mg, 94%).

trans isomer ^{1}H NMR: δ 11.48 (s, 1H, HN2), 8.07 (m, 2H, Hc), 7.81 (m, 1H, Ha), 7.20 (m, 2H, Hb), 5.89 (d, 1H, $J_{H1,H2}$ 8.4 Hz, H1), 5.38 (dd, 1H, $J_{H3,H4}$ 9.0 Hz, $J_{H2,H3}$ 10.0 Hz, H3), 5.24 (t, 1H, H4), 4.83 (dt, 1H, H2), 4.35 (dd, 1H, $J_{H5,H6b}$ 4.3 Hz, $J_{H6a,H6b}$ 12.5 Hz, H6b), 4.16 (dd, 1H, $J_{H5,H6a}$ 2.4 Hz, $J_{H6a,H6b}$ 12.5 Hz, H6a), 3.89 (m, 1H, H5), 2.20, 2.13, 2.12, 2.07 (4s, 12H, 4 × OAc) ppm. *cis* isomer ^{1}H NMR: δ 11.69 (s, 1H, HN2), 11.15 (d, 1H, $J_{H2,HN1}$ 9.5 Hz, HN1), 8.17 (m, 2H, Hc), 7.84 (m, 1H, Ha), 7.15 (m, 2H, Hb), 5.96 (d, 1H, $J_{H1,H2}$ 8.3 Hz, H1), 5.46 (dd, 1H, $J_{H3,H4}$ 9.0 Hz, $J_{H2,H3}$ 10.0 Hz, H3), 5.18 (t, 1H, H4), 4.73 (dt, 1H, H2), 4.34 (dd, 1H, $J_{H5,H6b}$ 4.9 Hz, $J_{H6a,H6b}$ 12.5 Hz, H6b), 4.16 (dd, 1H, $J_{H5,H6a}$ 2.4 Hz, $J_{H6a,H6b}$ 12.5 Hz, H6a), 3.92 (ddd, 1H, $J_{H5,H6a}$ 2.4 Hz, $J_{H5,H6b}$ 4.9 Hz, $J_{H4,H5}$ 9.7 Hz, H5), 2.24, 2.16, 2.09, 2.07 (4s, 12H, 4 × OAc) ppm. *Anal.* Calcd for $C_{40}H_{48}N_4O_{20}S_4Cl_2Pt$ (1299.068): C, 36.98; H, 3.72; N, 4.31. Found: C, 37.13; H, 3.80; N, 4.46. MS: *m/z*: 1227.128 (weak, $[M–2HCl+H]^+$, calc 1227.132), 1249.111 (medium, $[M–2HCl+Na]^+$, calc 1249.113), 1265.085 (strong, $[M–2HCl+K]^+$, calc 1265.087), 1285.084 (weak, $[M\text{-}HCl+Na]^+$ calc 1285.089), 1321.059 (weak, $[M+Na]^+$ calc 1321.065), 1337.034 (medium, $[M+K]^+$ calc 1337.039).

19a

19a was made using the same method as for **18a**, except the $K_2[PtCl_4]$ (30 mg, 0.0723 mmol) was stirred with NaBr (185.9 mg, 1.807 mmol, 25 M excess) for 1

hour in acetonitrile and water (8:1, 9 mL) before the addition of **8a** (73.8 mg, 0.145 mmol). Was worked up as above to give a yellow powder of **19a** (85.5 mg, 86%).

trans isomer: ^{1}H NMR: δ 11.23 (d, 1H, $J_{H2,HN1}$ 10.0 Hz, HN1), 11.30 (s, 1H, HN2), 8.11 (m, 2H, Hc), 7.66 (m, 1H, Ha), 7.54 (m, 2H, Hb), 5.93 (d, 1H, $J_{1,2}$ 8.4 Hz, H1), 5.41 (dd, 1H, $J_{H3,H4}$ 9.2 Hz, $J_{H2,H3}$ 10.1 Hz, H3), 5.26 (t, 1H, H4), 4.81 (dt, 1H, $J_{1,2}$ 8.4 Hz, $J_{H2,HN1}$; $J_{H2,H3}$ 10.0 Hz, H2), 4.35 (dd, 1H, $J_{5,6b}$ 4.5 Hz , $J_{6a,6b}$ 12.5 Hz, H6b), 4.17 (dd, 1H, $J_{5,6a}$ 2.4 Hz, $J_{6a,6b}$ 12.5 Hz, H6a), 3.91 (ddd, 1H, $J_{5,6a}$ 2.4 Hz, $J_{5,6b}$ 4.5 Hz, $J_{4,5}$ 9.8 Hz, H5), 2.21, 2.13, 2.13, 2.07 (4s, 12H, 4 × OAc) ppm. ^{13}C NMR: δ 178.2 (C=S), 170.8, 170.7, 169.5, 169.4 (4 × C=O, acetyl), 167.1 (C=O, amide), 134.8 (Ca), 130.0 (Cd), 129.4 (Cb), 128.6 (Cc), 92.2 (C1), 73.3 (C5), 72.4 (C3), 67.6 (C4), 61.6 (C6), 59.3 (C2), 21.3, 21.0, 20.9, 20.7 (4 × CH_3) ppm. *cis* isomer: ^{1}H NMR: δ 11.49 (s, 1H, HN2), 11.31 (d, 1H, $J_{H2,HN1}$ 10.0 Hz, HN1), 8.22 (m, 2H, Hc), 7.66 (m, 1H, Ha), 7.57 (m, 2H, Hb), 5.94 (d, 1H, $J_{1,2}$ 8.4 Hz, H1), 5.43 (dd, 1H, $J_{H3,H4}$ 9.1 Hz, $J_{H2,H3}$ 10.2 Hz, H3), 5.12 (t, 1H, H4), 4.67 (dt, 1H, $J_{1,2}$ 8.4 Hz, $J_{H2,HN1}$; $J_{H2,H3}$ 10.1 Hz, H2), 4.31 (dd, 1H, $J_{5,6b}$ 4.8 Hz , $J_{6a,6b}$ 12.4 Hz, H6b), 4.13 (dd, 1H, $J_{5,6a}$ 2.4 Hz, $J_{6a,6b}$ 12.4 Hz, H6a), 3.91 (ddd, 1H, $J_{5,6a}$ 2.4 Hz, $J_{5,6b}$ 4.8 Hz, $J_{4,5}$ 9.7 Hz, H5), 2.23, 2.17, 2.07, 2.06 (4s, 12H, 4 × OAc) ppm. ^{13}C NMR: δ 177.5 (C=S), 170.7, 170.6, 169.4, 169.3 (4 × C=O, acetyl), 167.3 (C=O, amide), 135.0 (Ca), 129.6 (Cd), 129.6 (Cb), 128.9 (Cc), 92.0 (C1), 73.2 (C5), 72.4 (C3), 67.6 (C4), 61.7 (C6), 59.4 (C2), 21.2, 20.9, 20.8, 20.7 (4 × CH_3) ppm. *Anal.* Calcd for $C_{44}H_{52}N_4O_{20}S_2Br_2Pt$ (1375.914): C, 38.41; H, 3.81; N, 4.07. Found: C, 38.89; H, 3.95; N, 4.20. MS: *m/z*: 1215.217 (weak, $[M–2HBr+H]^+$ calc 1215.219), 1237.205 (strong, $[M–2HBr+Na]^+$, calc 1237.201), 1253.177.

20a

20a was made using the same method as for **19a**, $K_2[PtCl_4]$ (30 mg, 0.072 mmol) and NaI (270.8 mg, 1.86 mmol, 25 M excess) in acetonitrile and water (8:1, 9 mL), followed by **8a** (73.8 mg, 0.145 mmol) and worked up as above to give **20a** (83.1 mg, 79%).

trans isomer: ^{1}H NMR: δ 11.02 (d, 1H, $J_{H2,HN1}$ 9.7 Hz, HN1), 10.92 (s, 1H, HN2), 8.08 (m, 2H, Hc), 7.67 (m, 1H, Ha), 7.57 (m, 2H, Hb), 6.07 (d, 1H, $J_{H1,H2}$ 8.6 Hz, H1), 5.58 (dd, 1H, $J_{H3,H4}$ 9.2 Hz, $J_{H2,H3}$ 10.3 Hz, H3), 5.28 (t, 1H, H4), 4.82 (dt, 1H, H2), 4.38 (dd, 1H, $J_{H5,H6b}$ 4.5 Hz, $J_{H6a,H6b}$ 12.5 Hz, H6b), 4.18 (dd, 1H, $J_{H5,H6a}$ 2.3 Hz, $J_{H6a,H6b}$ 12.5 Hz, H6a), 3.94 (ddd, 1H, $J_{H5,H6a}$ 2.3 Hz, $J_{H5,H6b}$ 4.5 Hz, $J_{H4,H5}$ 10.0 Hz, H5), 2.27, 2.18, 2.13, 2.08 (4s, 12H, 4 × OAc) ppm. ^{13}C NMR: δ 176.5 (C=S), 171.2, 170.7, 169.8, 169.5 (4 × C=O, acetyl), 166.3 (C=O, amide), 134.8 (Ca), 129.7 (Cd), 129.6 (Cb), 128.5 (Cc), 92.2 (C1), 73.1 (C5), 72.3 (C3), 67.9 (C4), 61.6 (C6), 59.6 (C2), 21.4, 21.2, 20.9, 20.7 (4 × CH_3) ppm. *cis* isomer: ^{1}H NMR: δ 11.80 (d, 1H, $J_{H2,HN1}$ 10.0 Hz, HN1), 8.28 (m, 2H, Hc), 7.67 (m, 1H, Ha), 7.57 (m, 2H, Hb), 6.05 (d, 1H, $J_{H1,H2}$ 8.3 Hz, H1), 5.56 (dd, 1H, $J_{H3,H4}$ 9.1 Hz, $J_{H2,H3}$ 10.3 Hz, H3), 5.22 (t, 1H, H4), 4.66 (dt, 1H, H2), 4.31 (dd, 1H, $J_{H5,H6b}$ 4.6 Hz, $J_{H6a,H6b}$ 13.0 Hz, H6b), 4.16 (dd, 1H, $J_{H5,H6a}$ 2.2 Hz, $J_{H6a,H6b}$ 12.4 Hz, H6a), 3.89 (m, 1H, H5), 2.22, 2.14, 2.12, 2.07 (4s, 12H, 4 × OAc) ppm. ^{13}C NMR: δ 175.5 (C=S), 171.0, 170.7, 169.6, 169.5 (4 × C=O, acetyl), 166.0 (C=O, amide), 135.1 (Ca), 129.9 (Cd), 129.7 (Cb), 128.7 (Cc), 92.0 (C1), 73.1 (C5), 72.3 (C3), 67.8 (C4), 61.6 (C6), 59.8 (C2), 21.3, 21.1, 20.8, 20.7 (4 × CH_3) ppm. *Anal.* Calcd for $C_{44}H_{52}N_4O_{20}S_2I_2Pt$ (1469.915): C, 35.95; H, 3.57; N 3.81,. Found: C, 36.21; H, 3.67; N, 3.89. MS: *m/z*: 1215.214 (weak, $[M–2HI+H]^+$ calc 1215.219), 1237.202 (strong, $[M–2HI+Na]^+$, calc 1237.201), 1253.178 (weak, $[M–2HI+K]^+$ calc 1253.175).

21a

8a (300 mg, 0.588 mmol) and $HgCl_2$ (79.7 mg, 0.294 mmol) were dissolved in a mixture of acetone and ethanol (1:1, 15 mL) and stirred for three hours. The solvent was removed under vacuum and the residue dissolved in CH_2Cl_2 and filtered through Celite. Addition of petroleum spirits gave **21a** (365.3 mg, 96%).

^{1}H NMR: δ 12.00 (d, 1H, $J_{H2,NH}$ 9.6 Hz, HN1), 10.65 (s, 1H, HN2), 8.12 (m, 2H, Hc), 7.63 (m, 1H, Ha), 7.48 (m, 2H, Hb), 5.90 (d, 1H, $J_{1,2}$ 8.2 Hz, H1), 5.37 (dd, 1H, $J_{H3,H4}$ 8.9 Hz, $J_{H2,H3}$ 9.9 Hz, H3), 5.21 (t, 1H, H4), 4.98 (m, 1H, H2), 4.34 (dd, 1H, $J_{5,6b}$ 4.6 Hz , $J_{6a,6b}$ 12.5 Hz, H6b), 4.17 (dd, 1H, $J_{5,6a}$ 2.4 Hz, $J_{6a,6b}$ 12.5 Hz, H6a), 3.92

(ddd, 1H, $J_{5,6a}$ 2.5 Hz, $J_{5,6b}$ 4.6 Hz, $J_{4,5}$ 9.5 Hz, H5), 2.18, 2.11, 2.10, 2.07 (4s, 12H, 4 × OAc) ppm. ^{13}C NMR: δ 181.2 (C=S), 170.7, 170.5, 169.4, 169.2 (4 × C=O, acetyl), 169.6 (C=O, amide), 134.8 (Ca), 130.1 (Cd), 129.5 (Cc), 129.0 (Cb), 92.0 (C1), 73.3 (C5), 72.0 (C3), 67.5 (C4), 61.6 (C6), 59.0 (C2), 21.2, 20.9, 20.9, 20.7 (4 × CH_3) ppm. *Anal.* Calcd for $C_{44}H_{52}N_4O_{20}S_2Cl_2Hg$ (1292.52): C, 40.89; H, 4.06; N, 4.33. Found: C, 41.09; H, 4.08; N, 4.24. MS: *m/z*: 1221.221 (weak, $[M–2HCl+H]^+$, calc 1221.224), 1243.201 (weak, $[M–2HCl+Na]^+$, calc 1243.206).

22a

22a was made using the same method as for **21a**, **8a** (100 mg, 0.196 mmol) and $HgBr_2$ (35.3 mg, 0.098 mmol) worked up to give **22a** (125.0 mg, 92%).

^{1}H NMR: δ 11.43 (d, 1H, $J_{H2,NH}$ 9.5 Hz, HN1), 9.58 (s, 1H, HN2), 7.98 (m, 2H, Hc), 7.65 (m, 1H, Ha), 7.52 (m, 2H, Hb), 5.91 (d, 1H, $J_{1,2}$ 8.2 Hz, H1), 5.36 (dd, 1H, $J_{H3,H4}$ 8.9 Hz, $J_{H2,H3}$ 9.8 Hz, H3), 5.21 (t, 1H, H4), 4.98 (m, 1H, H2), 4.33 (dd, 1H, $J_{5,6b}$ 4.6 Hz , $J_{6a,6b}$ 12.4 Hz, H6b), 4.17 (dd, 1H, $J_{5,6a}$ 2.5 Hz, $J_{6a,6b}$ 12.4 Hz, H6a), 3.91 (ddd, 1H, $J_{5,6a}$ 2.5 Hz, $J_{5,6b}$ 4.6 Hz, $J_{4,5}$ 9.4 Hz, H5), 2.15, 2.11, 2.08, 2.07 (4s, 12H, 4 × OAc) ppm. ^{13}C NMR: δ 181.6 (C=S), 170.8, 170.5, 169.4, 169.2 (4 × C=O, acetyl), 167.9 (C=O, amide), 134.5 (Ca), 130.6 (Cd), 129.2 (Cb), 128.6 (Cc), 92.2 (C1), 73.2 (C5), 72.2 (C3), 67.5 (C4), 61.7 (C6), 58.4 (C2), 21.2, 20.9, 20.9, 20.7 (4 × CH_3) ppm. *Anal.* Calcd for $C_{44}H_{52}N_4O_{20}S_2Br_2Hg$ (1381.426): C, 38.26; H, 3.79; N, 4.06. Found: C, 38.43; H, 3.94; N, 3.91. MS: *m/z*: 1301.147 (medium, $[M\text{-}Br]^+$, calc 1301.149).

21f

21f was made using the same method as for **21a**, **8f** (150 mg, 0.311 mmol) and $HgCl_2$ (42.1 mg, 0.155 mmol) worked up to give **21f** (191 mg, 99%).

^{1}H NMR: δ 10.87 (bs, 1H, HN2), 7.45 (m, 2H, Hb), 7.39 (m, 1H, Ha), 7.26 (m, 2H, Hc), 6.39 (bs, 1H, HN1), 5.63 (d, 1H, $J_{1,2}$, 8.5 Hz, H1), 5.17 (m, 1H, H4), 5.09 (m, 1H, H3), 4.79 (bm, 1H, H2), 4.22 (dd, 1H, $J_{5,6b}$ 4.6 Hz, $J_{6a,6b}$ 12.5 Hz, H6b), 4.08 (dd, 1H, $J_{5,6a}$ 2.1 Hz, $J_{6a,6b}$ 12.5 Hz, H6a), 3.74 (m, 1H, H5), 2.22, 2.12, 2.07, 1.99 (4s, 12H, 4 × OAc) ppm. ^{13}C NMR: δ 176.8 (C=S), 171.3, 170.7, 169.7, 169.3 (4 × C=O), 133.8 (Cd), 130.6 (Cb), 129.4 (Ca), 126.5 (Cc), 92.1 (C1), 73.0 (C5), 72.0 (C3), 67.7 (C4), 61.6 (C6), 58.9 (C2), 21.2, 21.0, 20.8, 20.6 (4 × CH_3) ppm. *Anal.* Calcd for $C_{42}H_{52}N_4O_{18}S_2Cl_2Hg$ (1236.504): C, 40.80; H, 4.24; N, 4.53. Found: C, 40.72; H, 4.36; N, 4.26.

22f

22f was made using the same method as for **21a**, **8f** (150 mg, 0.311 mmol) and $HgBr_2$ (56.0 mg, 0.155 mmol) worked up to give **22f** (194.5 mg, 95%).

^{1}H NMR: δ 9.95 (bs, 1H, HN2), 7.51 (m, 2H, Hb), 7.44 (m, 1H, Ha), 7.29 (m, 2H, Hc), 6.06 (bs, 1H, HN1), 5.62 (d, 1H, $J_{1,2}$, 8.4 Hz, H1), 5.17 (m, 1H, H4), 5.01 (t, 1H, H3), 4.82 (bm, 1H, H2), 4.26 (dd, 1H, $J_{5,6b}$ 4.5 Hz, $J_{6a,6b}$ 12.7 Hz, H6b), 4.12 (dd, 1H, $J_{5,6a}$ 2.4 Hz, $J_{6a,6b}$ 12.7 Hz, H6a), 3.72 (m, 1H, H5), 2.24, 2.15, 2.10, 2.01 (4s, 12H, 4 × OAc) ppm. ^{13}C NMR: δ 1767.5 (C=S), 171.3, 170.7, 169.7, 169.2 (4 × C=O), 133.6 (Cd), 130.7 (Cb), 129.6 (Ca), 126.7 (Cc), 92.3 (C1), 73.2 (C5), 72.1 (C3), 67.5 (C4), 61.6 (C6), 58.8 (C2), 21.4, 21.1, 20.8, 20.6 (4 × CH_3) ppm. *Anal.* Calcd for $C_{42}H_{52}N_4O_{18}S_2Br_2Hg$ (1325.406): C, 38.06; H, 3.95; N, 4.23. Found: C, 38.03; H, 4.07; N, 3.97.

23a

8a (100 mg, 0.196 mmol) and (THT)AuCl (62.8 mg, 0.196 mmol) were dissolved in CH_2Cl_2 (10 mL) under nitrogen and stirred overnight protected from light. The solvent was removed under vacuum and pumped for 2 hours, no further precautions were taken to exclude oxygen. The residue was taken up in CH_2Cl_2,

filtered through Celite, petroleum spirits were added to isolate a white solid of **23a** (104.1 mg, 72%).

^{1}H NMR: δ 11.20 (d, 1H, $J_{H2,HN1}$ 10.0 Hz, HN1), 10.29 (s, 1H, HN2), 7.76 (m, 2H, Hc), 7.70 (m, 1H, Ha), 7.56 (m, 2H, Hb), 6.07 (d, 1H, $J_{H1,H2}$ 8.3 Hz, H1), 5.56 (dd, 1H, $J_{H3,H4}$ 9.1 Hz, $J_{H2,H3}$ 10.1 Hz, H3), 5.23 (dd, 1H, $J_{H3,H4}$ 9.1 Hz, $J_{H4,H5}$ 9.9 Hz, H4), 4.65 (dt, 1H, H2), 4.35 (dd, 1H, $J_{H5,H6b}$ 4.5 Hz, $J_{H6a,H6b}$ 12.5 Hz, H6b), 4.17 (dd, 1H, $J_{H5,H6a}$ 2.4 Hz, $J_{H6a,H6b}$ 12.5 Hz, H6a), 3.93 (ddd, 1H, $J_{H5,H6a}$ 2.4 Hz, $J_{H5,H6b}$ 4.5 Hz, $J_{H4,H5}$ 9.9 Hz, H5), 2.21, 2.12, 2.09, 2.07 (4s, 12H, 4 × OAc) ppm. ^{13}C NMR: δ 179.6 (C=S), 170.9, 170.7, 169.7, 169.4 (4 × C=O, acetyl), 166.2 (C=O, amide), 135.7 (Ca), 130.1 (Cb), 128.6 (Cd), 128.0 (Cc), 91.8 (C1), 73.2 (C5), 72.2 (C3), 67.6 (C4), 61.5 (C6), 60.5 (C2), 21.2, 20.9, 20.8, 20.7 (4 × CH_3) ppm.

23b

The same method was used as for **23a**, **8b** (100 mg, 0.180 mmol), (THT)AuCl (57.7 mg, 0.180 mmol) and CH_2Cl_2 (10 mL) under nitrogen overnight. Worked up to give a pale yellow solid **23b** (121.7 mg, 86%).

^{1}H NMR: δ 11.08 (d, 1H, $J_{H2,HN1}$ 9.6 Hz, HN1), 10.55 (s, 1H, HN2), 8.30 (m, 2H, Hb), 8.09 (m, 2H, Hc), 6.00 (d, 1H, $J_{H1,H2}$ 8.2 Hz, H1), 5.46 (dd, 1H, $J_{H3,H4}$ 8.9 Hz, $J_{H2,H3}$ 9.8 Hz, H3), 5.21 (dd, 1H, $J_{H3,H4}$ 8.9 Hz, $J_{H4,H5}$ 9.6 Hz, H4), 4.81 (dt, 1H, H2), 4.33 (dd, 1H, $J_{H5,H6b}$ 4.7 Hz, $J_{H6a,H6b}$ 12.5 Hz, H6b), 4.16 (dd, 1H, $J_{H5,H6a}$ 2.6 Hz, $J_{H6a,H6b}$ 12.5 Hz, H6a), 3.95 (ddd, 1H, $J_{H5,H6a}$ 2.6 Hz, $J_{H5,H6b}$ 4.7 Hz, $J_{H4,H5}$ 9.6 Hz, H5), 2.17, 2.09, 2.08, 2.06 (4s, 12H, 4 × OAc) ppm. ^{13}C NMR: δ 180.2 (C=S), 170.7, 170.6, 169.4, 169.2 (4 × C=O, acetyl), 165.4 (C=O, amide), 151.2 (Ca), 135.3 (Cd), 129.9 (Cc), 124.3 (Cb), 91.9 (C1), 73.1 (C5), 72.0 (C3), 67.5 (C4), 61.6 (C6), 59.5 (C2), 21.2, 20.9, 20.8, 20.7 (4 × CH_3) ppm.

23c

The same method was used as for **23a**, **8c** (120 mg, 0.240 mmol), (THT)AuCl (76.9 mg, 0.240 mmol) and CH_2Cl_2 (10 mL) under nitrogen overnight. Worked up to give a white solid **23c** (137.9 mg, 78%).

^{1}H NMR: δ 10.75 (d, 1H, $J_{H2,HN1}$ 9.8 Hz, HN1), 9.82 (s, 1H, HN2), 7.61 (dd, 1H, 0.8 Hz, $J_{Ha,Hc}$; 1.7 Hz, $J_{Ha,Hb}$, Ha), 7.43 (dd, 1H, 0.8 Hz, $J_{Ha,Hc}$; 3.7 Hz, $J_{Hb,Hc}$, Hc), 6.68 (dd, 1H, 1.7 Hz, $J_{Hb,Hc}$; 3.7 Hz, $J_{Ha,Hb}$, Hb), 6.04 (d, 1H, $J_{H1,H2}$ 8.4 Hz, H1), 5.51 (dd, 1H, $J_{H3,H4}$ 9.1 Hz, $J_{H2,H3}$ 10.0 Hz, H3), 5.21 (dd, 1H, $J_{H3,H4}$ 9.1 Hz, $J_{H4,H5}$ 9.8 Hz, H4), 4.78 (dt, 1H, H2), 4.33 (dd, 1H, $J_{H5,H6b}$ 4.5 Hz, $J_{H6a,H6b}$ 12.5 Hz, H6b), 4.15 (dd, 1H, $J_{H5,H6a}$ 2.4 Hz, $J_{H6a,H6b}$ 12.5 Hz, H6a), 3.91 (ddd, 1H, $J_{H5,H6a}$ 2.4 Hz, $J_{H5,H6b}$ 4.5 Hz, $J_{H4,H5}$ 9.8 Hz, H5), 2.17, 2.10, 2.06, 2.05 (4s, 12H, 4 × OAc) ppm. ^{13}C NMR: δ 180.1 (C=S), 170.9, 170.7, 169.7, 169.4 (4 × C=O, acetyl), 156.0 (C=O, amide), 148.0 (Ca), 143.7 (Cd), 120.9 (Cc), 114.3 (Cc), 91.9 (C1), 73.1 (C5), 72.3 (C3), 67.6 (C4), 61.6 (C6), 59.7 (C2), 21.2, 20.8 × 2, 20.7 (4 × CH_3) ppm.

23d

The same method was used as for **23a**, **8d** (120 mg, 0.232 mmol), (THT)AuCl (74.5 mg, 0.232 mmol) and CH_2Cl_2 (10 mL) under nitrogen overnight. Worked up to give a white solid **23d** (143.2 mg, 82%).

^{1}H NMR: δ 10.78 (d, 1H, $J_{H2,HN1}$ 10.1 Hz, HN1), 10.05 (s, 1H, HN2), 7.92 (dd, 1H, 1.1 Hz, $J_{Ha,Hc}$; 5.0 Hz, $J_{Ha,Hb}$, Ha), 7.30 (dd, 1H, 1.1 Hz, $J_{Ha,Hc}$; 4.0 Hz, $J_{Hb,Hc}$, Hc), 7.07 (dd, 1H, 4.0 Hz, $J_{Hb,Hc}$; 5.0 Hz, $J_{Ha,Hb}$, Hb), 6.21 (d, 1H, $J_{H1,H2}$ 8.4 Hz, H1), 5.71 (dd, 1H, $J_{H3,H4}$ 9.2 Hz, $J_{H2,H3}$ 10.1 Hz, H3), 5.22 (dd, 1H, $J_{H3,H4}$ 9.2 Hz, $J_{H4,H5}$ 10.0 Hz, H4), 4.64 (dt, 1H, H2), 4.35 (dd, 1H, $J_{H5,H6b}$ 4.4 Hz, $J_{H6a,H6b}$ 12.5 Hz, H6b), 4.17 (dd, 1H, $J_{H5,H6a}$ 2.4 Hz, $J_{H6a,H6b}$ 12.5 Hz, H6a), 3.93 (ddd, 1H, $J_{H5,H6a}$ 2.4 Hz, $J_{H5,H6b}$ 4.4 Hz, $J_{H4,H5}$ 10.0 Hz, H5), 2.23, 2.11, 2.10, 2.07 (4s, 12H, 4 × OAc) ppm. ^{13}C NMR: δ 178.8 (C=S), 171.3, 170.7, 170.4, 169.4 (4 × C=O, acetyl), 160.2 (C=O, amide),

138.2 (Ca), 133.6 (Cd), 132.1 (Cc), 129.8 (Cb), 91.6 (C1), 73.1 (C5), 72.2 (C3), 67.8 (C4), 61.5 (C6), 60.8 (C2), 21.3, 21.0, 20.8, 20.7 (4 × CH_3) ppm.

24a

The same method was used as for **23a** except with a 2 molar equivalent of thiourea. **8a** (100 mg, 0.196 mmol), (THT)AuCl (31.4 mg, 0.098 mmol) and CH_2Cl_2 (10 mL) under nitrogen overnight. Worked up to give a white solid **24a** (84.7 mg, 71%).

^{1}H NMR: δ 11.12 (d, 1H, $J_{H2,HN1}$ 9.7 Hz, HN1), 9.76 (s, 1H, HN2), 7.82 (m, 2H, Hc), 7.67 (m, 1H, Ha), 7.54 (m, 2H, Hb), 5.99 (d, 1H, $J_{H1,H2}$ 8.3 Hz, H1), 5.45 (dd, 1H, $J_{H3,H4}$ 9.0 Hz, $J_{H2,H3}$ 9.9 Hz, H3), 5.23 (t, 1H, H4), 4.83 (dt, 1H, H2), 4.34 (dd, 1H, $J_{H5,H6b}$ 4.6 Hz, $J_{H6a,H6b}$ 12.4 Hz, H6b), 4.17 (dd, 1H, $J_{H5,H6a}$ 2.5 Hz, $J_{H6a,H6b}$ 12.5 Hz, H6a), 3.92 (ddd, 1H, $J_{H5,H6a}$ 2.5 Hz, $J_{H5,H6b}$ 4.6 Hz, $J_{H4,H5}$ 9.6 Hz, H5), 2.17, 2.11, 2.08, 2.07 (4s, 12H, 4 × OAc) ppm. ^{13}C NMR: δ 180.7 (C=S), 170.7, 170.6, 169.4, 169.4 (4 × C=O, acetyl), 166.4 (C=O, amide), 135.0 (Ca), 129.8 (Cd), 129.7 (Cb), 127.9 (Cc), 92.1 (C1), 73.2 (C5), 72.3 (C3), 67.6 (C4), 61.6 (C6), 59.4 (C2), 21.2, 20.9, 20.8, 20.7 (4 × CH_3) ppm. *Anal.* Calcd for $C_{44}H_{52}N_2O_{20}S_2ClAu$ (1253.448): C, 42.16; H, 4.18; N, 4.47. Found: C, 42.34; H, 4.37; N, 4.02.

2.14 References

1. Adams, R.D., Huang, M., Yamamoto, J.H., and Zhang, L., *The coordination of N,N-diethyl-N'-p-tolylthiourea to polynuclear rhenium carbonyl complexes.* Chem. Ber., 1996. **129**, 137-142.
2. Henderson, W., Nicholson, B.K., and Rickard, C.E.F., *Platinum(II) complexes of chelating and monodentate thiourea monoanions incorporating chiral, fluorescent or chromophoric groups.* Inorg. Chim. Acta, 2001. **320**, 101-109.
3. Dinger, M.B., Henderson, W., Nicholson, B.K., and Robinson, W.T., *Organogold(III) metallacyclic chemistry. Part 3[1]. Self-assembly of the*

nonametallic gold(III)-silver(I)-sulfido aggregates $[\{LAu(\mu\text{-}S)_2AuL\}_3Ag_3X_2]^+$ *(L=cycloaurated N,N-dimethylbenzylamine ligand; X=Cl, Br), by thiourea desulfurisation.* J. Organomet. Chem., 1998. **560**, 169-181.

4. Stocker, F.B. and Britton, D., *1,2-Dicyano-1,2-bis(imidazolidine-2-thione)digold(I) and 2,2-dicyano-1,1-bis(dimethylthiourea)digold(I).* Acta Crystallogr., Sect. C: Cryst. Struct. Commun., 2000. **56**, 798-800.
5. Melnick, J.G., Yurkerwich, K., and Parkin, G., *Synthesis, structure, and reactivity of two-coordinate mercury alkyl compounds with sulfur ligands: Relevance to mercury detoxification.* Inorg. Chem., 2009. **48**, 6763-6772.
6. Aldoshin, S.M., Lyssenko, K.A., Antipin, M.Y., Sanina, N.A., and Gritsenko, V.V., *Precision X-ray study of mononuclear dinitrosyl iron complex* $[Fe(SC_2H_3N_3)(SC_2H_2N_3)(NO)_2]\cdot 0.5H_2O$ *at low temperatures.* J. Mol. Struct., 2008. **875**, 309-315.
7. Beheshti, A., Clegg, W., Dale, S.H., and Hyvadi, R., *Synthesis, crystal structures, and spectroscopic characterization of the neutral monomeric tetrahedral* $[M(Diap)_2(OAc)_2] \cdot H_2O$ *complexes (M = Zn,Cd; Diap = 1,3-diazepane-2-thione; OAc = acetate) with N-H...O and O-H...O intra- and intermolecular hydrogen bonding interactions.* Inorg. Chim. Acta, 2007. **360**, 2967-2972.
8. Dago, A., Shepelev, Y., Fajardo, F., Alvarez, F., and Pomes, R., *Structure of 1-benzoyl-3-propylthiourea.* Acta Crystallogr., Sect. C: Cryst. Struct. Commun., 1989. **45**, 1192-1194.
9. Binzet, G., Arslan, H., Florke, U., Kulcu, N., and Duran, N., *Synthesis, characterization and antimicrobial activities of transition metal complexes of N,N-dialkyl-N'-(2-chlorobenzoyl)thiourea derivatives.* J. Coord. Chem., 2006. **59**, 1395-1406.
10. Cauzzi, D., Lanfranchi, M., Marzolini, G., Predieri, G., Tiripicchio, A., Costa, M., and Zanoni, R., *Anchoring rhodium(I) on benzoylthiourea-functionalized silca xerogels. Production of recyclable hydroformylation catalysts and the crystal structure of the model compound [Rh(cod)(Hbztu)Cl].* J. Organomet. Chem., 1995. **488**, 115-125.
11. Westra, A.N., Bourne, S.A., Esterhuysen, C., and Koch, K.R., *Reactions of halogens with Pt(II) complexes of N-alkyl- and N,N-dialkyl-N'-benzoylthioureas: oxidative addition and formation of an* I_2 *inclusion compound.* Dalton Trans., 2005. **17**, 2162-2172.

12. Cauzzi, D., Lanfranchi, M., Marzolini, G., Predieri, G., Tiripicchio, A., and Cambilini, M.T., *Metal complexes tethered to a functionalized xerogel containing the benzoylthiourea moiety. Crystal structures of trans-[Pd(Hbztu)$_2$Cl$_2$] and [Cu(Hbztu)$_2$Cl] (Hbztu = N-benzoyl-N'-propylthiourea.* Gazz. Chim. Ital., 1994. **124**, 417-421.

13. Bourne, S. and Koch, K.R., *Intramolecular hydrogen-bond controlled unidentate co-ordination of potentially chelating N-acyl-N'-alkylthioureas: Crystal structure of cis-bis(N-benzoyl-N'-propylthiourea) dichloroplatinum(II).* J. Chem. Soc., Dalton Trans., 1993. 2071-2072.

14. Koch, K.R., Wang, Y., and Coetzee, *Platinum(II) and palladium(II) complexes of N-benzoyl-N'-propyl-thiourea (H$_2$L): synthesis and geometric isomer distribution of [M(H$_2$L-S)$_2$X$_2$] (M = Pt^{II} or Pd^{II}; X = Cl$^-$, Br$^-$ or I$^-$); crystal structure of trans-[Pd(H$_2$L-S)$_2$Br$_2$].* J. Chem. Soc., Dalton Trans., 1999. **6**, 1013-1016.

15. Zhang, Y.-M., Xian, L., and Wei, T.-B., *Chlorobis[N'-ethoxycarbonyl-N-(4-methylphenyl)thiourea-kS]copper (I).* Acta Crystallogr., Sect. C: Cryst. Struct. Commun., 2003. **C59**, m473-m474.

16. Safin, D.A., Sokolov, F.D., Szyrwiel, L., Baranov, S.V., Babashkina, M.G., Gimadiev, T.R., and Kozlowski, H., *Monodentate S-vs. bidentate 1,5-O,S-coordination of N-phosphoryl-N'-(R)-thioureas with Pd(II).* Polyhedron, 2008. **27**, 1995-1998.

17. Rodríguez-Lucena, D., Ortiz Mellet, C., Jaime, C., Burusco, K.K., García Fernández, J.M., and Benito, J.M., *Size-tunable trehalose-based nanocavities: Synthesis, structure, and inclusion properties of large-ring cyclotrehalans.* J. Org. Chem., 2009. **74**, 2997-3008.

18. Tenchiu, A.-C., Kostas, I.D., Kovala-Demertzi, D., and Terzis, A., *Synthesis and characterization of new aromatic aldehyde/ketone 4-(β-D-glucopyranosyl)thiosemicarbazones.* Carbohydr. Res., 2009. **344**, 1352-1364.

19. Tournaire-Arellano, C., Younes-El Hage, S., Valès, P., Caujolle, R., Sanon, A., Bories, C., and Loiseau, P.M., *Synthesis and biological evaluation of ureido and thioureido derivatives of 2-amino-2-deoxy-D-glucose and related aminoalcohols as N-acetyl-β-D-hexosaminidase inhibitors.* Carbohydr. Res., 1998. **314**, 47-63.

20. López, Ó., Maza, S., Maya, I., Fuentes, J., and Fernández-Bolaños, J.G., *New synthetic approaches to sugar ureas. Access to ureido-β-cyclodextrins.* Tetrahedron, 2005. **61**, 9058-9069.

21. Jiménez Blanco, J.L., Bootello, P., Benito, J.M., Ortiz Mellet, C., and García Fernández, J.M., *Urea-, thiourea-, and guanidine-linked glycooligomers as phosphate binders in water.* J. Org. Chem., 2006. **71**, 5136-5143.

22. Blomberg, K. and Ulfstedt, A.-C., *Fluorescent europium chelates as target cell markers in the assessment of natural killer cell cytotoxicity.* J. Immunol. Methods, 1993. **160**, 27-34.

23. Felder, T., Röhrich, A., Stephan, H., and Schalley, C.A., *Fragmentation reactions of singly and doubly protonated thiourea- and sugar-substituted cyclams and their transition-metal complexes.* J. Mass Spectrom., 2008. **43**, 651-663.

24. Zhang, S.-S., Yang, B., Li, H.-X., and Jiao, K., *Facile synthesis and characterization of bioactive N-[(1-ferrocenylethylidene)amino]-N'-β-D-glycopyranosylthiourea.* Chin. J. Chem., 2005. **23**, 1253-1256.

25. Pill, T. and Beck, W., *Metal complexes of biologically important ligands. Rhodium(III), iridium(III), palladium(II), platinum(II), gold(I) complexes of N-(2,3,4,6-tetra-O-acetyl-β-D-glucopyranosyl)-thiocarbamate esters and β-D-glucopyranosylthiourea.* Z. Naturforsch., B: Chem. Sci., 1993. **48**, 1461-1469.

26. Roseman, S., *Reflections on glycobiology.* J. Biol. Chem., 2001. **276**, 41527-41542.

27. Myszka, H., Bednarczyk, D., Najder, M., and Kaca, W., *Synthesis and induction of apoptosis in B cell chronic leukemia by diosgenyl 2-amino-2-deoxy-β-D-glucopyranoside hydrochloride and its derivatives.* Carbohydr. Res., 2003. **338**, 133-141.

28. Ávalos, M., Babiano, R., Cintas, P., Jiménez, J.L., Palacios, J.C., and Valencia, C., *Condensation of 2-amino-2-deoxysugars with isothiocyanates. Synthesis of cis-1,2-fused glycopyrano heterocycles.* Tetrahedron, 1994. **50**, 3273-3296.

29. Fernández-Bolaños Guzmán, J., García Rodríguez, S., Fernández-Bolaños, J., Díanez, M.J., and López-Castro, A., *Reaction of 2-amino-2-deoxy-glucose with aryl and acyl isothiocyanates, and aryl isocyanates: structure of the intermediate products.* Carbohydr. Res., 1991. **210**, 125-143.

30. Brindley, J.C., Caldwell, J.M., Meakins, G.D., Plackett, S.J., and Price, S.J., *N'-substituted N-acyl- and N-imidoyl-thioureas: preparation and conversion of N',N'-disubstituted compounds into 2-(N,N-disubstituted amino)thiazol-5-yl ketones.* J. Chem. Soc., Perkin Trans. 1, 1987. 1153-1158.

31. Krüger, F. and Rudy, H., *Reaction of 2-amino-2-deoxy-D-glucose with acyl isothiocyanates.* Liebigs Ann. Chem., 1966. **696**, 214-219.

32. Zhou, G.-B., Guan, Y.-Q., Shen, C., Wang, Q., Liu, X.-M., Zhang, P.-F., and Li, L.-L., *A novel and convenient synthesis of thiazol-2(3H)-imine-linked glycoconjugates.* Synthesis, 2008. **2008**, 1994,1996.

33. Zhao, Q., Shen, C., Zheng, H., Zhang, J., and Zhang, P., *Synthesis, characterization, and cytotoxicity of some novel glycosyl thiazol-2-imines as antitumoral agents.* Carbohydr. Res., 2010. **345**, 437-441.

34. Duque, J., Estévez-Hernández, O., Reguera, E., Ellena, J., and S. Corrêa, R., *Synthesis, characterization, and single crystal X-ray structure of the 1-furoyl-3-cyclohexylthiourea cadmium chloride complex,* $Cd[C_4H_3OC(O)NHC(S)NHC_6H_{11}]_4Cl_2$. J. Coord. Chem., 2009. **62**, 2804 - 2813.

35. Silverstein, R.M., Webster, F.X., and Kiemle, D.J., *Spectrometric identification of organic compounds* 7th ed. 2005, Hoboken: John Wiley & Sons, Inc.

36. Anulewicz, R., Wawer, I., Piekarska-Bartoszewicz, B., and Temeriusz, A., *Crystal structure and solid state NMR analysis of N-(methyl 3,4,6-tri-O-acetyl-2-amino-2-deoxy-β-D-glucopyranoside)-N'-carbamoyl-D-valine ethyl ester.* J. Carbohydr. Chem., 1997. **16**, 739-749.

37. Vinogradov, S.N. and Linnell, R.H., *Hydrogen bonding*. 1971, New York: Van Nostrand Reinhold Company.

38. Bürgi, H.-B. and Dunitz, J.D., eds. *Structure correlation*. Vol. 2. 1994, New York: VCH Verlagsgesellschaft mbH.

39. Pimentel, G.C. and McClellan, A.L., *The hydrogen bond*. 1960, New York: W.H. Freeman and Company.

40. Jeffrey, G.A. and Lewis, L., *Cooperative aspects of hydrogen bonding in carbohydrates.* Carbohydr. Res., 1978. **60**, 179-182.

41. Ceccarelli, C., Jeffrey, G.A., and Taylor, R., *A survey of O-H•••O hydrogen bond geometries determined by neutron diffraction.* J. Mol. Struct., 1981. **70**, 255-271.

42. Rao, V.S.R., Qasba, P.K., Balaji, P.V., and Chandrasekaran, R., *Conformation of carbohydrates*. 1998, Amsterdam: Harwood academic publishers.

43. Collins, P. and Ferrier, R., *Monosaccharides: Their chemistry and their roles in natural products*. 1995, Chichester: John Wiley & Sons, Ltd.

44. Neuberger, A. and Fletcher, A.P., *Dissociation constants of 2-amino-2-deoxy-D-glucopyranose.* J. Chem. Soc., B, 1969. 178-181.

45. Horton, D., Jewell, J.S., and Philips, K.D., *Anomeric equilibria in derivatives of amino sugars. Some 2-amino-2-deoxy-D-hexose derivatives.* J. Org. Chem., 1966. **31**, 4022-4025.

46. Henderson, W. and Evans, C., *Electrospray mass spectrometric analysis of transition-metal halide complexes.* Inorg. Chim. Acta, 1999. **294**, 183-192.

47. Hutchings, A.M., McConnell, N.E., Faucher, R.A., VanDerveer, D., and Williams, D.J., *The preparation, characterization, and X-ray structural analysis of dichlorobis[1-methyl-3-(2-propyl) -2(3H)-imidazolethione]mercury(II).* J. Chem. Crystallogr., 2003. **33**, 619-623.

48. Groysman, S. and Holm, R.H., *A series of mononuclear quasi-two-coordinate copper(I) complexes employing a sterically demanding thiolate ligand.* Inorg. Chem., 2009. **48**, 621-627.

49. Scharwitz, M.A., Ott, I., Geldmacher, Y., Gust, R., and Sheldrick, W.S., *Cytotoxic half-sandwich rhodium(III) complexes: Polypyridyl ligand influence on their DNA binding properties and cellular uptake.* J. Organomet. Chem., 2008. **693**, 2299-2309.

50. Grgurić-Šipka, S., Alshtewi, M.A.M.A., Jeremić, D., Kaluđerović, G.N., Gómez-Ruiz, S., Žižak, Ž., Juranić, Z., and Sabo, T.J., *Synthesis, structural characterization and cytotoxic activity of two new organoruthenium(II) complexes.* J. Serb. Chem. Soc., 2008. **73**, 619-630.

51. Moro, A.C., Mauro, A.E., Netto, A.V.G., Ananias, S.R., Quilles, M.B., Carlos, I.Z., Pavan, F.R., Leite, C.Q.F., and Hörner, M., *Antitumor and antimycobacterial activities of cyclopalladated complexes: X-ray structure of [Pd(C^2,N-dmba)(Br)(tu)] (dmba = N,N-dimethylbenzylamine, tu = thiourea).* Eur. J. Med. Chem., 2009. **44**, 4611-4615.

52. Nadeem, S., Rauf, M., Ahmad, S., Ebihara, M., Tirmizi, S., Bashir, S., and Badshah, A., *Synthesis and characterization of palladium(II) complexes of thioureas. X-ray structures of [PdN,N'-dimethylthiourea)$_4$]Cl_2.2H_2O and [Pd(tetramethylthiourea)$_4$]Cl_2.* Transition Met. Chem., 2009. **34**, 197-202.

53. Huheey, J.E., *Inorganic chemistry*. 2nd ed. 1978, London: Harper and Row.

54. Ghassemzadeh, M., Heravi, M., M. , and Neumüller, B., *Synthesis, characterization and crystal structures of new palladium(II) complexes and the first platinum(III) complex containing ATT (ATT = 6-Aza-2-thiothymine).* Z. Anorg. Allg. Chem., 2005. **631**, 2401-2407.

55. Cotton, F.A., Wilkinson, G., Murillo, C.A., and Bochmann, M., *Advanced inorganic chemistry*. 6th ed. 1999: John Wikey & Sons, Inc.

56. Popović, Z., Matković-Čalogović, D., Soldin, Ž., Pavlović, G., Davidović, N., and Vikić-Topić, D., *Mercury(II) compounds with 1,3-imidazole-2-thione and its 1-*

methyl analogue. Preparative and NMR spectroscopic studies. The crystal structures of di-μ-iodo-bis[iodo(1,3-imidazolium-2-thiolato-S)mercury(II)], bis[bromo(1,3-imidazolium-2-thiolato-S)]mercury(II) and bis[μ-(1-N-methyl-1,3-imidazole-2-thiolato-S)]mercury(II). Inorg. Chim. Acta, 1999. **294**, 35-46.

57. Popović, Z., Pavlović, G., Matković-Čalogović, D., Soldin, Ž., Rajić, M., Vikić-Topić, D., and Kovaček, D., *Mercury(II) complexes of heterocyclic thiones. Part 1. Preparation of 1:2 complexes of mercury(II) halides and pseudohalides with 3,4,5,6-tetrahydropyrimidine-2-thione. X-ray, thermal analysis and NMR studies.* Inorg. Chim. Acta, 2000. **306**, 142-152.
58. Yusof, M.S.M., Yamin, B.M., and Kassim, M.B., *Bis(o-chlorophenylbenzoylthiourea-κS)-diiodomercury(II).* Acta Crystallogr. Sect. E: Struct. Rep. Online, 2004. **E60**, m98-m99.
59. Zhang, Y.-M., Yang, L.-Z., Lin, Q., and Wei, T.-B., *Synthesis and crystal structure of bis{(μ-chloro)-chloro-[N-benzoyl-N'-(2-hydroxyethyl)thiourea] mercury(II)}.* J. Coord. Chem., 2005. **58**, 1675-1679.
60. Sabounchei, S.J., Nemattalab, H., Salehzadeh, S., Bayat, M., Khavasi, H.R., and Adams, H., *New mono and binuclear mercury(II) complexes of phosphorus ylides containing DMSO as ligand: Spectral and structural characterization.* J. Organomet. Chem., 2008. **693**, 1975-1985.
61. Sabounchei, S.J., Nemattalab, H., and Khavasi, H.R., *Crystal structure of diiodo, (4'-chlorobenzoylmethylenetriphenylphosphorane), (dimethylsulfoxide), mercury(II) complex, $C_{28}H_{26}ClHgI_2O_2PS$.* X-ray Structure Analysis Online, 2009. **25**, 13-14.
62. Tschinkl, M., Schier, A., Riede, J., and Gabbai, F.P., *Complexation of DMF and DMSO by a monodentate organomercurial lewis acid.* Organometallics, 1999. **18**, 2040-2042.
63. Biscarini, P., Fusina, L., Nivellini, G.D., Mangia, A., and Pelizzi, G., *Crystal structure and spectroscopic properties of mercury(II) halide complexes. Part II. The dimethyl sulphoxide-mercury(II) chloride (2/3) adduct.* J. Chem. Soc., Dalton Trans., 1974. 1846-1849.
64. Zhang, Y., *Electronegativities of elements in valence states and their applications. 1. Electronegativities of elements in valence states.* Inorg. Chem., 1982. **21**, 3886-3889.

65. Isab, A.A. and Hussain, M.S., *Synthesis, ^{13}C NMR and IR spectroscopic studies of gold(I) complexes of imidazolidine-2-thione and its derivatives.* Polyhedron, 1985. **4**, 1683-1688.

66. Fabretti, A.C., Giusti, A., and Malavasi, W., *Reaction products between gold(III) bromide and tetramethylthiourea: Dibromobis(tetramethylthiourea)gold(III) dibromoaurate(I) and bromo(tetramethylthiourea)gold(I). Synthesis, crystal and molecular structure, and infrared spectra.* J. Chem. Soc., Dalton Trans., 1990. 3091-3093.

67. Eiter, L.C., Hall, N.W., Day, C.S., Saluta, G., Kucera, G.L., and Bierbach, U., *Gold(I) analogues of a platinum–acridine antitumor agent are only moderately cytotoxic but show potent activity against Mycobacterium tuberculosis.* J. Med. Chem., 2009. **52**, 6519-6522.

68. Shaw, C.F., *Gold-based therapeutic agents.* Chem. Rev., 1999. **99**, 2589-2600.

69. Shaw III, C.F., *The biochemistry of gold*, in *Gold: Progress in Chemistry, Biochemistry and Technology*, H. Schmidbaur, Editor. 1999, John Wiley & Sons Ltd: Chichester. p. 259-308.

70. Benedek, T.G., *The history of gold therapy for tuberculosis.* J. Hist. Med. All. Sci., 2004. **59**, 50-89.

71. Bensch, W. and Schuster, M., *Complex formation of gold with N,N-dialkyl-N'-benzoylthioureas: The crystal structure of N,N-diethyl-N'-benzoylthioureatogold(I) chloride.* Z. Anorg. Allg. Chem., 1992. **611**, 99-102.

72. Hussain, M.S. and Isab, A.A., *Chloro(N-ethyl-1,3-imidazolidine-2-thione)gold(I): Spectroscopic studies and x-ray structure.* Transition Met. Chem., 1984. **9**, 398-401.

73. Piro, O.E., Castellano, E.E., Piatti, R.C.V., Bolzan, A.E., and Arvia, A.J., *Two thiourea-containing gold(I) complexes.* Acta Crystallogr., Sect. C: Cryst. Struct. Commun., 2002. **58**, m252-m255.

74. Yan, K., Lok, C.-N., Bierla, K., and Che, C.-M., *Gold(I) complex of N,N'-disubstituted cyclic thiourea with in vitro and in vivo anticancer properties-potent tight-binding inhibition of thioredoxin reductase.* Chem. Commun., 2010. **46**, 7691-7693.

75. Isab, A.A., Fettouhi, M., Ahmad, S., and Ouahab, L., *Mixed ligand gold(I) complexes of phosphines and thiourea and X-ray structure of (thiourea-κS)(tricyclohexylphosphine)gold(I)chloride.* Polyhedron, 2003. **22**, 1349-1354.

76. White, C., Yates, A., Maitlis, P.M., and Heinekey, D.M., *(η^5-Pentamethylcyclopentadienyl)rhodium and -iridium compounds.* Inorg. Synth., 2007. **29**, 228-234.

77. Uson, R., Laguna, A., Laguna, M., Briggs, D.A., Murray, H.H., and Fackler, J.P., *(Tetrahydrothiophene)gold(I) or gold(III) complexes.* Inorg. Synth., 2007. **26**, 85-91.

Chapter Three
Sugar thioureas as anionic ligands

3.1 Thioureas as anionic ligands

The presence of at least one proton on a nitrogen of a thiourea allows it to be deprotonated and act as an anionic ligand. As mentioned on page 17, *N*,*N*-di-alkyl-*N´*-benzoyl thioureas generally prefer to act as bidentate monoanions through the sulfur and oxygen atoms and have been widely studied. Much less is known about *N*-alkyl-*N´*-benzoyl thioureas as monoanionic ligands.

3.1.1 Sugar thioureas as anionic ligands

As with the neutral complexes discussed in Chapter 2, while work has been done on thioureas in general as anionic ligands little research has been using sugar thioureas. The first example was reported by Zinner *et al* in 1970, where they took a sugar with a cyclic thiourea and formed a complex to mercury(II), Figure 3.1, giving a four-membered ring with *N*,*S* coordination [1]. More recently *N*-glucopyranosyl-*N´*-acetyl-*N´*-phenyl-thiourea was reacted with HgO to make the mercury(II) complex shown in Figure 3.1 with the thiourea acting as an anionic ligand with a six-membered ring with *O*,*S* coordination [2].

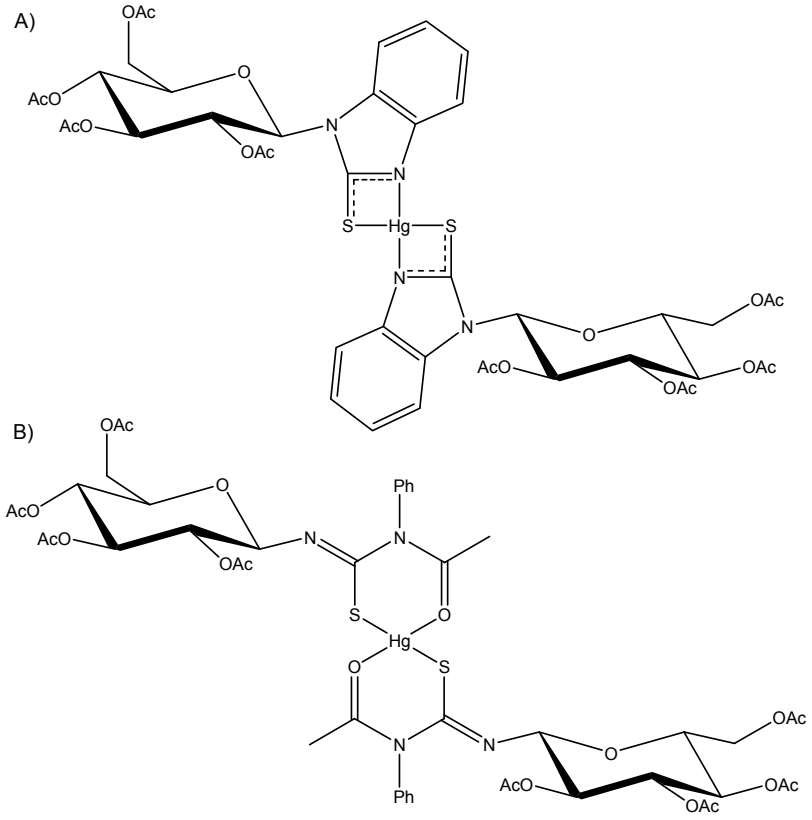

Figure 3.1 *Known sugar thioureas as anionic ligands: A) [2]; B) [1].*

3.1.2 Sugar thioureas tested as anionic ligands

As well as the acyl thioureas **8a-e** from the previous chapter, another sugar thiourea was used. Previously the analogue of the non-acyl thiourea **8f** with the thiourea on C1 instead of C2, was reacted with acetic anhydride and pyridine to acylate N2 [2]. This reaction was tried for **8f** and produced the new thiourea **8g**, Scheme 3.1. To see if the isomer with the acetate on N1 could be made, *N*-acetyl-1,3,4,6-tetra-*O*-acetyl-D-β-glucosamine [3] was reacted with phenyl isothiocyanate in CH_2Cl_2, Scheme 3.1. Unfortunately no reaction was observed, even after refluxing for 16 hours. It was thought that the electron withdrawing acetate group hindered the reaction.

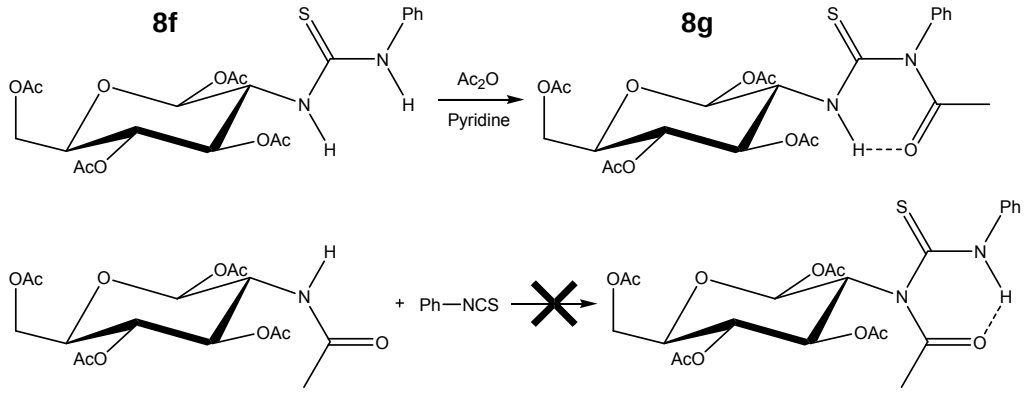

Scheme 3.1 *Reaction scheme for N-alkyl-N´-acetyl-N´-phenyl thioureas.*

The ^{1}H NMR spectrum of **8g**, Figure 3.2, showed that there was an internal hydrogen-bond as with other acyl thioureas by the large downfield position of HN1, even further than **8a**. NH2 was no longer present. As discussed in Chapter Two with the six-membered thiourea ring the coupling constant of HN1 can give information about the conformation. For **8g** it is 8.9 Hz suggesting that the thiourea has the same Z,E,Z-anti conformation seen for the acyl thioureas in Chapter Two. **8g** was of interest since its C1 analogue formed one of the complexes shown in Figure 3.1.

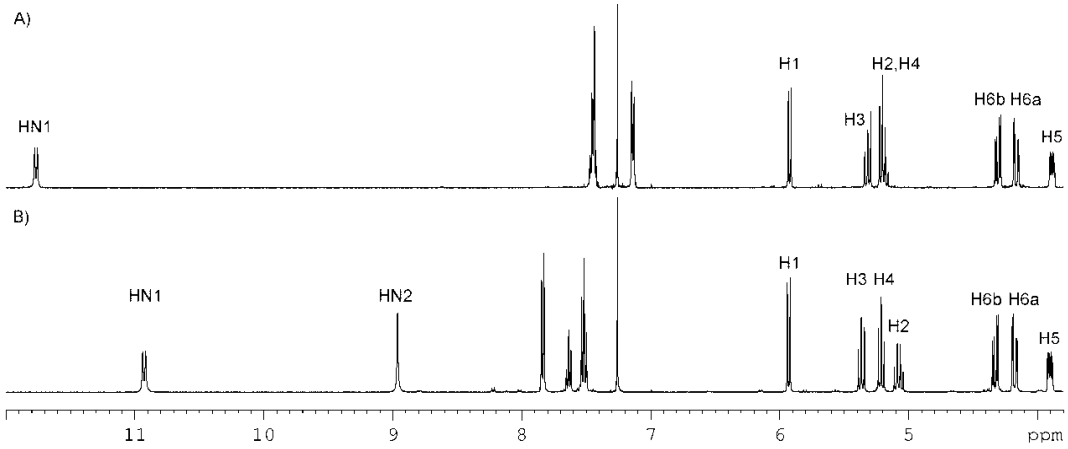

Figure 3.2 *Portion of the ^{1}H NMR spectrum comparing; A) **8g**; B) **8a**.*

3.2 Reaction of thioureas with $[Cp^*RhCl_2]_2$

$[Cp^*RhCl_2]_2$ and **8a** were stirred in a mixture of acetonitrile and water with a 1.2 molar excess of NaOAc. After removal of the solvent, the residue was dissolved in CH_2Cl_2 and filtered through Celite; addition of petroleum spirits gave a bright orange powder of **25a**. ESI-MS showed a number of ions consistent with the thiourea acting as an anionic chelating ligand forming a complex of the form [(**8a**–H)RhCp*Cl]. The main ion in the ESI-MS was $[M–Cl]^+$, with much weaker ions from $[M–HCl+Na]^+$, $[M+Na]^+$, $[2M–Cl]^+$, $[2M+Na]^+$ and $[2M+K]^+$. **25a** did show very weak molecular ions unlike the neutral complexes which generally only showed ions from the loss of one or two HCl molecules with no molecular ions observed. **25a** had essentially already lost one HCl which was why molecular ions were seen.

Since Cp* rhodium(III) has pseudo-tetrahedral geometry it was expected that if **8a** was bonding as a bidentate ligand the product, **25a**, would be chiral. The ^1H and ^{13}C NMR spectra confirmed two diastereoisomers showing two non-equivalent NMR environments of equal intensity. While the thiourea ligand showed two sets of signals, there was only one Cp* signal observed; this indicates that the NMR cannot distinguish between the two diastereoisomers of the Cp* ring. Part of the reason for investigating sugar ligands was for their use as chiral catalysts. Unfortunately in this case the carbohydrate group did not induce any apparent selectivity between the two diastereoisomers. Since complexes of this type can epimerise by loss of the chloride [4], if one isomer was to be preferred it would be expected that upon standing in solution the ratio of the two diastereoisomers would change. Recrystallisation of **25a** would be hindered by the interconversion between the two diastereoisomers so it is unsurprising that attempts to recrystallise **25a** failed.

There are three possible ways that the sugar acyl thioureas could bond as bidentate anionic ligands to a metal centre, Figure 3.3. The first two ways are through the sulfur and nitrogen atoms, or *N*,*S* bonding. This could either involve the amide nitrogen, class I, or the other nitrogen, class II. The bonding could also occur through the sulfur and oxygen atom, or *O*,*S* bonding, class III. Class I is the only one to retain the internal hydrogen-bond. The ^{1}H NMR spectrum was investigated to try and determine how the thiourea was bonding.

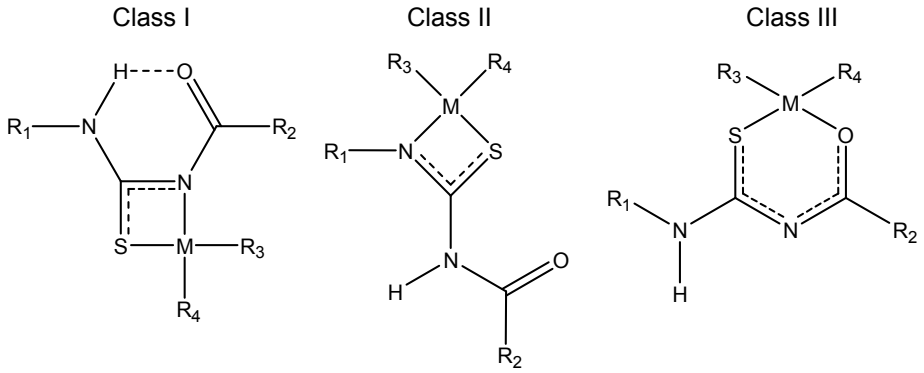

Figure 3.3 *Three classes of bonding acyl thioureas can have as bidentate anionic ligands to a metal centre.*

The ^{1}H NMR spectrum showed only one N–H signal suggesting that the thiourea was indeed bonding as a monoanionic ligand. The N–H signal was a doublet showing that it was the HN1 rather than the HN2 proton that was still present, which precludes class II bonding. The HN1 protons were still far downfield (11.06 and 11.00 ppm) indicating the intramolecular hydrogen-bond was still present, providing strong evidence that the thiourea is bonding as a class I ligand, as shown in Figure 3.4.

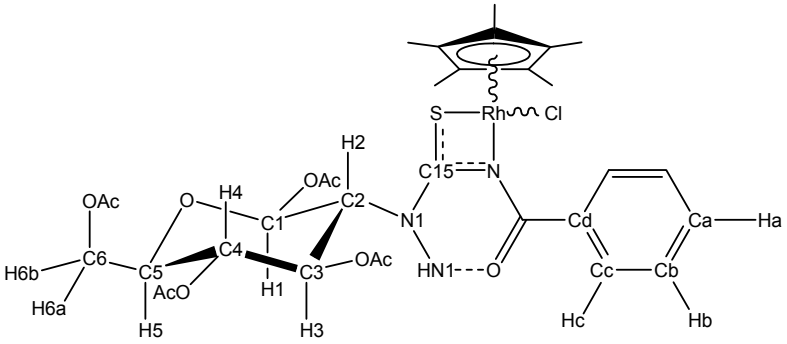

Figure 3.4 *Complex R,S-**25a** with **8a** acting as a monoanionic bidentate ligand and the NMR labelling scheme.*

As with the neutral thiourea the protonated thiourea still has the six-membered ring which prevents rotation around the N1–C15 bond. This means only rotation around the C2–N1 bond can occur. Since no X-ray quality crystals could be grown the only way to determine the orientation was through the coupling constants of HN1. The coupling constants were 10.3 and 10.2 Hz for the two diastereoisomers. This indicates that H2 and HN1 are anti to each other and that the thiourea has a Z,E,Z-anti conformation. While this isn't definitive proof, this orientation is seen for other thioureas with a secondary carbon on N1. There are only two structures of thioureas with a secondary carbon on N1 that show class I bonding; the *N*-isopropyl-*N´*-phosphoryl thiourea shown in Figure 3.5 forms complexes with Ni [5] and Pd [6] and has the Z,E,Z-anti conformation.

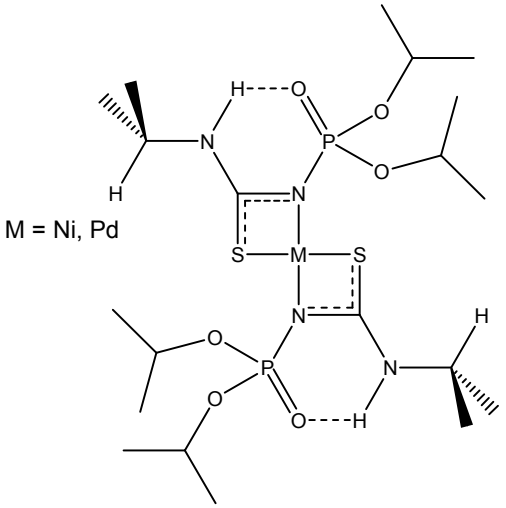

Figure 3.5 *Z,E,Z-anti conformation seen for thioureas with a secondary carbon on N1; Ni [5]; Pd [6].*

While some of the signals could be assigned as belonging to one of the two diastereoisomers others could not be and could only be identified as belonging to either diastereoisomer. For example the H1 and HN1 signals could be paired to each other, so that the isomer with an H1 signal at 5.78 ppm has the HN1 signal at 11.00 ppm and was called **25a**, while the isomer with an H1 signal at 5.60 ppm has the HN1 signal at 11.06 ppm and was called **25a´**. For an example of indistinguishable signals, in the aromatic region there is major overlap and the signal at 8.40 ppm can only be assigned as an overlap of Hc and Hc´.

Figure 3.6 shows the aromatic and N–H region of the ^{1}H NMR spectrum comparing **25a** to **8a**. The HN1 proton has moved downfield slightly. Of the aromatic signals Hc has shifted 0.58 ppm downfield, while Ha and Hb moved upfield. These are bigger changes as compared to **9a** where the thiourea is a neutral monodentate ligand to rhodium(III). This was expected as the thiourea portion has undergone a major change in its electron distribution on coordination.

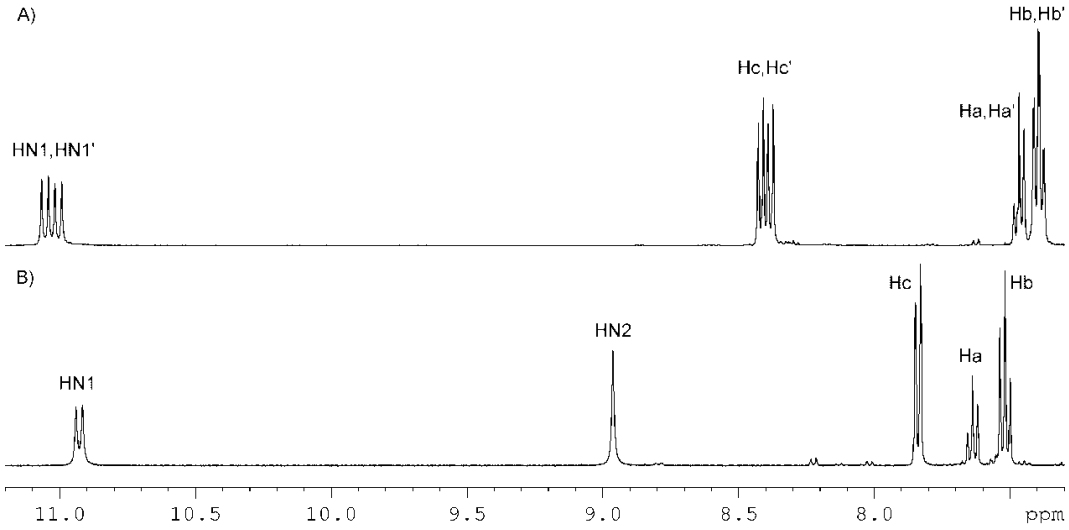

Figure 3.6 *N–H and aromatic portion of the ^{1}H NMR spectrum comparing; A) **25a**; B) **8a**.*

Figure 3.7 shows the sugar portion of the ^{1}H NMR spectrum comparing **25a** and **8a**. For the sugar region all of the signals have been shifted upfield, especially the signals closest to the thiourea (H1, H2, H3 and H4). H2 has shifted the most moving 0.70 ppm.

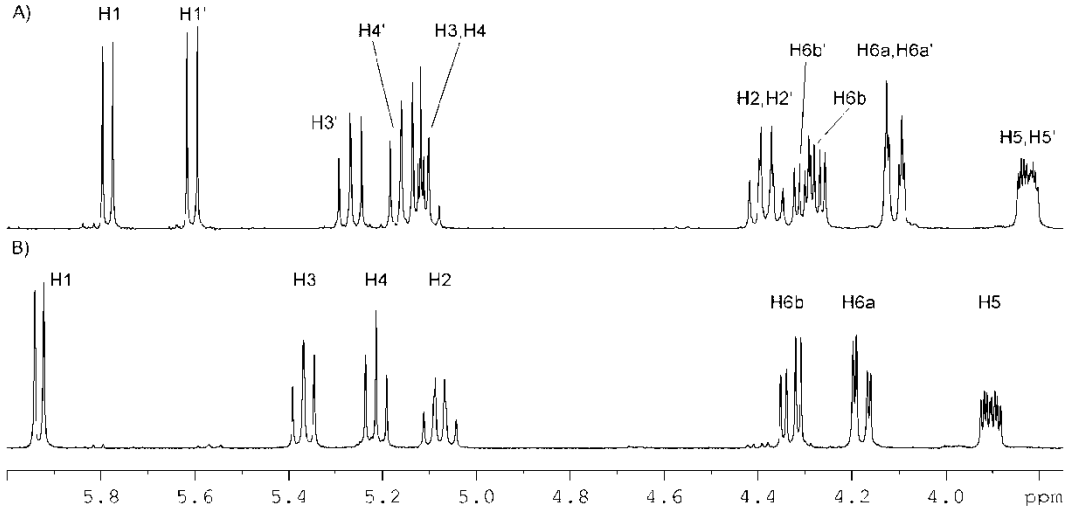

Figure 3.7 *Sugar portion of the ^{1}H NMR spectrum comparing; A) **25a**; B) **8a**.*

The ^{13}C NMR spectrum of **25a** also shows the two diastereoisomers that form. As with the ^{1}H NMR spectra many of the signals cannot be assigned to a specific diastereoisomer but can only be identified as belonging to either. In the HSQC experiment there is much less resolution in the carbon dimension than the proton. Only if there is a large difference in proton chemical shifts could two close carbon signals be distinguished. Only the H1 signals have a large enough separation to allow the two C1 signals to be assigned to each isomer.

Figure 3.8 shows the carbonyl and aromatic portion of the ^{13}C NMR spectrum comparing **25a** with **8a**. Both the C=S and amide carbonyl signals have been shifted downfield. The two diastereoisomers of C=S have moved 8.7 and 8.5 ppm, while for the amide carbonyl it is 10.1 and 10.0 ppm. The aromatic signals have also been shifted with Cd moving downfield and Ca upfield, while Cc and Cb have swapped positions. The carbons closest to the sulfur (C=S, amide carbonyl and Cd) have shifted the most. As with the ^{1}H NMR spectrum the shifts are much greater than for **9a**.

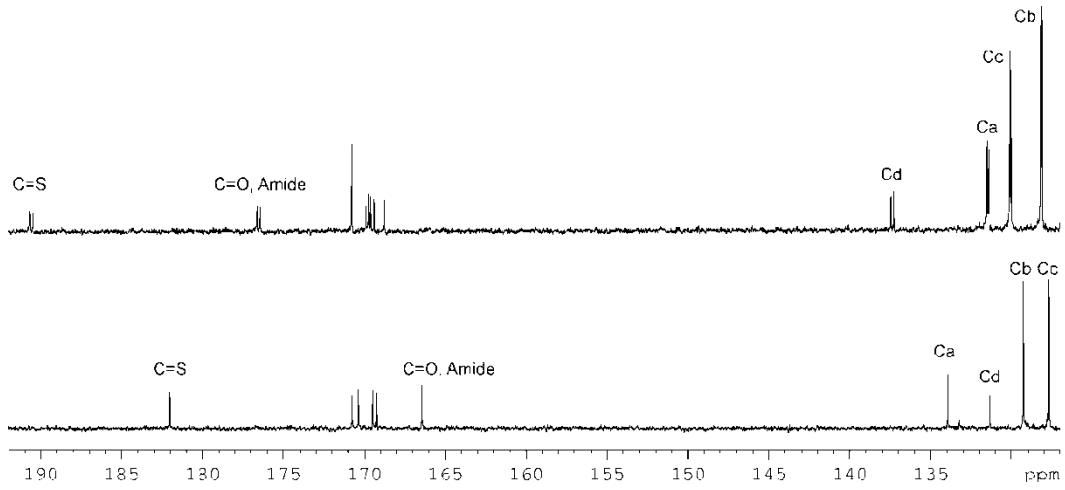

Figure 3.8 *Carbonyl and aromatic portion of the ^{13}C NMR spectrum comparing; A) **25a**; B) **8a**.*

Figure 3.9 shows the sugar portion of the ^{13}C NMR spectrum comparing **25a** with **8a**. For the sugar signals there is little change in chemical shift except C2 which has moved upfield 1.5 ppm. The ^{13}C NMR signals for Cp* like the ^{1}H signal show no sign of the two diastereoisomers. The quaternary carbons of Cp* show splitting from coupling to the rhodium atom of 8.1 Hz.

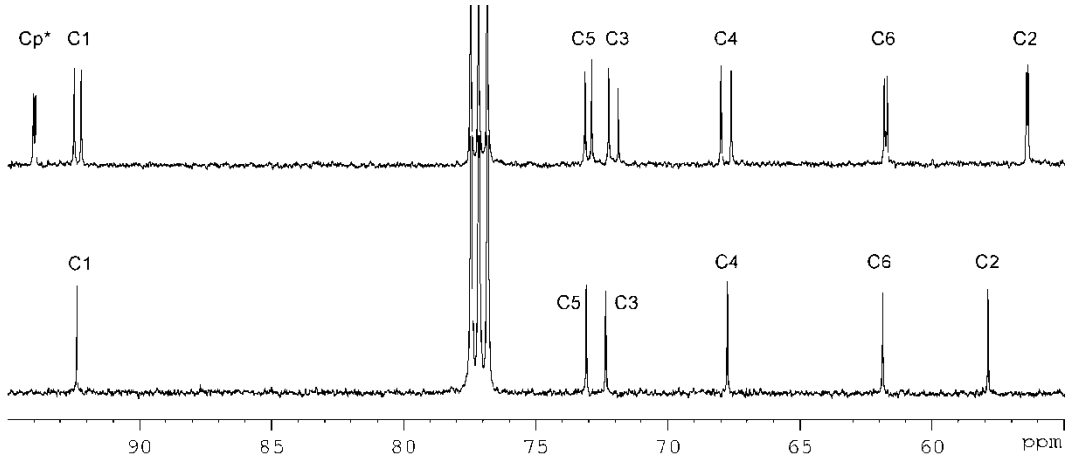

Figure 3.9 *Sugar portion of the ^{13}C NMR spectrum comparing; A) **25a**; B) **8a**.*

The acyl thioureas **8b** and **8d** also react with $[Cp^*RhCl_2]_2$ to produce similar products, Figure 3.10 shows the complex **25d**. ESI-MS of both complexes only showed the $[M–Cl]^+$ ion. Table 3.1 shows selected chemical shifts and coupling constants from the NMR spectra of the complexes **25a**, **25b** and **25d** and the thioureas.

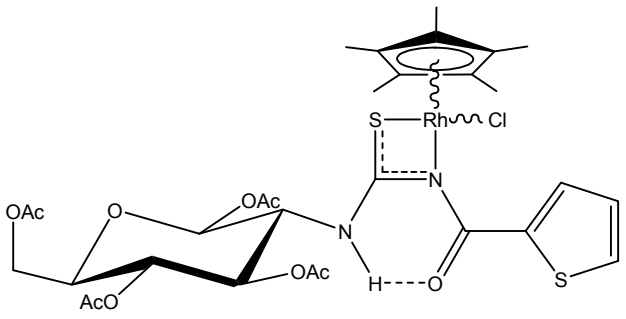

Figure 3.10 *Complex R,S-**25d** with **8d** acting as a monoanionic bidentate ligand.*

	HN1	Hc	H2	C=S	C=O, amide	C2
8a	10.92, 9.2 Hz	7.82	5.08	182.0	166.5	57.9
25a	11.00, 10.2 Hz	8.40,	4.38,	190.7,	176.6,	56.4,
	11.06, 10.3 Hz	8.40	4.38	190.5	176.5	56.4
8b	10.71, 9.4 Hz	8.04	5.06	181.3	164.5	58.0
25b	10.96, 10.4 Hz	8.64	4.43,	191.1,	174.4,	56.7,
	10.92, 10.1 Hz		4.48	190.9	174.3	56.6
8d	10.62, 9.5 Hz	7.55	5.06	181.5	160.5	57.8
25d	10.64, 7.0 Hz	8.90	5.40	189.7,	170.1,	56.2,
	10.61, 6.9 Hz			189.7	169.9	56.2

Table 3.1 *Selected chemical shifts and coupling constants from the NMR spectra of the complexes **25a**, **25b** and **25d** and the thioureas.*

The ^{1}H NMR spectrum shows the same features as **25a** and the signals have shifted in the same manner. Firstly two diastereoisomers have been formed in approximately equal concentrations, again showing no selectivity has been induced by the chiral ligand. The HN1 proton is still present and far downfield indicating that the intramolecular hydrogen-bond is still present. This shows that the thioureas are bonding as class I anionic ligands, with four-membered *N*,*S* chelation. The coupling constants for HN1 suggest the Z,E,Z-anti conformation for the thiourea. The ^{1}H NMR aromatic signals for **25b** and **25d** show similar shifts with Hc moving downfield, Figure 3.11 for a comparison of the aromatic region of the ^{1}H NMR spectrum of **25d** with **8d**. The ^{13}C NMR spectrum is also similar to **25a** with the C=S and amide carbonyl carbons moving downfield, and C2 shifting upfield.

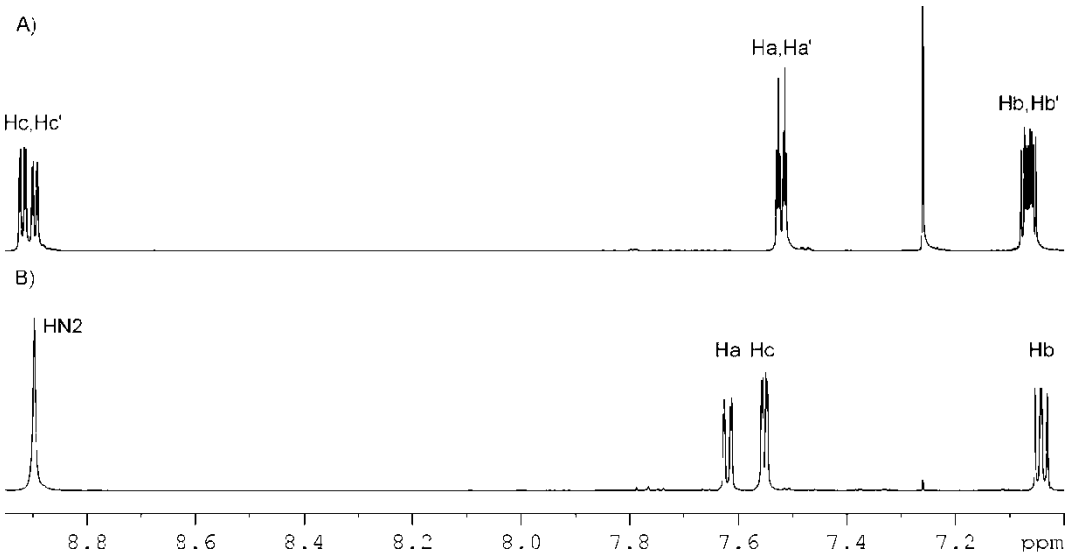

Figure 3.11 *Aromatic portion of the ^{1}H NMR spectrum comparing; A) **25d**; B) **8d**.*

As seen in Figure 3.7 there was severe overlap of some of the signals from the two diastereoisomers. Using a SELTOCSY the signals belonging to each isomer could be isolated, Figure 3.12 for an example SELTOCSY of **25a**.

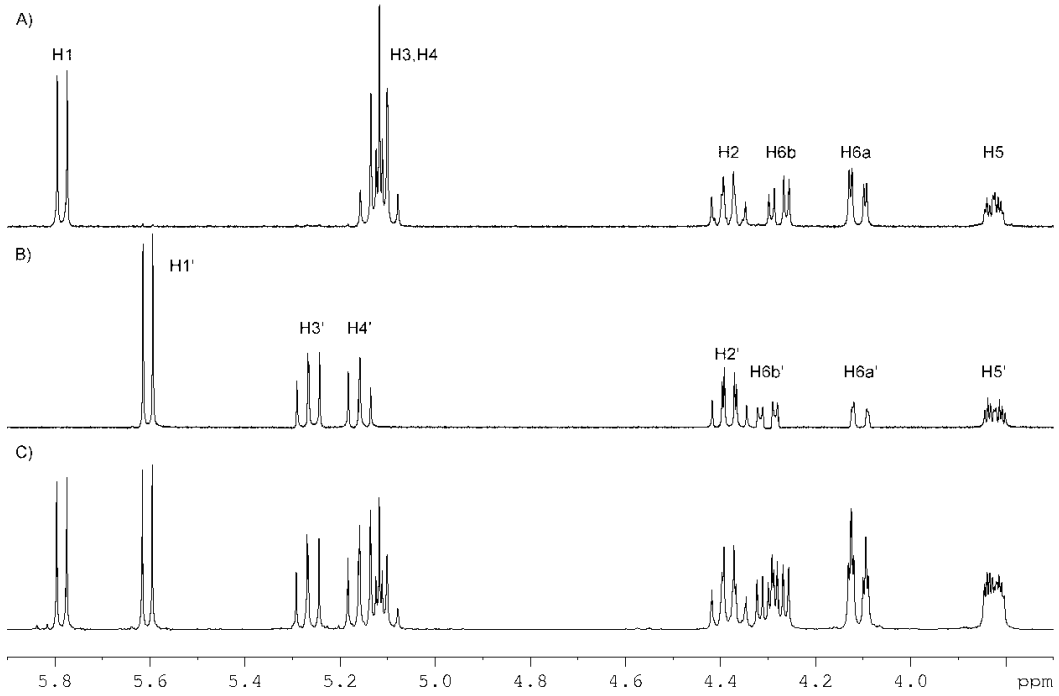

Figure 3.12 *Comparison of a portion of the SELTOSCY and ^{1}H NMR spectra for **25a**; A) SELTOCSY with irradiation of the 5.78 ppm H1 signal, mixing time of 150 milliseconds; B) SELTOCSY with irradiation of the 5.60 ppm H1 signal, mixing time of 150 milliseconds; C) Standard ^{1}H NMR spectrum.*

To see how labile the remaining N–H proton was, DBU was added to an NMR tube containing the complex **25a** in $CDCl_3$. While the N–H proton disappeared the rest of the spectrum had become very complex with very broad signals and nothing could be determined from it.

There are only a small number of complexes to Cp*Rh(III) involving anionic thioureas in the literature, Figure 3.13. These only involve non-acyl thioureas. The first has the thiourea acting as dianionic bridging ligand for a dinuclear metal complex, which was made by directly reacting $[Cp^*RhCl_2]_2$ with a thiourea and a base [7]. Indirect methods have been used, for example phenyl isothiocyanate undergoes an insertion reaction into [Cp*RhCl(Tol-N-CH=NTol)] to produce an *N*,*S* bonding thiourea [8], Figure 3.13.

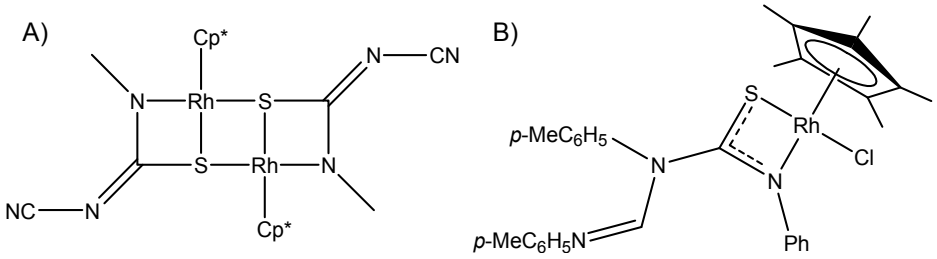

Figure 3.13 *Different complexes of anionic thioureas with Cp*Rh(III); A) [7]; B) [8].*

Since **8g** only has one N–H proton to lose, when it forms an anion there is no intramolecular hydrogen-bond that could drive *N*,*S* bonding. It was thought that *O*,*S* bonding might be observed. While a [(**8g**–H)RhCp*Cl] complex was observed by ESI-MS, no product could be isolated.

The reaction of $[Cp^*RhCl_2]_2$ was also attempted with the unprotected thiourea **8e**. Again while ESI-MS showed the presence of a [(**8e**–H)RhCp*Cl] complex the reaction only gave poorly soluble material from which nothing could be isolated. The NMR spectra of the residue was run in both D_2O and DMSO and no signals were observed that could be identified.

3.2.1 Attempted synthesis of *N*,*S*-[(8a–H)RhCp*PPh$_3$]BF$_4$

The complex **9a** where the thiourea **8a** was bonded as a neutral ligand was made in the previous Chapter. An attempt was made to make the cationic species **26** in Figure 3.14, by removing one of the chlorides from the rhodium and replacing it with PPh_3. To achieve this, **9a** was reacted with $NaBF_4$ and PPh_3 in methanol. The solvent was removed and the residue dissolved in CH_2Cl_2 and filtered. Since phosphorus couples to rhodium and the product would be chiral a pair of doublets was expected in the ^{31}P NMR due to the formation of a mixture of diastereoisomers. However the spectrum showed three sets of pairs of doublets and a doublet as shown in Figure 3.15 with coupling constants. The major

product was one of the pairs of doublets with a smaller pair of doublets at approximately half the intensity of the first. The other two signals were much lower intensity. The coupling constants are what would be expected for J_1 Rh–P values (~140 Hz).

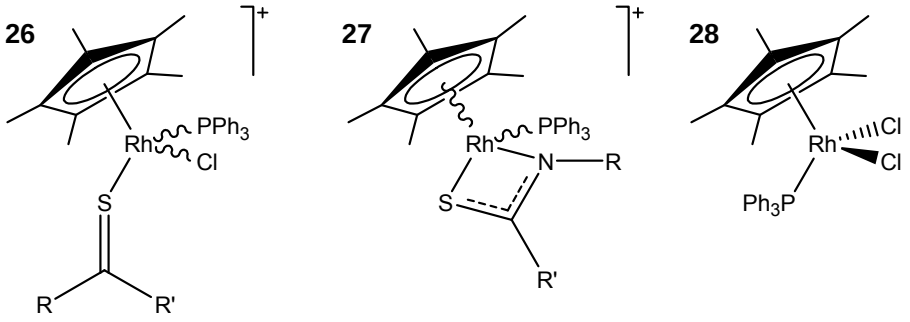

Figure 3.14 *Species seen in the ^{31}P NMR spectra where the thiourea is **8a**.*

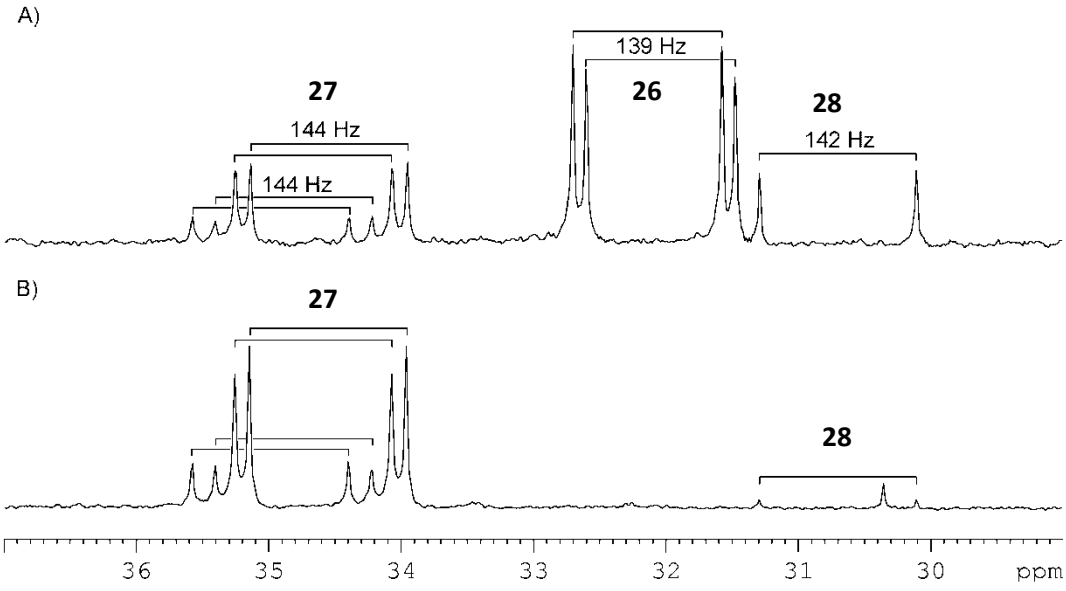

Figure 3.15 *Comparison of ^{31}P NMR spectrum of; A) Initial product from the reaction of **9a** with PPh_3 and $NaBF_4$; B) After the initial mixture was treated with NaOAc.*

It was obvious that other products were forming. The most likely candidate was that the initial complex, **26**, where the thiourea was monodentate was spontaneously losing HCl so that the thiourea was bonding as a bidentate anionic

ligand, to form **27**. This product would also produce a pair of doublets. To test this idea the initial mixture was treated with NaOAc in acetonitrile and water. Upon work up the ^{31}P NMR spectrum showed that the major product signal had disappeared and the minor product from the first reaction was now the largest signal with the two other signals still present. On this basis the signal at 32.3 ppm is assigned as **26** and 34.6 ppm as **27**. However no product could be isolated. When **25a**, where the thiourea was already deprotonated, was reacted with PPh_3 and NaOAc no product was isolated either. The small doublet was found to be $Cp^*RhCl_2PPh_3$. Any attempt to recrystallise the residue from the first reaction only crystallised this. The smallest pair of doublets which was seen in both spectra, could not be identified, but on the basis of the 144 Hz coupling constant was likely to involve some sort of Rh–P bonding.

3.3 Divergent behaviour in the bonding of acyl thioureas

Since the acyl thioureas reacted with $[Cp^*RhCl_2]_2$ as anionic ligands, the same reaction with NaOAc was carried out with the dimer $[(COD)RhCl]_2$. The reaction of **8a** with $[(COD)RhCl]_2$ gave an orange powder as before. ESI-MS showed a complex corresponding to (**8a**–H)Rh(COD), **29a**, with the ions $[M+H]^+$, $[M+Na]^+$ and $[M+K]^+$. **8b** reacted in a similar fashion to give **29b**.

When the ^1H NMR spectrum was recorded, again there was only one N–H signal belonging to HN1, indicating an anionic ligand. However the chemical shift of HN1 was now much further upfield at 6.36 ppm as compared to the HN1 proton in the ligand at 10.92 ppm. Figure 3.16 shows a portion of the ^1H NMR spectrum of **29b** showing the far upfield postion of HN1. This position is indicative of the intramolecular hydrogen-bond no longer being present. As shown in Chapter 2.2.5, this is close to the chemical shift of HN1 in the phenyl thiourea **8f** which also has no internal hydrogen-bond. The lack of this internal hydrogen-bond means that the thiourea is likely to be a class III anionic ligand as shown in Figure

3.17. As expected from the symmetrical COD ligand, no isomers were observed. Table 3.2 gives selected chemical shifts and coupling constants for **29a** and **29b**.

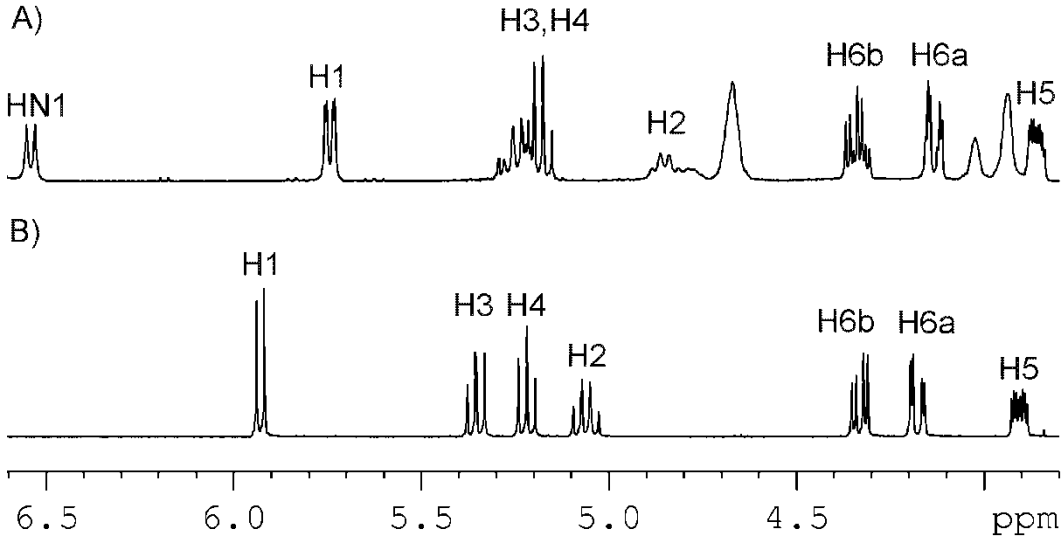

Figure 3.16 *Portion of the ^{1}H NMR spectrum comparing; A) **29b**; B) **8b**.*

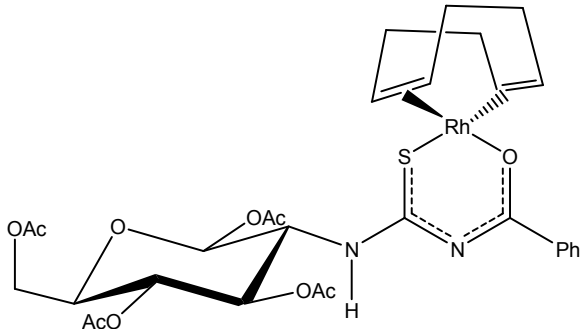

Figure 3.17 *The bonding mode of **29a**, with the thiourea binding through the S and O atoms breaking the intramolecular hydrogen-bond between HN1 and the carbonyl oxygen.*

	HN1	Hc	H2	C=S	C=O, amide	C2
8a	10.92, 9.2 Hz	7.82	5.08	182.0	166.5	57.9
29a	6.36, 9.1 Hz	8.15	4.91	178.5	172.5	56.1
8b	10.71, 9.4 Hz	8.04	5.06	181.3	164.5	58.0
29b	6.55, 9.0 Hz	8.26	4.85	180.1	170.2	56.3

Table 3.2 *Selected chemical shifts and coupling constants from the NMR spectra of complexes **29a** and **29b** and the thioureas.*

The coupling constants for HN1 of both complexes show that H2 and HN1 are still anti to each other. However since there is no longer the six-membered ring the N1–C15 bond is now free to rotate and it isn't possible to know the conformation from just the coupling constant. X-ray quality crystals could not be grown. Examples of acyl analogues that bond *O,S* have shown the protons to be anti to give the Z,Z,E-anti conformation, by rotating both of the bonds from the nitrogen atoms to the C=S carbon [9, 10]. Figure 3.18 gives an example which shows how this conformation puts the secondary carbon anti to the sulfur atom to minimise steric interaction. While it is possible for **29a** and **29b** to have this conformation it cannot be confirmed.

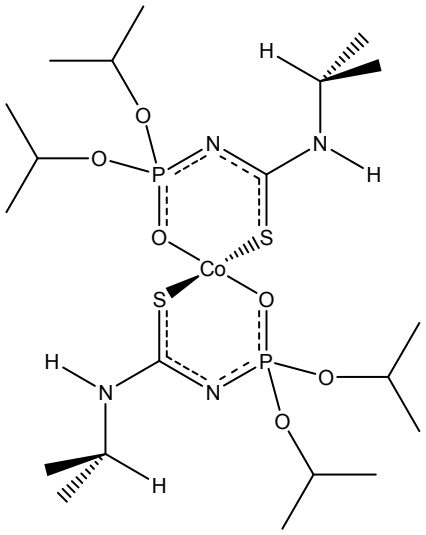

Figure 3.18 *O,S anionic thiourea with the Z,Z,E-anti conformation [10].*

This divergent behaviour between the *N*,*S* and *O*,*S* binding modes has been seen in other acyl thioureas and their analogues. When *N*-diisopropoxyphosphinyl-*N'*-phenylthiourea is reacted with base and Co(II), Ni(II) or Pd(II) two coordination modes are seen; *N*,*S* for Pd(II) and Ni(II), and *O*,*S* for Co(II), Scheme 3.2 [11]. The authors proposed two main reasons for Co(II) preferring to break the intramolecular hydrogen-bond and not bond through the strong electron donor of the N^- atom. Firstly the steric interactions required to distort the tetrahedral coordination of the Co(II) metal centre inhibits the *N*,*S* binding; and secondly that the CFSE for d^6 Co(II) is much lower than for low-spin d^8 Ni(II) and Pd(II) [11]. This can also be explained in terms of the bite angle that the ligand forms as discussed below.

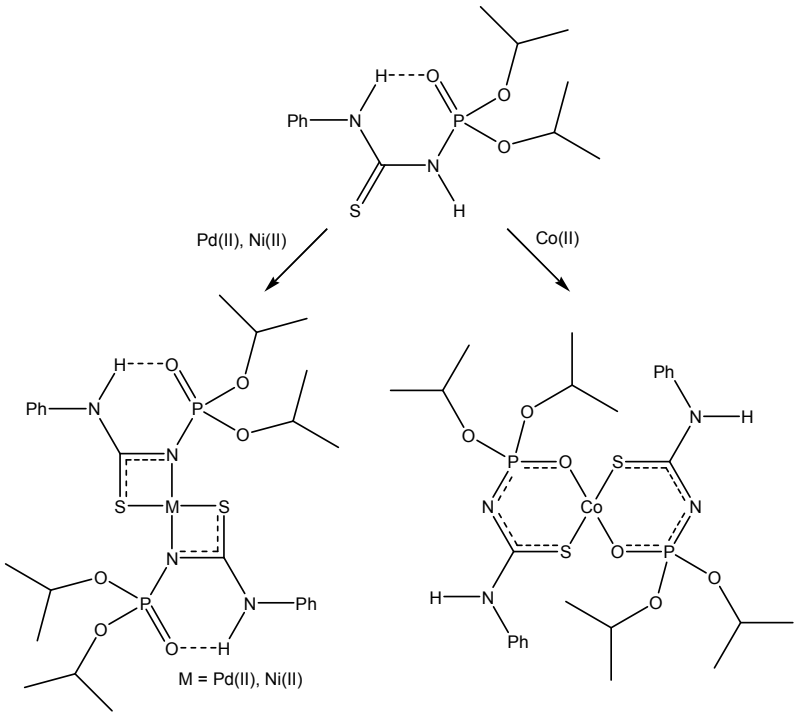

Scheme 3.2 *Reaction scheme showing the difference in coordination mode of N-diisopropoxyphosphinyl-N'-phenylthiourea with Co(II), Ni(II) and Pd(II) [11].*

Many *N,N*-di-alkyl-*N'*-benzoyl thioureas have been studied as anionic ligands and are well understood. These bond *O*,*S* since the first nitrogen is now unavailable for bonding as a class II ligand, and class I no longer has the N–H proton to drive

the formation of an intramolecular hydrogen-bond. For anionic complexes of *N*-alkyl-*N´*-benzoyl thioureas, the situation is less clear with limited reports of compounds.

While benzoyl thioureas bonding *N,S* class I have been reported, no crystal structures are known. For palladium complexes only a few compounds have been reported where the thiourea is bonded *O,S* to the metal centre [12, 13]. However the evidence for this assignment over *N*,*S* bonding is not strong with only the shift in the IR of the $\nu_{C=O}$ band as the indication of the bonding mode; for example the band in the ligand was 1672 cm^{-1} while the complex was 1626 cm^{-1} [12]. There are only two papers with unambiguous assignments with X-ray crystal structures. The first had a series of benzoyl thioureas reacted with an ortho-palladated imine acetate dimer, X-ray crystal structures of two of the compounds clearly showed the thiourea bonding *O,S* to the metal [14]. The second was based on another series of benzoyl thioureas forming platinum complexes [15]. Examples of both are shown in Figure 3.19. Of interest is the fact that the ortho metallated carbon in the complexes is *trans* to the sulfur for the palladium complex and trans to the oxygen in the platinum complex.

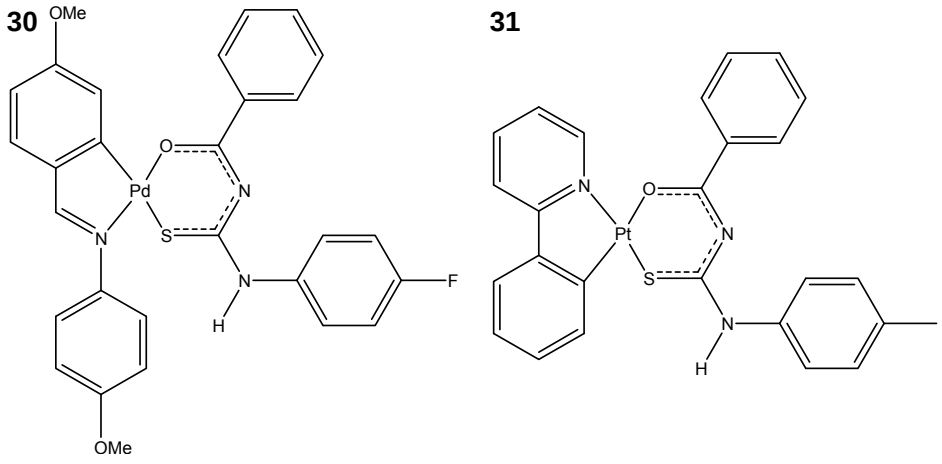

Figure 3.19 *Benzoyl thioureas binding as monoanionic O,S ligands;* ***30*** *[14]; B)* ***31*** *[15].*

There is slightly more information on acyl thioureas. There are a few X-ray crystal structures reported for acyl thioureas that bond *N,S*, class I. Two examples with coordination to cadmium(II) are shown in Figure 3.20 [16, 17]. The other crystal structure in the literature is an example where the thiourea is coordinated to $Re(CO)_4$; two isomers were seen with both class I and II bonding, rather than class III, Figure 3.20 [18]. The two isomers are both isolated from the reaction mixture, **32** was formed with higher yield, and if either compound was dissolved in $CDCl_3$ with pyridine an equilibrium of the two was formed which lies in favour of **32** [18]. In this case while having an internal hydrogen-bond was favoured, it wasn't enough to overcome other bonding factors. As mentioned above *N*-diisopropoxyphosphinyl-*N'*-phenylthiourea forms an *O,S* complex with Co(II).

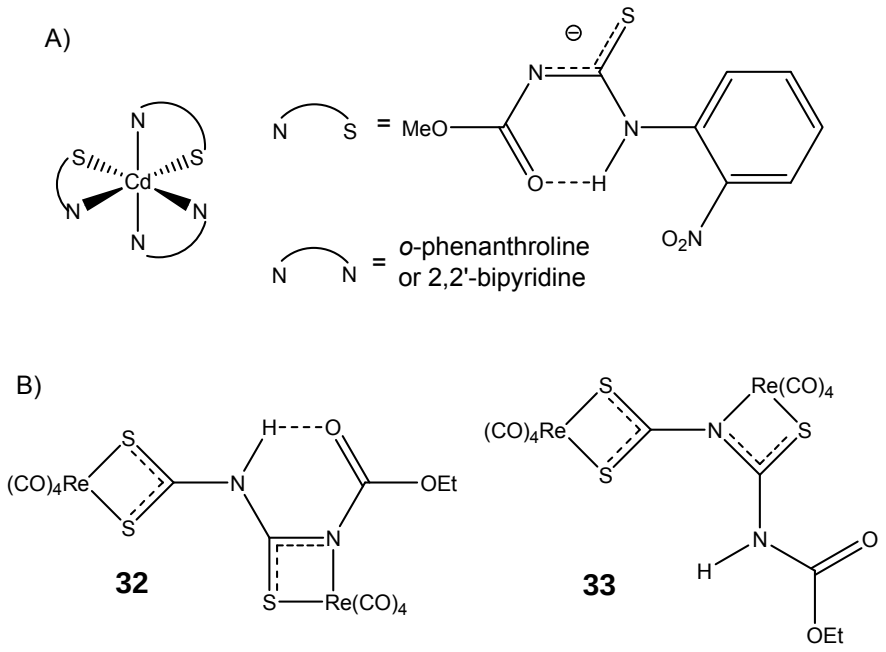

Figure 3.20 *Structurally characterised acyl thioureas that bond N,S; A) [16, 17]; B) Shows the two isomers of a thiourea with different bonding to $Re(CO)_4$, **32** has an internal hydrogen-bond that **33** doesn't [18].*

Since X-ray quality crystals could not be grown, the only evidence for the bonding was the ^{1}H NMR spectrum. It was hoped that a comparison with the literature values of complexes with crystal structures would help confirm *N,S* or

O,S assignment, but unfortunately there was a lot a variation between reported complexes. For benzoyl thiourea the *O*,*S* palladium analogues of **30** which had aromatic groups on N1, the N–H proton ranged from 8.11-8.02 ppm [14]. No chemical shifts for N–H were reported for the *O*,*S* platinum analogues of **31** [15]. This compares to 11.05 ppm for **25a** and 6.36 ppm for **29a**. The *N*,*S* *N*-phosphorylated thioureas from Scheme 3.2 and their analogues were looked at. For class I complexes with the internal hydrogen-bond, if the substituent on the nitrogen was an alkyl group the N–H proton was in the range of 8.47-8.55 ppm [6]; while for aromatic substituents the range was 10.30-10.55 ppm [11]. The alkyl values were lower than for those seen for the sugar thioureas. The ^{1}H NMR values for the class III complexes of these thioureas could not be compared since they were all to Co(III). For the acyl thioureas **32** and **33**, the N–H protons were 13.17 and 11.18 ppm respectively, showing that while the non hydrogen-bonded N–H signal was much higher than for the sugar thioureas, the formation of a hydrogen-bond does shift the signal further down-field.

A simple explanation for the difference in bonding can be made in terms of the bite angle that the anionic thiourea forms. For an ideal tetrahedral complex the angle is 109°, and 90° for an ideal square planar complex. The bite angle of the thiourea bonding *N*,*S* is much smaller than for *O*,*S* bonding, suggesting that *N*,*S* bonding is favoured for square planar complexes. For the tetrahedral Co(II) complex in Scheme 3.2 the two bite angles are 119.16(17)° and 118.25(18)°. While the Cp*Rh(III) complexes can be thought of as pseudo-tetrahedral, the bond angles have been shown to be quite small for thiourea complexes bonding *N*,*S*. For example the bite angle of the thiourea complex [Cp*RhCl(Tol-N-CH=NTol)] shown in Figure 3.13 is 67.3(1) [8]. Using this logic the rhodium(III) complex has a coordination preference for smaller angles and so would prefer *N*,*S* bonding, while square planar rhodium(I) has a coordination preference for larger angles and so prefers *O*,*S* bonding.

This doesn't fully explain the bonding however since *O,S* bonding has been observed for the square planar complexes **30** and **31**. The bite angles of the thioureas are 92.28(6)° for **30** [14] and 93.22(11)° for **31** [15]. As mentioned at the start of this Chapter this is also seen for *N,N*-di-alkyl-*N´*-benzoyl thioureas where *O,S* bonding is reported. For example the thiourea shown in Figure 3.21 has a bite angle of 93.43(8)° [19]. Obviously when bonding *O,S* the thiourea is quite flexible and has a wide range of bite angles that are viable. Since *N,S* bonding has been also been seen for square planar complexes, a bite angle of 90° seems to be a crossing point, where either type of bonding could occur.

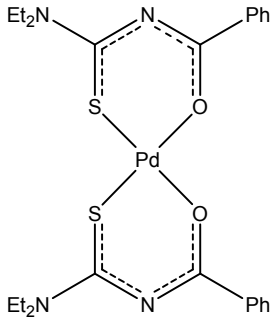

Figure 3.21 *N,N-di-alkyl-N´-benzoyl thiourea showing O,S bonding with a bite angle of 93.43(8)° [19].*

To investigate which mode of bonding was preferred for different metal systems, the acyl thioureas were reacted with a variety of metals.

3.4 8a with [(*p*-cymene)$RuCl_2$]$_2$

Other lower valence metals were investigated to see if the *O,S* binding mode could be observed with other metals. To that end [(*p*-cymene)$RuCl_2$]$_2$ was reacted with **8a** using the standard conditions used above. The ^{1}H NMR spectrum of **34a** is shown in Figure 3.22, compared to **8a**. The ^{1}H NMR spectrum showed that the thiourea was class III, by the presence of HN1 far downfield, as shown in

Figure 3.23. As with the rhodium(III) compound above the product was expected to be chiral, and the NMR spectrum clearly showed that the product contained both diastereoisomers in roughly equal proportions. This again showed that the chiral sugar was giving no selectivity to the conformation of the metal. The ^{1}H NMR spectrum has changed in similar ways to **25a**.

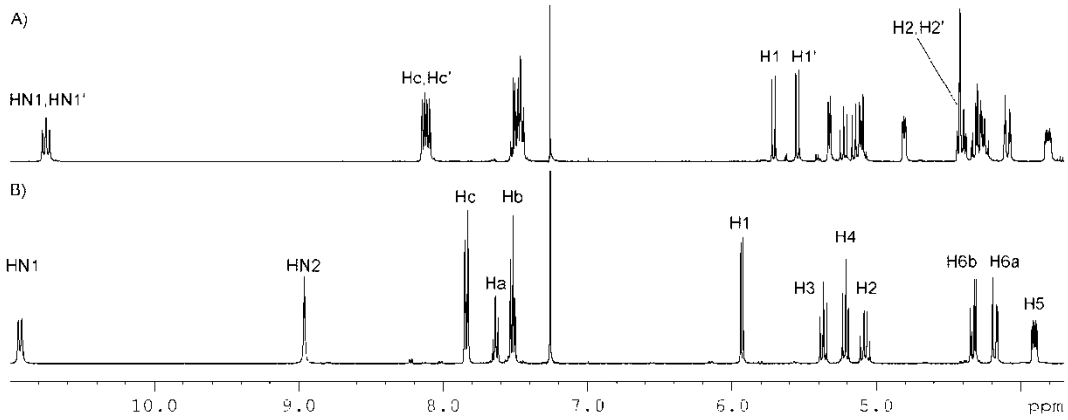

Figure 3.22 *Portion of the ^{1}H NMR spectrum comparing; A) R,S-**34a** showing the far downfield position of the HN1 proton and the two sets of signals seen; B) **8a**.*

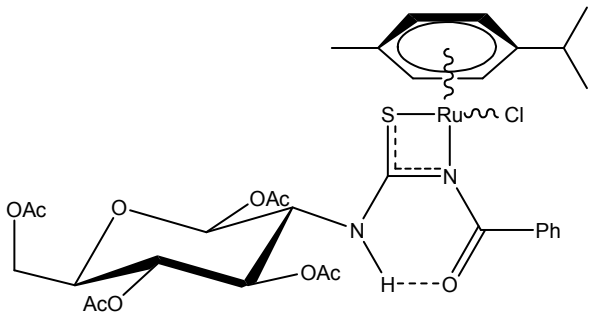

Figure 3.23 *R,S-**34a** with **8a** acting as a anionic bidentate ligand.*

The changes in the ^{13}C NMR spectrum of **34a** were similar to **25a**. Figure 3.24 shows a comparison with **8a** for the carbonyl and aromatic portion of the molecule while Figure 3.25 shows the sugar portion. Again both the C=S and amide carbonyl carbons are shifted downfield.

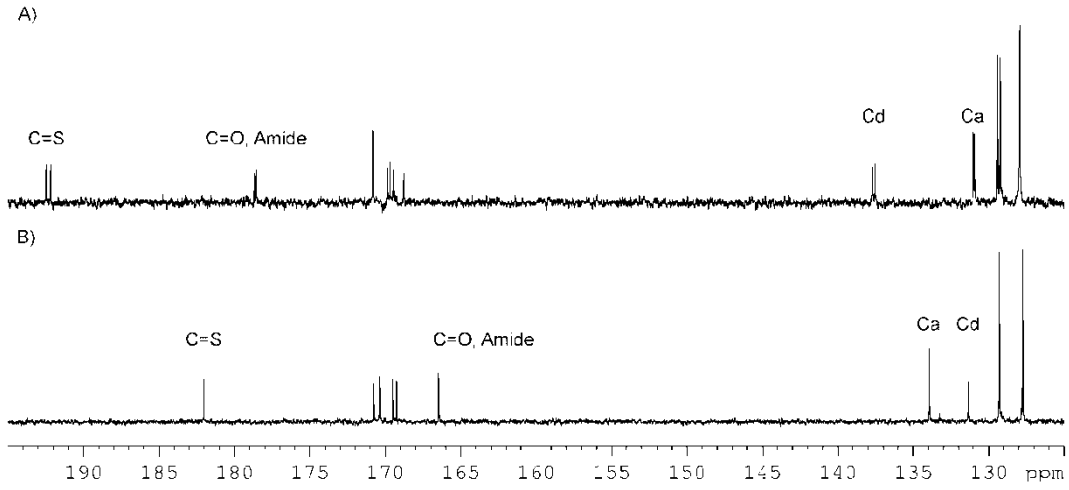

Figure 3.24 *Carbonyl and aromatic portion of the ^{13}C NMR spectrum comparing; A) **34a**; B) **8a**.*

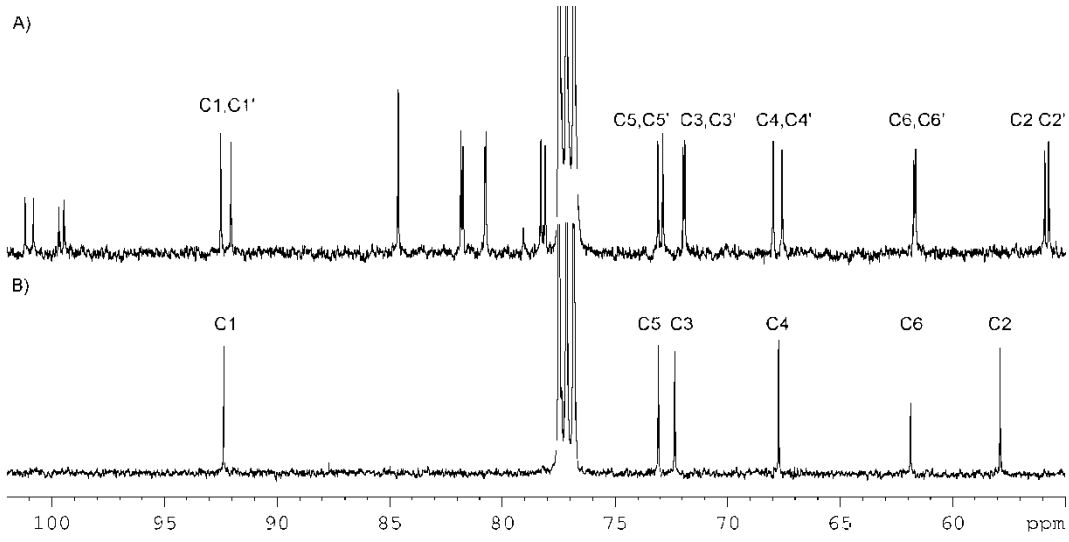

Figure 3.25 *Sugar portion of the ^{13}C NMR spectrum comparing; A) **34a**; B) **8a**.*

There are only a few reports of thiourea bonding as anionic ligands to ruthenium(II) with *p*-cymene, Figure 3.26 shows some examples with the bite angle of the thiourea. Henderson *et al* formed a thiourea dianion-bridged dinuclear complex, with *N*,*S* bonding [7]. Triazepine which is an acyl thiourea analogue, but because of the cyclic nature cannot undergo rotation to bond using the carbonyl oxygen, also bonds *N*,*S* [20]. The acyl thiourea *N,N*-diethyl-*N*-CO-2,6-$F_2C_6H_3$ bonds *O*,*S* with the metal [21], while the non-acyl *N,N*-dialkyl

thiourea $Me_2NSNHPh$ bonds *N*,*S* [22]. The bite angles of the thioureas in Figure 3.26 are all low at approximately 67°. This preference for a narrow bite angle would suggest that the *N*,*S* bonding seen for the sugar thiourea would be expected.

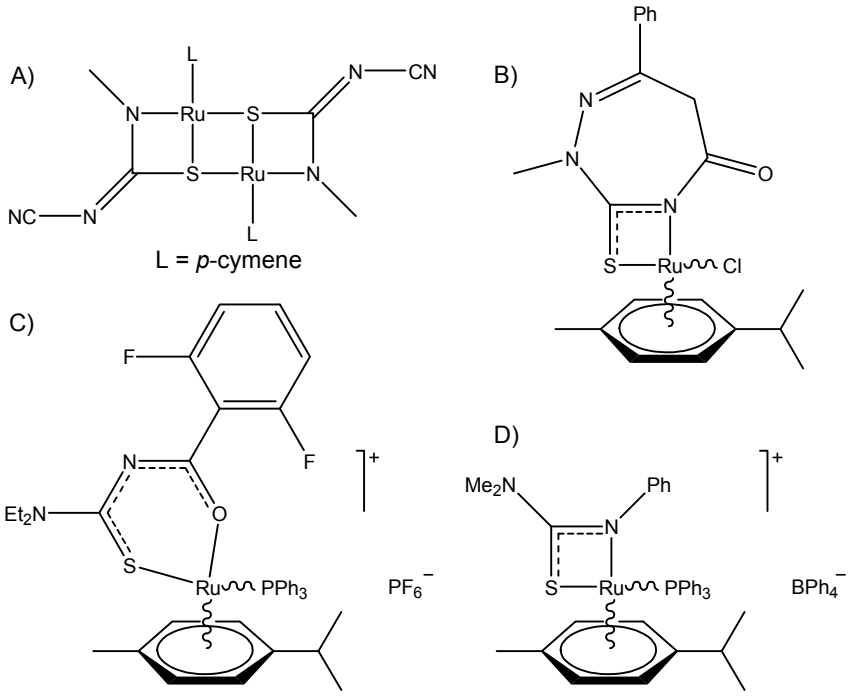

Figure 3.26 *Thioureas bonding as anionic ligands to ruthenium(II) with p-cymene with the bite angle of the thiourea if known; A) 67.23(8)°, 67.19(8)° [7]; B) 66.8(2)° (Average of two independent molecules) [20]; C) [21]; D) 67.07(5)° [22].*

34a was reacted with PPh_3 and $NaBF_4$ to see if the chloride could be displaced to form a cationic species to improve the chances of it crystallising. While the ESI-MS spectra showed the desired product with an ion tentatively assigned as [(**8a**–H)Ru(*p*-cymene)PPh_3]$^+$, nothing could be isolated.

3.5 8a with [Pd(*C,N*-DMBA)Cl]$_2$

In light of the *O,S* bonding seen for ortho-palladated imine [14], other palladated species were looked at. The dimer [Pd(*C,N*-DMBA)Cl]$_2$ was investigated. Reaction of the dimer with **8a** gave the product shown in Figure 3.27. The ^{1}H NMR spectrum showed the HN1 proton at an upfield position showing class III bonding. While the corresponding complex formed by the neutral thiourea discussed on page 55 was unstable, the complex with the chelated anionic thiourea was stable in chloroform. Since X-ray quality crystals of **35a** could not be grown the orientation of the thiourea with respect to the DMBA ligand could not be determined. It was assumed that it would be similar to **30** with the sulfur atom *trans* to the aryl carbon.

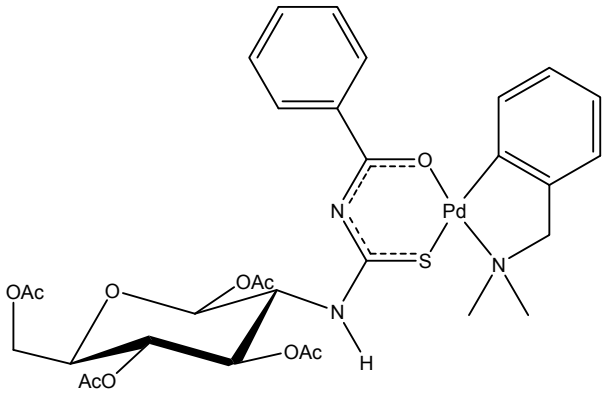

Figure 3.27 ***35a*** *with* ***8a*** *bonding class III.*

The ^{13}C NMR spectrum showed that the amide carbonyl had moved downfield as was typical for these complexes, but C=S had moved upfield.

3.6 Benzoyl thioureas with $PdCl_2$

When **8a** and $PdCl_2$ in a 2:1 ratio was stirred in a mixture of acetonitrile and water with a 1.2 molar excess of NaOAc the same *N*,*S* bonding as for $[Cp^*RhCl_2]_2$ is observed, Figure 3.28. The ^1H NMR spectrum only shows one set of signals, Figure 3.29, so no isomers are forming. Since crystals suitable for X-ray diffraction could not be grown the arrangement around the metal is unknown. Only crystal structures of palladium(II) bonding *N*,*S* with *N*-phosphorylated thioureas such as those in Scheme 3.2 have been reported and showed the sulfur atoms as *trans* to each other [6, 11]. As for the rhodium(III) complex the HN1 proton was present while the HN2 proton had disappeared. The HN1 proton signal was still far downfield indicating the intramolecular hydrogen-bond was present. Table 3.3 has selected chemical shifts and coupling constants for the complex. The coupling constant suggests the Z,E,Z-anti conformation.

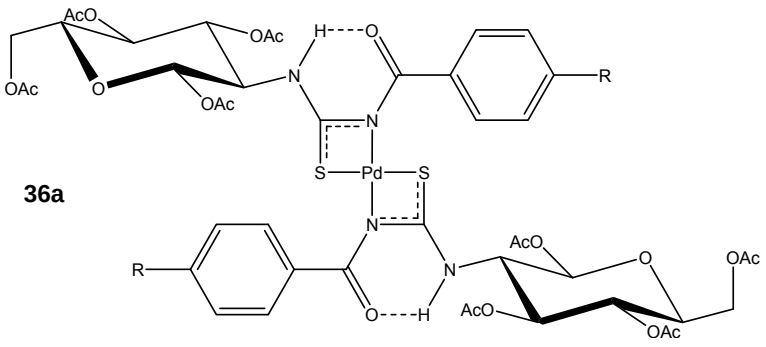

Figure 3.28 ***36a*** *with* ***8a*** *acting as a class I ligand with palladium(II).*

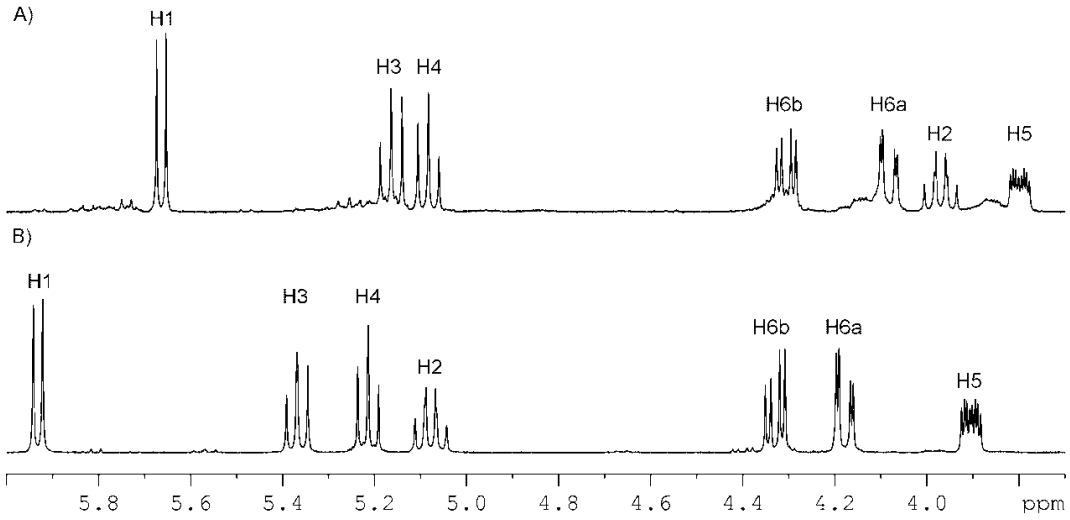

Figure 3.29 *Sugar portion of the ^{1}H NMR spectrum comparing; A) **36a**; B) **8a**.*

	HN1	Hc	H2	C=S	C=O	C2
8a	10.92, 9.2 Hz	7.82	5.08	182.0	166.5	57.9
36a	10.82, 10.0 Hz	7.77	3.97	191.8	177.3	55.5

Table 3.3 *Selected chemical shifts and coupling constants from the NMR spectra of **36a** and the thiourea.*

ESI-MS of the complex showed a strong ion corresponding to $[M+Na]^+$ and a very weak $[M+K]^+$ ion. Since there is no chloride on the metal the loss of HCl cannot occur.

3.7 Reaction of sugar thioureas with platinum(II)

This laboratory has previously studied anionic thioureas as ligands to a range of metals [7, 23]. Of particular interest were platinum(II) complexes with thioureas [24-27], Figure 3.30 shows some examples. These compounds were of interest as they display biological activity as well as that the thiourea groups can be made with a wide variety of different substituents with different properties. Different

sugar thioureas were reacted with two different platinum(II) compounds in an attempt to make complexes.

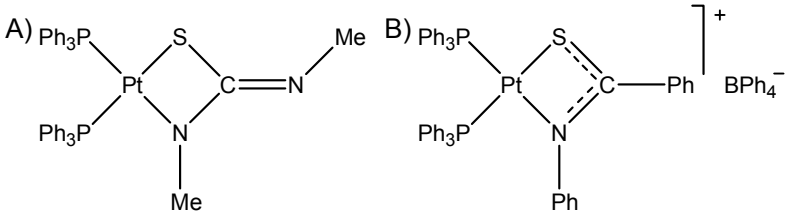

Figure 3.30 *Examples of thioureas acting as anionic ligands to platinum(II); A) [24]; B) [25].*

3.7.1 *cis*-$[PtCl_2(PPh_3)_2]$

Previously, reaction of thioureas with *cis*-$[PtCl_2(PPh_3)_2]$ was carried out in refluxing methanol with excess NEt_3 for 5 minutes [25]. This method was undesirable as methanol and base were likely to remove acetate groups from the sugar thiourea. Instead **8a** and *cis*-$[PtCl_2(PPh_3)_2]$ were stirred in dry CH_2Cl_2 and NEt_3. While ESI-MS indicated the formation of a complex with ions tentatively assigned as $[(\mathbf{8a}–H)_2Pt+Na]^+$ and $[(\mathbf{8a}–H)_2Pt+K]^+$, no product could be isolated from the reaction. The NaOAc, acetonitrile and water method was tried and the ^1H NMR spectrum suggested that the complex had formed. However upon anion metathesis to BF_4^- from Cl^- no product was observed. Attempts to isolate the complex with the chloride counter-ion failed.

The refluxing methanol and NEt_3 method was attempted but ESI-MS showed a mixture of the complex with increasing numbers of acetates removed. To try and isolate the fully deprotected complexes the mixture was left to reflux for longer, but no product could be isolated.

3.7.2 $K_2[PtCl_4]$

As discussed above there are a large number of complexes with *N*,*N*-dialkyl-*N´*-benzoyl thioureas with *O*,*S* bonding, many of which are to platinum(II) [21, 28-30]. **8a** was reacted with $K_2[PtCl_4]$ to try and make the analogue to the palladium(II) complex above. Reaction of **8a** with NaOAc in acetonitrile and water gave no product. Similarly reaction with **8e**, **8f** and **8g** also gave no product. It was not known why the platinum(II) analogues were so intractable compared to palladium(II).

3.8 Use of thioureas in gold chemistry

Thioureas have been reacted with gold(I) compounds to produce phosphine gold(I) thiourea complexes [23], Figure 3.31. There is interest in this class of compounds as there are biologically active examples such as Auranofin, Figure 3.31, which is a gold(I) compound with 2,3,4,6-tetra-*O*-acetyl-β-D-thioglucose and triethylphosphine as the two ligands. Auranofin is used in the treatment of arthritis [31]. This drug is of particular interest as it shows the potential of combining inorganic chemistry with carbohydrate chemistry.

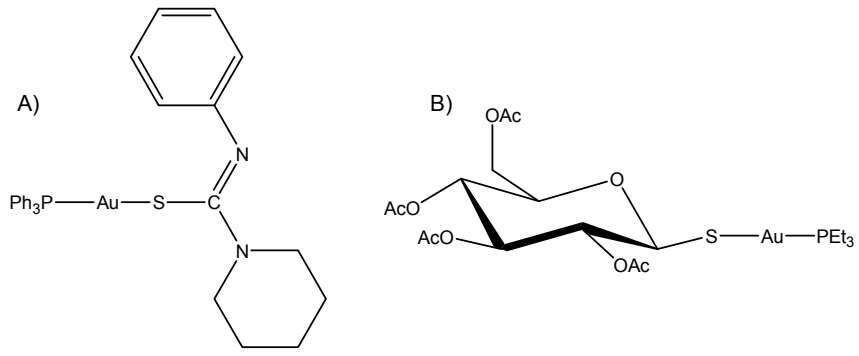

Figure 3.31 *A) An example of a phosphine gold(I) thiourea complex; B) 2,3,4,6-tetra-O-acetyl-β-D-glucopyranosato-S-(triethylphosphine) gold(I), Auranofin.*

3.8.1 Gold phosphines

When **8a** was reacted with Ph_3PAuCl and NaOAc, ESI-MS of the reaction mixture showed an intense peak that was assigned as $[Ph_3PAu\mathbf{8a}]^+$. However when the reaction was worked up unreacted Ph_3PAuCl was isolated. The reaction of **8g** with Ph_3PAuCl proved more successful, with the monodentate anionic complex shown in Figure 3.32 formed.

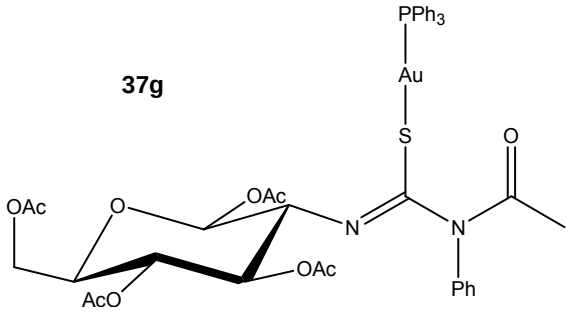

Figure 3.32 ***37g*** *with* ***8g*** *acting as a monodentate anionic ligand to* $AuPPh_3^+$.

ESI-MS showed clear $[M+H]^+$, $[M+Na]^+$ and $[2M+Na]^+$ ions. Also seen was a peak at 721 m/z from $[Au(PPh_3)_2]^+$, which is always seen for gold(I) phosphines. The molecular ion peaks were very intense, and dominated the spectra. The ^1H NMR spectra shows the change of the thiourea to an anionic ligand, Figure 3.33. The HN1 signal has disappeared and the H2 proton has become a doublet of doublets as it is no longer coupling to HN1 and is shifted upfield from the presence of the N=C bond.

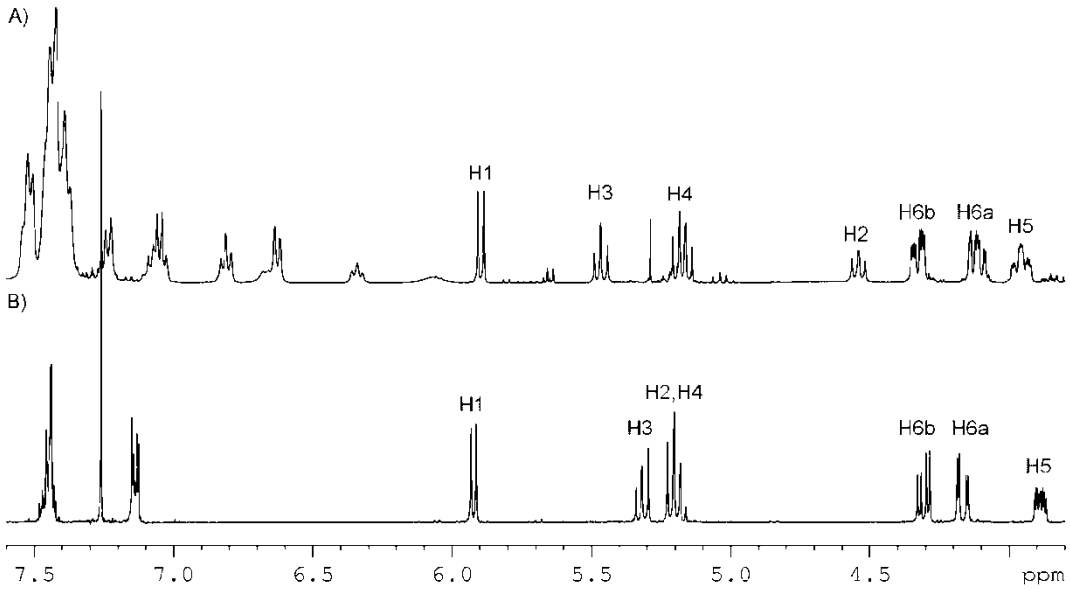

Figure 3.33 *Portion of the ^{1}H NMR spectrum showing the comparison of; A) **37g**; B) **8g**.*

There is no clear explanation for why **8g** but not **8a** acts as a monoanionic ligand to $AuPPh_3^+$ to form a complex.

3.9 Conclusion

The sugar acyl thioureas were shown to have the ability to form monoanionic bidentate ligands to a wide variety of metal systems. The particular metal system influences the mode of bonding. In general if the metal preferred small bite angles the *N*,*S* bonding was seen, while if it preferred larger bite angles *O*,*S* bonding was seen, with 90° as a cross over point where either type of bonding could occur. However this doesn't completely explain the details. The thiourea, **8a**, was flexible in its choice of bonding to palladium and complexes with both types of bonding could be made. There could be steric or electronic factors that determine what bonding is seen, especially for square planar metals, and this needs further investigation. While palladium(II) complexes were stable, platinum(II) analogues proved to be very intractable and no complexes could be isolated. It was also found that if the metal centre had the potential to be chiral

the sugar portion of the thiourea did not impart any selectivity on the distereoisomers forming.

The *N*′-acetyl thiourea **8g** was not as good a ligand as the acyl thioureas. Despite having one less bonding mode available no complexes could be made with $[Cp^*RhCl_2]_2$. However it formed a complex with the $AuPPh_3^+$ group, while **8a** did not.

3.10 Experimental

General experimental procedures are in Appendix One, NMR information is in Appendix Two. *N*-acetyl-1,3,4,6-tetra-*O*-acetyl-D-β-glucosamine [3], $[Cp^*RhCl_2]_2$ [32] and *cis*-$[PtCl_2(PPh_3)_2]$ [33] were made according to literature procedures.

8g

8g was made by slight modification to the literature procedure [2]. **8f** (269 mg, 0.558 mmol) was suspended in acetic anhydride (1 mL) and pyridine (1 mL) and stirred for 16 hours. The solution was added drop-wise to water (150 mL) resulting in a precipitate, filtration and drying under vacuum at room temperature gave **8g** (229.5 mg, 78.4%).

^{1}H NMR: δ 11.77 (d, 1H, $J_{H2,HN1}$ 8.9 Hz, HN1), 7.45 (m, 3H, Ha, Hc), 7.14 (m, 2H, Hb), 5.92 (d, 1H, $J_{1,2}$ 7.9 Hz, H1), 5.32 (dd, 1H, $J_{H3,H4}$ 8.6 Hz, $J_{H2,H3}$ 9.5 Hz, H3), 5.20 (m, 1H, H4), 5.19 (m, 1H, H2), 4.31 (dd, 1H, $J_{5,6b}$ 4.8 Hz , $J_{6a,6b}$ 12.4 Hz, H6b), 4.17 (dd, 1H, $J_{5,6a}$ 2.8 Hz, $J_{6a,6b}$ 12.4 Hz, H6a), 3.89 (ddd, 1H, $J_{5,6a}$ 2.8 Hz, $J_{5,6b}$ 4.8 Hz, $J_{4,5}$ 9.2 Hz, H5), 2.14, 2.10, 2.07, 2.07 (4s, 12H, 4 × OAc), 1.93 (s, 3H, NAc) ppm. ^{13}C NMR: δ 186.0 (C=S), 175.0 (C=O, amide), 170.8, 170.5, 169.5, 169.3(4 × C=O, acetyl), 142.4 (Cd), 129.6 (Cc), 129.6 (Cb), 129.2 (Ca), 92.6 (C1), 73.0 (C5), 72.7 (C3), 67.5 (C4), 61.9 (C6), 58.2 (C2), 28.1 (NAc) 21.2, 20.9, 20.9, 20.8 (4 ×

CH_3) ppm. *Anal.* Calcd for $C_{23}H_{28}N_2O_{10}S$ (524.541): C, 52.66; H, 5.38; N, 5.34. Found: C, 52.84; H, 5.16; N, 5.50. MS: *m/z*: 547.138 (strong, $[M+Na]^+$, calc 547.136), 563.112 (medium, $[M+K]^+$, calc. 563.110), 1071.281 (medium, $[2M+Na]^+$, calc. 1071.282), 1087.257 (weak, $[2M+K]^+$, calc. 1087.256).

25a

$[Cp^*RhCl_2]_2$ (60.5 mg, 0.098 mmol) and **8a** (100 mg, 0.196 mmol) were stirred in acetonitrile (10 mL) for ½ an hour. $NaOAc{\cdot}3H_2O$ (32.0 mg, 0.235 mmol) and water (8 mL) were added and the resulting solution stirred for 3 hours. The solvent was removed under vacuum and the residue dissolved in CH_2Cl_2 (20 mL) and filtered through Celite, addition of petroleum spirits gave **25a** (139.1 mg, 90.6%).

^{1}H NMR: δ 11.06 (d, 1H, $J_{H2',HN1'}$ 10.3 Hz, HN1′) 11.00 (d, 1H, $J_{H2,HN1}$ 10.2 Hz, HN1), 8.40 (m, 4H, Hc; Hc′), 7.46 (m, 2H, Ha; Ha′), 7.39 (m, 4H, Hb; Hb′), 5.78 (d, 1H, $J_{H1,H2}$ 8.3 Hz, H1), 5.60 (d, 1H, $J_{H1',H2'}$ 8.4 Hz, H1′), 5.27 (t, 1H, H3′), 5.16 (t, 1H, H4′), 5.12 (m, 2H, H3; H4), 4.38 (dt, 2H, H2; H2′), 4.35 (dd, 1H, $J_{H5',H6b'}$ 4.4 Hz, $J_{H6a',H6b'}$ 12.5 Hz, H6b'), 4.28 (m, 2H, $J_{H5,H6b}$ 4.6 Hz, $J_{H6a,H6b}$12.4 Hz, H6b), 4.11 (dd, 1H, $J_{H5,H6a}$ 2.4 Hz, $J_{H6a,H6b}$ 12.4 Hz, H6a; H6a′), 3.82 (m, 2H, H5; H5′), 2.18, 2.16, 2.10, 2.09 × 2, 2.08, 2.05, 1.99 (8s, 24H, 8 × OAc), 1.39 (Cp*) ppm. ^{13}C NMR: δ 190.7, 190.5 (C=S), 176.6, 176.5 (C=O, amide), 170.8 × 3, 169.9, 169.7, 169.6, 169.4, 168.8 (8 × C=O, acetyl), 137.5, 137.3 (Cd), 131.5, 131.4 (Ca), 130.1, 130.0 (Cc), 128.2, 128.2 (Cb), 94.0 ($J_{Rh,C}$ 8.1 Hz, Cp*, quart.), 92.5, 92.5 (C1), 73.1, 72.9 (C5), 72.2, 71.9 (C3), 68.0, 67.6 (C4), 61.8, 61.7 (C6), 56.4, 56.4 (C2), 21.3, 21.0, 21.0, 20.9, 20.8, 20.8, 20.7, 20.7 (8 × CH_3), 9.1 (Cp*, methyl) ppm. *Anal.* Calcd for $C_{32}H_{40}N_2O_{10}SClRh$ (783.091): C, 49.08; H, 5.15; N, 3.58. Found: C, 49.36; H, 5.27; N, 3.71. MS: *m/z*: 747.148 (strong, $[M–Cl]^+$, calc 747.145), 769.130 (weak, $[M–HCl+Na]^+$, calc 769.127), 783.121 (weak, $[M+H]^+$, calc 783.122), 805.107 (weak, $[M+Na]^+$, calc 805.1039), 1529.261 (weak, $[2M–Cl]^+$, calc 1529.260), 1589.220 (weak, $[2M+Na]^+$, calc 1589.218), 1605.195 (weak, $[2M+K]^+$, calc 1605.192).

25b

25b was produced using the same as for **25a**, $[Cp^*RhCl_2]_2$ (20.0 mg, 0.032 mmol) and **8b** (36.0 mg, 0.065 mmol), $NaOAc{\cdot}3H_2O$ (10.6 mg, 0.078 mmol), worked up to give **25b** (45.0 mg, 83.6%).

^{1}H NMR: δ 10.96 (d, 1H, $J_{H2',HN1'}$ 10.4 Hz, HN1′) 10.92 (d, 1H, $J_{H2,HN1}$ 10.2 Hz, HN1), 8.63 (m, 4H, Hc; Hc′), 8.25 (m, 4H, Hb; Hb′), 5.81 (d, 1H, $J_{H1,H2}$ 8.3 Hz, H1), 5.63 (d, 1H, $J_{H1,H2}$ 8.4 Hz, H1′), 5.33 (t, 1H, H3′), 5.22 (t, 1H, H4′), 5.13 (m, 2H, H3; H4), 4.43 (dt, 2H, H2′), 4.38 (dt, 2H, H2), 4.36 (dd, 1H, $J_{H5',H6b'}$ 4.1 Hz, $J_{H6a',H6b'}$ 12.6 Hz, H6b′), 4.29 (m, 1H, $J_{H5,H6b}$ 4.3 Hz, $J_{H6a,H6b}$12.5 Hz, H6b), 4.16 (dd, 1H, $J_{H5',H6a'}$ 1.5 Hz, $J_{H6a',H6b'}$ 12.6 Hz, H6a′), 4.13 (dd, 1H, $J_{H5,H6a}$ 1.5 Hz, $J_{H6a,H6b}$ 12.5 Hz, H6a), 3.88 (m, 1H, H5′), 3.84 (m, 1H, H5), 2.18, 2.17, 2.10, 2.09, 2.09, 2.09, 2.06, 2.01 (8s, 24H, 8 × OAc), 1.41 (Cp*) ppm. ^{13}C NMR: δ 191.1, 190.9 ($J_{Rh,C}$ 4.0, 3.9 Hz, C=S), 174.4, 174.3 (C=O, amide), 170.8, 170.8 × 2, 170.0, 169.7, 169.6, 169.4, 168.8 (8 × C=O, acetyl), 149.5, 149.4 (Ca), 143.1, 143.0 (Cd), 131.4, 131.2 (Cc), 123.2, 123.2 (Cb), 94.2, 94.1 ($J_{Rh,C}$ 8.1 Hz, quart. Cp*), 92.4, 92.1 (C1), 73.2, 72.9 (C5), 72.2, 71.9 (C3), 68.0, 67.5 (C4), 61.8, 61.7 (C6), 56.7, 56.6 (C2), 21.3, 21.0, 21.0, 20.9, 20.8, 20.8, 20.7, 20.7 (8 × CH_3), 9.2 (Cp*, methyl) ppm. *Anal.* Calcd for $C_{32}H_{39}N_3O_{12}SClRh$ (828.088): C, 46.41; H, 4.75; N, 5.07. Found: C, 46.58; H, 4.93; N, 5.14. MS: *m/z*: 792.131 (strong, $[M–Cl]^+$, calc 747.145).

25d

25d was produced using the same as for **25a**, $[Cp^*RhCl_2]_2$ (20.0 mg, 0.032 mmol) and **8d** (33.6 mg, 0.065 mmol), $NaOAc{\cdot}3H_2O$ (10.6 mg, 0.078 mmol), worked up to give **25d** (43.3 mg, 84.5%).

^{1}H NMR: δ 10.64 (d, 1H, $J_{H2,HN1}$ 10.3 Hz, HN1') 10.64 (d, 1H, $J_{H2,HN1}$ 10.2 Hz, HN1), 8.92, 8.90 (dd, 2H, Hc; Hc'), 7.52 (m, 2H, Ha; Ha'), 7.06 (m, 4H, Hb; Hb'), 5.74 (d, 1H, $J_{H1,H2}$ 8.2 Hz, H1), 5.55 (d, 1H, $J_{H1,H2}$ 8.6 Hz, H1'), 5.23 (t, 1H, H3'), 5.17 (t, 1H, H4'), 5.08 (m, 2H, H3; H4), 4.35 (dt, 2H, H2; H2'), 4.30 (m, 2H, H6b; H6b'),

4.11 (dd, 1H, $J_{H5,H6a}$ 2.4 Hz, $J_{H6a,H6b}$ 12.4 Hz, H6a), 4.10 (dd, 1H, $J_{H5,H6a}$ 2.3 Hz, $J_{H6a,H6b}$ 12.5 Hz, H6a'), 3.81 (m, 2H, H5; H5'), 2.15 × 2, 2.09, 2.09, 2.08× 2, 2.05, 2.00 (8s, 24H, 8 × OAc), 1.50 (Cp*) ppm. ^{13}C NMR: δ 189.7, 189.5 (C=S), 169.9, 169.5 (C=O, amide), 170.8 × 2, 170.8, 170.1, 169.7, 169.6, 169.4, 168.7 (8 × C=O, acetyl), 141.1, 141.1 (Cd), 134.5, 134.4 (Ca), 132.4, 132.1 (Cc), 127.8, 127.7 (Cb), 94.1 ($J_{Rh,C}$ 8.0 Hz, quart. Cp*), 92.6 (C1'), 92.0 (C1), 73.1, 72.8 (C5), 72.0, 72.0 (C3), 67.9, 67.5 (C4), 61.7, 61.6 (C6), 56.2, 56.2 (C2), 21.3, 21.0 × 2, 20.9, 20.9, 20.8, 20.7× 2 (8 × CH_3) ppm. *Anal.* Calcd for $C_{30}H_{38}N_2O_{10}SCl_2Rh$ (789.122): C, 45.66; H, 4.85; N, 3.55. Found: C, 45.95; H, 4.73; N, 3.48. MS: *m/z*: 753.103 (strong, $[M–Cl]^+$, calc 753.102).

29a

29a was produced using the same as for **25a**, $[(COD)RhCl]_2$ (25.0 mg, 0.051 mmol) and **8a** (52.1 mg, 0.102 mmol), $NaOAc·3H_2O$ (16.7 mg, 0.122 mmol), worked up to give **29a** (57.6 mg, 78.4%).

^{1}H NMR: δ 8.14 (m, 2H, Hc), 7.50 (tt, 1H, Ha), 7.41 (m, 2H, Hb), 6.36 (d, 1H, $J_{H2,HN1}$ 9.0 Hz, HN1), 5.74 (d, 1H, $J_{H1,H2}$ 8.6 Hz, H1), 5.25 (dd, 1H, $J_{H3,H4}$ 9.2 Hz, $J_{H2,H3}$ 10.2 Hz, H3), 5.17 (t, 1H, H4), 4.92 (dt, 1H, H2), 4.67 (m, 2H, CH), 4.33 (dd, 1H, $J_{H5,H6b}$ 4.9 Hz, $J_{H6a,H6b}$ 12.4 Hz, H6b), 4.12 (dd, 1H, $J_{H5,H6a}$ 2.4 Hz, $J_{H6a,H6b}$ 12.5 Hz, H6a), 3.90 (m, 2H, CH), 3.85 (ddd, 1H, $J_{H5,H6a}$ 2.4 Hz, $J_{H5,H6b}$ 4.9 Hz, $J_{H4,H5}$ 9.7 Hz, H5), 2.45 (m, 4H, CH_2), 2.10, 2.04, 2.02, 2.02 (4s, 12H, 4 × OAc), 1.95 (m, 4H, CH_2) ppm. ^{13}C NMR: δ 178.5 (C=S), 172.5 (C=O, amide), 170.9, 170.6, 169.4, 169.34 (4 × C=O, acetyl), 136.9 (Cd), 131.9 (Ca), 129.7 (Cb), 128.1 (Cc), 92.7 (C1), 87.4 ($J_{Rh,C}$ 10.0 Hz, CH), 87.2 ($J_{Rh,C}$ 10.0 Hz, CH), 72.9 (C5), 72.4 (C3), 71.3 ($J_{Rh,C}$ 13.0 Hz, CH), 71.0 ($J_{Rh,C}$ 14.0 Hz, CH), 67.8 (C4), 61.8 (C6), 55.9 (C2), 31.7, 31.4, 29.4, 29.2 (4 × CH_2), 21.0, 20.7, 20.7, 20.6 (4 × CH_3) ppm. *Anal.* Calcd for $C_{30}H_{37}N_2O_9SRh$ (720.595): C, 50.50; H, 5.18; N, 3.89. Found: C, 50.32; H, 5.46; N, 4.03. MS: *m/z*: 721.134 (weak, $[M+H]^+$, calc 721.130), 743.113 (strong, $[M+Na]^+$, calc 743.112), 759.090 (weak, $[M+K]^+$, calc 759.086).

29b

29b was produced using the same method as for **25a**, $[(COD)RhCl]_2$ (25.0 mg, 0.051 mmol) and **8b** (56.7 mg, 0.102 mmol), $NaOAc{\cdot}3H_2O$ (16.7 mg, 0.122 mmol), worked up to give **29b** (60.1 mg, 76.9%).

^{1}H NMR: δ 8.27 (m, 2H, Hc), 8.17 (m, 1H, Hc), 7.54 (m, 2H, Hb), 6.36 (d, 1H, $J_{H2,HN1}$ 9.0 Hz, HN1), 5.74 (d, 1H, $J_{H1,H2}$ 8.6 Hz, H1), 5.23 (m, 1H, H3), 5.18 (m, 1H, H4), 4.85 (dt, 1H, H2), 4.67 (b, 2H, CH), 4.35 (dd, 1H, $J_{H5,H6b}$ 4.9 Hz, $J_{H6a,H6b}$ 12.4 Hz, H6b), 4.13 (dd, 1H, $J_{H5,H6a}$ 2.3 Hz, $J_{H6a,H6b}$ 12.4 Hz, H6a), 3.94 (b, 2H, CH), 3.86 (ddd, 1H, $J_{H5,H6a}$ 2.3 Hz, $J_{H5,H6b}$ 4.9 Hz, $J_{H4,H5}$ 9.6 Hz, H5), 2.46 (b, 4H, CH_2), 2.10, 2.05, 2.03, 2.02 (4s, 12H, 4 × OAc), 1.98 (b, 4H, CH_2) ppm. ^{13}C NMR: δ 182.4 (C=S), 171.0, 170.8, 169.6, 169.3 (4 × C=O, acetyl), 170.2 (C=O, amide), 150.0 (Ca), 143.1 (Cd), 130.7 (Cb), 123.5 (Cc), 92.8 (C1), 89.3, 88.3 (2 × CH), 73.2 (C5), 72.5 (C3), 72.1, 71.8 (2 × CH), 67.9 (C4), 61.9 (C6), 56.3 (C2), 31.9, 31.7, 29.5, 29.4 (4 × CH_2), 21.1, 20.9 × 2, 20.7 (4 × CH_3) ppm. *Anal.* Calcd for $C_{30}H_{36}N_3O_{12}SRh$ (765.592): C, 47.06; H, 4.74; N, 5.49. Found: C, 47.30; H, 4.64; N, 5.63. MS: *m/z*: 721.134 (weak, $[M+H]^+$, calc 721.130), 743.113 (strong, $[M+Na]^+$, calc 743.112), 759.090 (weak, $[M+K]^+$, calc 759.086).

34a

34a was produced using the same method as for **25a**, $[(p\text{-cymene})RuCl_2]_2$ (30.0 mg, 0.049 mmol) and **8a** (50.0 mg, 0.098 mmol), $NaOAc{\cdot}3H_2O$ (16.0 mg, 0.118 mmol), worked up to give **34a** (63.2 mg, 82.6%).

^{1}H NMR: δ 10.76 (d, 1H, $J_{H2,HN1}$ 9.8 Hz, HN1') 10.74 (d, 1H, $J_{H2,HN1}$ 9.9 Hz, HN1), 8.12 (m, 4H, Hc; Hc'), 7.50 (m, 2H, Ha; Ha'), 7.46 (m, 4H, Hb; Hb'), 5.71 (d, 1H, $J_{H1,H2}$ 8.6 Hz, H1), 5.55 (d, 1H, $J_{H1,H2}$ 8.5 Hz, H1'), 5.33 (m, 2H, CH), 5.23 (dd, 1H, $J_{H3',H4'}$ 9.2 Hz, $J_{H2',H3'}$ 10.3 Hz, H3'), 5.14 (dd, 1H, $J_{H3,H4}$ 9.2 Hz, $J_{H2,H3}$ 9.9 Hz, H3'), 5.10 (m, 2H, H4; H4'), 4.81 (m, 2H, CH), 4.43 (m, 2H, CH), 4.41 (m, 2H, CH),

4.26 (dt, 2H, H2; H2'), 4.30 (m, 2H, H6b; H6b'), 4.09 (m, 2H, H6a; H6a'), 3.81 (m, 2H, H5; H5'), 2.60 (m, 2H, CH), 2.22, 2.15, 2.13, 2.10, 2.09, 2.07, 2.05, 2.00 (8s, 24H, 8 × OAc), 2.16 (m, 3H, Me), 2.16 (m, 3H, Me), 1.18, 1.16, 1.12, 1.11 (d, 12H, 4 × Me)ppm. ^{13}C NMR: δ 192.4, 192.2 (C=S), 178.7, 178.6 (C=O, amide), 170.8 × 3, 169.9, 169.7, 169.7, 169.7, 168.8 (8 × C=O, acetyl), 137.7, 137.5 (Cd), 131.0, 131.9 (Ca), 129.4, 129.2 (Cc), 127.9, 127.9 (Cb), 92.5, 92.0 (C1), 73.1, 72.9 (C5), 72.3, 71.8 (C3), 68.1, 67.6 (C4), 61.9, 61.6 (C6), 56.4, 56.4 (C2), 21.2, 21.0, 21.0, 20.9, 20.9, 20.8, 20.7, 20.7 (8 × CH_3) ppm. MS: *m/z*: 745.140 (strong, $[M–Cl]^+$, calc 745.137), 803.091 (weak, $[M+Na]^+$, calc 803.095).

35a

35a was produced using the same method as for **25a**, [Pd(*C,N*-DMBA)Cl]$_2$ (25.0 mg, 0.058 mmol) and **8a** (48.5 mg, 0.095 mmol), NaOAc·3H_2O (15.5 mg, 0.114 mmol), worked up to give **35a** (58.3 mg, 81.8%).

^{1}H NMR: δ 10.55 (d, 1H, $J_{H2,HN1}$ 9.2 Hz, HN1'), 8.19 (m, 2H, Hc), 7.54 (m, 1H, Ha), 7.46 (m, 2H, Hb), 5.82 (d, 1H, $J_{H1,H2}$ 8.2 Hz, H1), 5.31 (m, 1H, H3), 5.17 (m, 1H, H4), 4.98 (dt, 1H, H2), 4.34 (dd, 1H, $J_{H5,H6b}$ 4.8 Hz, $J_{H6a,H6b}$ 12.5 Hz, H6b), 4.10 (dd, 1H, $J_{H5,H6a}$ 2.2 Hz, $J_{H6a,H6b}$ 12.5 Hz, H6a), 3.84 (ddd, 1H, $J_{H5,H6a}$ 2.2 Hz, $J_{H5,H6b}$ 4.8 Hz, $J_{H4,H5}$ 9.9 Hz, H5), 2.11, 2.05, 2.03, 2.02 (4s, 12H, 4 × OAc) ppm. ^{13}C NMR: δ 177.1 (C=S), 173.4 (C=O, amide), 171.0, 170.8, 169.7, 169.4 (4 × C=O, acetyl), 137.9 (Cd), 132.0 (Ca), 129.6 (Cc), 128.4 (Cb), 92.9 (C1), 73.0 (C5), 72.2 (C3), 68.1 (C4), 61.9 (C6), 56.3 (C2), 21.1, 20.9, 20.9, 20.8 (4 × CH_3) ppm. MS: *m/z*: 750.135 (strong, $[M+H]^+$, calc 750.132), 772.111 (weak, $[M +Na]^+$, calc 772.114).

36a

36a was produced using the same method as for **25a**, $PdCl_2$ (26.1 mg, 0.147 mmol) and **8a** (150 mg, 0.294 mmol), NaOAc·3H_2O (48.0 mg, 0.353 mmol), worked up to give **36a** (149.4 mg, 90.3%).

^{1}H NMR: δ 10.82 (d, 1H, $J_{H2,NH}$ 10.0 Hz, HN1), 7.78 (m, 2H, Hc), 7.54 (tt, 1H, Ha), 7.42 (m, 2H, Hb), 5.66 (d, 1H, $J_{1,2}$ 8.3 Hz, H1), 5.16 (t, 1H, H3), 5.08 (t, 1H, H4), 4.31 (dd, 1H, $J_{5,6b}$ 4.6 Hz , $J_{6a,6b}$ 12.5, H6b), 4.08 (dd, 1H, $J_{5,6a}$ 2.3 Hz, $J_{6a,6b}$ 12.5 Hz, H6a), 3.97 (dt, 1H, H2), 3.80 (ddd, 1H, $J_{5,6a}$ 2.4 Hz, $J_{5,6b}$ 4.6 Hz, $J_{4,5}$ 9.5 Hz, H5), 2.16, 2.09, 2.09, 2.03 (4s, 12H, 4 × OAc) ppm. ^{13}C NMR: δ 191.8 (C=S), 177.3 (C=O, amide), 170.7, 170.1, 169.6, 168.8 (4 × C=O, acetyl), 134.5 (Cd), 132.0 (Ca), 128.9 (Cc), 128.2 (Cb), 92.2 (C1), 73.1 (C5), 72.0 (C3), 67.6 (C4), 61.6 (C6), 55.5 (C2), 21.2, 20.9, 20.9, 20.7 (4 × CH_3) ppm. *Anal.* Calcd for $C_{44}H_{50}N_4O_{20}S_2Pd$ (1125.432): C, 46.96; H, 4.48; N, 4.98. Found: C, 47.21; H, 4.37; N, 5.09. MS: *m/z*: 1125.161 (medium, $[M+H]^+$, calc. 1125.1583), 1147.144 (medium, $[M+Na]^+$, calc. 1147.140), 1163.114 (strong, $[M+K]^+$, calc. 1163.1188).

37g

8g (100 mg, 0.191 mmol) and PPh_3AuCl (94.5 mg, 0.191 mmol) were dissolved in CH_2Cl_2 (10 mL), triethylamine (0.053 mL, 0.382 mmol) was added and stirred for 3 hours. The organic phase was washed with water (2 × 50 mL), dried ($MgSO_4$), filtered and the volume reduced, addition of petroleum sprits gave **37g** (124.5 mg, 66.3%).

^{1}H NMR: δ 7.56-7.34 (m, 15H, PPh_3), 7.06, 6.82, 6.63 (m, 5H, N-Ph), 5.90 (d, 1H, $J_{H1,H2}$ 8.2 Hz, H1), 5.47 (t, 1H, H3), 5.18 (t, 1H, H4), 4.32 (dd, 1H, $J_{H5,H6b}$ 4.6 Hz, $J_{H6a,H6b}$ 12.6, H6b), 4.12 (dd, 1H, $J_{H5,H6a}$ 2.2 Hz, $J_{H6a,H6b}$ 12.6 Hz, H6a), 4.54 (dd, 1H, $J_{H1,H2}$ 8.2 Hz, $J_{H2,H3}$ 9.7 Hz, H2), 3.96 (ddd, 1H, $J_{H5,H6a}$ 2.2 Hz, $J_{H5,H6b}$ 4.6 Hz, $J_{H4,H5}$ 9.7 Hz, H-5), 2.23 (s, 3H, NAc), 2.09, 2.01, 1.90, 1.87 (4s, 12H, 4 × OAc) ppm. ^{31}P{^{1}H} NMR: δ 39.1 ppm. *Anal.* Calcd for $C_{41}H_{42}N_2O_{10}PSAu$ (982.785): C, 50.11; H, 4.31; N, 2.85. Found: C, 50.43; H, 4.41; N, 2.91. MS: *m/z*: 721 .147 (strong, $[Au(PPh_3)_2]^+$, calc. 717.142), 983.204 (weak, $[M+H]^+$, calc 983.204), 1005.185 (weak, $[M+Na]^+$, calc 1005.186), 1021.157 (weak, $[M+K]^+$, calc 1021.159).

3.11 References

1. Zinner, H. and Peseke, K., *Benzazoles. XXVI. Glucosidation of N-methyl- and N-(tetra-O-acetyl-β-D-glucopyranosyl)benzimidazolethione.* J. Prakt. Chem., 1970. **312**, 185-91.
2. Maza, S., López, Ó., Maya, I., and Fernández-Bolaños, J.G., *Synthesis and characterization of mercury(II)-sugar thioureas complexes.* Polyhedron, 2009. **28**, 4039-4043.
3. Tarasiejska, Z. and Jeanloz, R.W., *Acetohalogeno derivatives and glycosides of D-galactosamine.* J. Am. Chem. Soc., 1958. **80**, 6325-6327.
4. Brunner, H., Köllnberger, A., Burgemeister, T., and Zabel, M., *Optically active transition metal complexes: Part 125. Preparation and epimerization of chiral-at-metal pentamethylcyclopentadienyl-rhodium(III) and iridium(III) half-sandwich complexes.* Polyhedron, 2000. **19**, 1519-1526.
5. Sokolov, F.D., Baranov, S.V., Zabirov, N.G., Krivolapov, D.B., Litvinov, I.A., Khairutdinov, B.I., and Cherkasov, R.A., *Unusual structure of an N-phosphoryl-N'-isopropylthiourea chelate with the nickel(II) cation.* Mendeleev Commun., 2007. **17**, 222-223.
6. Sokolov, F.D., Baranov, S.V., Safin, D.A., Hahn, F.E., Kubiak, M., Pape, T., Babashkina, M.G., Zabirov, N.G., Galezowska, J., Kozlowski, H., and Cherkasov, R.A., *The influence of the intramolecular hydrogen bond on the 1,3-N,S- and 1,5-O,S-coordination of N-phosphoryl-N'-(R)-thioureas with Ni(II) and Pd(II).* New J. Chem., 2007. **31**, 1661-1667.
7. Henderson, W., Nicholson, B.K., Dinger, M.B., and Bennet, R.L., *Thiourea monoanion and dianion complexes of rhodium(III) and ruthenium(II).* Inorg. Chim. Acta, 2002. **338**, 210-218.
8. Piraino, P., Bruno, G., Tresoldi, G., Faraone, G., and Bombieri, G., *Reactivity of the rhodium(III) formamidinato-complex [Rh(η-C_5Me_5)Cl(p-MeC_6H_4N-CH-NC_6H_4Me-p)] with CO and heterocumulenes. Crystal and molecular structure of the thioureido-complex [Rh(η-C_5Me_5)Cl{PhN-C[N(C_6H_4Me-p)-CH=NC_6H_4Me-p)-S}]* J. Chem. Soc., Dalton Trans., 1983. 2391-2395.
9. Safin, D.A., Sokolov, F.D., Nöth, H., Babashkina, M.G., Gimadiev, T.R., Galezowska, J., and Kozlowski, H., *Studies on zinc(II) complexes with N-*

thioacylamidophosphates: X-ray crystal structure of the [Zn(RC(S)NP(O)(OiPr)$_2$)$_2$] (R = NH$_2$, tBuNH, c-C$_6$H$_{11}$NH). Polyhedron, 2008. **27**, 2022-2028.

10. Safin, D.A., Mlynarz, P., Sokolov, F.D., Kubiak, M., Hahn, F.E., Babashkina, M.G., Zabirov, N.G., Galezowska, J., and Kozlowski, H., *Rich magnetic chemistry of cobalt(II) complexes with N-phosphorylthioureas. Crystal structure and solution ^{1}H NMR spectral properties.* Z. Anorg. Allg. Chem., 2007. **633**, 2089-2096.
11. Sokolov, F.D., Zabirov, N.G., Yamalieva, L.N., Shtyrlin, V.G., Garipov, R.R., Brusko, V.V., Verat, A.Y., Baranov, S.V., Mlynarz, P., Glowiak, T., and Kozlowski, H., *Coordination diversity of N-phosphoryl-N'-phenylthiourea (LH) towards Co^{II}, Ni^{II} and Pd^{II} cations: Crystal structure of ML$_2$-N,S and ML$_2$-O,S chelates.* Inorg. Chim. Acta, 2006. **359**, 2087-2096.
12. Cârcu, V., Negoiu, M., Rosu, T., and Serban, S., *Synthesis, characterization of complexes of N-benzoyl-N'-2-nitro-4-methoxyphenyl-thiourea with Cu, Ni, Pt, Pd, Cd and Hg.* J. Therm. Anal. Calorim., 2000. **61**, 935-945.
13. Cauzzi, D., Marzolini, G., Predieri, G., Tiripicchio, A., Costa, M., Salviati, G., Armigliato, A., Basini, L., and Zanoni, R., *Sulfur ligand-stabilized palladium aggregates produced on the surface of benzoylthiourea-functionalized silica xerogels.* J. Mater. Chem., 1995. **5**, 1375-1381.
14. Tenchiu, A.C., Ilis, M., Dumitrascu, F., Whitwood, A.C., and Cîrcu, V., *Synthesis, characterization and thermal behaviour of ortho-metallated Pd(II) complexes containing N-benzoylthiourea derivatives.* Polyhedron, 2008. **27**, 3537-3544.
15. Cîrcu, V., Ilie, M., Ilis, M., Dumitrascu, F., Neagoe, I., and Pasculescu, S., *Luminescent cyclometallated platinum(II) complexes with N-benzoyl thiourea derivatives as ancillary ligands.* Polyhedron, 2009. **28**, 3739-3746.
16. Shen, X., Shi, X., Kang, B., Liu, Y., Tong, Y., Jiang, H., and Chen, K., *Syntheses, crystal structures and properties of Zn(II) and Cd(II) complexes derived from N-(o-nitrophenyl)-N'-(methoxycarbonyl) thiourea(H$_2$omt) and 2,2'-bipyridine(bpy) or o-phenanthroline(phen).* Polyhedron, 1998. **17**, 4049-4058.
17. Shen, X., Shi, X., Kang, B., Liu, Y., Gu, L., and Huang, X., *Syntheses, crystal structures and properties of cadmium(II) and manganese(II) complexes derived from N(o-nitrophenyl-N'-(methoxycarbonyl)thiourea and o-phenanthroline (or 2,2'-bipyridine).* J. Coord. Chem., 1999. **47**, 1 - 15.
18. Adams, R.D. and Huang, M., *Ring-opening insertion of a substituted dithiazole-3-thione into the Re–Re bond in a dirhenium carbonyl complex.* Organometallics, 1996. **15**, 2125-2131.

19. Domínguez, M., Anticó, E., Beyer, L., Aguirre, A., García-Granda, S., and Salvadó, V., *Liquid-liquid extraction of palladium(II) and gold(III) with N-benzoyl-N',N'-diethylthiourea and the synthesis of a palladium benzoylthiourea complex.* Polyhedron, 2002. **21**, 1429-1437.

20. Aitali, M., Ait Itto, M.Y., Hasnaoui, A., Riahi, A., Karim, A., Garcia-Granda, S., and Gutierrez-Rodriguez, A., *Chloro(η^6-p-cymene)(2-methyl-5-oxo-7-phenyl-5,6-dihydro-2H-1,2,4-triazepine-3-thiolato-κ^2N^4,S)ruthenium(II).* Acta Crystallogr., Sect. C: Cryst. Struct. Commun., 2000. **56**, e315-e316.

21. Pisiewicz, S., Rust, J., Lehmann, C.W., and Mohr, F., *Cationic palladium(II), platinum(II) and ruthenium(II) complexes containing a chelating difluoro-substituted thiourea ligand.* Polyhedron, **29**, 1968-1972.

22. Alagöz, C., Brauer, D.J., and Mohr, F., *Arene ruthenium metallacycles containing chelating thioamide ligands.* J. Organomet. Chem., 2009. **694**, 1283-1288.

23. Henderson, W., Nicholson, B.K., and Tiekink, E.R.T., *Synthesis, characterisation, supramolecular aggregation and biological activity of phosphine gold(I) complexes with monoanionic thiourea ligands.* Inorg. Chim. Acta, 2006. **359**, 204-214.

24. Dinger, M.B., Henderson, W., Nicholson, B.K., and Robinson, W.T., *Organogold(III) metallacyclic chemistry. Part 3[1]. Self-assembly of the nonametallic gold(III)-silver(I)-sulfido aggregates $[\{LAu(\mu\text{-}S)_2AuL\}_3Ag_3X_2]^+$ (L=cycloaurated N,N-dimethylbenzylamine ligand; X=Cl, Br), by thiourea desulfurisation.* J. Organomet. Chem., 1998. **560**, 169-181.

25. Henderson, W., Nicholson, B.K., and Rickard, C.E.F., *Platinum(II) complexes of chelating and monodentate thiourea monoanions incorporating chiral, fluorescent or chromophoric groups.* Inorg. Chim. Acta, 2001. **320**, 101-109.

26. Henderson, W., Kemmitt, R.D.W., Mason, S., Moore, M.R., Fawcett, J., and Russell, D.R., *Thiadiazatrimethylenemethane and N,N',P-triphenylphosphonothioic diamide complexes of platinum(II).* J. Chem. Soc., Dalton Trans., 1992. 59-66.

27. Henderson, W. and Nicholson, B.K., *Synthesis and electrospray mass spectrometry of platinum(II) complexes derived from thiourea dianions and the x-ray structure of [Pt{NMeC(=NCN)S}(COD)] (COD = cyclo-octa-1,5-diene).* Polyhedron, 1996. **15**, 4015-4024.

28. Westra, A.N., Bourne, S.A., Esterhuysen, C., and Koch, K.R., *Reactions of halogens with Pt(II) complexes of N-alkyl- and N,N-dialkyl-N'-benzoylthioureas:*

oxidative addition and formation of an I_2 inclusion compound. Dalton Trans., 2005. **17**, 2162-2172.

29. Mautjana, A.N., Miller, J.D.S., Gie, A., Bourne, S.A., and Koch, K.R., *Tailoring hydrophilic N,N-dialkyl-N'-acylthioureas suitable for Pt(II), Pd(II) and Rh(III) chloride pre-concentration from acid aqueous solutions, and their complex separation by reversed-phase HPLC.* Dalton Trans., 2003. **10**, 1952-1960.
30. Egan, T.J., Koch, K.R., Swan, P.L., Clarkson, C., Van Schalkwyk, D.A., and Smith, P.J., *In vitro antimalarial activity of a series of cationic 2,2'-bipyridyl- and 1,10-phenanthrolineplatinum(II) benzoylthiourea complexes.* J. Med. Chem., 2004. **47**, 2926-2934.
31. Shaw III, C.F., *The biochemistry of gold*, in *Gold: Progress in Chemistry, Biochemistry and Technology*, H. Schmidbaur, Editor. 1999, John Wiley & Sons Ltd: Chichester. p. 259-308.
32. White, C., Yates, A., Maitlis, P.M., and Heinekey, D.M., *(η^5-Pentamethylcyclopentadienyl)rhodium and -iridium compounds.* Inorg. Synth., 2007. **29**, 228-234.
33. Oliver, D.L. and Anderson, G.K., *Substitution reactions of (diphosphine)palladium(II) and -platinum(II) chloride and triflate complexes.* Polyhedron, 1992. **11**, 2415-2420.

Chapter Four

Sugar gold(III) iminophosphoranes

4.1 Iminophosphoranes

Iminophosphoranes have a four-coordinate tetrahedral phosphorus with a formal double bond to nitrogen, Figure 4.1, and are analogous to phosphorus ylides. An alternative view of the structure is to consider the nitrogen as negatively charged and the phosphorus positively charged. Unlike ylides there is little debate about the double bond nature between the phosphorus and nitrogen. They have a long history and have been known by many different names such as phosphinimines, phosphazo compounds, (mono-) phosphazenes and λ^5-phosphazenes amongst others. The first iminophosphorane was produced by Staudinger and Meyer in 1919, by reacting phenyl azide with PPh_3 to give *N*-phenyliminotriphenylphosphorane, **38** [1], Figure 4.1. After their initial discovery iminophosphoranes were largely neglected until the 1950's [2].

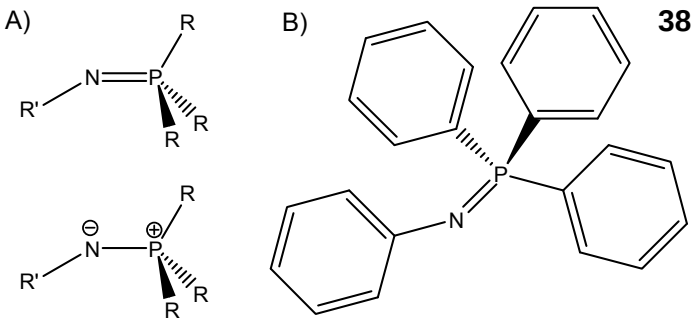

Figure 4.1 *A) Two representations of the general structure of an iminophosphorane; B)* ***38****, the first iminophosphorane synthesised.*

In comparison to their analogous ylides, iminophosphoranes are particularly stable. This is assumed to be from the delocalisation of electron density around

the nitrogen onto the phosphorus [2]. The lone pair of electrons on the nitrogen is accessible for bonding making the nitrogen a Lewis base.

4.2 Production of iminophosphoranes

There are two general routes to iminophosphoranes, either by directly forming the bond between nitrogen and phosphorus or by forming the parent imine (R_3P=NH) and reacting the nitrogen with an electrophile. A selection of the direct methods of synthesis will be discussed below.

4.2.1 Iminophosphoranes by direct methods

Scheme 4.1 summarises the direct methods discussed. The first method to produce iminophosphoranes was the Staudinger reaction [1]. One of the most elegant pathways, it is the reaction between an azide and a tertiary phosphine. The reaction is widely applicable and can be used with a vast number of different azides including but not limited to aromatic [1], aliphatic [3], silyl [4] and olefinic [5], with the only limit appearing to be if the azide can be synthesised [2]. The tertiary phosphines that will react are also numerous with alkyl, mixed aryl and alkyl, amino and polymeric phosphines as a small sample of the possibilities [2]. This shows the vast array of iminophosphoranes accessible through this reaction. The proposed mechanism for the Staudinger reaction, Scheme 4.2, starts with the nucleophilic attack on the terminal (γ) nitrogen to form a linear intermediate, and then N_2 dissociates via a probable four-centred transition state [2]. If a chiral phosphorus is used the reaction generally proceeds with retention of the configuration [6].

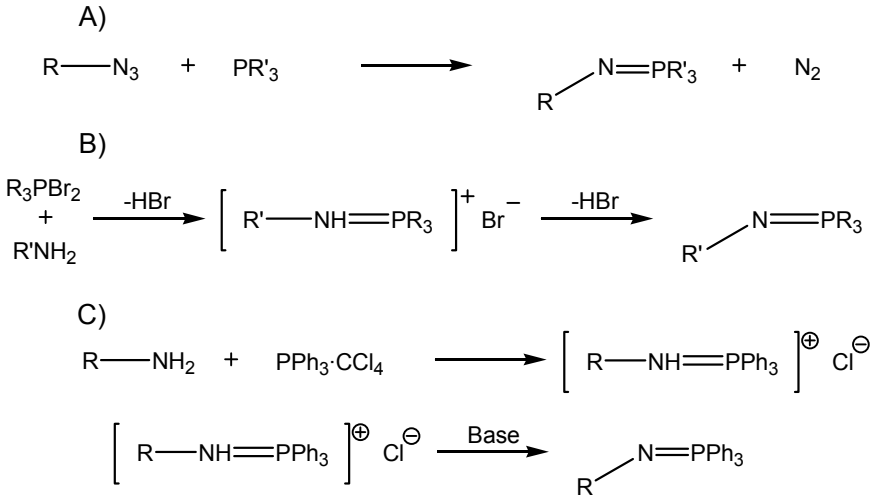

Scheme 4.1 *Overview of methods for directly synthesising iminophosphoranes. A) The Staudinger reaction between an azide and a tertiary phosphine; B) The Kirsanov reaction with an amine and tertiary phosphine dibromide; C) The Appel reaction between an amine and triphenylphosphine-carbon tetrachloride.*

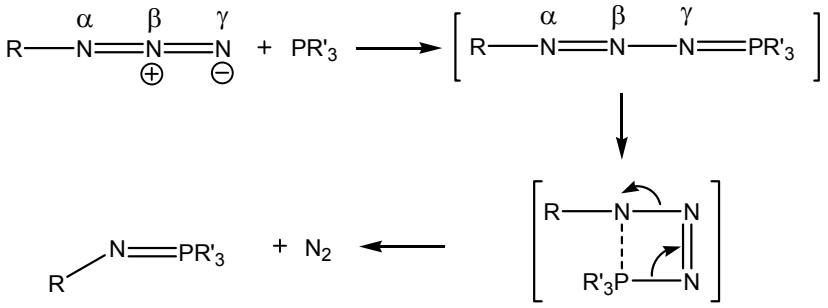

Scheme 4.2 *Proposed mechanism for the Staudinger reaction [2].*

Another route for the direct synthesis is the Kirsanov reaction [7], Scheme 4.1. When a tertiary phosphine is reacted with Br_2 a phosphine dibromide is formed, R_3PBr_2. This can be reacted with an amine to form an aminophosphonium bromide intermediate, $[R'–NH–PR_3]^+Br^-$, by nucleophilic displacement of the bromine by the nitrogen. With an aromatic amine the aminophosphonium bromide intermediate is deprotonated during the reaction to form the iminophosphorane; however with alkyl amines a deprotonating agent needs to be added to convert the salt to the iminophosphorane. Another method is the

Appel reaction [8], Scheme 4.1. This involves the reaction of an amine with a phosphine-carbon tetrachloride complex, this forms an aminophosphonium chloride; a base gives the iminophosphorane product.

4.3 Production of sugar iminophosphoranes

The first sugar iminophosphoranes produced were the acetylated glycosyl versions using glucose, galactose, xylose and cellobiose in 1964 [9], Figure 4.2. They were produced *via* the Staudinger reaction with the glycosyl azide and PPh_3 in Et_2O.

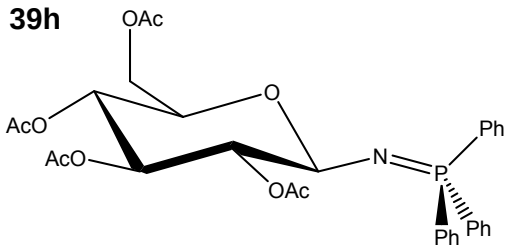

Figure 4.2 *One of the first sugar iminophosphoranes produced, N-(triphenyl-phosphoranylidene)-β-D-glucopyranosylamine,* ***39h****.*

The Appel reaction has also been used to produce sugar iminophosphoranes; **7** (Chapter 2.2.1) was reacted with PPh_3 and carbon tetrachloride to give the hydrochloride salt of the iminophosphorane which when treated with triethylamine gave the iminophosphorane [10]. The same reaction was attempted with 6-amino-6-deoxy-1,2:3,4-di-*O*-isopropylidene-α-D-galactopyranose but the iminophosphorane could not be isolated from the hydrochloride [10], while the 6-azido-6-deoxy derivative reacted with PPh_3 to give the iminophosphorane [11]. The Staudinger reaction can also be used with unprotected sugar azides; both β-D-glucopyranosyl azide and β-D-galactopyranosyl azide react with PPh_3 in dry 1,4-dioxane to produce the corresponding iminophosphoranes but these are susceptible to hydrolysis [12].

4.3.1 Reactions of sugar iminophosphoranes

The wide variety of reactions that iminophosphoranes undergo means that sugar iminophosphoranes have been used for a wide array of synthetic purposes. Some of the uses are discussed below.

4.3.1.1 Reduction of azides by hydrolysis of iminophosphoranes

The ease of hydrolysis of the iminophosphorane has lead to its use in sugar chemistry (and other fields) to reduce azide groups to amino groups with the phosphine oxide as the by-product, Scheme 4.3. It has been shown that PMe_3 at low temperatures can selectively reduce azides [13], Scheme 4.3.

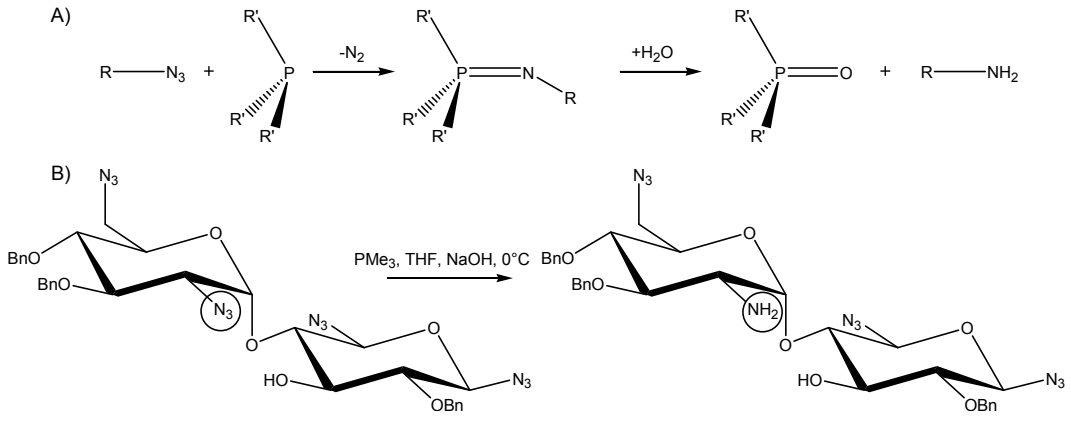

Scheme 4.3 *Reduction of azides by hydrolysis of iminophosphoranes. A) General scheme for reduction of an azide to an amine. B) Selective reduction of a sugar azide at low temperature [13].*

4.3.1.2 Synthesis of amides via the Staudinger reaction

The nitrogen of an iminophosphorane is nucleophilic allowing reactions to occur on it. It will react with acyl groups giving a variety of products. Previously synthesising glycoamides directly involved the acylation of glycosylamines. This

method had a number of limitations. In 1997 a synthetic route involving the Staudinger reaction was reported [14]. In a one-pot reaction glycosyl azides are reacted with PPh_3 and an acid chloride; after the addition of water the amide product was formed, Scheme 4.4.

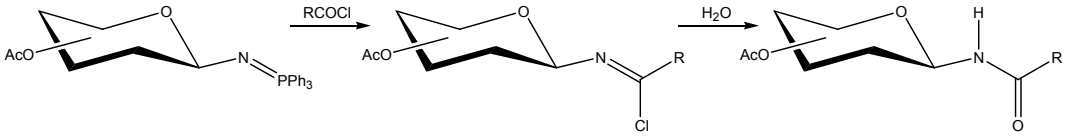

Scheme 4.4 *Synthesis of glycosylamides using PPh_3 and acid chlorides [14].*

In 2000 a new reaction was developed where a methyl ester was used as an electrophile trap with the nitrogen of the iminophosphorane undergoing an internal rearrangement to form an amide, which was termed Staudinger ligation [15], Scheme 4.5. Staudinger ligation has also been used to synthesis glycoproteins [16].

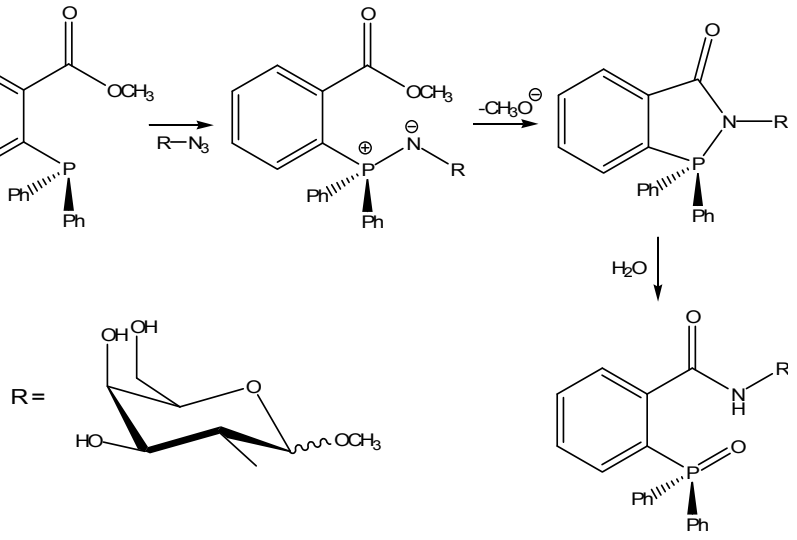

Scheme 4.5 *The first Staudinger ligation reaction [15].*

The addition of a group to the phosphine that can be traced allows Staudinger ligation to be used as a method for probing biological processes. For example a sugar with an azide group was attached to the enzyme β-galactosidase, a phosphine with the fluorescent molecular probe FLAG was added which reacted with the azide and gave easy detection of the enzyme and allowed investigation of its activity [17], Scheme 4.6. This method has also been used to study *N*-α-acetyl-galactosaminyltransferases [18]. This method can be carried out *in vivo*. An azido sugar was fed to mice; the sugar was incorporated into the cell walls of the mice with the azide group still free. The phosphine with a FLAG tracer could be fed to the mice and react with the tagged cells that had taken up the sugar allowing them to be observed [19].

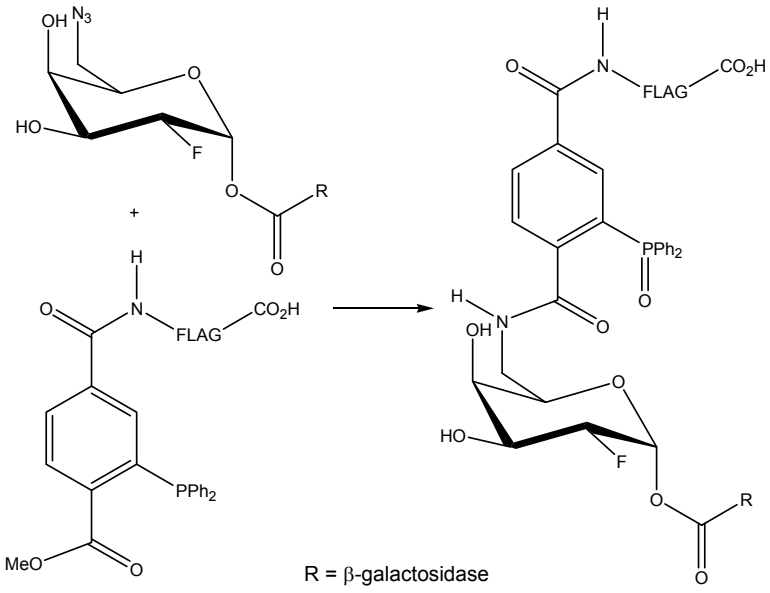

Scheme 4.6 *Use of Staudinger ligation to add the fluorescent molecular probe FLAG to an enzyme [18].*

Staudinger ligation can be used for acyl transfer to synthesise per-*O*-acetyl-β-glycosyl amides. If a glycosyl azide is reacted with a PPh_3 derivative modified with a *ortho* ester group, the resulting iminophosphorane undergoes acyl transfer to produce β-glycosyl amides [20], Scheme 4.7.

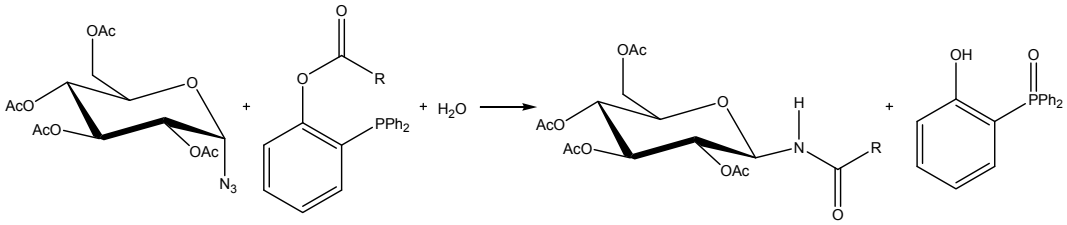

Scheme 4.7 *Reaction to produce per-O-acetyl-β-glycosyl amides, via Staudinger ligation [20].*

4.3.1.3 Aza-Wittig reaction

Another synthetic use of iminophosphoranes is the Aza-Wittig reaction where an iminophosphorane is reacted with a carbonyl to produce an imine, Scheme 4.8. This is a versatile reaction and an internal Aza-Wittig reaction can be used to produce nitrogen heterocycles [21]. It has been used in carbohydrate chemistry to produce sugar carbodiimides [22, 23].

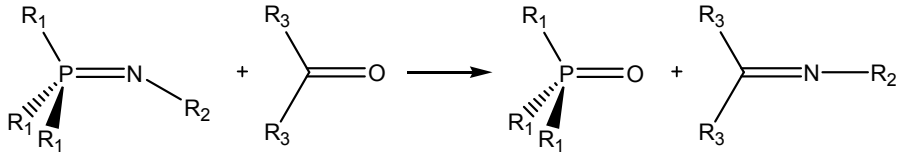

Scheme 4.8 *General form of the Aza-Wittig reaction.*

4.4 Reaction of iminophosphoranes with metals

Iminophosphoranes show a very wide variety of bonding modes to metal centres. Vicente *et al* divided the bonding modes into a series of classes [24], Figure 4.3. The first class, I, is when the iminophosphorane is acting as a simple nitrogen donor ligand; the basicity of the nitrogen is the driving force behind the complexes. When **38** is reacted with $PdCl_2$ the μ-chloride bridged dimer, $[PdCl(\mu\text{-}Cl)(N(Ph)=PPh_3)]_2$, is formed [25]; if half a molar equivalent of $PdCl_2(PhCN)_2$ in acetone is used, the similar *trans*-$PdCl_2[N(Ph)=PPh_3]_2$ species is formed [26],

Figure 4.4. The other classes are based around a carbon atom forming a σ bond to the metal centre. Groups IIa and IIb are cyclometalated compounds with the metal σ bond to an alkyl and aryl carbon respectively. IIc is the same as IIb except the metal is no longer coordinated to the nitrogen and so is not cyclometaled. Class III has the metal bonded to the ortho carbon on the nitrogen substituent. If the metal is bonded to the phosphorus substituent it is termed endo, while if it is bonded to the nitrogen substituent it is exo [24].

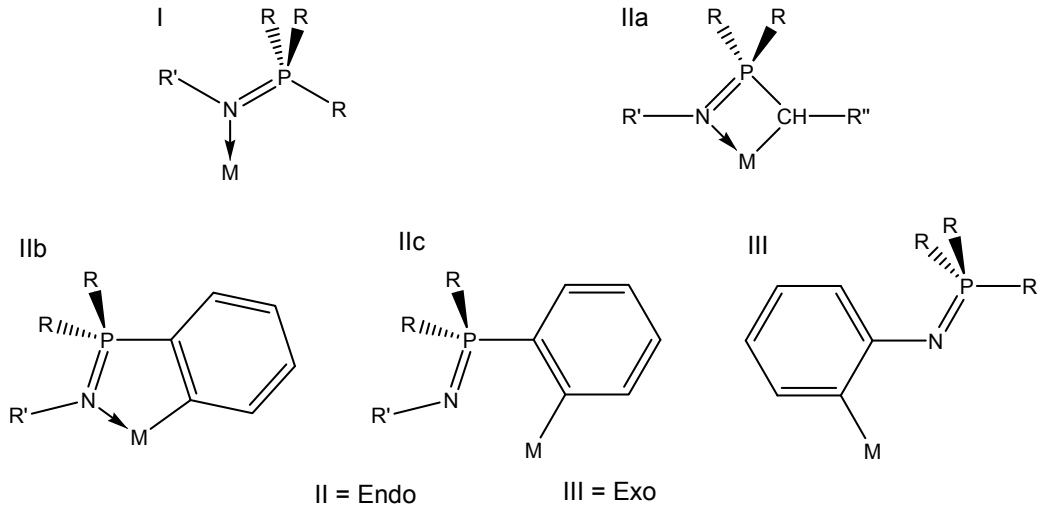

Figure 4.3 *I) Metal only coordinated to nitrogen; IIa) Cyclometalated to an alkyl carbon; IIb) Cyclometalated to an aryl carbon; IIc) Metal σ bonded to ortho carbon on phosphorus and not coordinated to nitrogen; III) Metal bonded to ortho carbon on nitrogen substituent, exo coordination. Class II are endo while class III are exo [24].*

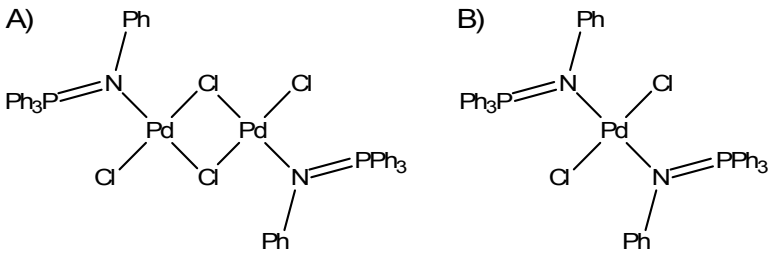

Figure 4.4 ***38*** *acting as a nitrogen donor to palladium. A) μ-chloride bridged dimer [25]; B) A trans-PdL_2Cl_2 type monomer [26].*

4.4.1 Cyclometalation reactions

This laboratory is interested in iminophosphoranes due to their ability to be involved in cyclometalation reactions [24, 27-30]. A cyclometalation reaction is a reaction of a transition metal complex in which a ligand undergoes an intramolecular metalation with the formation of a chelate ring containing a metal-carbon σ bond [31]. Figure 4.5 shows examples of cyclometalated iminophosphoranes derived from **38** that this laboratory has produced. The iminophosphorane acts as a mono-anionic *N*,*C*-chelating ligand with the ortho aromatic carbon forming a σ bond to the metal.

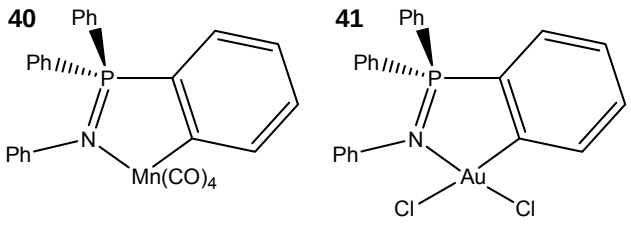

Figure 4.5 *Examples of **38** undergoing cyclometalation reactions to act as a monoanionic N,C-chelating ligand; **40** [30] and **41** [27].*

4.4.2 Routes to cyclometalation

Cyclometalated iminophosphoranes are accessible either by direct metalation or through ortho-lithiation of the iminophosphorane followed by transmetalation. Direct metalation was first developed by Alper who reacted $Ph_3P{=}NC_6H_4CH_3$ with $Na_2[PdCl_4]$ to form a μ-chloride bridged dimer [29]. It was shown that reacting **38** with $PhCH_2M(CO)_5$ (M = Mn or Re) would also directly metalate iminophosphoranes [30]. Vicente *et al* showed that direct metalation could give different products depending on the metal used [24]. When **38** is reacted with $Pd(OAc)_2$, it is metalated on the phenyl group attached to the phosphorus to give the endo product; while $Hg(OAc)_2$ metalates the phenyl group on the nitrogen to give the exo product, Scheme 4.9.

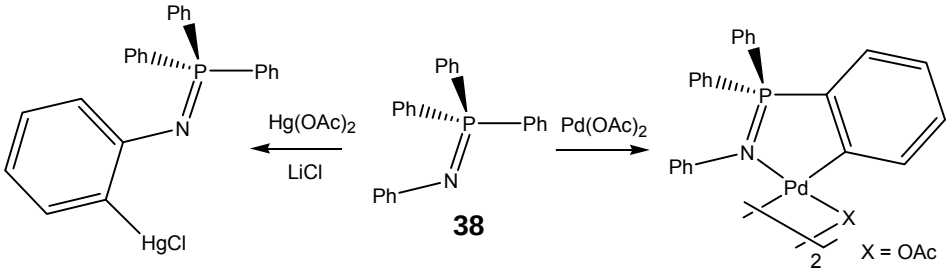

Scheme 4.9 *Scheme showing the difference in reactivity of **38** to direct metalation; $Hg(OAc)_2$ gives the N-phenyl metalated exo product, while $Pd(OAc)_2$ gives the P-phenyl metalated endo product [24].*

The metalation of the iminophosphorane in different positions is a problem if the endo product is wanted. To get around this problem, ortho-lithiation of the iminophosphorane can be used instead. Wei *et al* showed that reacting **38** with methyl or phenyl lithium would produce the ortho-lithiated iminophosphorane which could be transmetalated to a variety of metal chloride metalocycles including aluminium, gallium and palladium [32], Scheme 4.10.

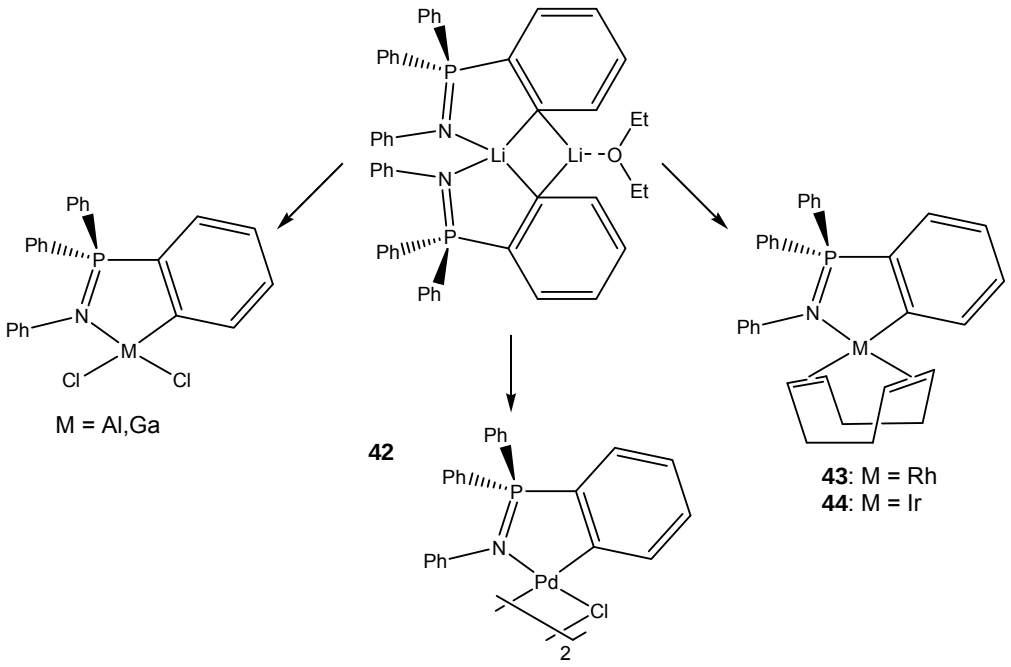

Scheme 4.10 *Scheme showing the reaction of the ortho-lithiated iminophosphorane to form a variety of different metalocycles. Al, Ga and Pd [32]; M(COD) (M = Rh or Ir) [33].*

Over the past 10 years a large number of articles have been published on cyclometaled iminophosphoranes with a wide variety of functional groups to produce many different structural features. Figure 4.6 shows a tridentate iminophosphorane platinum example.

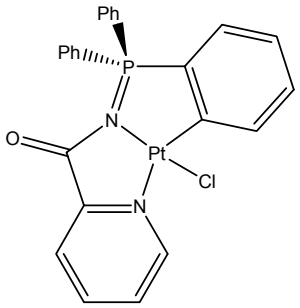

Figure 4.6 *A tridentate platinum iminophosphorane [34].*

If the group on the nitrogen is replaced with a carbohydrate it should be possible to produce a cyclometalated iminophosphorane with the associated benefits mentioned in Chapter One that carbohydrates contribute. This work was carried out to see if cyclometalated iminophosphoranes could be made with sugars.

4.5. Sugar azides

Three different types of sugar azides were used for this work; Glycosyl azides, an acetamido azide and a fructopyranoside based azide.

4.5.1 Glycosyl azides

Since the Staudinger reaction was the easiest way to produce iminophosphoranes, sugar azides were needed. They were easily synthesised from sugars and the general overall route to 1,2-*trans*-per-*O*-acetyl-β-glycosyl azides is shown in Scheme 4.11. Sugars can be readily acetylated using acetic

anhydride and a basic or acidic catalyst. Traditional catalysts have included pyridine, sodium acetate, zinc chloride and perchloric acid [35]. A more recent method involves using iodine as the catalyst [36, 37]. While this gives a mixture of anomers, the next step of bromination with HBr in acetic acid [38], reacts with both α and β acetates to give the thermodynamically favoured α-glycosyl bromide (due to the anomeric effect), removing the need to separate the anomers. The bromide is easily displaced with sodium azide by nucleophilic substitution in an acetone solution with water present to solubilise the azide ion [39]. This method is only applicable to 1,2-*trans* sugars, so mannose with the O2 oxygen in the axial position would not produce the azide product.

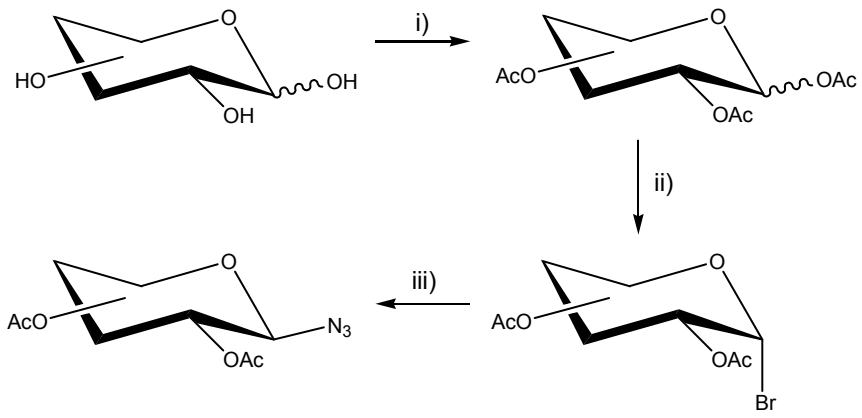

Scheme 4.11 *i) Acetic anhydride, cat. I_2; ii) HBr, acetic acid; iii) NaN_3, acetone, H_2O.*

Three sugars were used to synthesis glycosyl azides, D-glucose, D-galactose and L-arabinose, Figure 4.7. This reaction can be extended to many other sugars such as dissacharides.

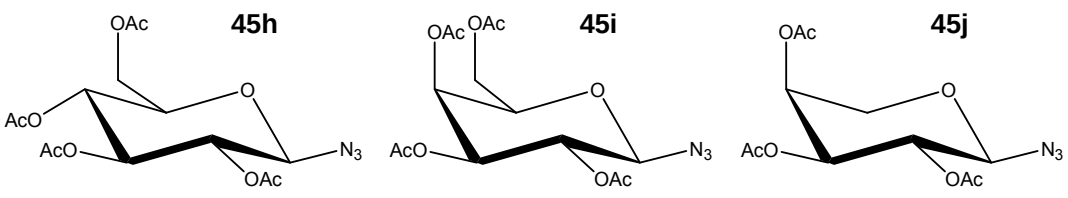

Figure 4.7 *The three glycosyl azides used for the Staudinger reaction.*

Azide compounds are notorious for their explosive nature. However as the percentage of nitrogen in the azide decreases they become less explosive. The Smith rule [21], shown in Figure 4.8, is an indication of whether an organic azide will be non-explosive. If the sum of the carbon and oxygen atoms divided by the number of nitrogen atoms is greater or equal to three, the azide will be non-explosive. Since the nitrogen content of all the sugar azides was so low no special precautions were taken with the manipulation of them.

$$\frac{N_C + N_O}{N_N} \geq 3$$

Figure 4.8 *The Smith rule for organic azides [21].*

4.5.2 Acetyl glucosamine acetamido azide

The second azide studied was based on the azide group $RCOCH_2N_3$. Iminophosphoranes derived from this azide have been previously looked at with $Ph_3P{=}NCH_2COR$ (R = OMe or NMe_2); these iminophosphoranes undergo direct metalation [40]. This group is able to be attached to different carbohydrate moieties such as an amine or hydroxyl. There are a number of possibilities to synthesize the $RCOCH_2N_3$ group. Bromo acetyl bromide, $BrCOCH_2Br$, appeared to be the best route to these azides. The acid bromide can easily react with alcohols or amines to give an ester or amide respectively. The CH_2Br derivative was chosen over CH_2Cl for the greater leaving potential of bromide over chloride. Once the ester or amide has been formed the bromide from the CH_2Br group could be displaced by an azide ion in a nucleophilic substitution.

7 provided an easily accessible amine group for the reaction with bromo acetyl bromide. By modification of several existing methods [39, 41], the azide **45k** could be synthesised in a one pot reaction, Scheme 4.12. **7** was dissolved in acetone with bromo acetyl bromide and an excess of 2,6-lutidene and stirred at

0°C for one hour. The use of a sterically hindered base prevents acylation of the base occuring. NaN_3 was added along with water and stirred for 16 hours. Water and HCl was added and **45k** extracted with CH_2Cl_2. Recrystallisation from hot ethanol gave the azide. The RCH_2Br compound shown in Scheme 4.12 has been made previously by reacting **7** with $(BrCH_2CO)_2O$ [42]. The RCH_2Cl derivative has been made by reacting **7** with chloro acetyl chloride in chloroform with 2,6-lutidene [41]. These RCH_2X compounds show anti-cancer properties [42, 43]. The azide has been produced by reacting the RCH_2Cl derivative with NaN_3 in DMF [44]. This current method is not only a one pot reaction but also avoids the use of DMF. The ^{1}H and ^{13}C NMR spectra of **45k** agree with the literature values [44].

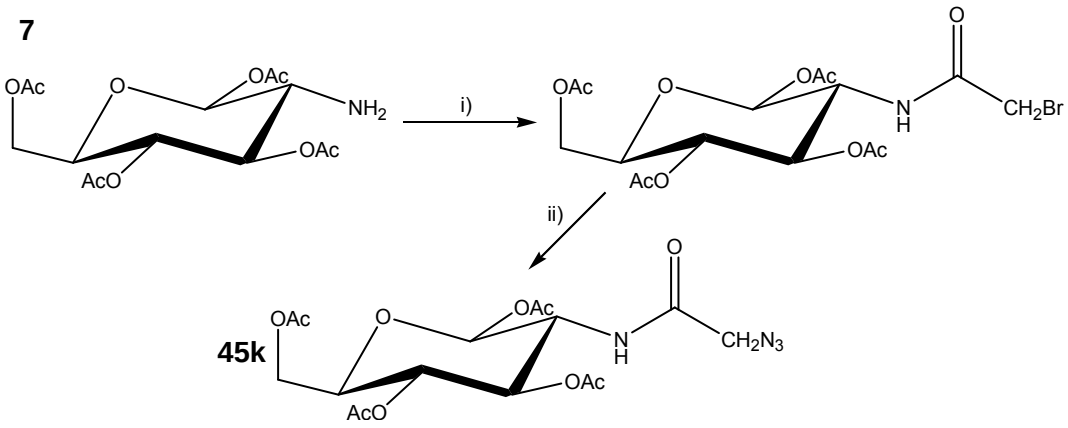

Scheme 4.12 *One pot synthesis of **45k** from **7**. i) $BrCH_2COBr$, acetone; ii) NaN_3, acetone, H_2O.*

4.5.3 Fructopyranoside azide

The final azide that was investigated was 2′-azidoethyl 1,3,4,5-tetra-*O*-acetyl-β-D-fructopyranoside, **45l** [45]. Scheme 4.13 shows the production of **45l**. This was of interest as the azide now had an ethylene spacer between the azide and the sugar.

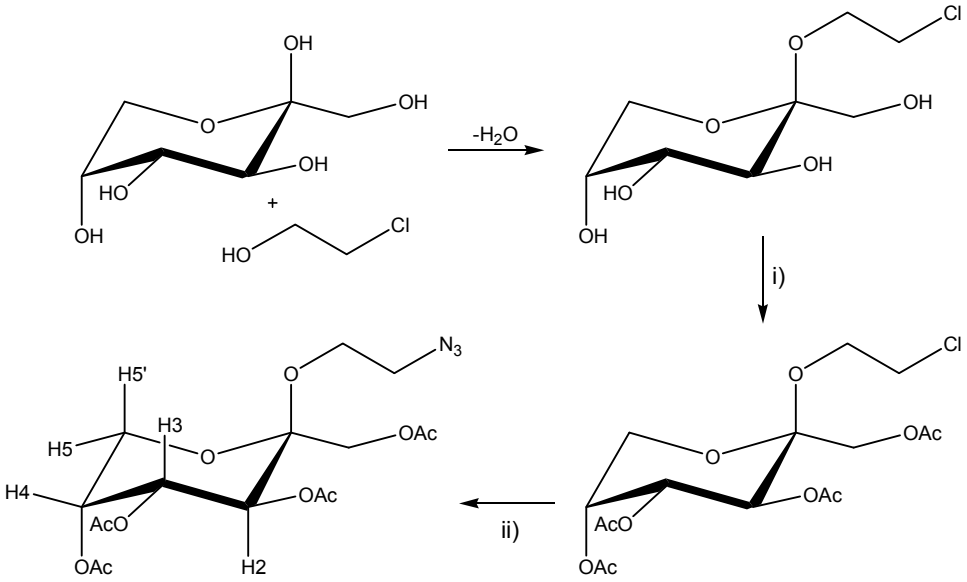

Scheme 4.13 *Synthesis of **45l**; i) Acetic anhydride, pyridine; ii) DMF, $NaNa_3$ [45].*

Since the literature on the azide only partially assigned the NMR spectrum, a full range of experiments were run to fully assign the spectra. The NMR data supports the $^2C_5$ conformation. The coupling constant for $J_{H3,H4}$ is 10.2 Hz which is indicative of a dihedral angle of 180° between the two protons (from the vicinal Karplus correlation), while a much smaller coupling constant would be expected for $^5C_2$ (~2 Hz for a 60° dihedral angle). On the same grounds the coupling constants for $J_{H5,H6}$ and $J_{H5',H6}$ of 1.3 and 1.7 Hz is also as expected; in the $^2C_5$ conformation both H6 protons are at a 60° dihedral angle to the H5 proton and would be expected to give the same coupling constant. Since the anomeric effect is stronger in non-polar solvents it would be expected that in chloroform the O-CH_2CH_2-N_3 group would be in the axial position.

4.6 Reaction of azides with phosphines

With the azides in hand, it was a simple reaction to produce iminophosphoranes with a slight modification of the method of Messmer *et al* [9]. The azides were dissolved in CH_2Cl_2 with the phosphine under nitrogen and stirred for 1.5 hours, and solvent removed under vacuum.

4.6.1 Reaction of sugar azides with PPh_3

When **45h** was reacted with PPh_3 it produced the reported product **39h** [9] which was stable and produced X-ray quality crystals as discussed below. **45k** also reacted cleanly with PPh_3 as shown by ESI-MS but the product was only characterised by NMR and used directly in cyclometalation attempts. Figure 4.9 shows the two iminophosphoranes. When the fructoside **45l** was reacted with PPh_3 the iminophosphorane was observed by ESI-MS as $[M+H]^+$ but attempts to isolate it only lead to decomposition, the ethylene group leaves the iminophosphorane vulnerable to hydrolysis.

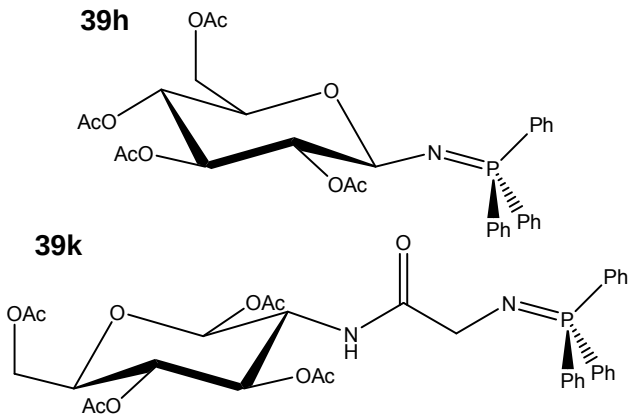

Figure 4.9 *The two sugar iminophosphoranes derived from PPh_3.*

^{31}P NMR of **39h** and **39k** showed the typical chemical shift for iminophosphoranes at 22.1 and 23.6 ppm respectively. As discussed later this is indicative of an iminophosphorane that has not been cyclometaled.

4.6.1.1 Crystal structure of 39h

Recrystallisation of **39h** with dichloromethane and hexane gave crystals suitable for X-ray diffraction. **39h** formed monoclinic crystals in the space group $P2_1$. This structure was slightly unusual with a β angle of exactly 90°; there was no ambiguity with the orthorhombic system with a successful refinement in $P2_1$ and only two molecules in the unit cell. Appendix Two gives the details of solving the structure. Figure 4.10 shows the geometry of **39h**.

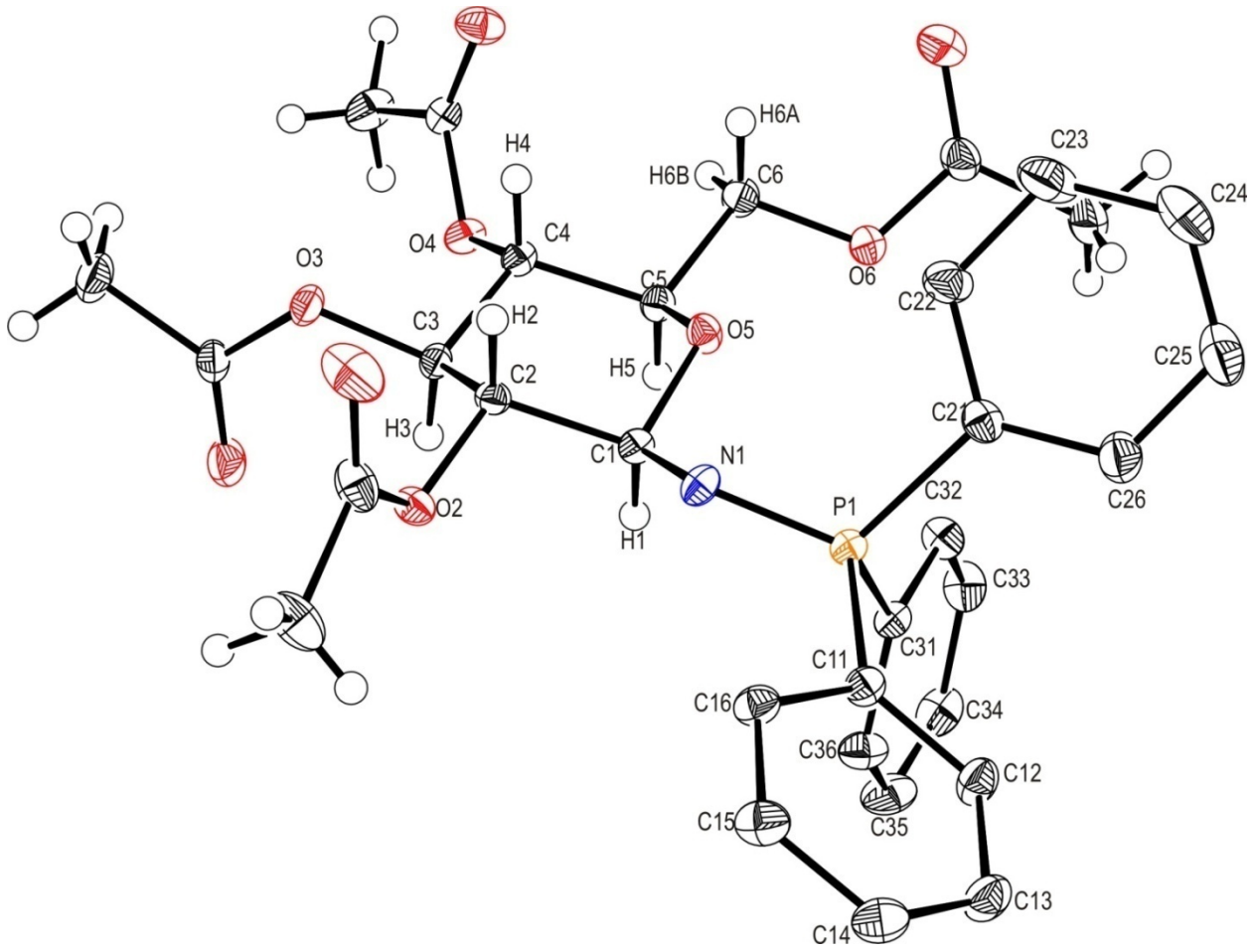

Figure 4.10 *The geometry of **39h** showing the atom labelling scheme and thermal ellipsoids at the 50% probability level. Phenyl hydrogen atoms have been omitted for clarity.*

Table 4.1 gives selected bond lengths and angles for **39h**. Compared with other iminophosphoranes with alkyl groups on the nitrogen the C–N and N=P bond lengths are similar as is the C–N=P bond angle [46, 47]. The C–N=P bond angle for **38** is larger at 130.4(3)°. While the phosphorus is approximately tetrahedral there is a slight distortion in the N=P–C angles, with the carbons *cis* to the nitrogen substituent having slightly larger angles. This is seen in the structure of **38** [48] and for some alkyl iminophosphoranes [46, 47]. The torsion angle for C2–C1–N1–P1 is 176.8(1)°. The sugar portion of the molecule is as expected. The ring is in the expected $^4C_1$ conformation which puts the N=PPh_3 group in the most stable equatorial position as opposed to the axial position. The acetylated hydroxylmethyl group has adopted the *gt* conformation.

	39h
C1–N1	1.408(12)
N1=P1	1.5708(9)
C1–N1=P1	120.8(7)
N1=P1–C11	108.80(5)
N1=P1–C21	113.07(5)
N1=P1–C31	115.52(5)

Table 4.1 *Selected bond lengths (Å) and angles (°) for **39h**.*

4.7 Metalation of sugar iminophosphoranes

With **39h** in hand metalation was attempted. The presence of the acetyl groups precluded the use of lithium reagents so direct metalation methods were attempted. The method of Vicente *et al* [24], using $Hg(OAc)_2$ and $Pd(OAc)_2$, was tried as was the Leeson *et al* $PhCH_2Mn(CO)_5$ method [30]. None of the reactions gave any sign of cyclometalation occuring. ESI-MS of the reaction mixture showed no indication of metal coordination to the iminophosphorane. To test this **39h** was stirred with $PdCl_2$ in acetonitrile. ESI-MS again showed no sign of any coordination. A space filling model based on the crystal structure showed

that the nitrogen was very sterically crowded. Figure 4.11 shows a comparison of the space filling model of **39h** with **38**. The acetate group on O2 is blocking access to the nitrogen. Since the cyclometalation reactions are assumed to require the metal to coordinate to the nitrogen first, this appeared to be a major stumbling block to carbohydrate derived cyclometalated iminophosphoranes.

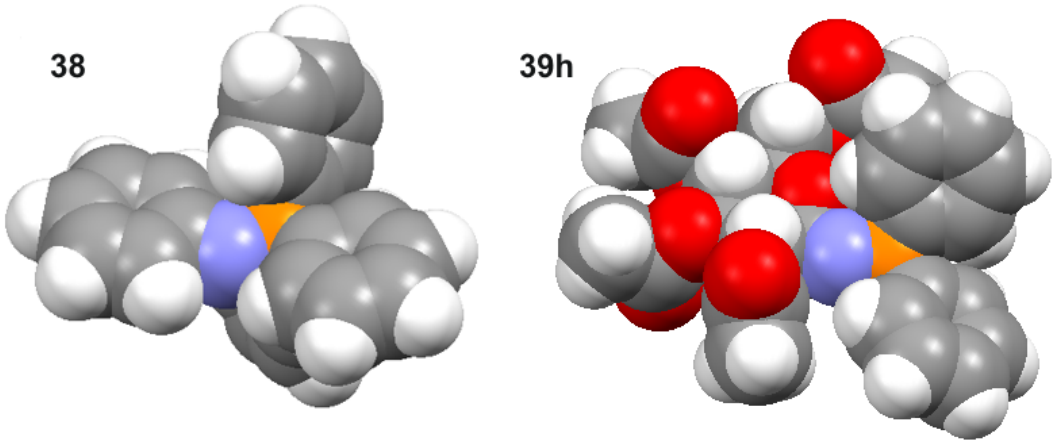

Figure 4.11 *Comparison of the space filling diagram of; A) **38**; B) **39h**. This shows the crowded nature of the nitrogen atom in **39h**.*

Direct metalation was also attempted with **39k**, but again no product could be detected or isolated. Some proposed mechanisms for direct cyclometalation start with the coordination of the metal to the nitrogen, Scheme 4.14 shows the proposed mechanism for the direct metalation by $Pd(OAc)_2$. It can be hypothesised that the lack of availability of the nitrogen hinders the direct metalation.

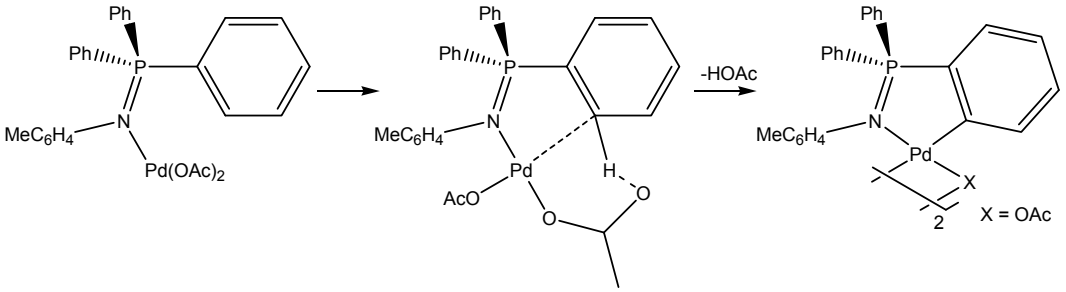

Scheme 4.14 *Proposed mechanism for cyclometalation of $MeC_6H_4N{=}PPh_3$ by palladium acetate [24].*

Since the sugar iminophosphoranes couldn't be directly metalated, another route to cyclometalated compounds was needed. To get around this issue two methods were investigated. Firstly a less sterically crowded phosphine was used. Secondly premetalation of a phosphine was investigated.

4.7.1 Reaction of 45h with Me_2PhP

The phosphine Ph_2MeP has been used to produce cyclometalated iminophosphoranes [49]. To investigate the possibility that a much less sterically hindered phosphine would allow direct metalation, **45h** was reacted with Me_2PhP using the above method. The product was an impure oil and attempts to purify the product only lead to decomposition. Evidently the sterically crowded nature of the PPh_3 phosphine also helps to prevent the hydrolysis of the iminophosphorane bond in **39h**.

4.7.2 Pre-metalation of a phosphine

The second method was the pre-metalation of a phosphine. For this the ortho-mercurated diphosphine $[Hg(2\text{-}C_6H_4PPh_2)_2]$, **46**, shown in Figure 4.12 was used. Since it has a phosphine group free it reacts with azides to produce mercurated iminophosphoranes which can be transmetalated. This method of producing cyclometalated iminophosphoranes was developed by Kilpin *et al*, who used it to

produce the gold(III) iminophosphorane shown in Figure 4.12 [50]. The diphosphine is synthesised by reacting 1,2-dibromobenzene, ^{n}BuLi and Ph_2PCl to produce 2-$BrC_6H_4PPh_2$ which can be lithiated to give 2-$LiC_6H_4PPh_2$ [51]. When reacted with $HgCl_2$ in Et_2O **46** is produced [52], Scheme 4.15.

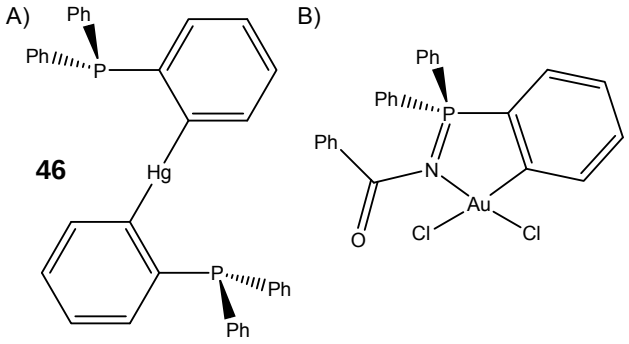

Figure 4.12 *A) **46**; B) A gold(III) iminophosphorane made via **46** [50].*

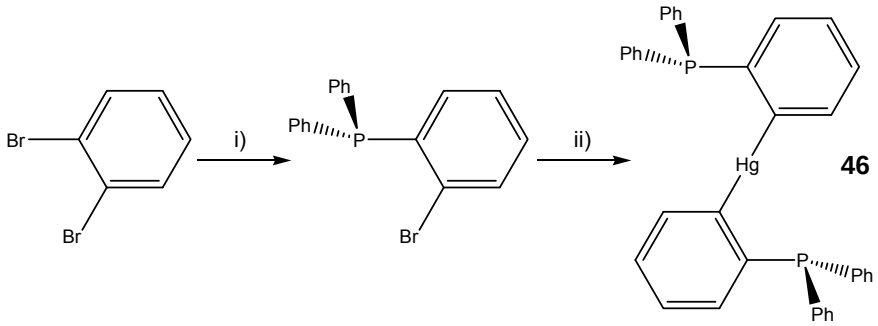

Scheme 4.15 *Reaction scheme for **46**. i) Ph_2PCl, ^{n}BuLi, THF, Et_2O, -110°C; ii) ^{n}BuLi, $HgCl_2$, Et_2O.*

With **46** in hand it could be reacted with the sugar azides to produce the ortho-mercurated iminophosphane intermediate **47**, which could be transmetalated, Scheme 4.16. The details of the transmetalation to gold(III) iminophosphoranes for each sugar azide is detailed below. The intermediate, **47**, was not isolated but used directly *in situ* for cyclometalation. This method of producing pre-metalated iminophosphoranes side steps the steric issues with directly metalating sugar iminophosphoranes. While gold(III) iminophosphoranes were produced there is potential to transmetalate to a wide variety of different metals.

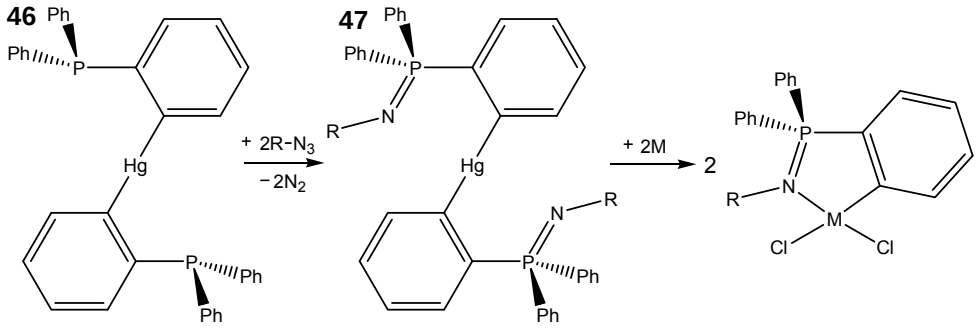

Scheme 4.16 *General reaction scheme to form the cyclometaled sugar iminophosphoranes from **46**.*

4.8 Gold(III) iminophosphoranes

4.8.1 Glycosyl gold(III) iminophosphoranes

The azide sugar **45h** was reacted with **46** the same as for the other phosphines above. Monitoring of the reaction by ^{31}P NMR and ESI-MS showed that the intermediate mercurated iminophosphorane, **47h**, had fully formed after 1.5 hours. Removal of the solvent gave **47h** which could be used directly. The ion $[AuCl_4]^-$ has been used to produce gold(III) iminophosphoranes [27, 28, 50] as well as other gold(III) *C,N* compounds [53-55] by transmetalation. To **47h** was added $[NMe_4][AuCl_4]$ and dry acetonitrile and stirred for several days in the dark. $[NMe_4]Cl$ is sometimes added to transmetalations to speed up the reaction by forming the insoluble salt $[NMe_4][HgCl_3]$, this was tried for these reactions but no significant increase in yield or decrease in reaction time was seen. Monitoring by ESI-MS showed the slow disappearance of the mercurated sugar iminophosphorane and the appearance of the cyclometaled gold(III) compound. After removal of $HgCl_2$ by filtration, the solvent was removed under vacuum and recrystallisation of the residue with $CHCl_3$ and petroleum spirits gave yellow crystals of **48h**, Figure 4.13. While they were air and moisture stable, if left at room temperature after 1 month decomposition was seen to occur with the compounds turning purple because of the presence of colloidal elemental gold.

However if they were stored at -15 °C, they were stable for over a year. The other glycosyl azides **45i** and **45j** reacted the same way.

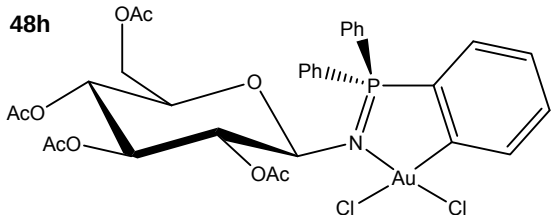

Figure 4.13 *The cyclometaled gold(III) sugar iminophosphorane **48h**.*

4.8.2 ESI-MS

ESI-MS of the compounds **48h-j** showed several consistent ions. The main ion was from the loss of a chloride to give $[M–Cl]^+$ with a less intense ion from $[M+Na]^+$. This is a different mode of ionisation from that seen for the intermediate **47**, which is seen while monitoring the reaction and forms the ion $[M+H]^+$. This difference is because of the availability of the nitrogen to be protonated, since mercury only weakly interacts with the nitrogen while gold forms a strong bond.

4.8.3 ^{31}P, ^{1}H and ^{13}C NMR

^{31}P NMR is a very useful tool and allows quick, direct and diagnostic detection of changes in the phosphorus environment. Figure 4.14 shows the clear changes in chemical shift of the series of iminophosphoranes using the sugar azide **45h**. With the free phosphine **46** the shift is 0.38 ppm. Upon reaction with the azide to form **47h** there is a clear shift downfield to 21.2 ppm. Once the compound has been cyclometaled and the phosphorus contained in a cyclic system, there is another large downfield shift to 60.3 ppm. This large downfield shift is a

diagnostic indication that the phosphorus is in a cyclic system [56]. For **46** and **47h** ^{199}Hg satellite peaks can be seen from $^{3}J_{Hg,P}$ coupling.

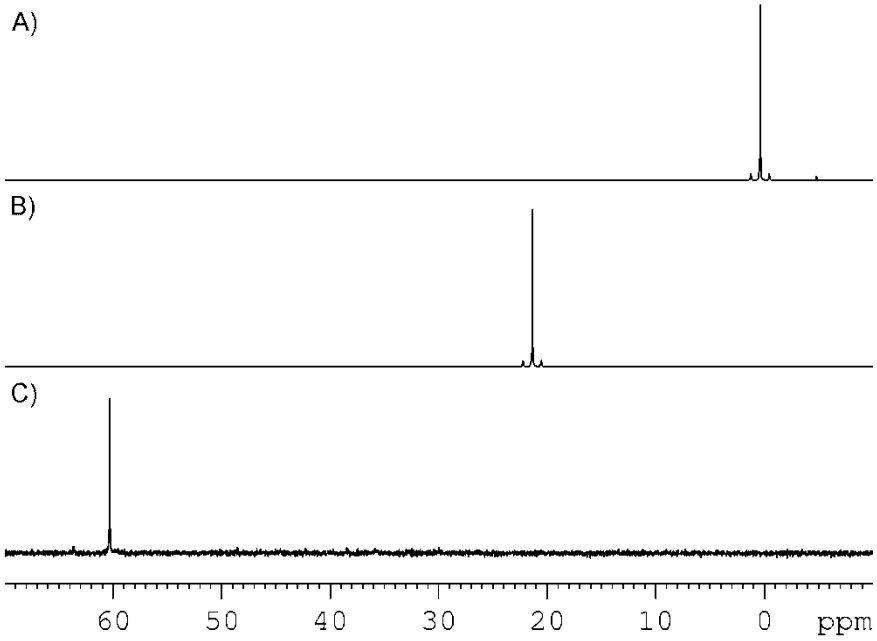

Figure 4.14 *^{31}P NMR spectra comparing the changes of chemical shift for; A) **46** B) **47h** C) **48h**.*

^{1}H NMR also has some diagnostic signals with the anomeric proton, H1. The changes in this signal can clearly indicate what is happening to the group attached to the anomeric carbon. Figure 4.15 shows a series of ^{1}H NMR spectra showing the change in the anomeric proton signal for galactose (**i**). For the fully acetylated sugar (A) it is at 5.65 ppm and the coupling constant (8.3 Hz) shows it is the β anomer. Once it has been brominated (B) the bromine has shifted the signal downfield to 6.69 ppm, and the coupling constant (4.0 Hz) shows the α anomer has formed. For the azide, **45i**, it has shifted upfield to 4.59 ppm and is back to the β anomer. In the gold(III) chloride iminophosphorane the normal doublet signal becomes a doublet of doublets at 6.21 ppm. This is due to the three bond coupling to the phosphorus atom and gives a $^{3}J_{H1,P}$ coupling constant of 18.1 Hz. The β anomer has been retained.

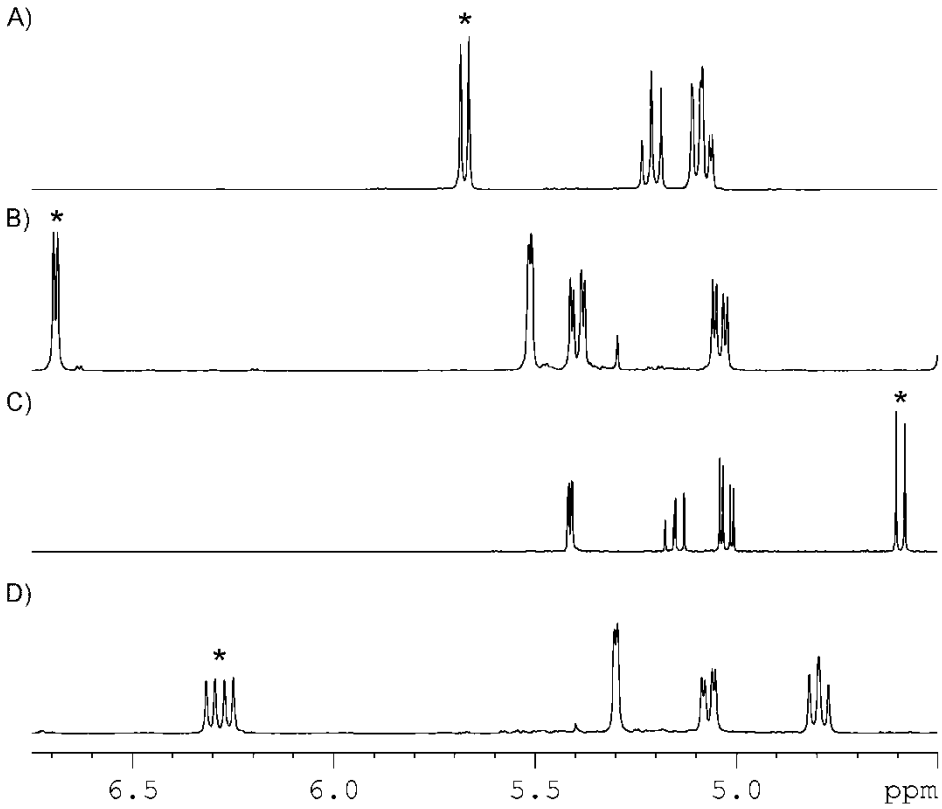

Figure 4.15 *^{1}H NMR spectra showing the change in the anomeric proton signal by comparing. A) R-OAc B) R-Br C) **45i** D) **48i**. R = Per-O-acetyl galacosyl. The anomer proton is marked with an asterisk.*

For the rest of the ^{1}H NMR spectrum the typical sugar signals are seen and could be easily assigned. The difference in the position of the hydroxyl group at C4 for glucose (**h**) and galactose (**i**), Figure 4.16, was easy to see in the ^{1}H NMR spectrum, Figure 4.17. H4 in glucose is in the axial position and has a vicinal angle of 180° with H3 and H5, while for galactose it is equatorial and the vicinal angle is 60°. This smaller angle leads to small coupling constants for H3, H4 and H5 which can be seen in Figure 4.17. This is also seen in the ^{1}H-^{1}H COSY with no cross peak seen between H4 and H5. The spectrum for **48j** was harder to interpret since H1 and H2 were very broad signals. **48j** also has an equatorial proton at C4 and small coupling constants were also seen.

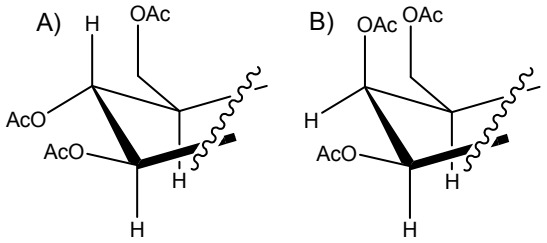

Figure 4.16 *Difference at C4 between; A) Glucose; B) Galactose.*

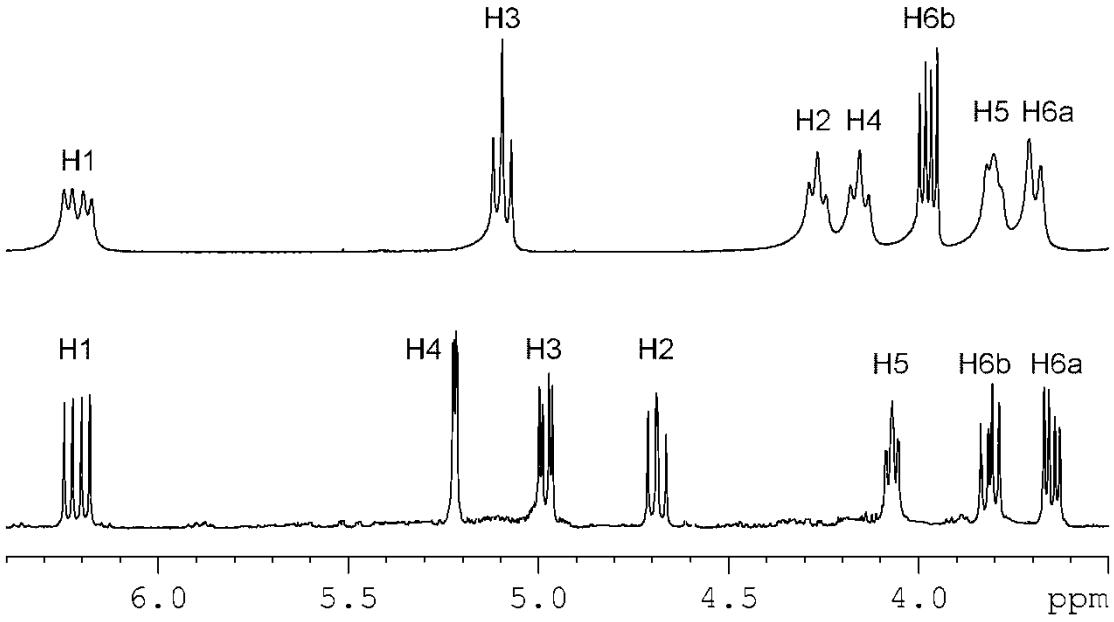

Figure 4.17 *Portion of the ^{1}H NMR spectrum comparing; A) **48h**; B) **48i**.*

The aromatic region in the ^{1}H NMR spectrum is difficult to interpret because of the number of slightly inequivalent protons leads to large amounts of overlapping signals and was not assigned.

In the ^{13}C NMR spectrum sugar signals were as expected; the anomeric carbon (C1) showed splitting from $^{2}J_{C,P}$ coupling of ~5 Hz. The aromatic region was complex with many slightly inequivalent carbon atoms as well as coupling to the phosphorus atom and this area was not assigned.

4.8.4 Crystal Structure of 48h and 48j

Recrystallisation of **48h** and **48j** with dichloromethane and hexane produced X-ray quality crystals. They both formed monoclinic crystals in the $P2_1$ space group. **48j** had two independent molecules in the unit cell, with two chloroform molecules and a hexane molecule in the lattice with disorder in one of the chloroform molecules. Appendix Two gives details of the structure solution. Figure 4.18 shows the geometry of **48h**, while Figure 4.19 shows **48j**. The final solution for **48j** contained a large residual peak close to the gold, caused by ripples from the gold atom.

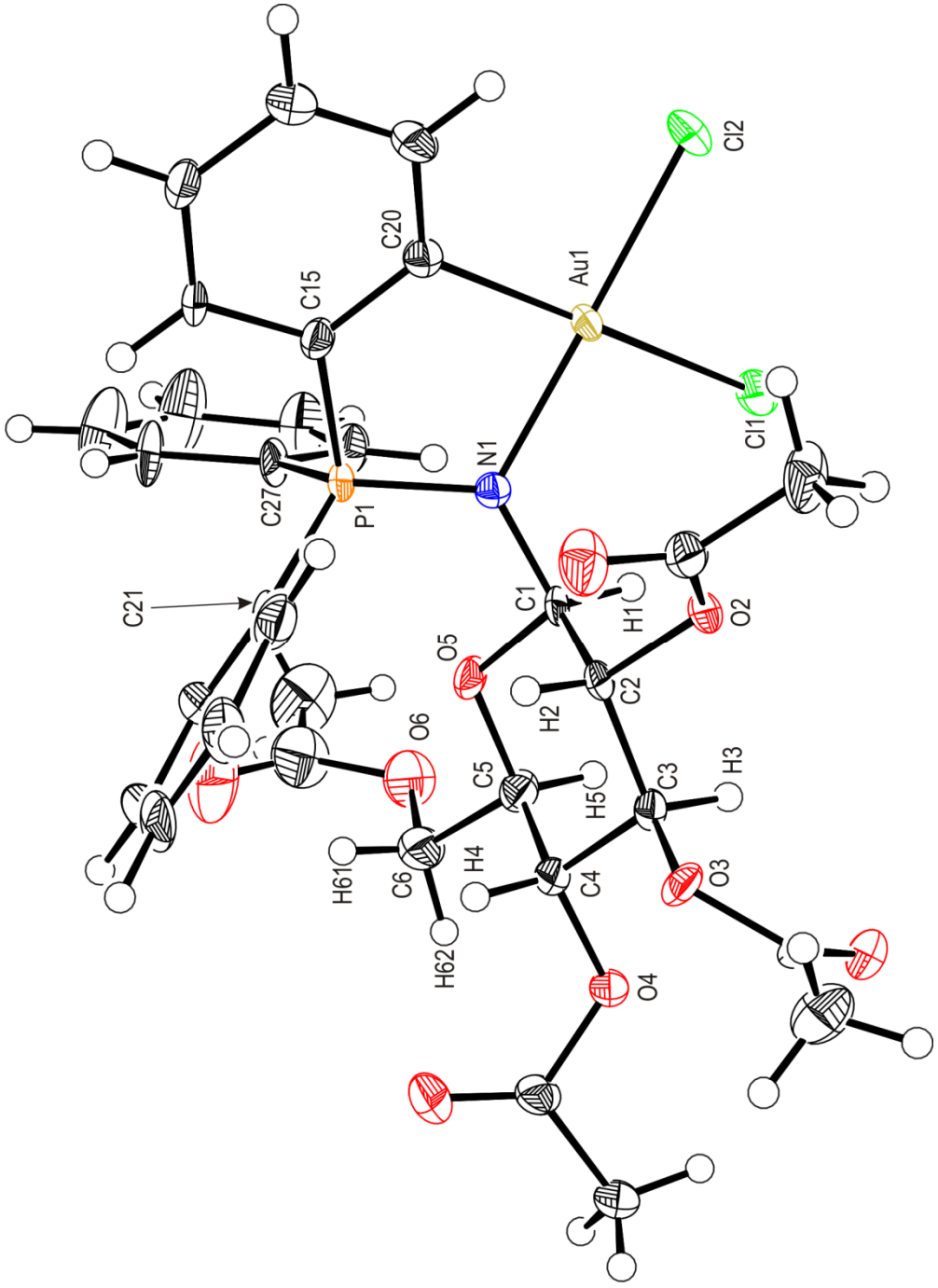

Figure 4.18 *The geometry of **48h** showing the atom labelling scheme and thermal ellipsoids at the 50% probability level.*

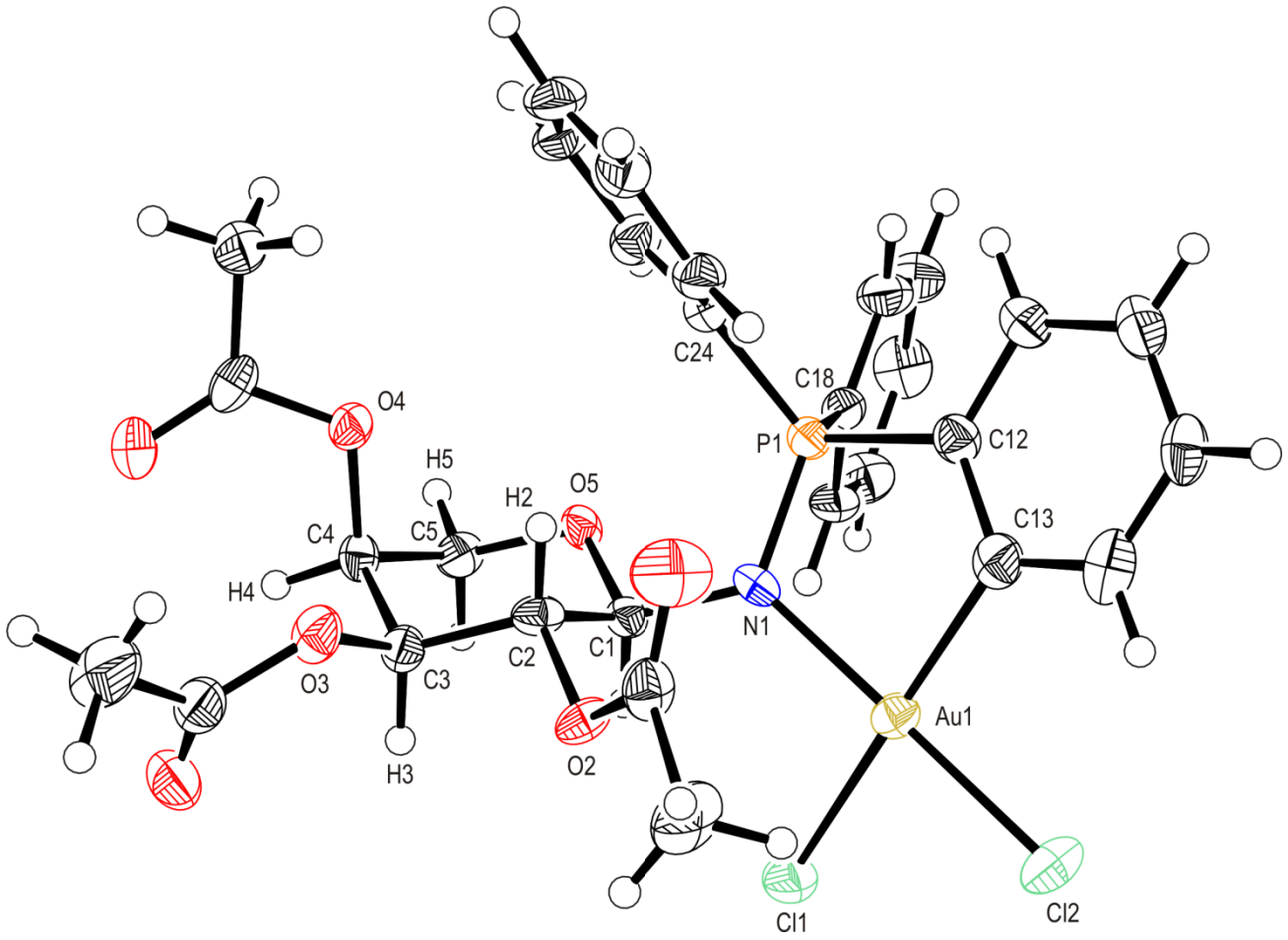

Figure 4.19 *The geometry of one of the independent molecules in the unit cell of **48j** showing the atom labelling scheme and thermal ellipsoids at the 50% probability level. Solvent molecules have been omitted for clarity.*

Table 4.2 shows selected bond lengths, bond angles and torsion angles for **48h** and **48j** and a comparison with **39h**. All the Au, C–N and N=P bond lengths are similar to those reported for **41** [27]. Both sugar portions of the molecules show the $^4C_1$ conformation. In comparison to the D-glucose structure the L-arabinose compound lacks the hydroxymethyl group on C5 and O4 is axial instead of equatorial. The acetylated hydroxylmethyl group of **48h** has the *gt* conformation. As a note, even though **48j** has the same configuration as the glucose version, it is assigned the α configuration since it is an L-sugar rather the β configuration for the D-sugar of **48h**. Despite the major change in the environment around the carbohydrate of **48j** compared to **48h** there are major similarities with the triphenylphosphine and metalocyclic rings essentially identical between the two compounds.

	39h	**48h**	**48j**	
			Molecule A	**Molecule B**
Au1–Cl1	NA	2.348(2)	2.377(2)	2.366(2)
Au1–Cl2	NA	2.272(2)	2.283(2)	2.274(3)
Au–C	NA	2.068(7)	2.043(10)	2.040(9)
Au–N1	NA	2.038(5)	2.026(8)	2.041(9)
C1–N1	2.272(2)	1.449(8)	1.421(11)	1.437(11)
N1–P1	1.5708(9)	1.612(6)	1.644(7)	1.608(8)
C–Au–N	NA	85.6(3)	85.6(3)	85.1(3)
C–N=P	120.8(1)	121.9(4)	121.1(6)	123.4(7)
P1=N1–C1–C2	176.8(1)	93.1(6)	94.9(8)	91.6(9)

Table 4.2 *Selected bond lengths (Å), bond angles (°) and torsion angles (°) for **39h**, **48h** and **48j**.*

In both compounds the gold(III) is square planar. If a plane is calculated through Au1, Cl1, Cl2, N1 and the metalated carbon, for **48h** the largest deviation is 0.065(3) Å for the metalated carbon, C20. For **48j** the largest deviations are also for the metalated carbon, C13, with 0.124(4)Å and 0.065(4)Å for molecule A and B respectively. The *trans* influence can be seen in the lengthening of the Au–Cl

bond *trans* to the carbon for **48h** (2.348(2) Å and 2.272(2) Å for Au1–Cl1 and Au1–Cl2 respectively), and this is also seen in **48j**.

Both metalocyclic rings show puckering with an envelope conformation with the nitrogen out of the plane. If a plane is defined by Au–C–C–P it is essential planar; for **48h** the largest deviation is 0.008(4) Å. The plane is slightly less planar for **48j** with the largest deviations being 0.068(6) Å and 0.062(6) Å for molecule A and B respectively. The nitrogen is displaced from the plane by 0.411(7) Å for **48h** while for **48j** it is 0.472(9) Å and 0.38(1) Å respectively. While there are examples of iminophosphoranes having a relatively flat metalocyclic ring, such as **40** [30], all reported Au(III) compounds give envelope conformations with large deviations for the nitrogen atom [27, 28].

The torsion angle of C2–C1–N1–P1 is 93.1(6)° for **48h**, while for molecule A and B of **48j** the angles are 94.9(8)° and 91.6(9)° respectively. For **39h** it is 176.8(1)° showing that the triphenylphosphine group has been twisted substantially which points the lone pair of electrons on the nitrogen away from the acetate group on C2 of the sugar and instead points them down. It can be assumed that this provides steric relief which allows the complex to form. It is unclear why this rotation could not happen in **39h** to allow direct metalation to occur if steric hindrance of the nitrogen prevents it from happening. Figure 4.20 shows this twisting with a comparison between **39h** and **83h**. This puts one of the phenyl rings above the carbohydrate ring. Despite having an axial acetate group at C4, **48j** has the phenyl ring in a similar position.

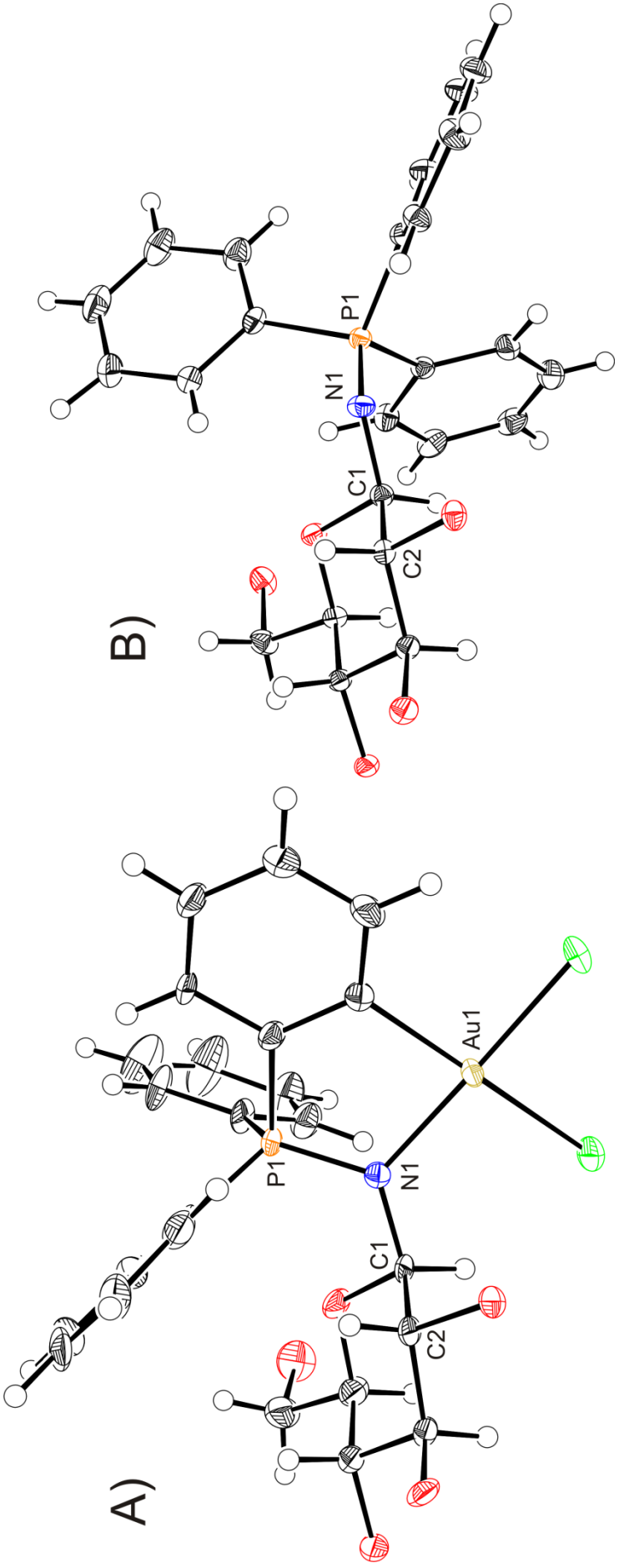

Figure 4.20 *Comparison of the torsion angle C2–C1–N1–P1, for* ***48h*** *(A) and* ***39h*** *(B), showing the twisting of the C1–N1 bond. Acetate groups have been omitted for clarity.*

The strength of the nitrogen bond to the gold can be seen by the lengthening of the N1–P1 and C1–N1 bond as electron density is removed from the nitrogen-phosphorus bond by the gold centre. For example if **39h** and **48h** are compared N1–P1 has increased to 1.612(6) Å from 1.5708(9) Å, while C1–N1 has increased to 2.348(2) Å from 2.272(2) Å). The C–N=P bond angle for **48h** is similar to **39h** showing little change upon cyclometalation.

The bite angle of C–Au–N is 85.6(3)° for **48h** and 85.6(3)° and 85.1(3)° for A and B of **48j**. This is comparable to known cyclometalated iminophosphoranes such as **40** (83.5(2)° [30]), **41** (84.9(2)° [27]) and **42** (85.45(10)° [32]).

4.8.5 Deviation of the nitrogen in the metalocyclic ring

Looking at the differences in the deviation of the nitrogen in the metalocyclic ring for the sugar iminophosphoranes with other complexes, it was wondered if any reason for the differences could be found and quantified. An obvious feature to look at is the size of the metal. A number of different cyclometalated compounds derived from **38** have been reported in the literature, and made a good basis for examining any trends. Table 4.3 summarises the nitrogen deviations for some reported complexes.

	Metal	Deviation of the nitrogen atom (Å)	Bite angle (°)
40 [30]	Mn(I)	0.166	83.5(2)
43 [33]	Rh(I)	0.247	84.90(9)
44 [33]	Ir(I)	0.268	84.77(19)
41 [27]	Au(III)	0.55	84.9(2)
42 [32]	Pd(II)	0.612	85.45(10)

Table 4.3 *Table of the nitrogen deviations for some of the C,N metalated compounds derived from **38**, and the bite angle.*

Even with a wide variety of different metals and ligands attached to them, the bite angle of the iminophosphorane is remarkably consistent at ~84°. This bite angle is also seen for iminophosphoranes with non-aromatic groups on the nitrogen such as the sugar compounds above or tertiary butyl examples [28]. If a different sized metal is inserted into the five-membered metalocyclic ring, the ring must deform to retain the same bite angle, and apparently the iminophosphorane prefers to push the nitrogen atom out of plane to do so. A search of the CCDC database for PPh_3 derived cylcometalated iminophosphoranes confirmed this with all examples where there was puckering of the five membered ring was from the displacement of the nitrogen atom. The relationship between the amount of deviation versus the size of the metal was investigated to quantify it. This was hampered by a lack of an appropriate measurement scale to relate the different metals, oxidation states and coordination geometries. Several different data sets of covalent radii [57, 58] were tried but no relationship could be found. Using ionic radii for the metals surprisingly gave a good fit (R factor of ~0.95) but this is likely a coincidence, and their use cannot be justified for these compounds. The size of the metal is likely to be a factor since a plot of deviation verses atomic number or mass number shows a rough correlation (R factor of ~0.753) but unfortunately the relationship could not be quantified.

4.8.6 Acetyl glucosamine acetamido iminophosphorane

The azide **45k** was reacted with **46** and $[NMe_4][AuCl_4]$. There are two potential binding modes for the acetamido group, as either a bidentate or tridentate ligand, Figure 4.21. The ligand $Me_2NCOCH_2NPPh_3$ shows the tridentate form of bonding with palladium [40], Figure 4.22. When the reaction mixture was analyzed by ESI-MS an ion was observed corresponding to the tridentate binding mode as $[M+Na]^+$. When the reaction was worked up the ^1H NMR spectrum showed a complex spectrum from which nothing could be determined. Upon standing the sample decomposed and so was not investigated further.

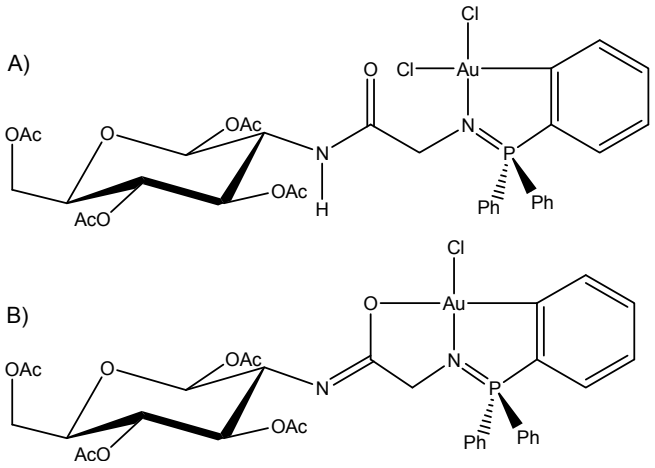

Figure 4.21 *The two forms of bonding the acetyl glucosamine acetamido iminophosphorane could have; A) Bidentate; B) Tridentate.*

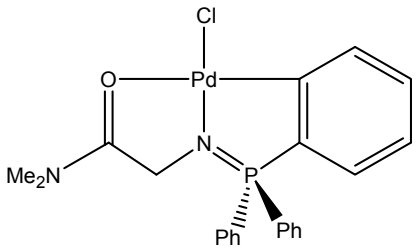

Figure 4.22 *Form of bonding seen for the metalated $RCOCH_2NPPh_3$ type iminophosphorane [40].*

4.8.7 Ethyl fructopyranoside iminophosphorane

The iminophosphorane derived from **45l** and PPh_3 was unstable to hydrolysis. It was thought that if the iminophosphorane was cyclometalated it might be more stable since the gold(III) would block access to the nitrogen. **45l** was reacted with **46** and $[NMe_4][AuCl_4]$ as above. ESI-MS showed ions that suggested the complex, **48l**, shown in Figure 4.23 had formed with ions tentatively assigned as $[M+Na]^+$, $[M+K]^+$ and $[M+NMe_4]^+$. The reaction mixture was worked up to give a yellow residue which decomposed forming colloidal gold and producing a gold mirror on an NMR tube. This showed that the ethylene spacer was still very susceptible to hydrolysis and was not investigated further.

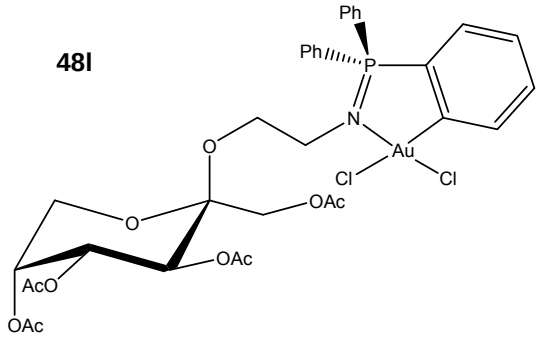

Figure 4.23 *Cyclometalated iminophosphorane observed in ESI-MS.*

4.9 Reactions at the Au(III) centre

For *C*,*N* cyclometalated gold(III) dichlorides, a variety of different ligands can displace the chlorides on the gold(III) atom. Three examples are looked at below.

4.9.1 Reaction with PPh_3

There are a large number of *C*,*N*-cyclometaled gold(III) dichloride compounds. An important property of these compounds is how strong the gold–nitrogen bond is. The strength can be gauged by the reaction with various reagents to see if a gold–chloride or the gold–nitrogen bond is broken; PPh_3 has been used to test this [59]. Scheme 4.17 shows the two possible pathways; either one of the chlorides is displaced to form a cation or the nitrogen is displaced to form a neutral compound. Previous work has shown that the gold–nitrogen bond in iminophosphoranes are very strong and resist displacement by PPh_3 [28]. It was not expected that the carbohydrate iminophosphoranes would be different.

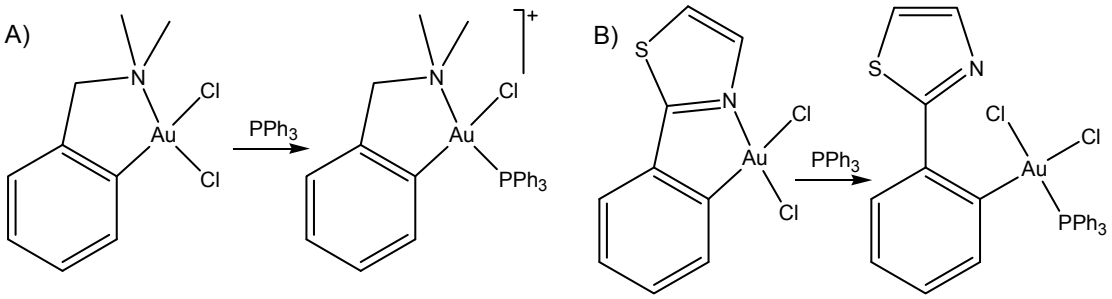

Scheme 4.17 *Two possible products of reacting a C,N-cyclometaled gold(III) dichloride with PPh_3; A) [53]; B) [60].*

48h was reacted with PPh_3 using the reported procedure [28], where the iminophosphorane, PPh_3 and NH_4PF_6 were stirred in CH_2Cl_2 to produce **49h**. Scheme 4.18 shows the two possible products. ESI-MS of the product showed a very intense ion corresponding to the cation in Scheme 4.18. If the cation had formed this would be expected since it wouldn't have to ionise in the machine to be seen and so would be easily observed.

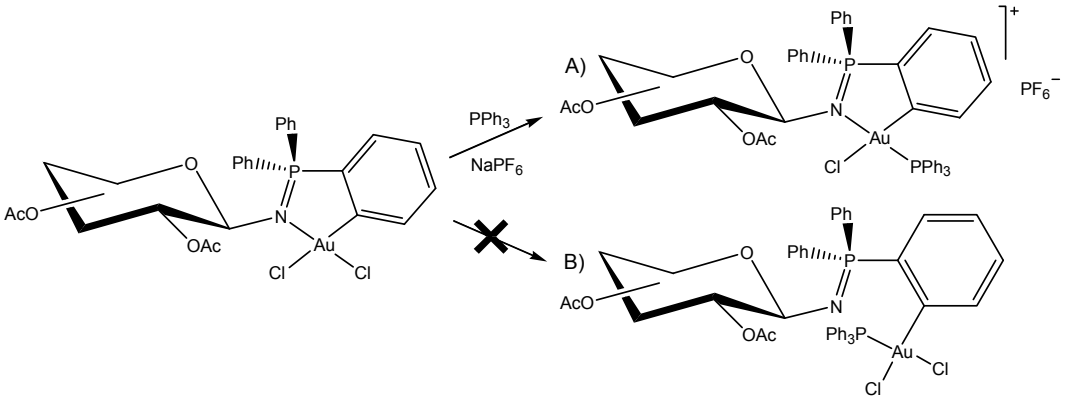

Scheme 4.18 *Reaction of gold(III) dichloride iminophosphoranes with PPh_3 showing the two possible reaction paths; A) PPh_3 displaces one of the chloride ligands; B) PPh_3 displaces the Au–N bond.*

While this was only moderate evidence for the cation formation, the ^{31}P NMR spectrum of **49h** was definitive. It showed two signals, one at 63.5 ppm from the iminophosphorane and one at 37.5 ppm from PPh_3, Figure 4.24. The high

downfield position of the iminophosphorane phosphorus indicated that it is still in a metalocyclic ring.

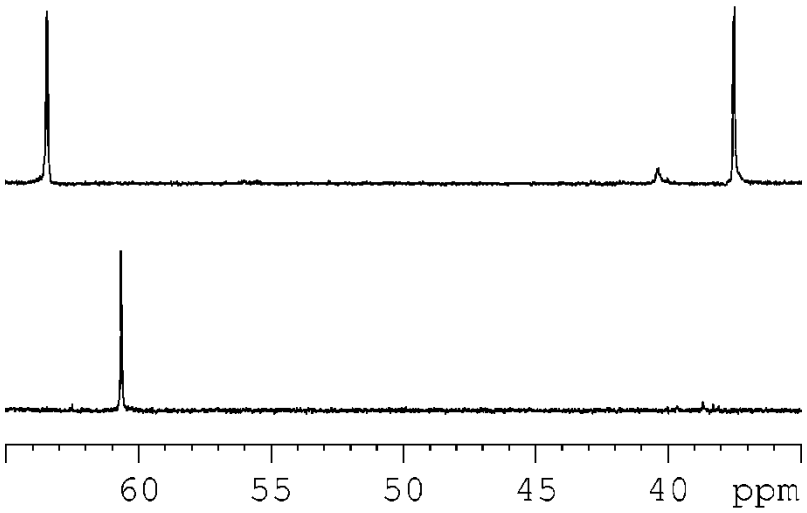

Figure 4.24 *^{31}P NMR spectrum comparing; A) **49h**; B) **48h**.*

The ^{1}H NMR spectrum showed large changes. The carbohydrate signals were very broad so the multiplicity was difficult to determine, and the anomeric proton had been shifted upfield 1.80 ppm. Figure 4.25 shows a comparison between the ^{1}H NMR spectra of **49h** and **48h**. In the ^{13}C NMR spectrum the anomeric carbon barely shifted, only moving 0.2 ppm downfield, it also no longer had any coupling to phosphorus. Interestingly C2 now showed ^{3}J coupling to the phosphorus (15.8 Hz for **49h**). The rest of the spectrum was similar to the dichloride.

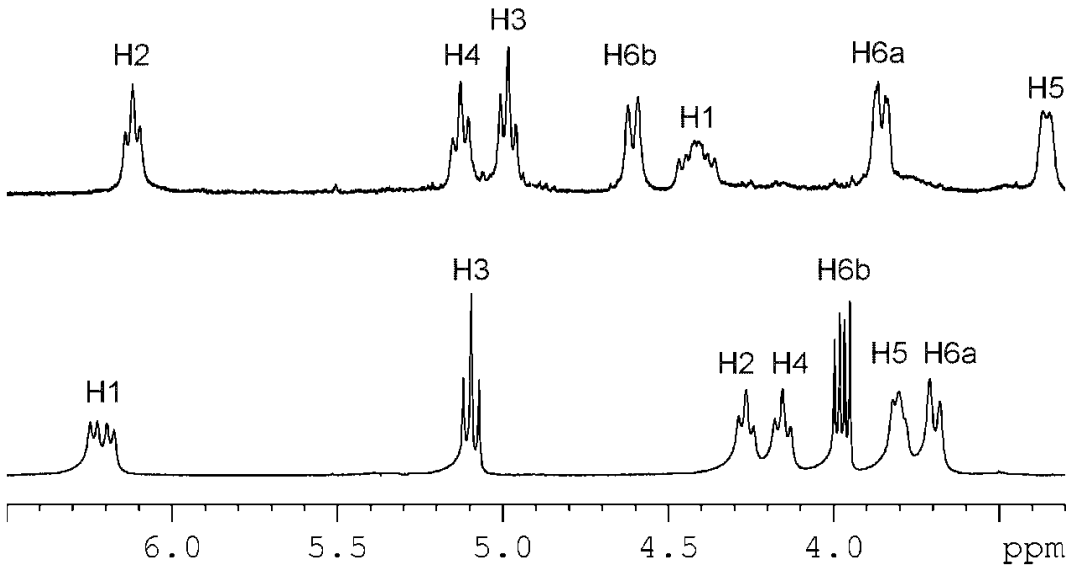

Figure 4.25 *Portion of the ^{1}H NMR spectrum comparing; A) **49h**; B) **48h**.*

Although crystals of X-ray quality could not be grown, it was assumed that the PPh_3 was *trans* to the nitrogen as in previous examples [28]. This is caused by antisymbiosis which is the preference for a hard donor ligand *trans* to a soft ligand on a soft metal [61]. Since ligands *trans* to each other compete for the same σ and π metal orbitals, having the phosphine and carbon *trans* to each other would destabilise the complex.

4.9.2 Reaction with thiosalicylic acid

There is interest in replacing the chlorides on *C,N* cycloaurated compounds with the dianionic thiosalicylate ligand to form a second six-membered chelate ring [62, 63]. This is because they show good anti-tumour effects [63], which are often greater than their parent dichlorides [28]. While this has been previously carried out in methanol with triethylamine [63], this was undesirable with the acetate protecting groups; therefore a different method was wanted. This reaction has also been carried out with Ag_2O in CH_2Cl_2 [62]. Since this involved no protic solvent it was the chosen method. The reaction with the gold dichlorides

went smoothly to give the products in high yields, Scheme 4.19. These products were also much more stable than the dichlorides with the thiosalicylic acid derivatives stable at room temperature for over a year. ESI-MS of the compounds only showed the ions $[M+H]^+$, $[M+Na]^+$ and $[M+K]^+$. This compares with the dichlorides which only showed a weak $[M+Na]^+$ peak; the thiosalicylate ligand provides additional ionisation sites.

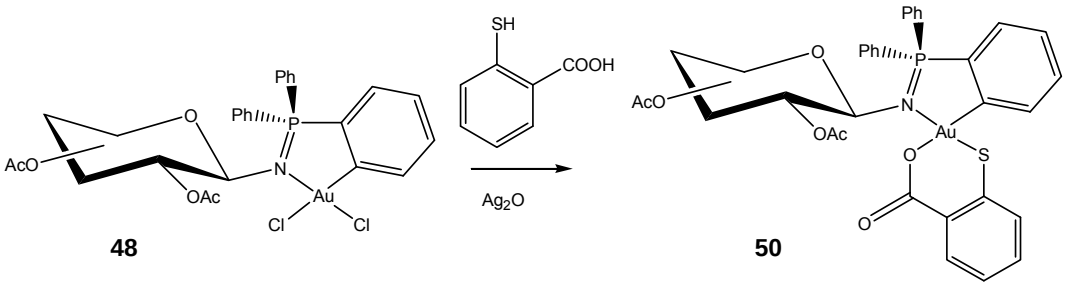

48 **50**

Scheme 4.19 *Reaction of gold(III) dichloride iminophosphoranes with thiosalicylic acid.*

The NMR spectra of the complexes were similar to the starting dichlorides. The main changes were the phosphorus and anomeric proton. The anomeric proton has shifted upfield as the new ligand changes the amount of electron density on the gold, Figure 4.26. The same effect is seen in the ^{31}P NMR, Figure 4.27, as the phosphorus signal for **50i** is 51.7 ppm compared to 60.3 ppm for **48i**. Similar shifts were seen for the other compounds. The anomeric carbon still showed coupling to phosphorus (6.1 Hz for **50i**)

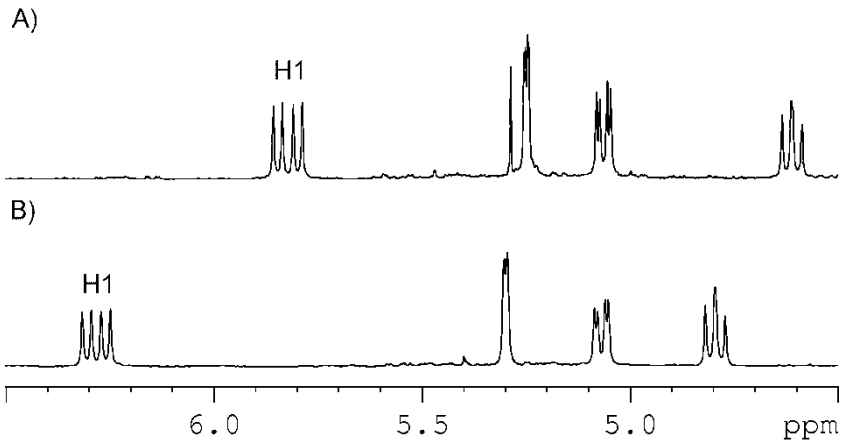

Figure 4.26 *Comparison of the anomeric proton of A)* ***50i****; B)* ***48i****.*

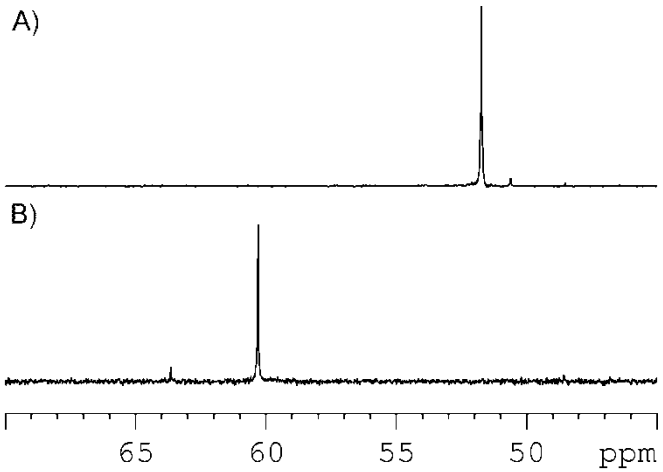

Figure 4.27 *Portion of the ^{31}P NMR spectrum comparing; A)* ***50i****; B)* ***48i****.*

Although crystals of X-ray quality could not be grown, it was assumed that the sulfur atom of the thiosalicylate was *trans* to the nitrogen for two reasons. Firstly because of antisymbiosis, and secondly the gold(III) iminophosphorane **51**, Figure 4.28, has had a structure determination that showed that configuration.

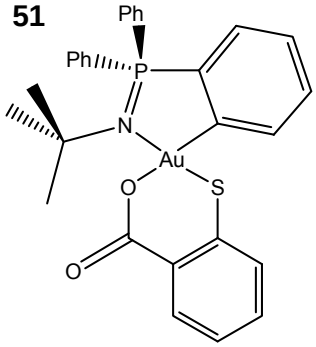

Figure 4.28 *Previous thiosalicylate complex of a gold(III) iminophosphorane showing the oxygen trans to the carbon [28].*

4.9.2.1 Biological activity

A number of gold(III) compounds have shown biological activity [59]. To see if the carbohydrate had any effect **48h** and its thiosalicylate derivative **50h** were tested for anti-tumor activity against a P388 Murine Leukaemia cell line (detailed in general procedures). Table 4.4 summarizes the IC_{50} values with a comparison to **41** and its thiosalicylate derivative **52**. **48h** was essentially inactive with an IC_{50} value of >62500 ng mL^{-1}. This is extremely poor compared to **41** with an activity of 7546 ng mL^{-1} [28]. **50h** had much better activity although less than **52**. This shows that replacing the substituent on the nitrogen atom with a carbohydrate moiety does not provide any extra activity to the iminophosphorane. It can also be seen that the derivatising the iminophosphorane with thiosalicylate does boost the activity significantly. This could be because the gold centre is now more protected than the dichloride.

	IC_{50} Values ng mL^{-1}
48h	>62500
50h	1665
41 [28]	7546
52 [28]	<487

Table 4.4 *Summary of anti-tumor activity of tested sugar gold(III) iminophosphoranes with IC_{50} values against P388 Murine Leukaemia cell line.*

4.9.3 Reaction with catechol

As well as displacement of the chlorides with thiosalicylate an analogous substitution can be carried out using catecholate to form a new five-membered chelate ring [28, 64]. When the carbohydrate gold(III) iminophosphoranes were stirred with catechol and AgO in CH_2Cl_2, Scheme 4.20, after 1 hour in the dark the yellow solution had turned a dark brown and no product could be isolated or seen in the ESI-MS of the mixture. Since catechol is a reducing agent, it is likely that it is reducing the silver producing the dark brown product.

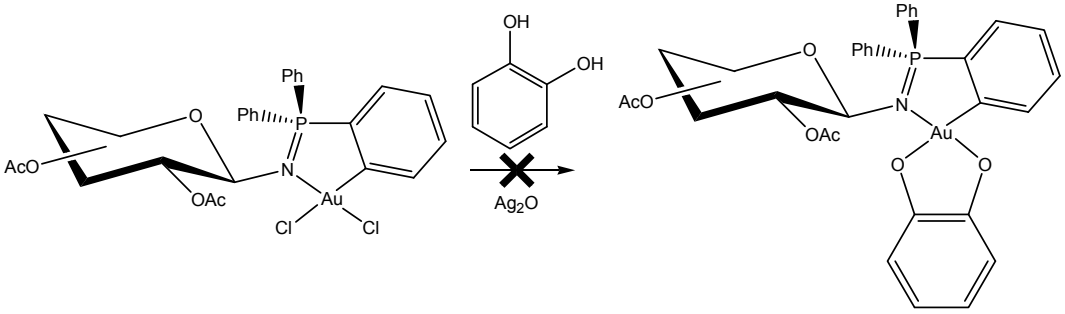

Scheme 4.20 *Attempt to make catechol derivatives.*

4.10 Conclusion

The reaction of acetylated sugar azides proceeded smoothly with PPh_3 to produce iminophosphoranes. All attempts at direct metalation of the

iminophosphoranes failed and was thought to be because of steric crowding of the nitrogen atom. The premetalation of PPh_3 with mercury gave access to C,N cycloaurated iminophosphoranes via transmetalation with $[Me_4N][AuCl_4]$. The reaction worked with different acetylated glycosyl sugars and it should be possible to extend this reaction to the wide range of glycosyl sugars available. Two other sugar azides were investigated but the gold complexes derived from them proved to be very unstable.

^{31}P NMR was an excellent tool for tracking the changes in the iminophosphorane environment with a chemical shift of ~60 ppm observed when the iminophosphorane was in a five-membered metalocyclic ring, compared with ~20 ppm in the iminophosphorane. The anomeric proton of the sugar also showed changes for the different products formed.

A number of reactions could occur at the gold atom. PPh_3 readily displaces one of the chlorides to form a cation. This shows the strength of the Au–N bond that forms. The reaction with thiosalicylic acid to form a new six-membered ring goes smoothly while the catechol derivative could not be made via the AgO method.

4.11 Experimental

General procedures

General experimental procedures are in Appendix One. X-ray crystallography is detailed in Appendix Two. 2′-Chloroethyl 1,3,4,5-tetra-*O*-acetyl-β-D-fructopyranoside [45], 2-$LiC_6H_4PPh_2$ [51] and $Hg(2\text{-}C_6H_4PPh_2)_2$ [52] were made by literature procedures. Anti-tumour assays were carried out at the University of Canterbury using previously described methods [65].

Table 4.5 *Summary of the crystallographic data for the structures in Chapter Four.*

	39h	**48h**	**48j**
Molecular formula	$C_{32}H_{34}NO_9P$	$C_{32}H_{33}NO_9PCl_2Au{\cdot}2CH_2Cl_2$	$2(C_{29}H_{29}NO_7PCl_2Au).2CHCl_3.C_6H_{14}$
Lattice	Monoclinic	Monoclinic	Monoclinic
Space group	$P2_1$	$P2_1$	$P2_1$
Z	2	2	2
a (Å)	8.6161(8)	9.1905(2)	13.4315(5)
b (Å)	9.9944(10)	12.6953(3)	13.4103(4)
c (Å)	18.1458(18)	17.4863(4)	20.9413(7)
α (°)	90	90	90
β (°)	90.705(1)	99.4860(10)	90.785(2)
γ (°)	90	90	90
Unit cell volume ($Å^3$)	1562.6(3)	2012.34(8)	3771.6(2)
Calculated density (g cm^{-3})	1.291	1.723	1.699
θ range (°)	2.62 to 34.88	1.99 to 28.01	2.15 to 30.65
Reflections collected, unique	32712, 12241	32579, 9497	101907, 23064
R(int)	0.0306	0.0286	0.0580
Data, restraints, parameters	12241, 1, 524	9497, 7, 471	23064, 12, 858
Goodness-of-fit on F^2	1.031	1.134	1.035
Final R indices [I>2σ(I)]; R1, wR2	0.0353, 0.0852	0.0394, 0.1044	0.0594, 0.1504
R indices (all data); R1, wR2	0.0426, 0.0901	0.0409, 0.1049	0.0862, 0.1675
Largest diff. peak and hole (e $Å^{-3}$)	0.415 and -0.220	2.272 and -2.918	8.942 and -2.740
Flack parameter	0.02(4)	0.053(7)	-0.011(7)

General procedure for acetylation of glucosyl sugars

The compounds were synthesized by literature methods with slight modifications [36, 37]. The sugar was suspended in acetic anhydride (1.2 M excess) and a catalytic amount of I_2 (0.2 mmol) was added and the suspension stirred for 18 hours. CH_2Cl_2 was added, washed with sodium thiosulphate, water (×3), saturated $NaHCO_3$, dried ($MgSO_4$) and evaporated under reduced pressure. The product was used without further purification.

General procedure for bromination of glucosyl sugars

The compounds were synthesized by literature methods with slight modifications [39]. The crystalline per-acetylated sugars were directly added to a solution of HBr in acetic acid (30% w/v, 1.2 M excess). Per-*O*-acetylated sugars that formed syrups were first dissolved in the minimum amount of CH_2Cl_2 to help dissolution of the starting material before addition of HBr. The solution was stirred for 2 hours. CH_2Cl_2 was added, washed with water (×3) saturated $NaHCO_3$ solution (×1), dried ($MgSO_4$) and evaporated under reduced pressure. The product was used without further purification.

General procedure for 1,2-trans-per-O-acetyl-β-glycosyl azides

The compounds were synthesized by literature methods with slight modifications [39]. Glycosyl bromide was dissolved in acetone (10 mL per 1 mmol). Sodium azide (1.2 M excess) was dissolved in water (5 mL) and added to the acetone solution and stirred for 2 hours. The solvent was removed under reduced pressure and the residue taken up in dichloromethane, washed with water (×3), dried ($MgSO_4$) and evaporated under reduced pressure. The residue was recrystallised from hot ethanol to give the crystalline azides.

45k

7 (2.00 g, 5.76 mmol) was dissolved in acetone (25 mL) with 2,6-lutidine (1.3 mL, 11.5 mmol, 2 M excess). The solution was cooled in an ice-bath and bromo acetyl bromide (0.50 mL, 5.76 mmol) was added and stirred for 1 hour with a white precipitate forming immediately. The solution was allowed to warm to room temperature and sodium azide (0.41 g, 6.34 mmol, 1.1 M excess) and water (5 mL) added and left to stir for 16 hours. Solvent was removed under vacuum and the residue suspended in CH_2Cl_2 (15 mL) and washed with water (20 mL), HCl (2M, 20 mL) and water (20 mL), dried ($MgSO_4$), filtered and the solvent removed under vacuum. The residue was recrystallised from hot ethanol to give a white powder of **45k** (1.92 g, 78.2%).

^{1}H NMR: δ 6.45 (d, 1H, $J_{NH,H2}$ 9.4 Hz, NH) 5.79 (d, 1H, $J_{H1,H2}$ 8.7 Hz, H1), 5.25 (dd, 1H, $J_{H3,H4}$ 9.3 Hz, $J_{H2,H3}$ 10.5 Hz, H3), 5.14 (t, 1H, H4), 4.28 (dd, 1H, $J_{H5,H6b}$ 4.7 Hz, $J_{H6a,H6b}$ 12.5, H6b), 4.23 (m, 1H, H2), 4.13 (dd, 1H, $J_{H5,H6a}$ 2.4 Hz, $J_{H6a,H6b}$ 12.5 Hz, H6a), 3.91 (s, 2H, CH_2N_3), 3.84 (ddd, 1H, $J_{H5,H6a}$ 2.4 Hz, $J_{H5,H6b}$ 4.7 Hz, $J_{H4,H5}$ 9.8 Hz, H5), 2.11, 2.09, 2.05, 2.04 (4s, 12H, 4 × OAc) ppm. ^{13}C NMR: δ 171.1, 170.8, 169.5, 169.4 (4 × C=O, acetyl), 167.2 (C=O, amide), 92.4 (C1), 73.1 (C5), 72.3 (C3), 67.9 (C4), 61.8 (C6), 53.4 (C2), 52.8 (CH_2N_3), 20.0, 20.9, 20.7 × 2 (4 × CH_3) ppm.

45l

45l was made according to literature procedures [45]. 2′-Chloroethyl 1,3,4,5-tetra-*O*-acetyl-β-D-fructopyranoside (2.00 g, 4.87 mmol) and NaN_3 (1.90 g, 29.2 mmol, 6 M excess) were heated in DMF at 90°C with stirring for 18 hours. Water (40 mL) was added and extracted with Et_2O (3 × 25 mL), the organic fractions were combined, dried ($MgSO_4$), filtered and the solvent removed under reduced pressure to give **45l** (1.47 g, 72.3%)

^{1}H NMR: δ 5.51 (d, 1H, $J_{H3,H4}$ 10.2 Hz, H3), 5.38 (m, 1H, H5), 5.35 (dd, 1H, $J_{H5,H6}$ 3.3 Hz, $J_{H3,H4}$ 10.2 Hz, H4), 4.30 (d, 1H, $J_{H1a,H1b}$ 12 Hz ,H1a), 4.10 (d, 1H, $J_{1a,1b}$ 12 Hz ,H1b), 3.97 (dd, 1H, $J_{5,6}$ 1.3 Hz, $J_{H6ax,H6eq}$ 13 Hz, H6), 3.83 (dd, 1H, $J_{H5,H6}$ 1.7 Hz, $J_{H6ax,H6eq}$ 13 Hz, H6), 3.70 (m, 2H, O-C**H$_2$**-CH$_2$-N), 3.45 (m, 2H, O-CH$_2$-C**H$_2$**-N), 2.16, 2.10, 2.05, 1.98 (4s, 12H, 4 × OAc) ppm. ^{13}C NMR: δ 170.6 (C=O), 170.4 (C=O), 170.3 (C=O), 99.0 (C2), 68.9 (C4), 68.3 (C5), 67.6 (C3), 62.8 (C1), 62.1 (C6), 61.2 (**C**H$_2$-CH$_2$-N), 50.6 (CH$_2$-**C**H$_2$-N), 21.0, 20.7, 20.7, 20.6 (4 × CH$_3$) ppm.

39h

45h (200 mg, 0.536 mmol) and PPh_3 (140.5 mg, 0.536 mmol) were dissolved in dry CH_2Cl_2 (15 mL) under nitrogen and stirred for 1.5 hours. Removal of the solvent gave **39h** (322.4 mg, 99 %) which was used for reactions without further purification. Crystals suitable for X-ray diffraction were grown by cooling a CH_2Cl_2/hexane solution of **39h**.

^{1}H NMR: δ 7.67 -7.10 (m, 15H, arom.), 5.93 (dd, 1H, $J_{H1,H2}$ 8.4 Hz, $J_{H1,P}$ 19.6 Hz, H1) 5.08 (t, 1H, H3), 4.25 (t, 1H, H2), 4.16 (t, 1H, H4), 3.99 (dd, 1H, $J_{H5,H6b}$ 6.3 Hz $J_{H6a,H6b}$ 12.2 Hz, H6b), 3.80 (bm, 1H, H5), 3.70 (bm, 1H, H6a), 2.19, 2.17, 1.93, 1.86 (s, 12H, 4 × OAc) ppm. ^{13}C NMR: δ 170.5, 170.2, 169.6, 169.5 (C=O), 88.5 (d, $J_{C1,P}$ 5.8 Hz, C1), 74.7 (C5), 72.1 (C2), 72.6 (C3), 68.4 (C4), 62.2 (C6), 21.4, 20.9, 20.5 × 2 (4 × CH$_3$) ppm. ^{31}P{H} NMR: δ 21.1 ppm. MS: *m/z:*

39k

39k was made using the same method as **39h**. **45k** (100 mg, 0.232 mmol) and PPh_3 (60.9 mg, 0.232 mmol) worked up to give **39k** (152.7 mg, 99 %) which was used for reactions without further purification.

^{1}H NMR: δ 8.23 (b, 1H, NH), 7.61-7.44 (m, 15H, Ar), 5.75 (d, 1H, $J_{H1,H2}$ 8.8 Hz, H1), 2.29 (dd, 1H, $J_{H3,H4}$ 9.2 Hz, $J_{H2,H3}$ 10.6 Hz, H3), 5.14 (t, 1H, H4), 4.31 (b, 1H,

H2), 4.28 (dd, 1H, $J_{H5,H6b}$ 4.6 Hz, $J_{H6a,H6b}$ 12.4, H6b), 4.13 (dd, 1H, $J_{H5,H6a}$ 2.3 Hz, $J_{H6a,H6b}$ 12.4 Hz, H6a), 3.67 (d, 1H, $J_{H,P}$ 12.0 Hz, C*H*H'N_3), 3.66 (d, 1H, $J_{H,P}$ 13.2 Hz, CH*H'*N_3), 3.85 (ddd, 1H, $J_{H5,H6a}$ 2.3 Hz, $J_{H5,H6b}$ 4.5 Hz, $J_{H4,H5}$ 9.9 Hz, H5), 2.09, 2.07, 2.02, 1.93 (4s, 12H, 4 × OAc) ppm. ^{13}C NMR: δ 175.8 (d, $J_{C,P}$ 24.8 Hz, C=O, amide), 170.9, 170.6, 169.5, 169.5 (4 × C=O, acetyl), 132.5 (d, $J_{C,P}$ 9.3 Hz, Cb), 131.9 (d, $J_{C,P}$ 2.8 Hz, Ca), 130.6 (d, $J_{C,P}$ 97.4 Hz, Cd), 128.8 (d, $J_{C,P}$ 11.6 Hz, Cc), 93.0 (C1), 73.0 (C5), 72.6 (C3), 68.3 (C4), 61.9 (C6), 52.5 (C2), 49.3 (d, $J_{C,P}$ 3.5 Hz, CH_2N=P), 21.2, 20.9, 20.8 × 2 (4 × CH_3) ppm. ^{31}P{H} NMR: δ 23.6 ppm.

48h

45h (200 mg, 0.536 mmol) and **46** (193.8 mg, 0.268 mmol) were dissolved in dry CH_2Cl_2 (15 mL) under N_2 and stirred for 2 hours, solvent was removed under vacuum and [NMe_4][$AuCl_4$] (221 mg, 0.536 mmol) was added and the solids dissolved in dry acetonitrile (15 mL) and left to stir under N_2 and protected from light for 3 days. Solvent was removed under vacuum and the residue dissolved in CH_2Cl_2 and filtered through Celite. Addition of petroleum spirits and cooling to -15°C gave yellow crystals of **48h** (397 mg, 88.3%). Crystals suitable for X-ray diffraction were grown by cooling a CH_2Cl_2/hexane solution of **48h**.

^{1}H NMR: δ 8.16-7.10 (m, 14H, arom.), 6.21 (dd, 1H, $J_{H1,H2}$ 8.7 Hz, $J_{H1,P}$ 20.4 Hz, H1) 5.09 (t, 1H, H3), 4.27 (t, 1H, H2), 4.16 (t, 1H, H4), 3.98 (dd, 1H, $J_{H5,H6b}$ 6.3 Hz $J_{H6a,H6b}$ 12.2 Hz, H6b), 3.80 (bm, 1H, H5), 3.70 (bm, 1H, H6a), 2.17, 1.93 × 2, 1.86 (s, 12H, 4 × OAc) ppm. ^{13}C NMR: δ 170.4, 170.2, 169.6 × 2 (C=O), 86.9 (d, $J_{C1,P}$ 5.6 Hz, C1), 74.8 (C5), 72.9 (C2), 72.6 (C3), 68.4 (C4), 62.3 (C6), 21.3, 20.9, 20.6 × 2 (4 × CH_3) ppm. ^{31}P{H} NMR: δ 61.6 ppm. *Anal.* Calcd for $C_{32}H_{33}NO_9PCl_2Au$ (874.452): C, 43.95; H, 3.80; N, 1.60. Found: C, 44.07; H, 3.80; N, 1.70. MS: *m/z*: 838.122 (strong, $[M–Cl]^+$, calc. 838.124), 896.086 (weak, $[M+Na]^+$, calc. 896.083), 947.193 (weak, $[M+NMe_4]^+$, calc. 947.191).

48i

48i was made using the same method as **48h**, with **45i** (200 mg, 0.536 mmol), **46** (193.8 mg, 0.268 mmol) and $[NMe_4][AuCl_4]$ (221 mg, 0.536 mmol). Worked up to give **48i** (378 mg, 80.7%).

^{1}H NMR: δ 8.12 (m, 1H, arom.), 8.00-7.21 (m, 12H, arom.), 7.05 (m, 1H, arom.), 6.21 (dd, 1H, $J_{H1,H2}$ 8.8 Hz, $J_{H1,P}$ 18.2 Hz, H1) 5.22 (dd, 1H, $J_{H4,H5}$ 1.4 Hz, $J_{H3,H4}$ 3.4 Hz, H4), 4.98 (dd, 1H, $J_{H3,H4}$ 3.4 Hz, $J_{H2,H3}$ 10.5 Hz, H3), 4.69 (dd, 1H, $J_{H1,H2}$ 8.8 Hz, $J_{H2,H3}$ 10.5 Hz, H2), 4.06 (m, 1H, H5), 3.81 (dd, 1H, $J_{H5,H6b}$ 7.5 Hz $J_{H6a,H6b}$ 11.4 Hz, H6b), 3.65 (dd, 1H, $J_{H5,H6a}$ 5.2 Hz, $J_{H6a,H6b}$ 11.4 Hz, H6a), 2.24, 1.90, 1.87, 1.69 (s, 12H, 4 × OAc) ppm. ^{13}C NMR: δ 170.8, 170.4, 169.9, 169.7 (C=O), 86.9 (d, $J_{C1,P}$ 4.9 Hz, C1), 74.2 (C5), 70.7 (C3), 70.5 (C2), 67.3 (C4), 61.4 (C6), 21.6, 20.8, 20.7, 20.6 (4 × CH_3) ppm. ^{31}P{H} NMR: δ 60.3 ppm. *Anal.* Calcd for $C_{32}H_{33}NO_9PCl_2Au$ (874.452): C, 43.95; H, 3.80; N, 1.60. Found: C, 44.10; H, 3.85; N, 1.84. MS: *m/z*: 838.123 (strong, $[M–Cl]^+$, calc. 838.124), 896.083 (weak, $[M+Na]^+$, calc. 896.083), 947.187 (weak, $[M+NMe_4]^+$, calc. 947.191).

48j

48j was made using the same method as **48h**, with **45j** (200 mg, 0.664 mmol), **46** (240 mg, 0.332 mmol) and $[NMe_4][AuCl_4]$ (274 mg, 0.664 mmol). Worked up to give **48j** (456 mg, 85.6 %).

^{1}H NMR: δ 8.15 (m, 1H, arom.), 7.99-7.54 (m, 9H, arom.), 7.42-7.25 (m, 3H, arom.), 7.04 (m, 1H, arom.), 6.06 (b, 1H, H1) 5.13 (dd, 1H, $J_{H4,H5}$ 1.7 Hz, $J_{H3,H4}$ 3.5 Hz, H4), 4.96 (dd, 1H, $J_{H3,H4}$ 3.5 Hz, $J_{H2,H3}$ 10.3 Hz, H3), 4.73 (b, 1H, H2), 3.76 (mm, 2H, H5a, H5b), 2.20, 1.89, 1.72 (s, 9H, 3 × OAc) ppm. ^{13}C NMR: δ 170.3, 170.1, 169.5 (C=O), 88.7 (d, $J_{C1,P}$ 5.2 Hz, C1), 70.4 (C3), 68.7 (C2), 67.7 (C4), 65.9 (C5), 21.0, 20.8, 20.7 (3 × CH_3) ppm. ^{31}P{H} NMR: δ 60.6 ppm. *Anal.* Calcd for $C_{29}H_{29}NO_7PCl_2Au$ (802.389): C, 43.41; H, 3.64; N, 1.75. Found: C, 43.63; H, 3.91;

N, 1.83. MS: *m/z*: 766.106 (strong, $[M - Cl]^+$, calc. 766.103), 1569.178 (weak, $[2M - Cl]^+$, calc. 1569.174).

49h

48h (50 mg, 0.0572 mmol), PPh_3 (15.0 mg, 0.0572 mmol) and $[NH_4][PF_6]$ (9.3 mg, 0.0572 mmol) were suspended in dry CH_2Cl_2 (10 mL) under N_2 and stirred for 4 hours. The suspension was filtered through Celite and the addition of petroleum spirits gave **49h** (47.4 mg, 66.5%).

^{1}H NMR: δ 8.28 (m 1H, arom.), 7.95-7.21 (m, 26H, arom.), 6.82 (m 1H, arom.), 6.66 (m 1H, arom.), 6.12 (t, 1H, H2), 5.13 (t, 1H, H4), 4.99 (t, 1H, H3), 4.61 (bd, 1H, H6b), 4.12 (m, 1H, H1), 3.85 (bd, 1H, H6a), 3.3.36 (bm, 1H, H5), 1.97, 1.94, 1.89, 1.77 (s, 12H, 4 × OAc) ppm. ^{13}C NMR: δ 170.6 × 2, 170.3, 169.3 (C=O), 87.1 (C1), 73.2 (C5), 72.9 (C3), 72.4 (C2), 68.5 (C4), 61.2 (C6), 21.0, 20.8, 20.7, 20.6 (4 × CH_3) ppm. ^{31}P{H} NMR: δ 63.5, 37.5 (PPh_3) ppm. *Anal.* Calcd for $C_{50}H_{48}NO_9F_6P_3ClAu$ (1246.249): C, 48.19; H, 3.88; N, 1.12. Found: C, 48.29; H, 3.91; N, 1.26. MS: *m/z:* MS: *m/z*: 1101.288 (strong, $[M–PF_6]^+$, calc. 1101.284).

50h

48h (50 mg, 0.057 mmol) and thiosalicylic acid (8.8 mg, 0.057 mmol) were dissolved in CH_2Cl_2 (10 mL). Ag_2O (67.2 mg, 0.29 mmol) was added and the suspension stirred for 1 hour protected from light. The suspension was filtered through Celite and the solvent removed under vacuum. The residue was recrystallized from $CHCl_3$ and petroleum spirits to give **50h** (48.0 mg, 88.2%).

^{1}H NMR: δ 8.16-7.20 (m, 18H, arom.), 5.78 (dd, 1H, $J_{1,2}$ 8.7 Hz, $J_{1,P}$ 21.2 Hz, H1), 5.13 (t, 1H, H3), 4.25 (m, 1H, H4), 4.17 (m, 1H, H2), 3.98 (m, 1H, H6b), 3.92 (m, 1H, H5), 3.68 (dd, 1H, H6a), 1.95, 1.93, 1.81, 1.57 (4s, 12H, 4 × OAc) ppm. ^{13}C NMR: δ 170.3, 170.2, 169.8, 169.7 (C=O), 169.5 (C=O, thiosalicylic), 83.8

(d, $J_{C1,P}$ 6.5 Hz, C1), 74.6 (C5), 73.1 (C2), 72.8 (C3), 68.4 (C4), 62.4 (C6), 20.9, 20.7, 20.7, 20.3 (4 × CH_3) ppm. $^{31}P\{H\}$ NMR: δ 52.8 ppm. *Anal.* Calcd for $C_{39}H_{37}NO_{11}PSAu$ (955.72): C, 49.01; H, 3.90; N, 1.47. Found: C, 49.04; H, 4.24; N, 1.53. MS: *m/z:* 978.141 (strong, $[M + Na]^+$, calc 978.138), 956.159 (weak, $[M + H]^+$, calc 956.156), 1933.289 (weak, $[2M + Na]^+$, calc 1933.287).

50i

50i was made using the same method as **50h**, with **48i** (50 mg, 0.057 mmol), thiosalicylic acid (8.8 mg, 0.057 mmol) and Ag_2O 67.2mg, 0.29 mmol) in CH_2Cl_2 (10 mL). Worked up to give **50i** (50.4 mg, 92.5%).

^1H NMR: δ 8.16 (m, 1H, arom.), 8.06-7.05 (m, 17H, arom.), 5.82 (dd, 1H, $J_{H1,H2}$ 8.6 Hz, $J_{1,P}$ 19.1 Hz, H1), 5.25 (dd, 1H, $J_{H4,H5}$ 1.4 Hz, $J_{H3,H4}$ 3.4 Hz, H4), 5.06 (dd, 1H, $J_{H3,H4}$ 3.4 Hz, $J_{H2,H3}$ 10.4 Hz, H3), 4.61 (dd, 1H, $J_{H1,H2}$ 8.6 Hz, $J_{H2,H3}$ 10.4 Hz, H2), 4.23 (ddd, 1H, $J_{H4,H5}$ 1.4 Hz, $J_{H5,H6b}$ 4.9 Hz, $J_{H5,H6a}$ 7.6 Hz, H5), 3.81 (dd, 1H, $J_{H5,H6a}$ 7.6 Hz, $J_{H6a,H6b}$ 11.4 Hz, H6a), 3.69 (dd, 1H, $J_{H5,H6b}$ 4.9 Hz, $J_{H6a,H6b}$ 11.4 Hz, H6b), 1.89, 1.82, 1.69, 1.67 (4s, 12H, 4 × OAc) ppm. ^{13}C NMR: δ 170.5, 170.4, 169.4 × 2 (C=O), 169.4 (C=O, thiosalicylic), 84.0 (d, $J_{C1,P}$ 6.0 Hz, C1), 74.1 (C5), 71.0 (C2), 70.9 (C3), 67.0 (C4), 61.8 (C6), 20.8, 20.7, 20.6, 20.5 (4 × CH_3) ppm. $^{31}P\{H\}$ NMR: δ 51.7 ppm. *Anal.* Calcd for $C_{39}H_{37}NO_{11}PSAu$ (955.72): C, 49.01; H, 3.90; N, 1.47. Found: C, 49.14; H, 3.98; N, 1.56. MS: *m/z:* 978.140 (strong, $[M + Na]^+$, calc 978.138), 956.160 (weak, $[M + H]^+$, calc 956.156).

4.12 References

1. Staudinger, H. and Meyer, J., *New organic compounds of phosphorus. III. Phosphinemethylene derivatives and phosphinimines.* Helv. Chim. Acta, 1919. **2**, 635-646.
2. Johnson, A.W., *Ylides and imines of phosphorus*. 1993, New York: John Wiley & Sons, Inc.

3. Staudinger, H. and Hauser, E., *New organic phosphorus compounds. IV. Phosphinimines.* Helv. Chim. Acta, 1921. **4**, 861-886.

4. Birkofer, L., Ritter, A., and Richter, P., *Siliconorganic compounds. XIX. Thermolysis of silylated tetrazoles.* Chem. Ber., 1963. **96**, 2750-2757.

5. Nitta, M., Lino, Y., Hara, E., and Kobayashi, T., *On the reaction of N-vinyliminophosphoranes. Part 7. A short new 1-aza-azulene synthesis.* J. Chem. Soc., Perkin Trans. 1, 1989. 51-56.

6. Gololobov, Y.G. and Kasukin, L.F., *Recent advances in the Staudinger reaction.* Tetrahedron, 1992. **48**, 1353-1406.

7. Kirsanov, A.V., *Chemistry of amides of sulfuric acid.* Izvestiya Akademii Nauk SSSR, Seriya Khimicheskaya, 1950. 426-437.

8. Appel, R., Kleinstück, R., Ziehn, K.D., and Knoll, F., *The simultaneous action of ammonia (amines, imines) together with carbon tetrachloride on phosphines, I.* Chem. Ber., 1970. **103**, 3631-3639.

9. Messmer, A., Pintér, I., and Szegö, F., *Triphenylphosphine N-acetylglycosylimides and N,N'-bis(acetylglycosyl)carbodiimides.* Angew. Chem. Int. Ed., 1964. **3**, 228.

10. Pintér, I., Kovács, J., and Messmer, A., *Synthesis of sugar phosphinime derivatives from amino sugars.* Carbohydr. Res., 1977. **53**, 117-122.

11. Szarek, W.A. and Jones, J.K.N., *Carbohydrates containing nitrogen in a five-membered ring and an attempted synthesis of a carbohydrate with nitrogen in a seven-membered ring.* Can. J. Chem., 1965. **43**, 2345-2356.

12. Kovács, J., Pintér, I., and Messmer, A., *Unprotected sugar phosphinimines: A facile route to cyclic carbamates of amino sugars.* Carbohydr. Res., 1985. **141**, 57-65.

13. Nyffeler, P.T., Liang, C.-H., Koeller, K.M., and Wong, C.-H., *The chemistry of amine-azide interconversion: Catalytic diazotransfer and regioselective azide reduction.* J. Am. Chem. Soc., 2002. **124**, 10773-10778.

14. Maunier, V., Boullanger, P., and Lafont, D., *A one-pot synthesis of glycosyl amides from glycosyl azides using a modified Staudinger reaction.* J. Carbohydr. Chem., 1997. **16**, 231 - 235.

15. Saxon, E. and Bertozzi, C.R., *Cell surface engineering by a modified Staudinger reaction.* Science, 2000. **287**, 2007.

16. Malkinson, J.P., Falconer, R.A., and Toth, I., *Synthesis of C-terminal glycopeptides from resin-bound glycosyl azides via a modified Staudinger reaction.* J. Org. Chem., 2000. **65**, 5249-5252.

17. Hang, H.C., Yu, C., Pratt, M.R., and Bertozzi, C.R., *Probing glycosyltransferase activities with the staudinger ligation.* J. Am. Chem. Soc., 2003. **126**, 6-7.

18. Vocadlo, D.J. and Bertozzi, C.R., *A Strategy for functional proteomic analysis of glycosidase activity from cell lysates.* Angew. Chem. Int. Ed., 2004. **43**, 5338-5342.

19. Prescher, J.A., Dube, D.H., and Bertozzi, C.R., *Chemical remodelling of cell surfaces in living animals.* Nature, 2004. **430**, 873.

20. Bianchi, A. and Bernardi, A., *Traceless staudinger ligation of glycosyl azides with triaryl phosphines: Stereoselective synthesis of glycosyl amides.* J. Org. Chem., 2006. **71**, 4565-4577.

21. Bräse, S., Gil, C., Knepper, K., and Zimmermann, V., *Organic azides: An exploding diversity of a unique class of compounds.* Angew. Chem. Int. Ed., 2005. **44**, 5188-5240.

22. Fernández, J.M.G., Mellet, C.O., Pérez, V.M.D., Fuentes, J., Kovács, J., and Pintér, I., *Aza-Wittig reaction of sugar isothiocyanates and sugar iminophosphoranes: An easy entry to unsymmetrical sugar carbodiimides.* Tetrahedron Lett., 1997. **38**, 4161-4164.

23. Fernández, J.M.G., Mellet, C.O., Pérez, V.M.D., Fuentes, J., Kovács, J., and Pintér, I., *Synthesis of (1→6)-carbodiimide-tethered pseudooligosaccharides via aza-Wittig reaction.* Carbohydr. Res., 1997. **304**, 261-270.

24. Vicente, J., Abad, J.-A., Clemente, R., López-Serrano, J., Ramírez de Arellano, M.C., Jones, P.G., and Bautista, D., *Mercurated and palladated iminophosphoranes. Synthesis and reactivity.* Organometallics, 2003. **22**, 4248-4259.

25. Comrie, D., *Unpublished results*, University of Waikato.

26. Aguilar, D., Aznárez, F., Bielsa, R., Falvello, L.R., Navarro, R., and Urriolabeitia, E.P., *Versatility of iminophosphoranes and noninnocent behavior of the 1,5-cyclooctadiene ligand in palladium(II) complexes. Synthesis of σ-allyl derivatives.* Organometallics, 2007. **26**, 6397-6402.

27. Brown, S.D.J., Henderson, W., Kilpin, K.J., and Nicholson, B.K., *Orthomercurated and cycloaurated derivatives of the iminophosphorane Ph_3P=NPh.* Inorg. Chim. Acta, 2007. **360**, 1310-1315.

28. Kilpin, K.J., Henderson, W., and Nicholson, B.K., *Synthesis and reactivity of gold(III) complexes containing cycloaurated iminophosphorane ligands.* Inorg. Chim. Acta, 2009. **362**, 3669-3676.

29. Alper, H., *Cyclopalladation of phosphine imides.* J. Organomet. Chem., 1977. **127**, 385-389.

30. Leeson, M.A., Nicholson, B.K., and Olsen, M.R., *Orthomanganation of the iminophosphorane Ph_3P=NPh, and of triphenylarsine-oxide and -sulfide.* J. Organomet. Chem., 1999. **579**, 243-251.

31. Bruce, M.I., *Cyclometalation reactions.* Angew. Chem. Int. Ed., 1977. **16**, 73-86.

32. Wei, P., Chan, K.T.K., and Stephan, D.W., *Metallated triphenylphosphinimine complexes.* Dalton Trans., 2003. 3804-3810.

33. Chan, K.T.K., Spencer, L.P., Masuda, J.D., McCahill, J.S.J., Wei, P., and Stephan, D.W., *Anionic phosphinimine-chelate complexes of rhodium and iridium: Steric and electronic influences on oxidative addition of CH_2Cl_2.* Organometallics, 2004. **23**, 381-390.

34. Bielsa, R., Larrea, A., Navarro, R., Soler, T., and Urriolabeitia, E.P., *Synthesis, structure, reactivity, and catalytic activity of C,N- and C,N,N-orthopalladated iminophosphoranes.* Eur. J. Inorg. Chem., 2005. **9**, 1724-1736.

35. Wolfrom, M.L. and Thompson, A., *Acetylation*, in *Methods in Carbohydrate Chemistry*, R.L. Whistler and M.L. Wolfrom, Editors. 1963, Academic Press, Inc: New York. p. 211-215.

36. Kartha, K.P.R. and Field, R.A., *Iodine : A versatile reagent in carbohydrate chemistry IV. Per-O-acetylation, regioselective acylation and acetolysis.* Tetrahedron, 1997. **53**, 11753-11766.

37. Mukhopadhyay, B., Kartha, K.P.R., Russell, D.A., and Field, R.A., *Streamlined synthesis of per-O-acetylated sugars, glycosyl iodines, or thioglycosides from unprotected reducing sugars.* J. Org. Chem., 2004. **69**, 7758-7760.

38. Alcaro, S., Arena, A., Neri, S., Ottanà, R., Ortuso, F., Pavone, B., and Vigorita, M.G., *Design and synthesis of DNA-intercalating 9-fluoren-β-O-glycosides as potential IFN-inducers, and antiviral and cytostatic agents.* Biorg. Med. Chem., 2004. **12**, 1781-1791.

39. Ibatullin, F.M. and Shabalin, K.A., *A simple and convenient synthesis of glycosyl azides.* Synth. Commun., 2000. **30**, 2819-2823.

40. Bielsa, R., Navarro, R., Soler, T., and Urriolabeitia, E.P., *Orthopalladation of iminophosphoranes: synthesis, structure and study of stability.* Dalton Trans., 2008. 1203-1214.

41. Kiso, M. and Anderson, L., *Protected glycosides and disaccharides of 2-amino-2-deoxy-D-glucopyranose by ferric chloride-catalyzed coupling.* Carbohydr. Res., 1985. **136**, 309-323.

42. Fondy, T.P., Roberts, S.B., Tsiftsoglou, A.S., and Sartorelli, A.C., *Haloacetamido analogs of 2-amino-2-deoxy-D-glucose and 2-amino-2-deoxy-D-galactose. Syntheses and effects on the Friend murine erythroleukemia.* J. Med. Chem., 1978. **21**, 1222-1225.

43. Simon, P., Burlingham, W.J., Conklin, R., and Fondy, T.P., *N-Bromoacetyl-β-D-glucosamine tetra-O-acetate and N-bromoacetyl-β-D-galactosamine tetra-O-acetate as chemotherapeutic agents with immunopotentiating effects in Ehrlich Ascites tumor-bearing mice.* Cancer Research, 1979. **39**, 3897-3902.

44. Witte, M.D., Florea, B.I., Verdoes, M., Adeyanju, O., Van der Marel, G.A., and Overkleeft, H.S., *O-GlcNAc peptide epoxyketones are recognized by mammalian proteasomes.* J. Am. Chem. Soc., 2009. **131**, 12064-12065.

45. Chan, J.Y.C., Cheong, P.P.L., Hough, L., and Richardson, A.C., *The preparation and reactions of a new glycoside: 2'-Chloroethyl-β-D-fructopyranoside.* J. Chem. Soc., Perkin Trans. 1, 1985. **7**, 1447-1455.

46. Szmuszkovicz, J., Kane, M.P., Laurian, L.G., Chidester, C.G., and Scahill, T.A., *New synthesis of azetidine.* J. Org. Chem., 1981. **46**, 3562-3564.

47. Reetz, M.T. and Bohres, E., *Chiral diiminophosphoranes: a new class of ligands for enantioselective transition metal catalysis.* Chem. Commun., 1998. 935-936.

48. Boehm, E., Dehnicke, K., Beck, J., Hiller, W., Straehle, J., Maurer, A., and Fenske, D., *The crystal structures of Ph_3PNPh, $[Ph_3PN(H)Ph][AuI_2]$ and of 2,3-bis(triphenylphosphoranimino)maleic acid N-methylimide.* Z. Naturforsch., B: Chem. Sci., 1988. **43**, 138-144.

49. Aguilar, D., Aragüés, M.A., Bielsa, R., Serrano, E., Soler, T., Navarro, R., and Urriolabeitia, E.P., *Synthesis and structure of orthopalladated complexes derived from prochiral iminophosphoranes and phosphorus ylides.* J. Organomet. Chem., 2008. **693**, 417-424.

50. Kilpin, K.J., Linklater, R.A., Henderson, W., and Nicholson, B.K., *Synthesis and characterisation of isomeric cycloaurated complexes derived from the iminophosphorane $Ph_3PNC(O)Ph$.* Inorg. Chim. Acta, 2010. **363**, 1021-1030.

51. Harder, S., Brandsma, L., Kanters, J.A., Duisenberg, A., and van Lenthe, J.H., *The structure of 2-(diphenylphosphino)phenyllithium: the significance of P–Li bonding.* J. Organomet. Chem., 1991. **420**, 143-154.

52. Bennett, M.A., Contel, M., Hockless, D.C.R., Welling, L.L., and Willis, A.C., *Bis{(2-diphenylphosphino)phenyl}mercury: A P-donor ligand and precursor to mixed metal-mercury (d^8–d^{10}) cyclometalated complexes containing 2-$C_6H_4PPh_2$.* Inorg. Chem., 2002. **41**, 844-855.

53. Vicente, J., Chicote, M.T., and Bermúdez, M.-D., *2-[(Dimethylamino)methyl]phenylgold(III) complexes.* J. Organomet. Chem., 1984. **268**, 191-195.

54. Vicente, J., Bermúdez, M.-D., Carrión, F.-J., and Jones, P.G., *Synthesis of mono-, di-, and tri-arylgold(III) complexes using organomercury compounds – Synthesis of the first aurated Schiff bases.* Chem. Ber., 1996. **129**, 1301-1306.

55. Parish, R.V., Wright, J.P., and Pritchard, R.G., *Mercury(II) and gold(III) derivatives of 2-phenyl pyridines and 2-phenyl-4-(methylcarboxylato)quinoline.* J. Organomet. Chem., 2000. **596**, 165-176.

56. Garrou, P.E., *Δ_R Ring contributions to ^{31}P NMR parameters of transition-metal-phosphorus chelate complexes.* Chem. Rev., 1981. **81**, 229-266.

57. Orpen, A.G., Brammer, L., Allen, F.H., Kennard, O., Watson, D.G., and Taylor, R., *Supplement. Tables of bond lengths determined by X-ray and neutron diffraction. Part 2. Organometallic compounds and co-ordination complexes of the d- and f-block metals.* J. Chem. Soc., Dalton Trans., 1989. S1-S83.

58. Cordero, B., Gomez, V., Platero-Prats, A.E., Reves, M., Echeverria, J., Cremades, E., Barragan, F., and Alvarez, S., *Covalent radii revisited.* Dalton Trans., 2008. 2832-2838.

59. Henderson, W., *The chemistry of cyclometallated gold(III) complexes with C,N-donor ligands.* Adv. Organomet. Chem., 2006. **54**, 207-265.

60. Ieda, H., Fujiwara, H., and Fuchita, Y., *Synthesis and reactivity of the five-membered cycloaurated complexes of 2-phenylthiazole.* Inorg. Chim. Acta, 2001. **319**, 203-206.

61. Pearson, R.G., *Antisymbiosis and the trans effect.* Inorg. Chem., 1973. **12**, 712-713.

62. Dinger, M.B. and Henderson, W., *Organogold(III) metallacyclic chemistry. Part 4. Synthesis, characterisation, and biological activity of gold(III)-thiosalicylate and -salicylate complexes.* J. Organomet. Chem., 1998. **560**, 233-243.

63. Henderson, W., Nicholson, B.K., Faville, S.J., Fan, D., and Ranford, J.D., *Gold(III) thiosalicylate complexes containing cycloaurated 2-arylpyridine, 2-*

anilinopyridine and 2-benzylpyridine ligands. J. Organomet. Chem., 2001. **631**, 41-46.

64. Goss, C.H.A., Henderson, W., Wilkins, A.L., and Evans, C., *Synthesis, characterisation and biological activity of gold(III) catecholate and related complexes.* J. Organomet. Chem., 2003. **679**, 194-201.

65. Henderson, W., Nicholson, B.K., and Wilkins, A.L., *Facile syntheses of four-membered aurathietane dioxide [Au-CHR-SO_2-CHR] ring systems, and the first isonitrile insertion reaction into a gold(III)-carbon bond.* J. Organomet. Chem., 2005. **690**, 4971-4977.

Chapter Five
Catalytic activity of sugar thioureas and iminophosphoranes

5.1 Gold(III) iminophosphorane catalysis

5.1.1 Gold as a catalyst

While not traditionally thought of as catalysts, gold compounds are finding many uses in catalysis. Two reasons for neglecting this area have been proposed. Firstly the inert nature of elemental gold lead people to think it was catalytically inactive, and secondly the expensive nature of gold meant it was unfeasible as a catalyst [1]. These assumptions have been shown to be very wrong and the field is now growing extremely rapidly. A lot of the work done is on heterogeneous catalysis but homogeneous catalysis is becoming a growing part of this field. While various papers have been published over the years showing the possibilities [2], it is within the past decade that the area has taken off [3]. The field of gold catalysis was extensively reviewed by Hashmi in 2007 [4], and a number of other recent reviews have been published in selected areas [5-7]. Much of the homogeneous catalytic work has been carried out with the simple inorganic gold compound $AuCl_3$. While it is often a potent catalyst it does have some issues as it is deliquescent, very acidic and can be difficult to handle. Gold compounds that are air and moisture sensitive that can catalyse the reaction offer much better applications as catalysts being easier to use. For example work has shown that gold(III) iminophosphoranes can catalyze the formation of propargylamines from a terminal alkyne and an amine [8]. This short chapter describes some preliminary studies on the catalytic activities of some of the new complexes prepared as part of this thesis.

5.1.2 Addition of methyl vinyl ketone to 2-methyl furan

The reaction that was chosen for investigation was the addition of methyl vinyl ketone, **53**, to 2-methyl furan, **54**, to produce 4-(5-methyl-2-furanyl)butan-2-one, **55**, Scheme 5.1.

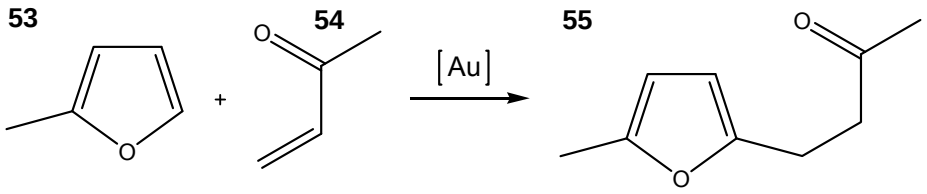

Scheme 5.1 *Addition of **53** to **54** catalyzed by gold.*

A number of different gold systems have been used for this reaction. $AuCl_3$ was the first gold compound shown to catalyze this reaction, and two mechanisms were suggested [9]. First was the direct auration of **53** followed by the addition of **54**, the second was the gold activating the alkene and the arene acting as a nucleophile in a Friedel-Crafts-like electrophilic substitution. NMR studies indicate that the auration of **53** is the most likely mechanism [10]. The gold(I) compounds Et_3PAuCl and (THT)AuCl also acted as catalysts but only if $AgBF_4$ was added [10]. *C*,*N* cycloaurated gold(III) iminophosphoranes were also shown to be catalysts, with the addition of either $AgBF_4$ or AgOTf increasing the activity of the compounds [11]. Recently *N*,*N* cycloaurated gold(III) iminophosphoranes, Figure 5.1, were shown to catalyze the reaction, however the addition of AgOTf did not increase the yields [12].

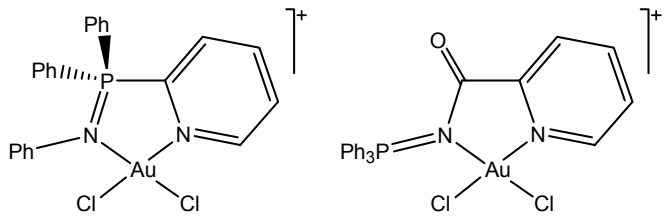

Figure 5.1 *Examples of N,N cycloaurated gold(III) iminophosphoranes that catalyze the coupling of **53** to **54**.*

The coupling of **54** is not limited to **53**, and is widely applicable with the gold compounds catalyzing the reaction of **54** to a number of electron-rich arenes such as azulene [10-12]. At this laboratory a wide range of different cycloaurated complexes including iminophosphoranes were tested and shown to be catalysts for this reaction [13]. The carbohydrate gold(III) iminophosphoranes were investigated to see if they were also active.

5.1.3 Gold(III) iminophosphoranes as catalysts

The reactions were carried out using the previously developed method from this laboratory by Kilpin [13]. The reactants **53**, **54**, the catalyst and $AgBF_4$ (if appropriate) were stirred in acetonitrile under N_2 for 18 hours. The solvent was removed and the residue dissolved in Et_2O/hexane (3:1). *O*-xylene was added as an internal standard and the percentage conversion to **55** determined by GC-MS.

The sugar gold(III) iminophosphoranes were tested with the above method, with either no $AgBF_4$ or a 2.2% loading of $AgBF_4$; the results are summarised in Table 5.1. A series of previously known cycloaurated iminophosphoranes [14, 15] were also tested, Figure 5.2.

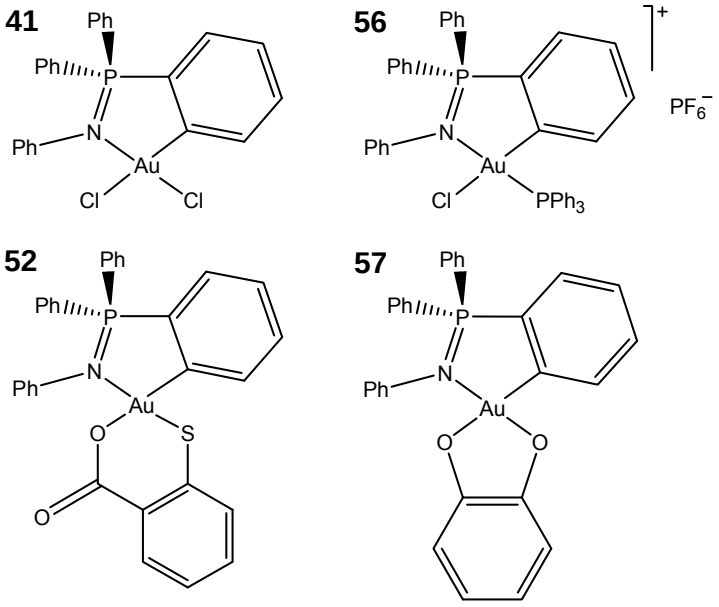

Figure 5.2 *Non-sugar cycloaurated iminophosphoranes also tested for catalytic activity.*

	Percentage conversion[1]	
	No $AgBF_4$	**2.2% $AgBF_4$**
48h	0	41
48i	14	45
49h	16	53
49i	21	51
50h	0	NA
50i	0	NA
41	7	86
56	37	85
52	0	NA
57	0	NA
$AgBF_4$	0	NA
$[NMe_4][AuCl_4]$	62	NA

1: Conditions: 1% catalyst loading, acetonitrile, 18 hours, 25°C.

Table 5.1 *Percentage conversion to **55** for different sugar gold(III) iminophosphoranes.*

From the result it can be seen that without the addition of $AgBF_4$ the sugar based compounds are generally very poor catalysts. While **48h** had no activity, **48i** showed a small amount. When one of the chlorides was replaced with PPh_3 the activity was increased, this is not surprising since for the gold(III) to take part in the reaction it needs a vacant coordination site. The PPh_3 is much more labile than chloride, so would more readily dissociate thus exposing the gold(III) centre. Both of the thiosalicylate derivatives were catalytically inactive. Again this is not surprising in terms of the ability to form a vacant coordination site. The thiosalicylate dianion binds to the gold much more firmly than the monodentate chloride ions. This may also relate back to the stability of the thiosalicylate derivatives over the dichlorides, since there would need to be access to the gold(III) centre for decomposition to occur.

When $AgBF_4$ was added the catalytic activity was greatly increased. It removes the chlorides from the iminophosphoranes, leaving vacant coordination sites which can be temporarily filled by the weakly coordinating acetonitrile solvent, greatly increasing the catalytic potential. While the dichloride **48h** showed no activity, the addition of $AgBF_4$ increased this to 41%. With the PPh_3 derivative the presence of $AgBF_4$ also increased the activity.

The *N*-phenyl derived iminophosphoranes generally performed better than the sugar based complexes. The results showed the same trends with the activity greatly increased when $AgBF_4$ was added.

As a blank $AgBF_4$ was tested without any gold compound present and showed no activity. The simple salt $[NMe_4][AuCl_4]$ (without $AgBF_4$) was also tested for a comparison. It showed better activity than the sugar iminophosphoranes.

5.1.4 Conclusions

The sugar gold(III) iminophosphoranes could catalyse the coupling of **53** to **54**. The presence of a vacant coordination site was very important with changes in activity correlated to how labile the ligands on the gold(III) centre were. While they did catalyse the reaction, $[NMe_4][AuCl_4]$ performed better. It appears that the very bulky sugar on the nitrogen (compared to the *N*-phenyl derivative) hinders the catalytic ability of the gold(III) centre, with the *N*-phenyl derivatives outperforming the sugar based compounds. Further testing that could be done on the sugar iminophosphoranes is to use a pro-chiral derivative of the alkene to see if any enantiomeric excess could be generated by the sugar moiety.

5.2 Rhodium catalysis

Despite the extreme expense of rhodium (it is more expensive than gold), its compounds are widely used for catalysis. The main use of rhodium is in the catalytic converters of cars; in 2007 81% of all the rhodium mined went to this purpose. It is also widely used as a catalyst in the Monsanto process for producing acetic acid by the carbonylation of methanol. Perhaps the best known rhodium catalyst is Wilkinson's catalyst, used for the hydroformylation and hydrogenation of alkenes. Because of the high activity of rhodium, the sugar thioureas and their rhodium complexes were investigated to see if they had any catalytic properties.

5.2.1 Hydrogen transfer catalysis

Hydrogen transfer was chosen as a reaction to study. Hydrogen transfer is the addition of hydrogen to a molecule from a source other than H_2. A common substrate for testing catalysts for this reaction is acetophenone, **58**, Scheme 5.2. It was hoped that the rhodium thiourea complexes would act as catalysts for this

reaction since partly similar thioamides derived from α amino acids had been used with $[RhCp^*Cl_2]_2$ and base to reduce **58**, Figure 5.3 [16].

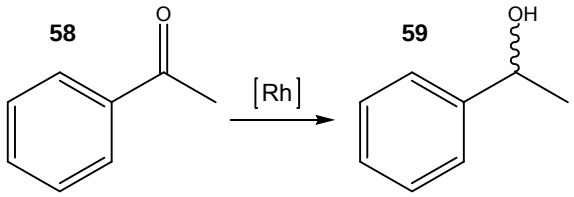

Scheme 5.2 *Hydrogen transfer of **58** to **59**.*

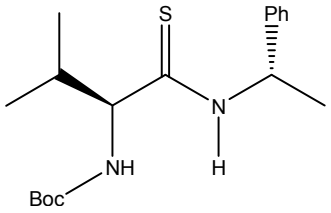

Figure 5.3 *Examples of a thioamide ligand used for the asymmetric hydrogen transfer of **58** [16].*

5.2.2 Sugar thioureas as hydrogen transfer catalysts

The chosen proton source was 2-propanol which was used as the solvent for the reactions. The general method involved stirring the catalyst, **58**, and KOH for 2 hours. The mixture was passed through a silica column and the solvent volume reduced by rotary evaporation. The conversion was determined by ^1H NMR spectroscopy of the residue and comparing the integration of the methyl peaks of **58** and **59**.

The reactions were carried out with a 1% loading of the catalyst. Different conditions were used with the temperature of the reaction run at 25 or 75 °C. Different concentrations of KOH were also added at 1.2, 5 and 10 mole equivalent per mole of catalyst. The first trials were with **25**, where the sugar thiourea acts as a bidentate ligand. To see if the *in situ* formation of a complex

would make a difference the thiourea and $[RhCp^*Cl_2]_2$ were also added to the mixture. It has been previously found with the thioamide ligands that the pre-formed complex from reacting the ligand with $[RhCp^*Cl_2]_2$ and base performs worse than species formed *in situ* [16].

The results for the sugar thiourea complexes were very unsatisfactory. The best conversion was for **25b** using a 1.2 M equivalent of KOH at 75 °C with a 11% conversion; as a comparison $[RhCp^*Cl_2]_2$ and $RhCp^*Cl_2PPh_3$ under the same conditions showed conversions of 80 and 68% respectively [17]. The other conditions gave essentially no conversion. No differences were seen between the use of a pre-made complex and *in situ* formation. Since under the basic conditions the acetate groups would be removed, it was thought that the unprotected thiourea **8e** might fare better. However it also showed very little conversion (<0.2%).

5.2.3 Conclusions

The sugar thiourea rhodium(III) complexes were very poor catalysts for the hydrogen transfer reaction of **58** to **59**. The best conversion was 11%, much less than that for the starting material.

5.3 Experimental

2-Methyl furan and methyl vinyl ketone were purchased from Aldrich and used as received. Reactions were run in HPLC grade acetonitrile. Samples of **41**, **52**, **56** and **57** were kindly provided by Dr Kelly Kilpin. NMR instrument details are in Appendix Two.

Gold catalysis

53 (2.00 mmol, 0.179 mL), **54** (2.00 mmol, 0.167 mL), the gold catalyst (0.02 mmol, 1% catalyst loading) and, if desired, $AgBF_4$ (0.044 mmol, 8.6 mg, 2.2% loading) were stirred in acetonitrile (5 mL) under N_2 for 18 hours. The flasks were maintained at 25°C in a bath. Solvent was removed under vacuum and the residue taken up in Et_2O/hexane (3:1) and made up to 20 mL in a volumetric flask containing *o*-xylene (1.00 mmol, 0.121 mL). The solution was passed through a silica column, 0.050 mL was transferred to a GC vial and made up to ~1.5 mL with hexanes.

GC-MS analysis

GC-MS experiments were run on a HP 68990 Series GC System coupled to a HP 5973 Mass Selective Detector running in TIC mode. 3 μL of sample was injected onto a non-polar column (ZB-5, 30 m × 0.25 mm, 0.25 μm film thickness) with an autosampler. The oven was initially held at 50 °C, the temperature was increased at 8 °C per minute. The relative response factor of **55** and *o*-xylene was determined allowing integration of the area of the peaks to determine the number of moles of **55** formed, Figure 5.4.

$$mmol\ of\ \mathbf{55} = \frac{area\ of\ \mathbf{55}}{area\ of\ o-xylene} \div 1.08$$

Figure 5.4 *Equation for determining the mmol of **55** produced.*

Rhodium catalysis

Either a thiourea complex (0.01 mmol) or the thiourea (0.01 mmol) and $[RhCp^*Cl_2]_2$ (0.005 mmol) were added to a vial with **58** (0.1 mmol) and 2-propanol (4.875 mL). KOH (0.125 mL, 0.1 M in 2-propanol) was added and left to

stir for 2 hours at 25 or 75 °C. If more base was added, the first amount of 2-propanol was reduced so that the total volume was 5 mL. After 2 hours the mixture was passed through a short column of silica which was washed with ethyl acetate (5 mL). The solvent volume was reduced under vacuum and the residue analysed by ^{1}H NMR. The methyl signal of **58** comes at 2.47 ppm, while for **59** it is 1.35 ppm; they were integrated and the equation shown in Figure 5.5 was used.

$$\%\ conversion = \frac{area\ of\ \mathbf{59}}{area\ of\ \mathbf{58} + area\ of\ \mathbf{59}}$$

Figure 5.5 *Equation for calculating percentage conversion by the integration of ^{1}H NMR spectra.*

5.4 References

1. Hashmi, A.S.K. and Rudolph, M., *Gold catalysis in total synthesis.* Chem. Soc. Rev., 2008. **37**, 1766-1775.
2. Ito, Y., Sawamura, M., and Hayashi, T., *Catalytic asymmetric aldol reaction: reaction of aldehydes with isocyanoacetate catalyzed by a chiral ferrocenylphosphine-gold(I) complex.* J. Am. Chem. Soc., 1986. **108**, 6405-6406.
3. Hashmi, A.S.K. and Hutchings, G.J., *Gold catalysis.* Angew. Chem. Int. Ed., 2006. **45**, 7896-7936.
4. Hashmi, A.S.K., *Gold-catalyzed organic reactions.* Chem. Rev., 2007. **107**, 3180-3211.
5. Xu, B., Wang, W., Liu, L.-P., Han, J., Jin, Z., and Hammond, G.B., *Synthetic evolutions in the nucleophilic addition to alkynes.* J. Organomet. Chem., 2011. **696**, 269-276.
6. Hashmi, A.S.K., *Homogeneous gold catalysis beyond assumptions and proposals—Characterized intermediates.* Angew. Chem. Int. Ed., 2010. **49**, 5232-5241.
7. Sengupta, S. and Shi, X., *Recent advances in asymmetric gold catalysis.* ChemCatChem, 2010. **2**, 609-619.

8. Aguilar, D., Contel, M., and Urriolabeitia, E., P., *Mechanistic insights into the one-pot synthesis of propargylamines from terminal alkynes and amines in chlorinated solvents catalyzed by gold compounds and nanoparticles.* Chem. Eur. J., 2010. **16**, 9287-9296.

9. Hashmi, A.S.K., Schwarz, L., Choi, J.-H., and Frost, T.M., *A new gold-catalyzed C−C bond formation.* Angew. Chem. Int. Ed., 2000. **39**, 2285-2288.

10. Dyker, G., Muth, E., Hashmi, A.S.K., and Ding, L., *Gold(III) chloride-catalyzed addition reactions of electron-rich arenes to methyl vinyl ketone.* Adv. Synth. Catal., 2003. **345**, 1247-1252.

11. Aguilar, D., Contel, M., Navarro, R., and Urriolabeitia, E.P., *Organogold(III) iminophosphorane complexes as efficient catalysts in the addition of 2-methylfuran and electron-rich arenes to methyl vinyl ketone.* Organometallics, 2007. **26**, 4604-4611.

12. Aguilar, D., Contel, M., Navarro, R., Soler, T., and Urriolabeitia, E.P., *Gold(III) iminophosphorane complexes as catalysts in C-C and C-O bond formations.* J. Organomet. Chem., 2009. **694**, 486-493.

13. Kilpin, K.J., *PhD Thesis*. 2009, University of Waikato.

14. Brown, S.D.J., Henderson, W., Kilpin, K.J., and Nicholson, B.K., *Orthomercurated and cycloaurated derivatives of the iminophosphorane Ph_3P=NPh.* Inorg. Chim. Acta, 2007. **360**, 1310-1315.

15. Kilpin, K.J., Henderson, W., and Nicholson, B.K., *Synthesis and reactivity of gold(III) complexes containing cycloaurated iminophosphorane ligands.* Inorg. Chim. Acta, 2009. **362**, 3669-3676.

16. Ahlford, K., Ekström, J., Zaitsev, A.B., Ryberg, P., Eriksson, L., and Adolfsson, H., *Asymmetric transfer hydrogenation of ketones catalyzed by amino acid derived rhodium complexes: On the origin of enantioselectivity and enantioswitchability.* Chem. Eur. J., 2009. **15**, 11197-11209.

17. Marr, A.C., Nieuwenhuyzen, M., Pollock, C.L., and Saunders, G.C., *Synthesis of piano stool complexes employing the pentafluorophenyl-substituted diphosphine $(C_6F_5)_2PCH_2P(C_6F_5)_2$ and the effect of phosphine modifiers on hydrogen transfer catalysis.* Organometallics, 2007. **26**, 2659-2671.

Appendix One

General experimental procedures

Dry CH_2Cl_2, THF, ether and hexane were produced from a Pure Solv solvent purification system [1]. High resolution ESI-MS was carried out on a Bruker Daltonics MicrOTOF instrument. Samples were dissolved in methanol and were run using methanol as the eluent at 180 µL min^{-1}. The instrument was calibrated over the appropriate mass range with sodium formate, and all spectra were acquired in positive ion mode. Peak intensities were given a qualitative label depending on the intensity of the peak relative to the most intense peak; Strong (100 – 65%), medium (65 – 30%), weak (30 – 1%) and very weak (>1%). Microelemental analysis was carried out at the Campbell Microanalytical Laboratory at the University of Otago. IR was carried out on a PerkinElmer Spectrum 100 FT-IR, samples were prepared in KBr discs.

Synthesis of sugars

1,3,4,6-Tetra-*O*-acetyl-β-D-glucosamine hydrochloride salt [2]

D-Glucosamine hydrochloride (14.2 g, 66.0 mmol) was dissolved in water (70 mL) containing sodium hydroxide (2.64 g, 66.0 mmol). 4-Methoxybenzaldehyde was added (9.68 mL, 10.8 g, 79.6 mmol) and vigorously stirred for 2 hours producing a white precipitate which was filtered and washed with diethyl ether:ethanol (1:1, 3 × 30 mL) yielding 17.1 g. This was dissolved in pyridine (40 mL) and acetic anhydride (35 mL) and stirred overnight. The solution was poured into a beaker of ice cold water (300 mL) and stirred until a white precipitate formed (approximately 10 minutes) which was filtered and washed with water (3 × 30 mL) and dried under reduced pressure yielding 11.6 g. The product was dissolved in acetone (30 mL) and HCl (6M, 4.15 mL, 24.9 mmol) was added and stirred for 2 hours to produce a white precipitate, diethyl ether (60 mL) was added and kept

at 4°C overnight. The precipitate was filtered and washed with diethyl ether (3 × 50 mL) and dried under reduced pressure to give **7**·HCl (7.12 g, 28%).

1,3,4,6-Tetra-*O*-acetyl-β-D-glucosamine, 7

7·HCl (1.37 g, 3.57 mmol) was dissolved in water (30 mL) and sodium bicarbonate (0.45 g, 5.36 mmol) was added and stirred for 30 minutes. The solution was extracted with dichloromethane (3 × 20 mL), the organic phase was dried with magnesium sulphate, filtered and evaporated under reduced pressure to give **7** (1.18 g, 95.2%).

^{1}H NMR: δ 5.45 (d, 1H, $J_{1,2}$, 8.6 Hz, H1), 5.38 (m, 1H, H4), 5.21 (m, 1H, H3), 4.30 (dd, 1H, $J_{5,6b}$ 4.6 Hz, $J_{6,6b}$ 12.4 Hz, H6b), 4.08 (dd, 1H, $J_{5,6a}$ 2.2 Hz, $J_{6a,6b}$ 12.4 Hz, H6a), 3.80 (ddd, 1H, $J_{5,6a}$ 2.2 Hz, $J_{5,6}$ 4.6 Hz, $J_{4,5}$ 9.7 Hz, H5), 3.01 (m, 1H, H2), 2.16, 2.08, 2.07, 2.02 (4s, 12H, 4 × OAc), 1.27 (s, 2H, NH_2) ppm. ^{13}C NMR: δ 170.8, 170.7, 169.8, 169.3 (4 × C=O), 95.4 (C1), 75.3 (C3), 72.9 (C5), 68.4 (C4), 62.0 (C6), 55.2 (C2), 21.1, 20.9, 20.8, 20.8 (4 × CH_3) ppm.

Appendix Two

NMR details

A.2.1 General NMR details

^{1}H and ^{13}C NMR spectra were recorded on a Bruker Avance III 400 FT NMR spectrometer at 400.13 and 100.61 MHz respectively at 300 K, while $^{31}P\{H\}$ was run on a Bruker DRX 300 FT NMR spectrometer at 121.5 MHz. ^{1}H and ^{13}C NMR spectra were referenced to the solvent line, while $^{31}P\{H\}$ NMR spectra were referenced using an external standard of H_3PO_4. For $CHCl_3$-d1 and DMSO-d6 the referencing for ^{1}H NMR spectra was 7.26 and 2.50 ppm and for ^{13}C NMR spectra was 77.16 and 39.52 ppm respectively. ^{1}H NMR spectra were processed with no line broadening applied and were baseline corrected. ^{13}C NMR spectra were routinely run with a 70° tip angle and a 2 second delay for better signal to noise from the carbonyl signals. HSQC 135 spectra were run with a default coupling constant of 145 Hz as the best compromise value.

A.2.2 NMR assignment

The compounds reported were all characterized by a suite of NMR experiments. To show how assignment and characterisation was carried out, a representative example is shown below detailing how **12a** was characterised. Figure A.2.1 shows **12a** and its labelling scheme.

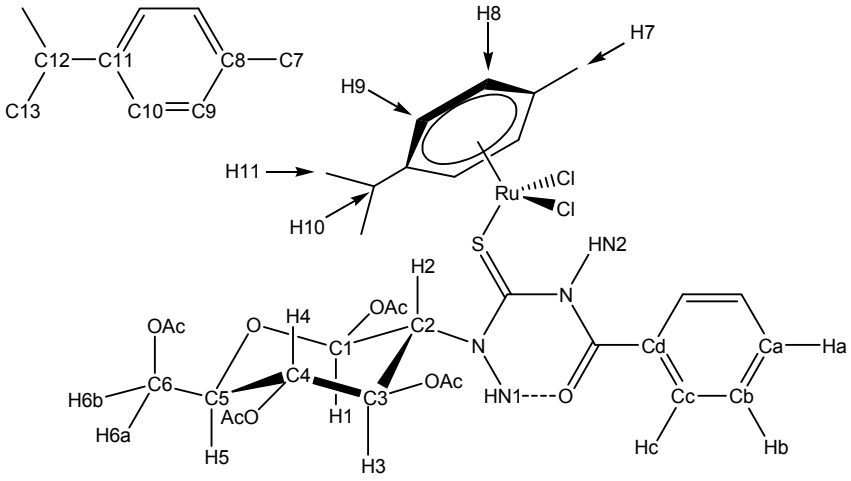

Figure A.2.1 ***12a**, the compound used for the explanation of the NMR assignment with its labelling scheme.*

The first experiment run was a ^{1}H NMR shown in Figure A.2.2. A number of signals could be assigned immediately, with the anomeric proton H1, being very distinctive as a doublet at 5.83 ppm. The H6 protons could be seen as two sets of doublet of doublets, and the H5 proton was distinctive as a doublet of doublet of doublets. To see some of the coupling patterns, resolution enhancement was often needed. This was carried out using Gaussian processing; the typical setting used were lb = -2 and gb = 0.33. Figure A.2.2 shows the difference that resolution enhancement gives for Ha, H9 and H2. The acetates were seen as singlets that integrated to 3 protons between 2.0-2.2 ppm. In the aromatic region, Ha could be identified through integration as there were two multiplets that integrated to 2 protons and one triplet of triplet that integrated to 1 proton. Most of the signals from the *p*-cymene could be identified at this stage. The methyl's from the isopropyl group were a 6 proton doublet at 1.35 ppm, the other methyl was a singlet slightly downfield of the acetates at 2.28 ppm. The CH from the isopropyl group was a quartet at 3.03 ppm. A signal was seen at 5.45 ppm, shown in Figure A.2.2, which appeared to be a doublet of doublet of doublets that integrated as 2 protons. The most likely interpretation of this was that these were the two protons opposite each other on the *p*-cymene ring, and were slightly inequivalent and thus were each of doublet of doublets, that overlapped

each other. The N–H protons could be identified, HN1 was a doublet at 11.71 ppm, HN2 was a singlet at 11.28 ppm.

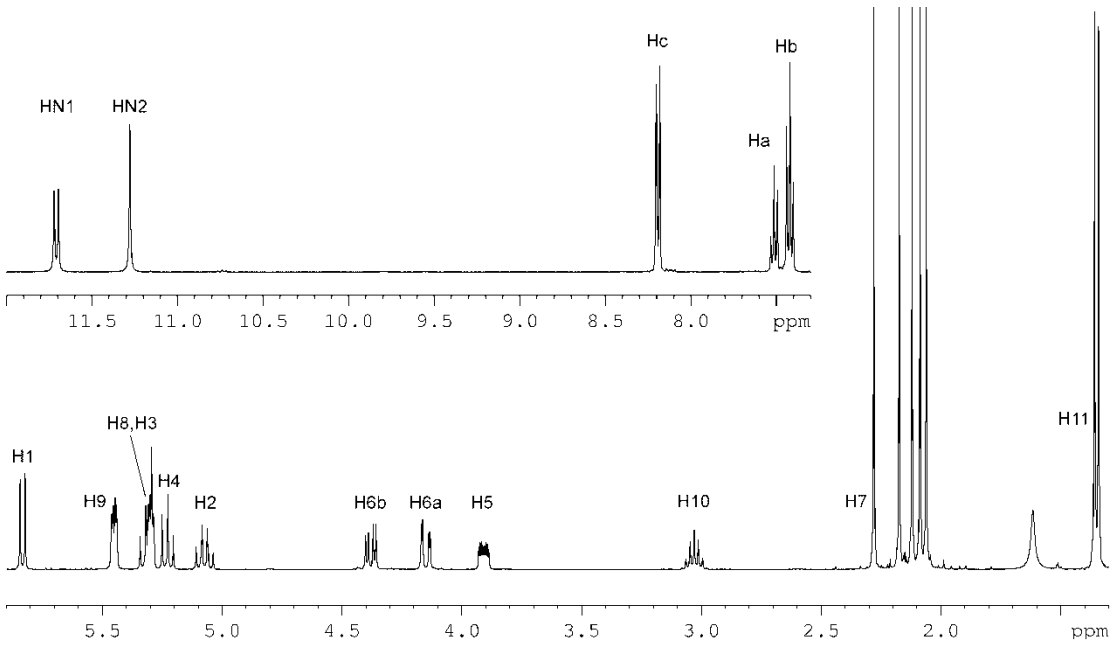

Figure A.2.2 *^{1}H NMR spectrum of **12a**; inset shows the N–H and aromatic signals.*

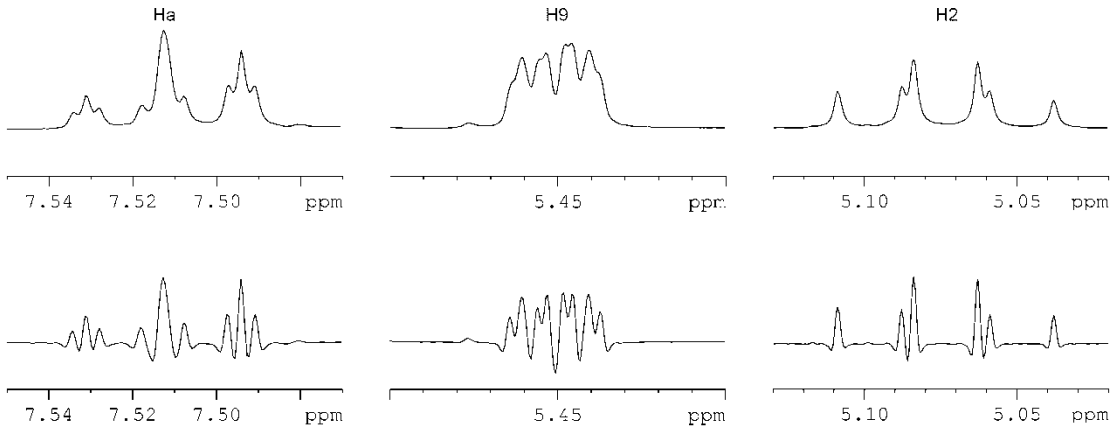

Figure A.2.3 *Effect of resolution enhancement on ^{1}H NMR spectra. Top row shows standard processing of signals with no line broadening. Bottom row shows the same signals processed with resolution enhancement.*

To assign the rest of the ^{1}H NMR signals the 2D ^{1}H-^{1}H COSY experiment was run, where the spectrum is observed along the diagonal, and the correlated signals have cross peaks showing which protons are coupled. Since the H1 proton was

already known, the rest of the sugar signals could be easily identified. Figure A.2.4 shows a portion of the COSY spectrum with the tracing of signals from H1 which allows the sugar protons H2, H3 and H4 to be determined. There is difficulty with H3 however as it overlaps with another signal. The overlapped signal couples to the aromatic *p*-cymene signal at 5.45 ppm, this can then be assigned as the other aromatic *p*-cymene signal. Integration confirms this as the overlapping region integrates to three protons. Other signals could be confirmed; for example the signals assigned as H5, H6a and H6b show the correct correlation. In the COSY spectrum there is no coupling seen between H5 to H6a unlike between H5 and H6b. This is because there is a smaller coupling constant between H5 and H6a than H5 and H6b; $J_{H5,H6a}$ is 2.4 Hz compared with 4.9 Hz for $J_{H5,H6b}$. A standard COSY spectra is biased towards larger coupling constants. Coupling is seen between the methyl (H11) and CH (H10) signals of the isopropyl group on the *p*-cymene.

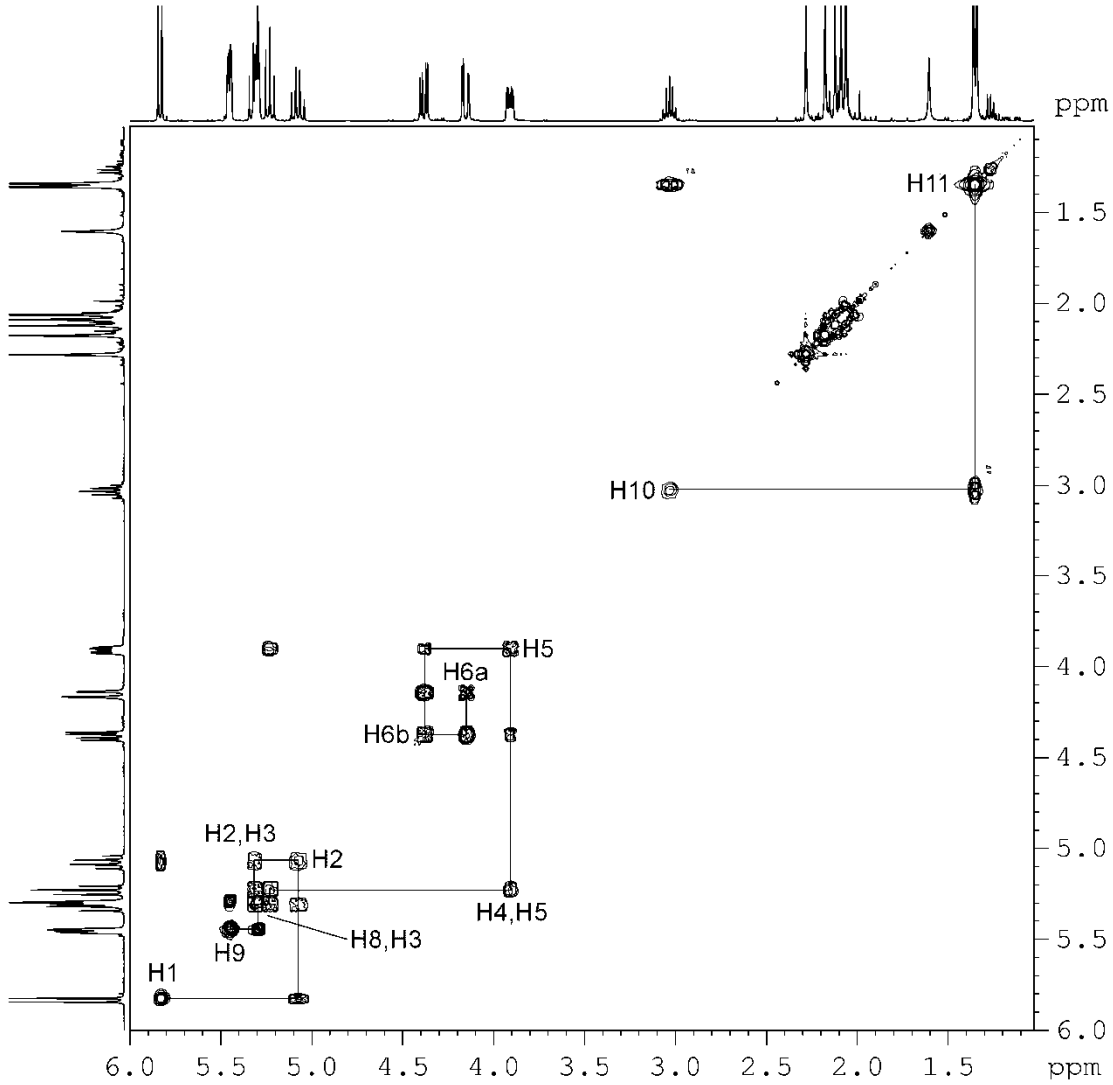

Figure A.2.4 *^{1}H-^{1}H COSY spectrum of the sugar and cymene region of **12a**. There is no cross peak between H5 and H6a.*

Figure A.2.5 shows the aromatic portion of the COSY spectrum. Since Ha is known from integration, Hb and Hc can be identified. Figure A.2.6 shows the coupling from H2 to HN1, confirming the assignment of HN1 and H2.

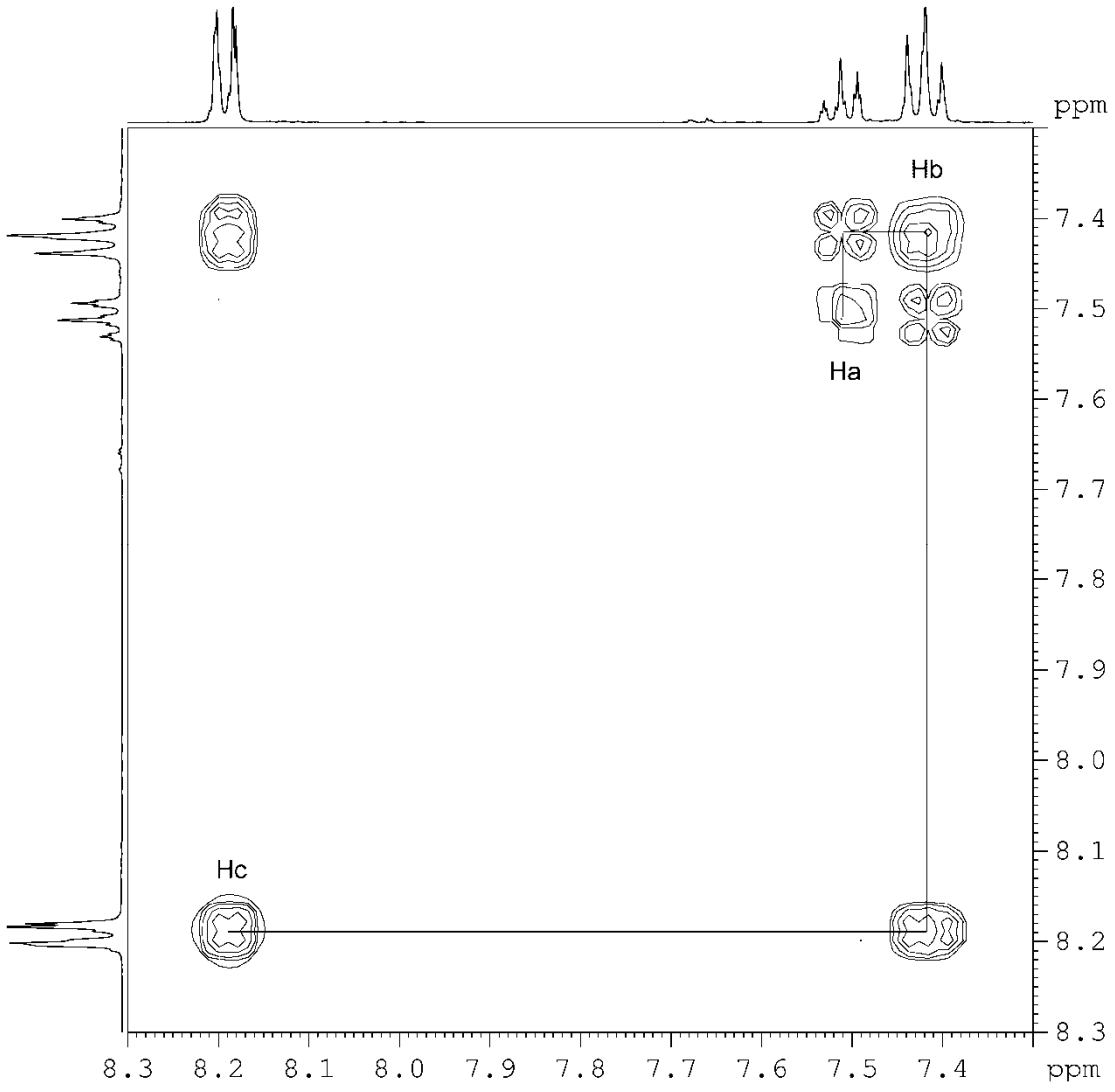

Figure A.2.5 *Aromatic portion of the ^{1}H-^{1}H COSY spectrum of **12a**.*

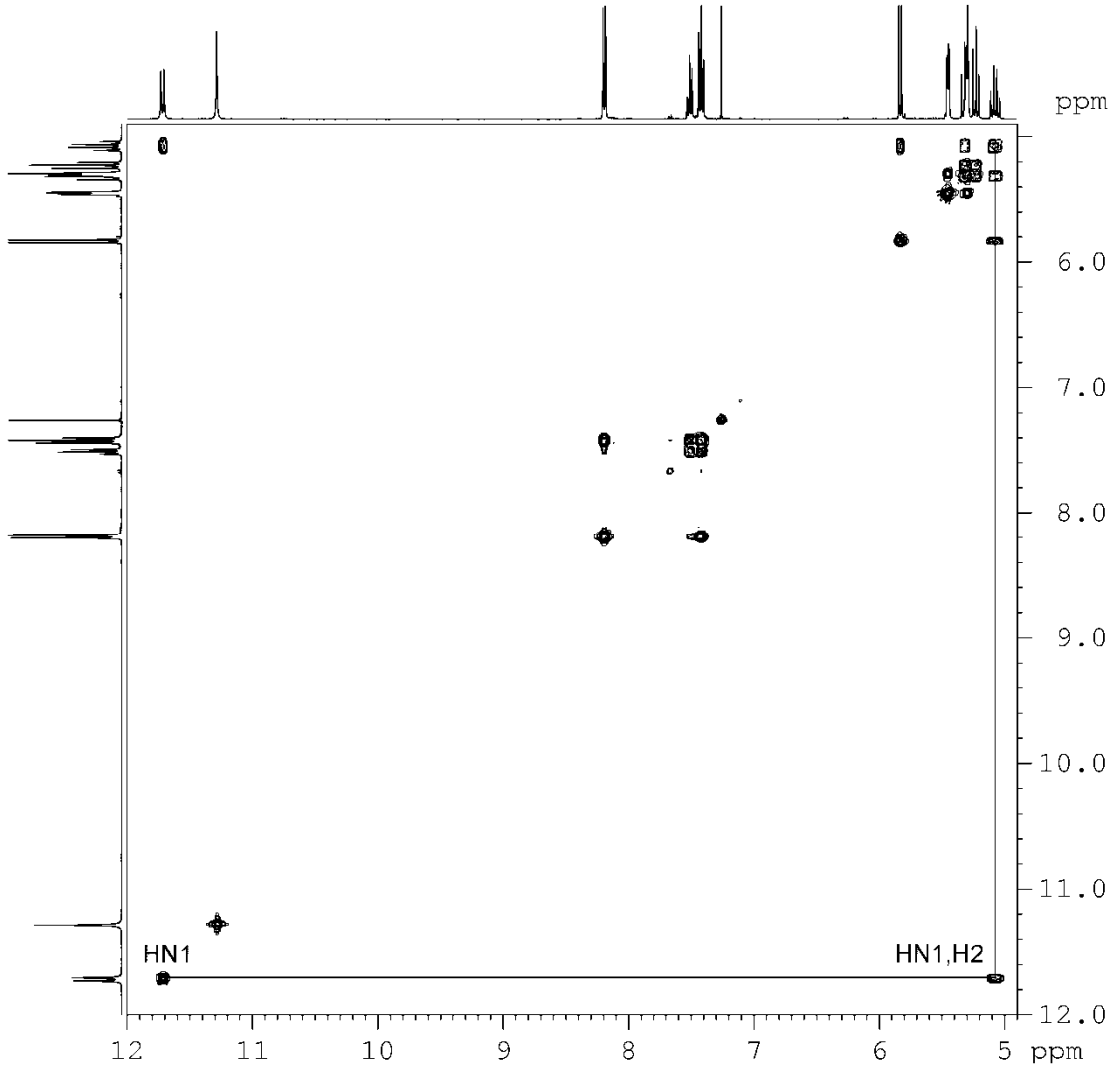

Figure A.2.6 *^{1}H-^{1}H COSY spectrum of **12a** showing the coupling between H2 and HN1.*

The ^{13}C NMR spectrum was acquired next, shown in Figure A.2.7. Rough assignment could be carried out, with the sugar signals coming between 55-95 ppm, with the anomeric carbon C1, generally coming at ~92 ppm. The aromatic carbons came at 125-135 ppm; carbonyl carbons were between 165-175 ppm and the methyl groups of the acetates were approximately 20 ppm.

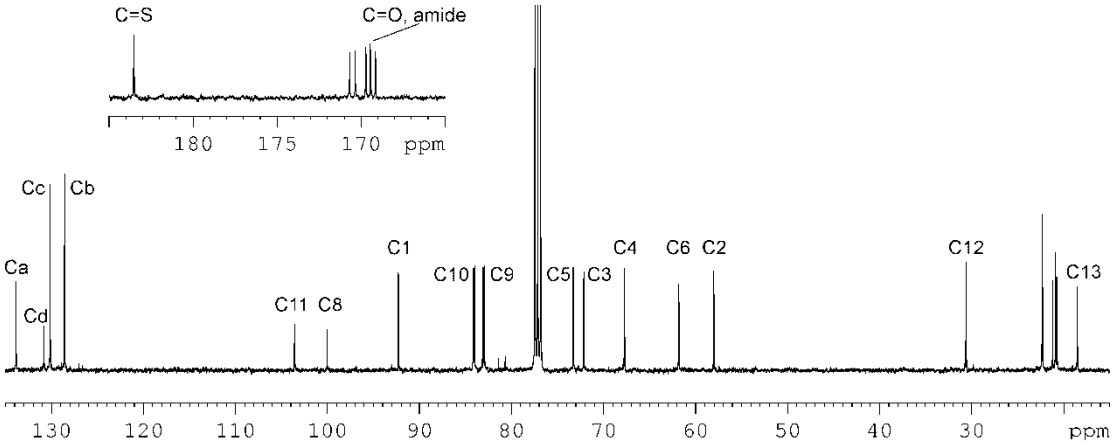

Figure A.2.7 *^{13}C NMR spectrum of **12a**; inset shows the carbonyl and C=S carbon signals.*

To properly identify the carbon signals a ^{1}H-^{13}C HSQC experiment was needed. This gives the one bond coupling between proton and carbon, Figure A.2.8. The standard HSQC was modified to an HSQC-135 experiment to give additional information on the carbon type with CH and CH_3 signals appearing as positive peaks and the CH_2 appearing as negative peaks. N–H protons show no signals as they are not attached to carbon atoms. Since all the proton signals have been assigned, the identity of any primary, secondary and tertiary carbon atoms are known.

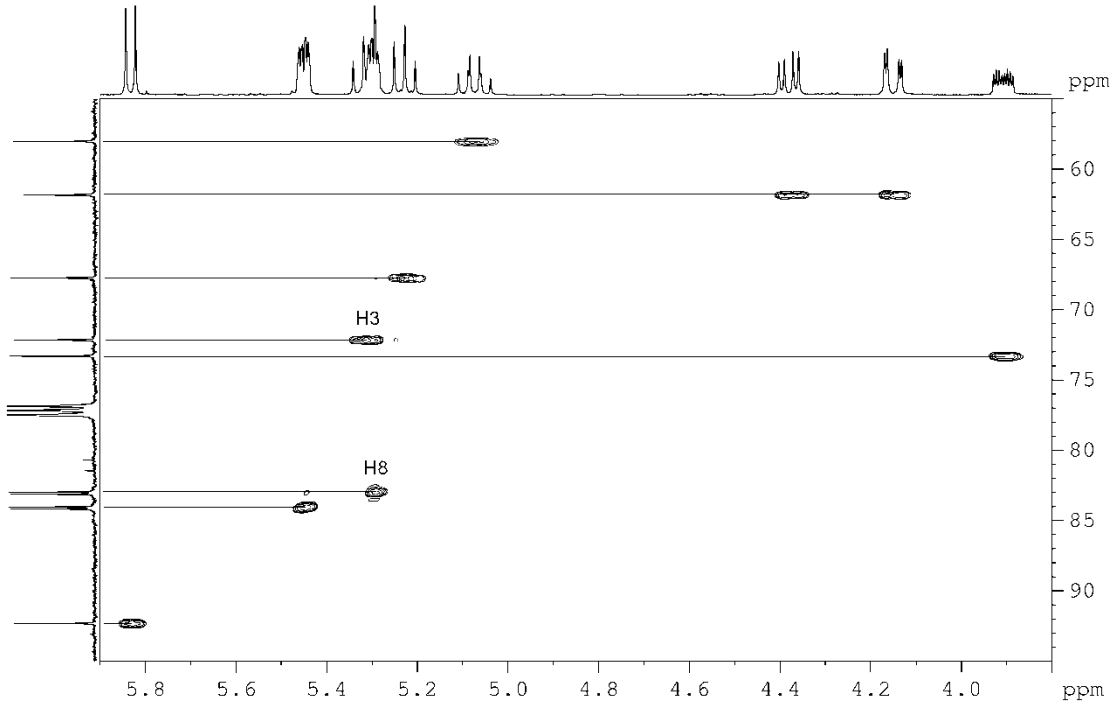

Figure A.2.8 *A ^{1}H-^{13}C HSQC135 spectrum of **12a** showing the one bond couplings between proton and carbon. The H3 and H8 signals are now separated.*

If two proton signals overlap, generally the HSQC experiment can separate them, as they will often have different carbon signals. For example H3 and H8 of the *p*-cymene signals overlap. The carbons that they are attached to have different chemical shifts (~11 ppm), and so can be distinguished and the chemical shift of the proton signals determined, this is shown in Figure A.2.8. If the coupling information of the signal is wanted as well a SELTOCSY experiment can be run. This is a 1D version of the TOCSY experiment. The experiment gives through the bond correlations from a chosen irradiated signal. The mixing time (d9) is varied and as it increases the further the through bond correlation can be seen. It has a number of advantages over the traditional TOCSY experiment; such as shorter acquisition time; very specific irradiation of the spectrum and much higher resolution (While less than a standard ^{1}H NMR spectrum, many coupling constants can be obtained). Figure A.2.9 shows a series of SELTOCSY spectra with increasing d9 values (15-150 ms) where the H1 signal has been irradiated. With the long mixing time only the signals from the irradiated spin system are seen.

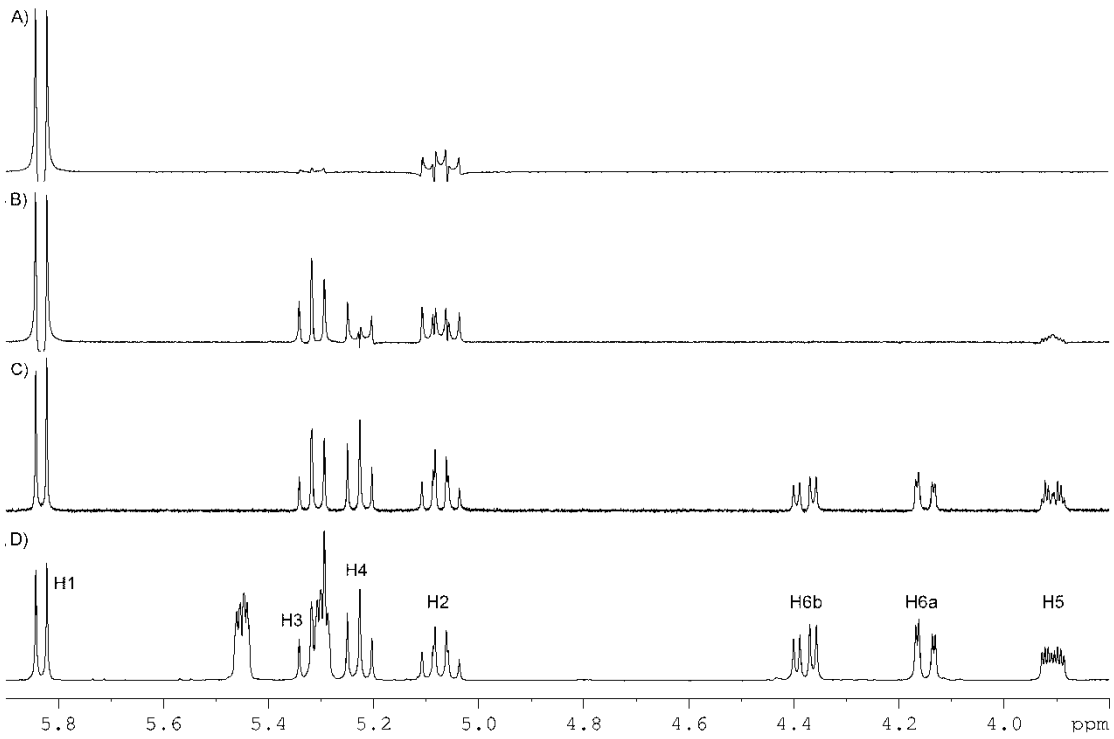

Figure A.2.9 *A series of SELTOCSY spectra of **12a** with increasing mixing times (d9), the H1 signal has been irradiated; A) d9 = 15 ms; B) d9 = 60 ms; C) d9 = 200 ms; D) Standard ^{1}H NMR spectrum.*

The final signals left unidentified were the quaternary carbonyl, C=S and aromatic signals. To distinguish them a ^{1}H-^{13}C HMBC experiment was run Figure A.2.10. This gives the two and three bond proton to carbon coupling while cancelling the 1 bond coupling. The standard experiment was modified to an HMBC cigar experiment. This removes some of the residual 1 bond coupling leftover in the standard experiment. The acetyl and amide carbonyl carbon atoms are all close together. To distinguish them the long range coupling was investigated. The acetyl carbonyl carbons show correlation to the carbohydrate signals H1, H3, H4, H6a and H6b which all have acetates on their respective oxygen's. The carbonyl of the amide showed no coupling to a carbohydrate proton but to HN2 and Hc, while the C=S carbon showed coupling to H2 and a weak coupling to HN1.

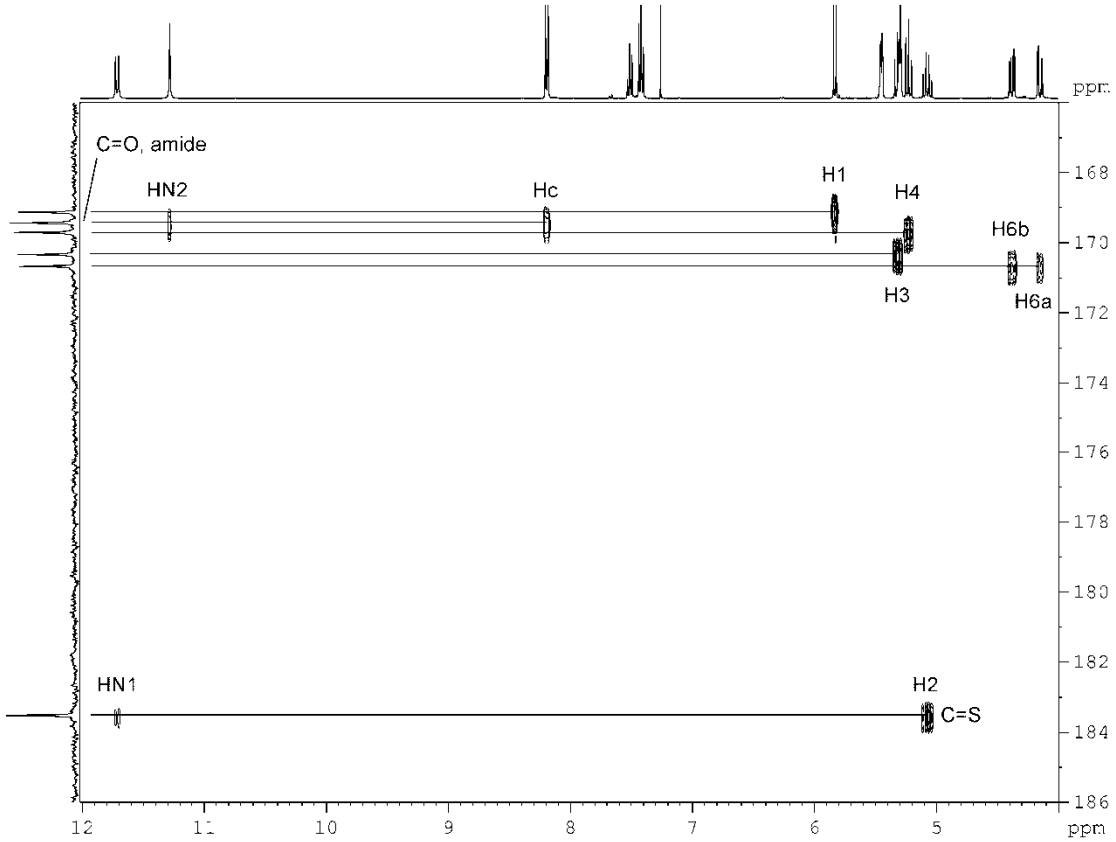

Figure A.2.10 *Portion of the ^{1}H-^{13}C HMBC cigar spectrum of **12a** showing the long range coupling to the carbonyl and C=S carbons.*

The quarternary carbons on the *p*-cymene could also be identified. The isopropyl and the methyl group show coupling to different parts of the aromatic ring, allowing them to be distinguished. Figure A.2.12 shows a summary of the long range coupling seen in **11a**.

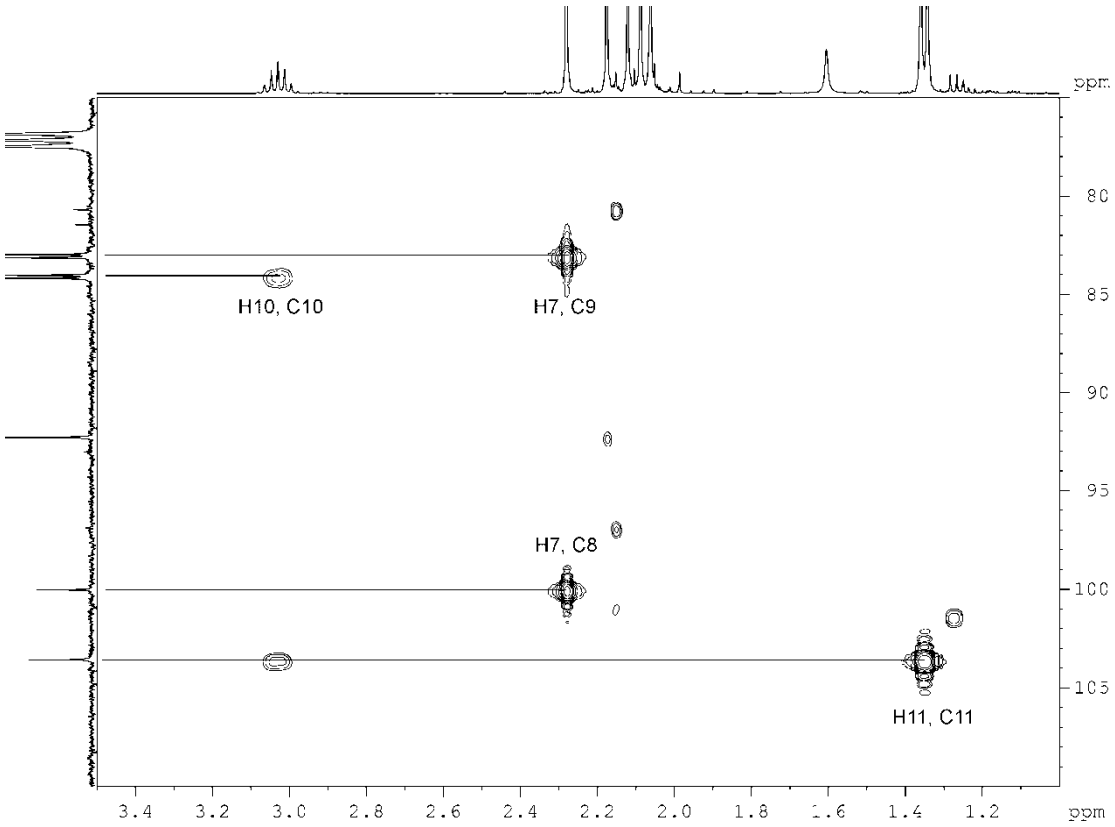

Figure A.2.11 *Portion of the ^{1}H-^{13}C HMBC cigar spectrum of **12a** showing the long range coupling on the p-cymene ring.*

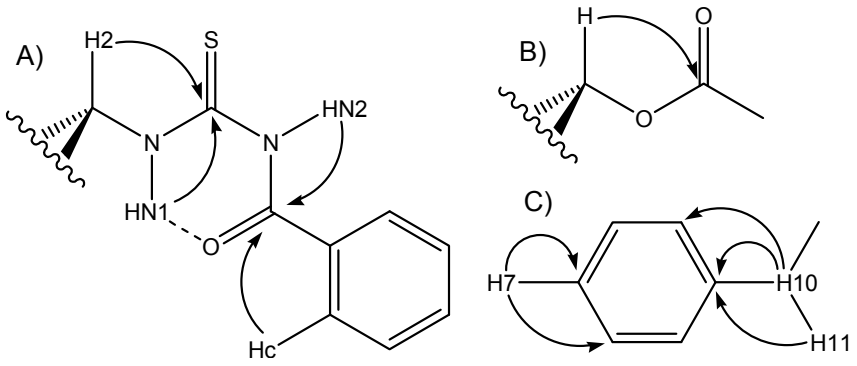

Figure A.2.12 *Diagram showing the long range coupling between the various protons and quaternary carbons on different portions of **12a**; A) Thiourea; B) Acetate; C) p-Cymene.*

Appendix Three

X-ray diffraction details

A.3.1 Data Collection

Intensity data and unit cell dimensions for **8e**, **14b** and **48h** were collected at the University of Auckland on a Bruker SMART CCD diffractometer at 89 K, while data for **8a**, **9a**, **39h** and **48j** were collected at the University of Canterbury on a Bruker APEX II CCD diffractometer at 93 K.

A.3.2 Solution and Refinement

Structures were solved by the direct methods option of SHELXS97 [3]. All non-hydrogen atoms were either initially located or were found in subsequent difference maps. Full-matrix least-squares refinement (SHELXL97 [4]) was based on F_0^2 with all non-hydrogen atoms anisotropic, unless otherwise stated. Hydrogen atoms on carbon atoms were refined using a riding model, hydrogen atoms on oxygen or nitrogen were treated in two different manners. For good data they were in a difference map and their positions were allowed to refine and isotropic *U* values were constrained to 1.2 times the U_{eq} value of the atom they were bound to. For data of poorer quality they were refined using a riding model. All calculations were carried out by the SHELXL97 suite of programs [4] and were run under WinGX [5]. All crystal structure graphics were generated using ORTEP-3 [6]. The compounds crystallised in non-centrosymmetric space groups; to get the correct absolute structure the Flack-*x* parameter [7, 8] was used for structures with heavy atoms as well as inspecting the stereochemistry of the sugar moiety and comparing to accepted literature stereochemistry.

A.3.3 Statistical Analysis

To test the significance of the difference between two X-ray diffraction measurements, the following formula was used, with a differences of more than 3σ being considered significantly different.

$$\sigma(A-B) = \sqrt{\sigma^2(A) + \sigma^2(B)}$$

Figure A.3.1 *Formula for determining the significance of the difference between two measurements.*

Appendix references

1. Pangborn, A.B., Giardello, M.A., Grubbs, R.H., Rosen, R.K., and Timmers, F.J., *Safe and convenient procedure for solvent purification.* Organometallics, 1996. **15**, 1518-1520.
2. Myszka, H., Bednarczyk, D., Najder, M., and Kaca, W., *Synthesis and induction of apoptosis in B cell chronic leukemia by diosgenyl 2-amino-2-deoxy-β-D-glucopyranoside hydrochloride and its derivatives.* Carbohydr. Res., 2003. **338**, 133-141.
3. Sheldrick, G.M., *SHELXS-97: A program for automatic solution of crystal structures*. 1997, University of Göttingen, Germany.
4. Sheldrick, G.M., *SHELXL-97: A program for the refinement of crystal structures*. 1997, University of Göttingen, Germany.
5. Farrugia, L.J., *WinGX suite for small-molecule single-crystal crystallography.* J. Appl. Crystallogr., 1999. **32**, 837-838.
6. Farrugia, L.J., J. Appl. Crystallogr., 1997. **30**, 565.
7. Flack, H.D., *On enantiomorph-polarity estimation.* Acta Crystallogr., Sect. A, 1983. **39**, 876-881.
8. Bernardinelli, G. and Flack, H.D., *Least-squares absolute-structure refinement. Practical experience and ancillary calculations.* Acta Crystallogr., Sect. A, 1985. **41**, 500-511.

1

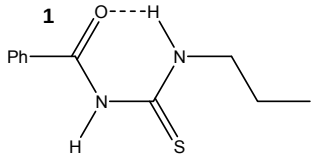

2: X = Cl
3: X = Br
4: X = I

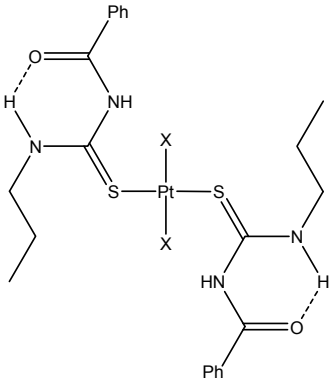

5: X = Cl
6: X = Br

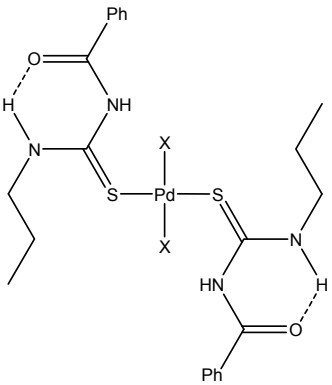

7

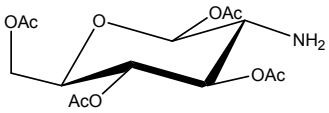

8a

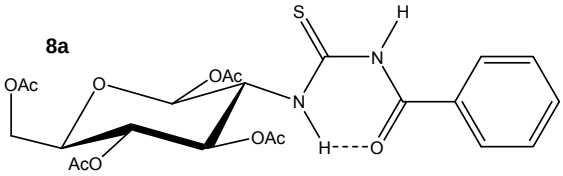

8b

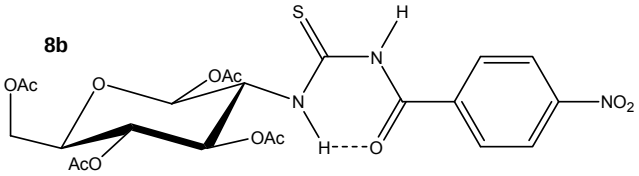

8c

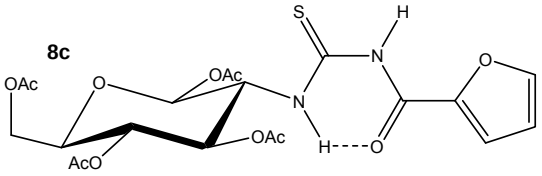

8d

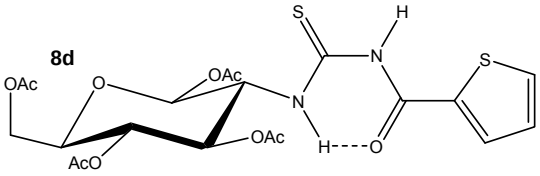

8e

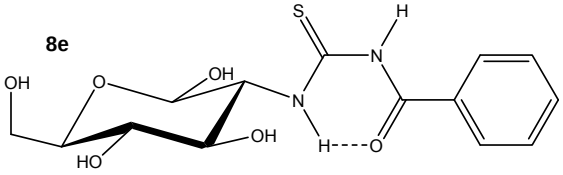

8f

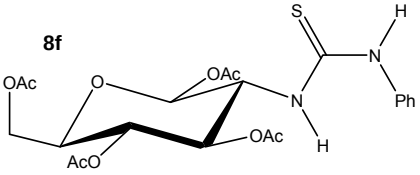

9a

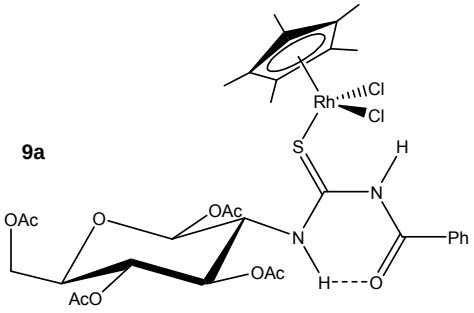

10

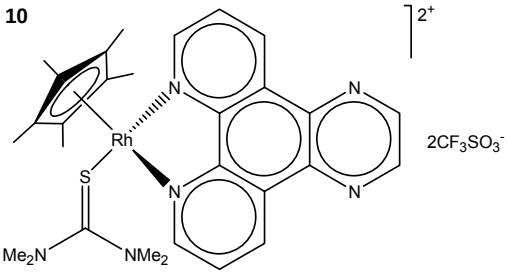

11a

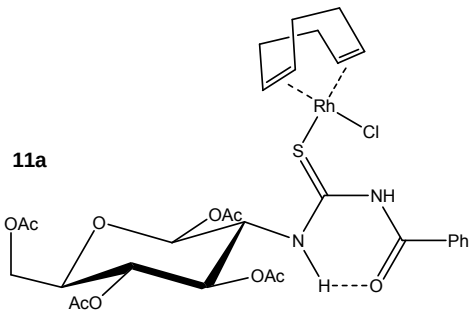

12a

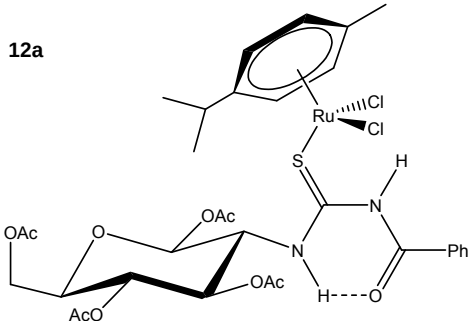

13a

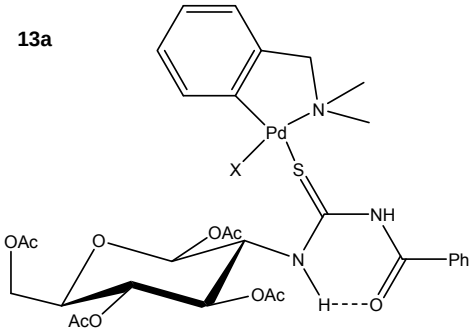

14a: X = Cl
15a: X = Br
16a: X = I

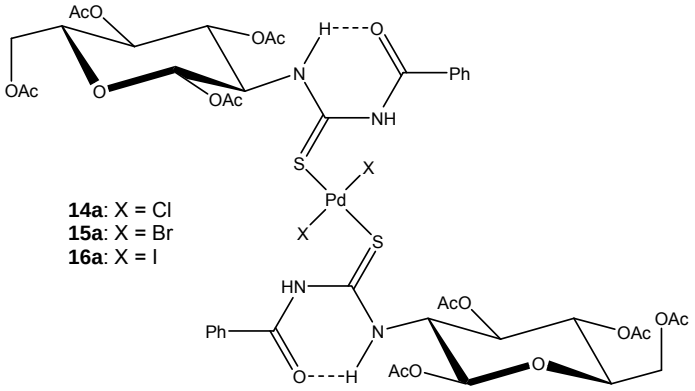

17a

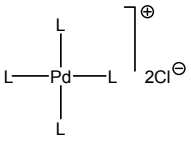

L =

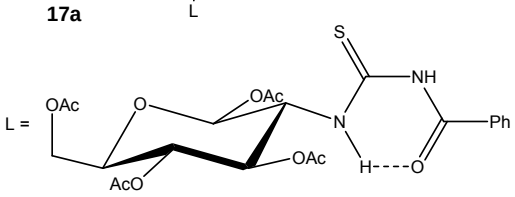

18a: X = Cl
19a: X = Br
20a: X = I

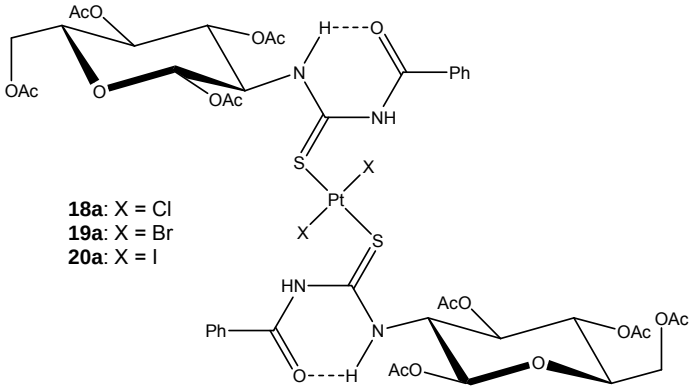

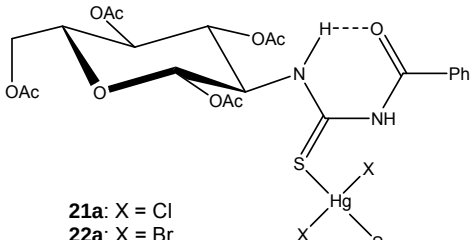

21a: X = Cl
22a: X = Br

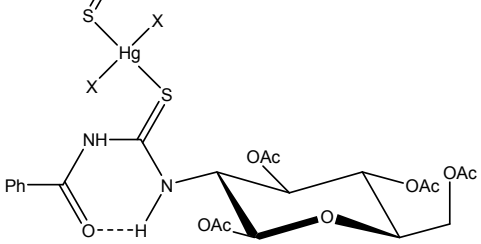

23a

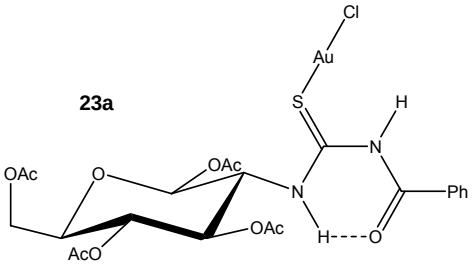

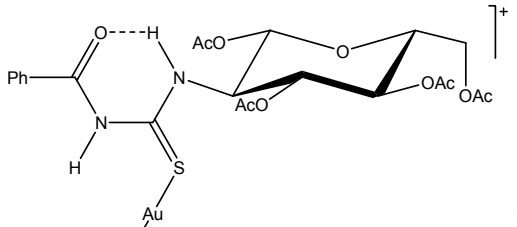

24a

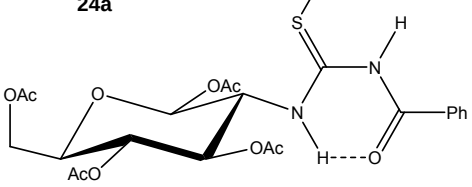

25a

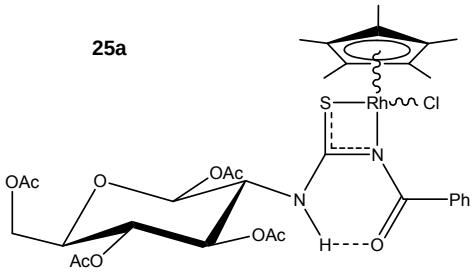

26

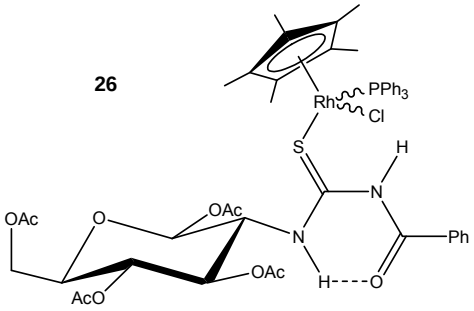

27

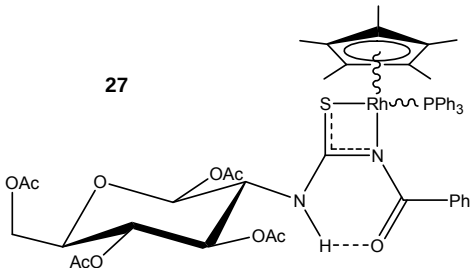

28

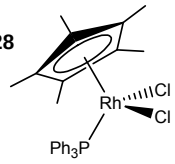

29a

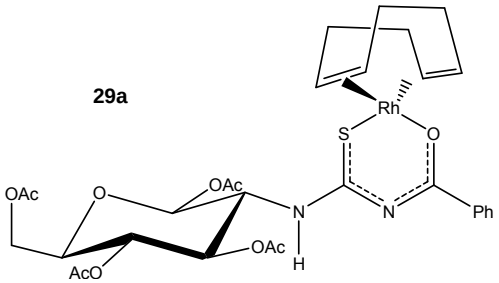

30

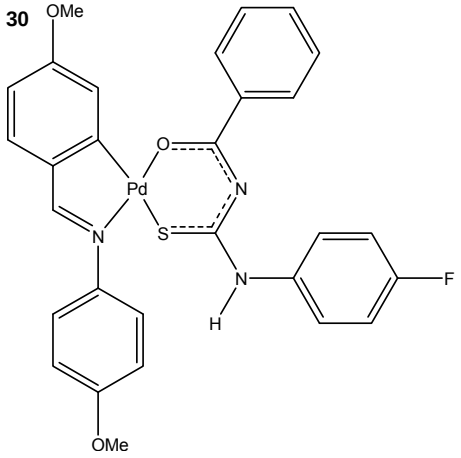

31

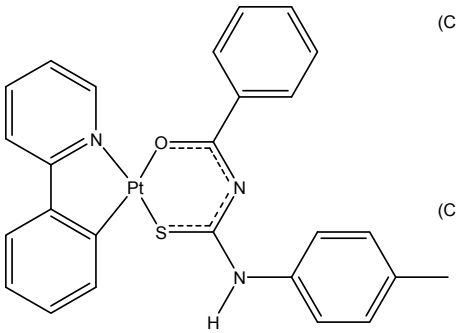

32

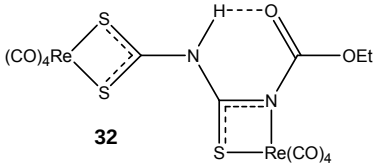

33

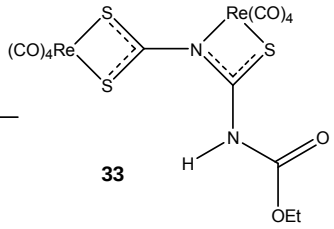

34a

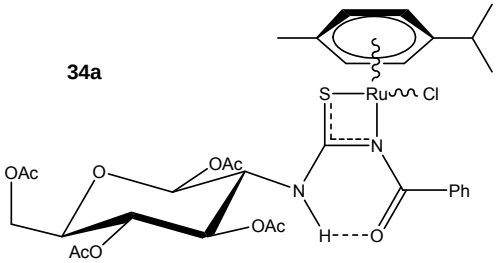

35a

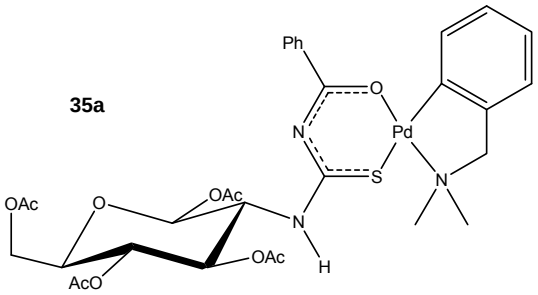

36a

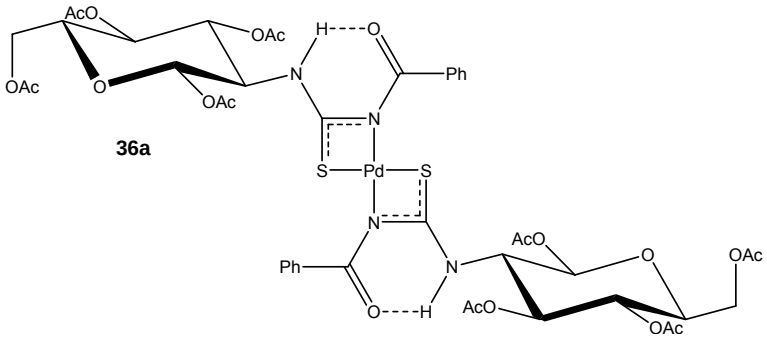

37g

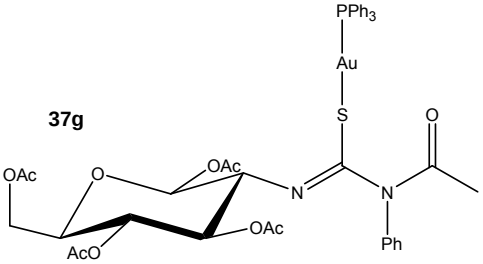

38

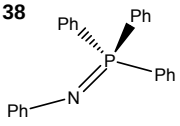

39h

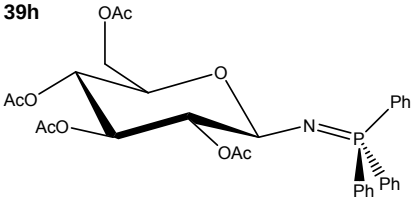

39k

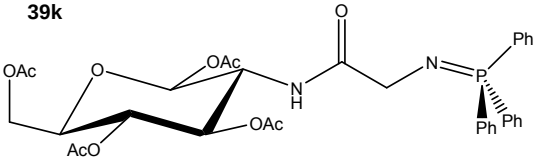

40

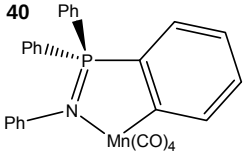

41

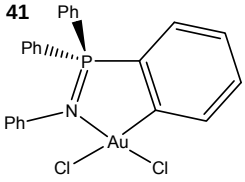

42

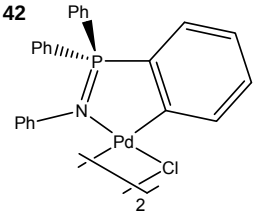

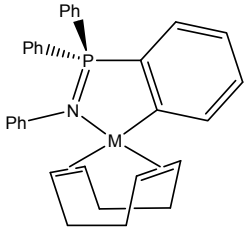

43: M = Rh
44: M = Ir

45h

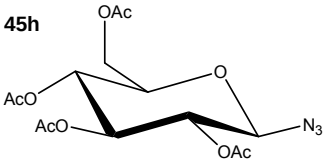

45i

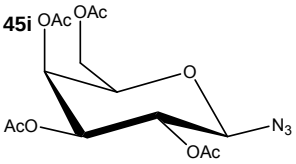

45j

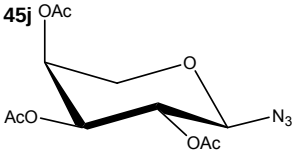

45k

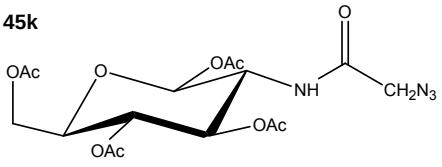

45l

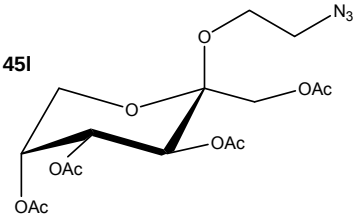

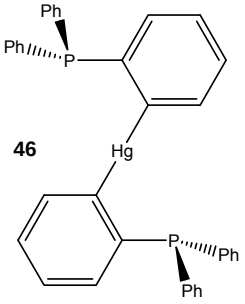

46

47

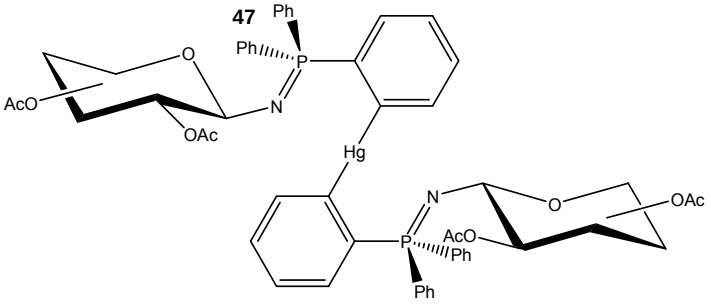

48l

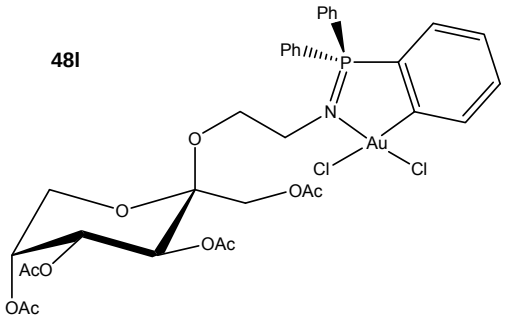

48

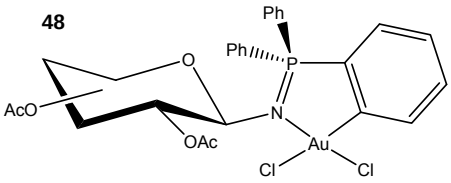

49

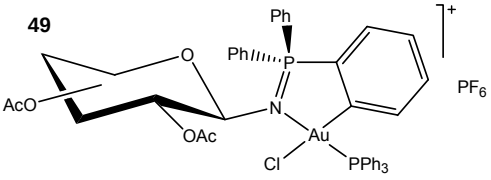

50

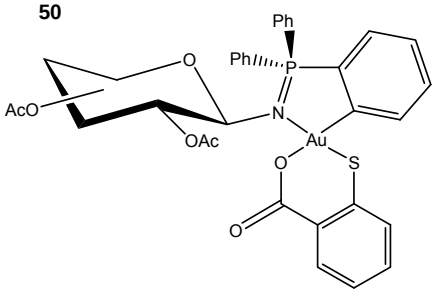

51

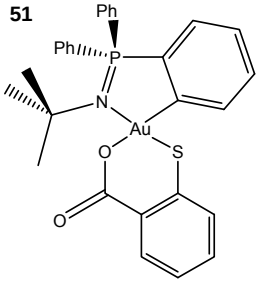

52

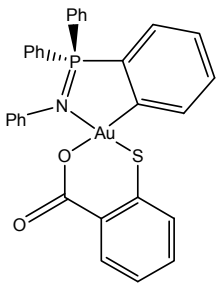

53

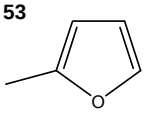

54

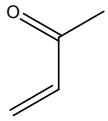

55

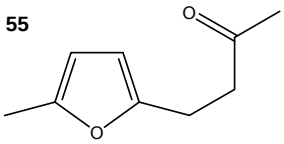

56

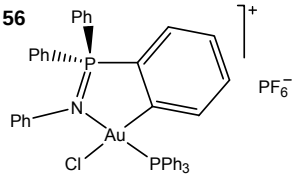

57

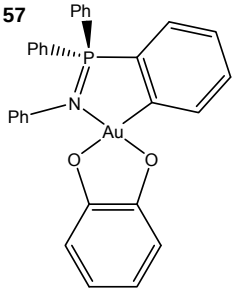

58

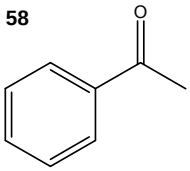

59